Department of Water, Atmosphere and Environment

Institute of Meteorology

University of Natural Resources and Life Sciences, Vienna

Novel methods and data sources in crop growth models – an application in Austria

Mag. Mag. Sabina Thaler

Dissertation to obtain a doctoral degree (Dr. nat. techn.) in Engineering Sciences, Agriculture, at the University of Natural Resources and Applied Life Sciences (BOKU) Vienna

Supervisor: Ao.Univ.Prof. Dipl.-Ing. Dr.nat.techn.Josef Eitzinger

Vienna, April, 2019

Abstract

Crop growth models are widely used as a tool to assess the consequences of the changing climate and various management strategies for crop production at the field level. These outcomes are increasingly implemented in a spatial model at the regional level. The analysis and modelling of crop growth, in combination with Geographic Information Systems (GIS), allows integrating e.g. topography, soil or weather data over a larger area. Currently, remote sensing data is becoming increasingly more available in terms of quality and quantity and can be applied for spatial crop growth modelling. These different technologies together form the basis for the spatial and temporal analysis presented here.

The assessment of the possible impacts of climate change on spring barley and winter wheat production in the Marchfeld region (NE Austria) was carried out in my previous studies on the basis of the Decision Support System for Agrotechnology Transfer (DSSAT) model in combination with three different Global Circulation Models (GCMs). In this present dissertation, some of the practicable regional- and farm-based adaptation measures (management options) to the crop yield as well as water and nitrogen balance under the climate scenarios were simulated. The results showed that increasing air temperature by e.g. 2°C would shorten the growing period by up to 20 days (winter wheat) and reduce the potential winter wheat and spring barley yield on almost all soil types in the region. Additional irrigation would maintain the yield, but at the same time lead to higher nitrogen leaching rates. Nevertheless, the use of specific management options, such as minimum tillage and windbreaks (e.g. hedges), could help mitigate increasing water demand.

Furthermore, DSSAT was applied for the analysis of five grid-shaped precipitation data as model input at three sites in Austria. The Integrated Calibration and Application Tool (INCA) of the Austrian Met Service (ZAMG), two satellite precipitation data sources (Multisatellite Precipitation Analysis (TMPA) and Climate Prediction Centre MORPHing (CMORPH)) and two precipitation estimations on the basis of satellite soil moisture data were used. The latter was calculated by applying the SM2RAIN algorithm and regression analysis to the soil moisture product Metop-A/B Advanced SCATtermonter (ASCAT) over 2007-2015. For the evaluation, the impact on the winter wheat and spring barley yield by the various precipitation input sets at a spatial resolution of about 25 km was computed. The highest variance was achieved for the driest region e.g. in combination with light-textured soils; TMPA and the two soil moisture products gave very good results under more humid conditions. The statistical weakest results at all three sites and for both crops were obtained with the CMORPH input data.

Keywords: crop growth model, model calibration and validation, climate change impacts, adaptation options, ASCAT soil moisture data, INCA, SM2RAIN, satellite precipitation data

Kurzfassung

Pflanzenwachstumsmodelle werden häufig als Instrument zur Abschätzung der Folgen eines Klimawandels und verschiedener Managementstrategien für die Pflanzenproduktion auf Feldebene eingesetzt. Diese Ergebnisse werden zunehmend in ein räumliches Modell auf regionale Ebene übertragen. Die Analyse und Modellierung dieser Daten in Kombination mit Geographischen Informationssystemen (GIS) ermöglicht es, Informationen aus z.B. Boden-, Klima- und Topographiedaten in eine größere Region zu übertragen. Fernerkundungsdaten sind in zunehmender Qualität und Quantität für die räumliche Anwendung von Modellen für Ertragssimulationen verfügbar. Diese verschiedenen Technologien bilden gleichzeitig die Grundlage für eine räumliche und zeitliche Analyse des Pflanzenwachstums.

Die möglichen Auswirkungen des Klimawandels auf die Sommergerste- und Winterweizenproduktion in der Region Marchfeld (NE Österreich) wurden in den ersten beiden Studien auf der Grundlage des Modells Decision Support System for Agrotechnology Transfer (DSSAT) in Kombination mit drei verschiedenen Global Circulation Models (GCMs) ermittelt. Darüber hinaus wurden einige praktikable regionale und betriebliche Anpassungsmaßnahmen (betreffend Produktionstechniken) an den Ernteertrag sowie die Wasser- und Stickstoffbilanz in den Klimaszenarien simuliert. Die Ergebnisse zeigen, dass eine Zunahme der Lufttemperatur um z.B. 2°C die Wachstumsperiode um bis zu 20 Tage verkürzen (Winterweizen) und den potenziellen Winterweizen- und Sommergersteertrag auf fast allen Bodenarten in der Region reduzieren würde. Eine zusätzliche Bewässerung würde den Ertrag erhalten, aber gleichzeitig zu höherer Nitratauswaschung führen. Spezielle Bewirtschaftungsoptionen, wie reduzierte Bodenbearbeitung und Windschutzelemente (z.B. Hecken), könnten jedoch dazu beitragen, den steigenden Wasserbedarf zu reduzieren.

Darüber hinaus wurde DSSAT für die Evaluierung von fünf rasterförmigen Niederschlagsdaten als Modelleingabe an drei Standorten in Österreich verwendet, bestehend aus dem Integrated Calibration and Application Tool (INCA) des Österreichischen Wetterdienstes, zwei Satelliten-Niederschlagsdaten - Multisatellite Precipitation Analysis (TMPA) und Climate Prediction Centre MORPHing (CMORPH) - und zwei Niederschlagsschätzungen auf Basis von Satelliten-Bodenfeuchtedaten. Letzteres wurde durch die Anwendung des SM2RAIN-

Algorithmus und einer Regressionsanalyse basierend auf das Bodenfeuchteprodukt Metop-A/B Advanced SCATtermonter (ASCAT) über den Zeitraum 2007-2015 ermittelt. Für die Bewertung wurden die Auswirkungen auf die Winterweizen- und Sommergersteerträge durch die verschiedenen Niederschlagseingabedaten bei einer räumlichen Auflösung von ca. 25 km berechnet. Die höchste Varianz wurde für die trockenste Region in Kombination mit sandigen Böden ermittelt; TMPA und die beiden Bodenfeuchteprodukte lieferten sehr gute Ergebnisse bei den feuchteren Gebieten. Die statistisch schwächsten Ergebnisse an allen drei Standorten und für beide Kulturen wurden mit den CMORPH-Eingabedaten erzielt.

Schlagwörter: Pflanzenwachstumsmodell, Modellkalibrierung und -validierung, Klimawandel, Anpassungsmöglichkeiten, ASCAT Bodenfeuchtedaten, INCA, SM2RAIN, Satelliten-Niederschlagsdaten

Affidavits

I hereby declare that I am the sole author of this work; no assistance other than that permitted has been used and all quotes and concepts taken from unpublished sources, published literature or the internet in wording or in basic content have been identified by footnotes or with precise source citations.

Acknowledgements

I would like to thank my supervisor, Univ.Prof. Dr. Josef Eitzinger, for the opportunity to carry out this dissertation in his working group, and for the support he has always given me. Thanks also to Delia Arnold, Katja Berger, Luca Brocca, Luca Ciabatta, Martin Dubrovsky, Herbert Formayer, Sebastian Hahn, Petr Hlavinka, Franz Holawe, Gerhard Kubu, Pablo Rischbeck, Mirek Trnka, Wolfgang Wagner and my colleagues from the Institute of Meteorology at BOKU, without whose help this work would certainly not have been possible.

My special thanks go to my family and friends who believed in me and always supported me. Here heartfelt thanks to my partner Filippo and our three children Alan, Mara and Ella, my parents Matthias and Notburga as well as siblings Florian, Karin, Monika, Thomas and Daniela.

Contents

1 Introduction 1

2 Objectives 3

3 Materials and methods 5

3.1 Crop growth simulation models 5

3.1.1 Types of crop growth simulation models 6

3.1.2 Brief history of crop modeling 7

3.1.3 Current limitations of crop growth simulation models 11

3.1.4 The Decision Support System for Agrotechnology Transfer (DSSAT) 11

3.2 Satellite Remote Sensing 12

3.2.1 Brief history of remote sensing 13

3.2.2 Basics of Satellite remote sensing 16

3.2.3 Resolution 17

3.3 GIS and Remote Sensing combined with crop growth models 18

3.3.1 Interfacing crop growth models to GIS 18

3.3.2 Linking crop growth models with remote sensing data 19

3.4 Study area 22

3.5 Input data of the crop model DSSAT 23

3.5.1 Weather data 23

3.5.2 Soil data 25

3.5.3 Genetic data 26

3.5.4 Management data 26

3.6 Simulation and model performance analysis 27

4 Results 29

4.1 Consequences of climate change in the Marchfeld, Austria 29

4.1.1 Climate change effects 29

4.1.2 Climate change impacts on winter wheat and spring barley yield 30

4.1.3 Technical adaptation strategies in response to a changing climate 31

4.2 Influence of various spatial precipitation input data on the results of the crop model 36

4.2.1 Comparison of the different precipitation dataset 36

4.2.2 Crop model response 37

5 Discussion and conclusion 40

6 References 45

7 Full list of publications 63

8 Appendix 67

List of figures

Figure 1. A simplified draft, which indicates how real world observations are brought into a descriptive model (source: Penning de Vries *et al.* 1989) 6

Figure 2. A simplified draft, which indicates how real world observations are analyzed and integrated into an explanatory model to simulate behavior of the system (source: Penning de Vries *et al.* 1989)... 7

Figure 3. Representation of the development of cropping systems modelling: starting with the comprehension of the basic plant and soil processes to models for more integrated plant-soil interactions up to cropping and farming systems (source: Keating and Thorburn 2018)... 11

Figure 4. Schematic overview of the DSSAT Cropping System Model (sources: Jones *et al.* 2003; Hoogenboom *et al.* 2017) 12

Figure 5. The wavelength ordered electromagnetic spectrum, which contains energy measurements within the ultraviolet, visible, reflective infrared, thermal infrared, and microwave ranges (source: Landgrebe 2003)... 13

Figure 6. A schematic representation of the three methods to assimilate state variables from remote sensing data in crop growth models: (a) calibration, (b) forcing, and (c) updating method (source: Dorigo *et al.* 2007 adapted from Delécolle *et al.* 1992).............................. 21

Figure 7. The four soil classes applied for the agricultural land use for Austria, the Marchfeld region and the three study sites 23

Figure 8. Changes of temperature (°C) as well as precipitation (%) in 2035 (2021-2050) in respect to present conditions (1961-1990) according to the SRES-A1B scenario (source: Thaler *et al.* 2009) 30

Figure 9. Relative change (%) in winter wheat (a) and spring barley yield (b) compared to baseline (1961-1990) and climate scenarios 2035s conditions (2021-2050) (source: Thaler *et al.* 2009)... 31

Figure 10. Relative change (%) of winter wheat yield (a) and spring barley yield (b) in 2035 (2021-2050) when ploughing would be replaced by minimum tillage in the Marchfeld region (source: Thaler *et al.* 2009) 33

Figure 11. Relative changes (%) of winter wheat yield in 2035 (2021-2050) with average wind speed decreases of 25%, 50% and 75% due to hedges on ploughed fields compared to reference management (1961-1990) (source: Thaler *et al.* 2012) 34

Figure 12. Monthly precipitation variations $INCA_{23km}$ (benchmark) versus $SM2R_{ASC}$, RA_{ASC}, TRMMRT, CMORPH for the period March to July 2007-2015 in (a) Groß-Enzersdorf, (b) Hartberg, (c) Kremsmünster (source: Thaler *et al.* 2018*a*) 37

Table index

Table 1. Different categories of models' application (source: Soltani and Sinclari 2012) 5

Table 2. Landmarks in the remote sensing history (source: Campbell and Wynne 2011) 15

Table 3. Canopy state and driving variables, which are derived from remote sensing data and applied in modelling studies for agroecosystems (source: Dorigo *et al.* 2007)....................... 20

Table 4. Four soil classes according to the available water capacity for Austria (according to AG Boden 1994, source: Thaler *et al.* 2018*a*) 25

Table 5. Estimated genetic coefficients of winter wheat (cultivar Capo) (source: Rischbeck 2007; Thaler *et al.* 2012) and spring barley (cultivar Magda) (source: Rischbeck 2007) used in the crop model simulation 26

Table 6. Changes of water demand (absolute in mm) across the various climate and management scenarios (2021-2050) against the baseline (1961-1990) 35

Table 7. Statistical characteristics (MAE, RMSE and r^2) of daily rainfall differences $INCA_{23km}$ (benchmark) versus $SM2R_{ASC}$, RA_{ASC}, TRMMRT, CMORPH for the period March to July 2007-2015 in Groß-Enzersdorf, Hartberg and Kremsmünster (source: Thaler *et al.* 2018*a*) 36

Table 8. Mean yield (kg/ha) with $INCA_{23km}$ input data and comparative statistics (RMSE, PBias, d, and r^2) of model performance in simulated crop yield using $SM2R_{ASC}$, RA_{ASC}, TRMMRT and CMORPH precipitation inputs against $INCA_{23km}$ inputs for the three study areas: (a) winter wheat (b) spring barley (source: Thaler *et al.* 2018*a*) 38

1 Introduction

Changes in the variability and the mean of climatic parameters have a critical influence on agricultural cropping systems, especially under water-limit production conditions, such as in the semi-arid areas of Central Europe (Trnka *et al.* 2010). It can be assumed that water scarcity, drought frequency, and its severity are increasing in many European regions. Dubrovsky *et al.* (2008) and Trnka *et al.* (2010, 2011*a*,*b*) stated that droughts and heat stress in especially sensitive developmental stages of crops are expected to increase in these areas of Central Europe. For instance, in Austria in 2013, the total damage to crops caused by drought and heat in agriculture was EUR 200 million; the damages in 2015 amounted up to EUR 175 million, in 2017 to EUR 140 million and in 2018 increased to EUR 210 million, paid by the Austrian Hail insurances for farmers to those insured against drought. Still, these do not include additional direct state disaster support for drought damage, such as in 2018 (BMNT 2018).

Drought and heat stress in plants can reduce biomass accumulation (Barlow *et al.* 2015; Lobell *et al.* 2011), accelerate senescence (Wardlaw and Moncur 1995) and – in specific cases – infertile florets (Saini *et al.* 1983; Grant *et al.* 2011), which reduce significantly, grain numbers (Tashiro and Wardlaw 1990; Stone and Nicolas 1995; Nendel *et al.* 2018). Heat stress, which often occurs in combination with drought stress, can be seen as a complex feature of the timing and duration of high-temperature events, characteristics of varieties and the phenological stage of the crop (Rezaei *et al.* 2015*a*,*b*; Prasad *et al.* 2017). In this case, temperatures reach a threshold level for a certain period of time, which is adequate to affect the crop growth and development in an irreversible way (Wahid *et al.* 2007). The critical thresholds for temperature differ strongly with the developmental stages of crops and plants (Hall 2018). Cereals, millets, oilseeds and other field crops are most vulnerable during the main reproductive stages, i.e. gametogenesis and flowering (Hedhly 2011; Prasad and Djanaguiraman 2014; Prasad *et al.* 2015; Shi *et al.* 2015; Singh *et al.* 2015).

Drought is regarded as a slow-onset natural disaster that can be defined as an extended period of time where less water is disposable than expected in an ecological system (Zhang *et al.* 2016). Agricultural dryness occurs if soil moisture is insufficient to fulfill the crop water requirement at a given time during growth (Razzaghi *et al.* 2017) and increase risks in particular in rainfed agricultural production (Sayago *et al.* 2017). Indeterminate plants like cowpea, cotton and tomatoes may adapt better to mid-season droughts than determinate plants like rice, maize, sorghum, pearl millet, and wheat (Hall 2018). Since drought stress is mainly connected with temperature stress, leaf temperatures usually increase above air temperature as a result of stomata closure and reduced transpiration (Hatfield 1979), having therefore in most cases negative effects on the crop growth and yield.

Another aspect of the changing climate is the ongoing enrichment of atmospheric CO_2, which is expected to rise from a current 400 ppm (2016) to 421 ppm (Regional Climate Model 2.6 (RCP)) - 936 ppm (RCP 8.5), respectively, by the year 2100 (IPCC 2014), enhancing the photosynthetic rate and biomass accumulation.

Changes in rainfall patterns and the increases in atmospheric CO_2 concentration and temperature operate quite differently on crop yields (Asseng *et al.* 2013, 2015; Porter *et al.* 2014; Trnka *et al.* 2014) and product quality (Martre *et al.* 2006; Myers *et al.* 2014), which may improve or decline depending on the region (Wheeler and von Braun 2013; Challinor *et al.* 2014; IPCC 2014; Nendel *et al.* 2018). Due to higher temperature changes in the crop's phenological development are expected. It may besides affect its vulnerability to adverse weather conditions, shifting sensitive phases into or out of periods in which late frost, critical heat, drought or heavy rain is more likely to occur (Siebert and Ewert 2012; Teixeira *et al.* 2013; Rezaei *et al.* 2015*a*,*b*; Trnka *et al.* 2015*a*,*b*). In addition to changes in climatic means, climate variability, with more frequent occurrence of climate extremes, increases the risk of adverse weather conditions during the cropping season, pushing crop performance beyond critical thresholds (Rötter *et al.* 2011*a*; Nendel *et al.* 2018).

For the assessment and interpretation of the behavior of agronomic systems under diverse environmental conditions, such as climate change and management options, mechanistic crop simulation models are suitable tools (Tsuji *et al.* 1998; Challinor 2011; Rötter *et al.* 2011*b*; Li *et al.* 2015*a*; Jones *et al.* 2017*a*). They are based on biophysical processes and their interactions are constructed to determine system feedbacks. In such a way, a better understanding and predicting of the system's behavior is given. Notably is their capability to explore genotype × environment × management interactions that make them so indispensable in agriculture studies (Porter *et al.* 2014; Chenu *et al.* 2017). However, crop models are only a simplification of the complex soil-crop-atmosphere system. Uncertainties are thus abundant, such as the model representation of the involved processes and model inputs (Eitzinger *et al.* 2008; Challinor 2011; Rötter *et al.* 2011*b*). For example, deficient process descriptions for response to temperature, drought, and CO_2 are given, lack of standardized protocols for their application, including inappropriate scaling methods and uncertainty reporting, can be found (Rötter *et al.* 2011*b*; White et al 2011; Rosenzweig *et al.* 2013). The use of crop simulation models is also a main tool to describe the effects of climatic conditions and management strategies on the field level. Increasingly their outcomes are implementing in a spatial application model on the regional level. Limits for crop model applications are frequently related to the availability and quality of model input data. So, an important uncertainty factor in simulated outputs is a poor quality of input data (beyond the representation of significant natural processes in the model); e.g. the spatial representation of the weather and soil model input data, which are mainly from scattered point locations such as weather stations (de Wit *et al.* 2005) and local spots (e.g. soil pit). With the help of spatial data analysis techniques and geographical information system (GIS) those model outputs can incorporate their information into a larger area (Delécolle *et al.* 1992). For instance, topographical, soil, and climate data provide a link between these two technologies and are at the same time groundwork for spatial and temporal analysis. Before using these data, comparing model results with field observations (model calibration and validation) or intercomparison of models (e.g. by sensitivity analysis) of different nature should be done. In this way, information on the performance of the models are given and their strength and their weakness discovered (e.g. Palosuo *et al.* 2011; Rötter *et al.* 2012; Eitzinger *et al.* 2013*a*; Huang *et al.* 2015; Kollas *et al.* 2015; Battisti *et al.* 2017).

2 Objectives

The overall objectives of this work are (i) to identify the potential impacts of climate change on agriculture in Austria's driest regions and possible adaptation strategies as well as (ii) to evaluate various precipitation crop model inputs derived from remote sensing products through crop model outputs such as simulated yield.

(i) In the first two studies presented (Thaler *et al.* 2012; Eitzinger *et al.* 2013*b*), the manifold impacts and possible adaptation strategies to climate change at farm level under semi-arid crop production regions of Central Europe for winter wheat and spring barley production were investigated by means of crop growth simulation. For this purpose, detailed input data for the parameterisation and validation of the crop growth model DSSAT (Decision Support System for Agrotechnology Transfer) were collected. GIS was applied to link and visualise the results for the entire investigated region Marchfeld (NE Austria). Special attention was given to (i) the range of potential future crop development and yields under different climate change scenarios and (ii) the effects of tillage and windbreak effects (hedges) on yield-limiting factors (i.e. soil water and N balance) as adaptation options.

(ii) The third paper (Thaler *et al.* 2018*a*) analyses different types of spatially gridded precipitation data used as crop model inputs and their influences of winter wheat and spring barley yield. For this purpose, remote sensing derived precipitation data were linked with the crop model DSSAT. The determination of site-representative precipitation estimates is of great importance since precipitation patterns during the vegetation period play a central role for crop growth and development conditions. Three case study sites in Austria were selected, which are characterized by different climate and soil conditions. The main purpose of this study was to test and compare whether the different free available satellite-based precipitation data (25 km spatial resolution) were suitable sources as input data for crop models and to identify their limitations compared to the 1 km grid precipitation data of Integrated Calibration and Application Tool (INCA) of Meteorological Service Austria. INCA data sets are distinguished by the high spatial resolution of 1 km but are not available freely, so that an overview of acceptable alternatives for different applications is of special interest. Besides, there is further relevancy in determining under which conditions and to which extent errors in the rainfall data are carried over to the final results of the crop model (simulated crop yield). Precipitation is the key uncertainty factor for crop growth simulation in the investigated area and therefore, information on the circumstances to replace this critical weather input parameter with alternative spatial sources is of interest.

The structure of the work is as follows. The Materials and Methods section presents crop growth models and remote sensing as well as their linking, followed by a description of the data used for application and evaluation in the crop growth model. Selected results from the three papers are then presented in the Results section. Finally, the Discussion and Conclusion section examines the approach and highlights some of the key findings of this work. Three peer-reviewed scientific publications form the Appendix of the thesis.

3 Materials and methods

3.1 Crop growth simulation models

Crop growth simulation models integrate available information on cultivar physiology, soil chemistry, management practices, agro-climatology data, and simulate key processes in order to determine crop performance in a given environment (Hodson and White 2010). They have a wide range of applications, e.g. climate change impact assessment and adaptation options, irrigation and fertilizer management, plant breeding and crop improvement, gene-based modeling, pest and diseases management, spatial analysis, tillage simulation and long-term effects of crop rotations (productivity and sustainability) (Jones *et al.* 2003; Hoogenboom *et al.* 2017). Generally, they can be divided into three main application categories (i) tools for decision making, (ii) research tools and (iii) tools for education and technology transfer (Murthy 2003). A brief summary of different types of models' application can be found in table 1.

Table 1. Different categories of models' application (source: Soltani and Sinclari 2012)

Using crop models in research
• Integration of research knowledge
• Integration of knowledge across disciplines
• Improvement in experiment documentation
• Crop genetic improvement
• Crop management improvement
• Yield analysis
• Response to climate variability and change
• Environmental impact of crop production
Using crop models as a tool in crop management
• Best management practices
• Pre-sowing and in-season decision aid for farmers
• Site-specific or precision farming
• Pre-harvest yield forecasting
Using crop models in education
• Student education
• Farmer education

3.1.1 Types of crop growth simulation models

Crop growth models, a simple representation of a crop based on physical plant processes, can be classified in descriptive and explanatory models. The first one describes the behaviour of a system in a basic way and involves normally one or more mathematical equations (Fig 1) (Penning de Vries *et al.* 1989). The relationship between variables is described without referring to any underlying biological or physical structure that may exist between the variable (Gowda *et al.* 2013).

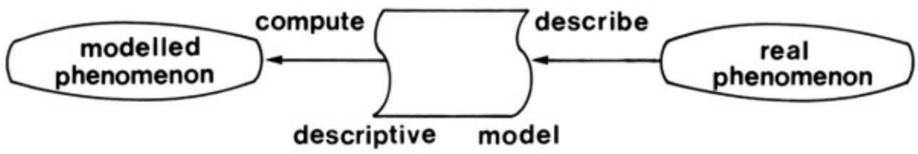

Figure 1. A simplified draft, which indicates how real world observations are brought into a descriptive model (source: Penning de Vries et al. 1989)

The explanatory model consists of a quantitative description of the mechanisms and processes, which influence the behaviour of a system (Fig 2). They are also called dynamic models or process-based models (Kasampalis *et al.* 2018). After the analysis, the process and mechanisms of the system are quantified separately. The model is constructed by integrating the different descriptions for the entire system with rate, state and driving variables (Penning de Vries *et al.* 1989). The state variables are quantities, which can be measured at specific times; for example biomass, amount of nitrogen in the soil, soil water content. Driving variables define the influence of the environment on the system at its borders, and their values have to be continuously controlled, as for example meteorological variables. Each state variable is coupled with rate variables, which define their rate of change at a given point in time as a result of certain processes. These variables characterized the flow of biomass or material between state variables. Their value relies on the state and driving variables, which are based on the knowledge of the biological, chemical, and physical processes involved in crop growth and development (Dadhwal 2003). In these ways, growth rates can be determined in each plant phase during the vegetation period, assuming the state of culture, soil, and weather (Gowda *et al.* 2013). The software application program DSSAT was used in these three studies, which comprises dynamic crop growth simulation models for over 40 crops.

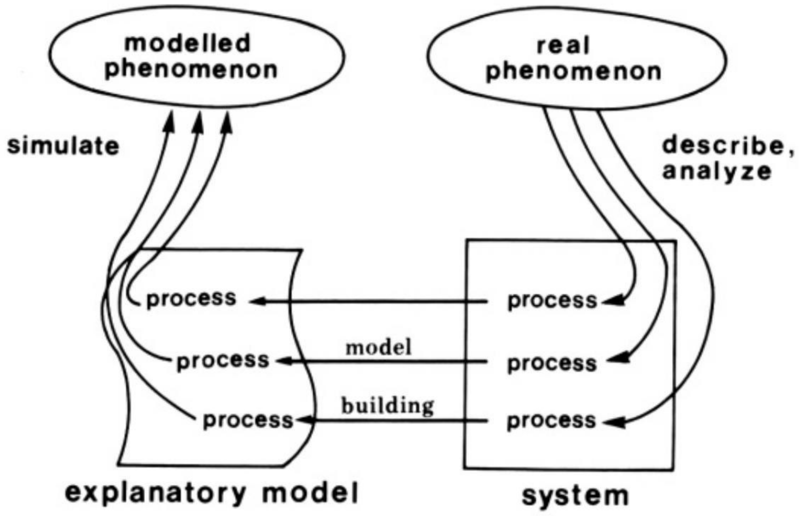

Figure 2. A simplified draft, which indicates how real world observations are analyzed and integrated into an explanatory model to simulate behavior of the system *(source: Penning de Vries et al. 1989)*

3.1.2 Brief history of crop modeling

The classical and functional growth analysis phase, also called the first generation, was from the 1910's to 1970's (Fig 3). At this time, first mathematical descriptions of plant and crop growth (Gregory 1917; Blackman 1919; West *et al.* 1920; Fisher 1921) as well as soil processes were defined (Heath and Gregory 1938; Williams 1946; Evans 1972; Venus and Causton 1979; Hunt 1982; Yin *et al.* 2003). The main focus was to describe growth functions, which fitted to plant growth data and frame plant growth according to leaf canopy for light capture and photosynthetic capacity (Keating and Thorburn 2018). These studies created the conditions for the next crop modelling efforts, the second generation. Here, one of the first models of agricultural production systems were conceived in the mid-1960s from the physicist C.T. de Wit of the Wageningen University in the Netherlands, a pioneer of agricultural system modeling. He assumed that agricultural systems can be modeled by uniting physical and biological principles. Another pioneer was the chemical engineer W.G. Duncan, who made the attempt to model canopy photosynthesis (Duncan *et al.* 1967) and developed some of the early crop-specific simulation models for maize, cotton, and peanut (Duncan 1972).

These first models, which simulated photosynthetic rates of crop canopies, were applied to estimate potential food production for some regions of the world and to make available indications for crop management and breeding (de Wit 1967; Linneman *et al.* 1979; Oteng-Darko *et al.* 2013). So de Wit *et al.* (1970) created in 1970 an Elementary Crop growth Simulator (ELCROS). It is a static photosynthesis model in which crop respiration is used as a fixed fraction per day of biomass and an amount proportional to the growth rate is added. Furthermore, a functional equation between root and shoot growth was established (Penning de Vries *et al.* 1974).

The work by de Wit (1958, 1965; Brouwer and Wit 1968; de Wit *et al.* 1970) and Duncan *et al.* (1967) were the inspiration for many scientists and engineers who began to develop and apply crop models (Jones *et al.* 2017*a*).

A significant improvement was the consideration of micrometeorology in the models (Goudriaan 1977) and the quantification of canopy resistance to gas exchanges, which was supplemented, for example, in the Basic Crop growth Simulator (BACROS) (de Wit and Gourdiaan 1978; Oteng-Darko *et al.* 2013).

In 1972, the Huffaker Integrated Pest Management (IPM) was established in the USA to tackle the huge problems associated with the increasing use of pesticide and the emergence of pesticide resistance in many target insects and diseases (Pimentel and Peshin 2014). A set of dynamic models for insect and disease were technologically further developed; some of them were linked to growth models for cotton and soybean (Wilkerson *et al.* 1983; Batchelor *et al.* 1993), like the SOYGRO model, which is now integrated into DSSAT (Jones *et al.* 2003). Additionally, the elaboration of a generic framework for coupling crop models with insect and disease information to assess the impact on crop growth and yield were undertaken (Boote *et al.* 1983; Jones *et al.* 2017*a*).

In the 1970s and 1980s, more and more cropping systems models were developed, which integrated plant physiology for the crop components and soil science for the soil water and nitrogen components, the third generation. So in the 1980s, the CERES Models (Maize and Wheat) by Joe Richie and his colleagues in Texas (Ritchie and Otter 1984; Jones and Kiniry 1986) as well as CROPGRO (SOYGRO and PNUTGRO) models at the University of Florida were developed (Wilkerson et al 1983; Boote et al 1986). These models coupled crop growth and yield, soil water, and soil nitrogen in a comprehensive way for the first time (Jones *et al.* 2017*a*). In 1982, the IBSNAT (International Benchmark Sites Network for Agrotechnology

Transfer) project was initiated, which aim was to collect and distribute a portable, user-friendly, computerized decision support system. This system contains (i) a database management system, where a minimum set of weather, soil, crop, site and management data can be entered, collected and saved to validate and use the software, (ii) crop growth models, which are able to simulate the interaction of genotype × environment × management, and (iii) application programs that permit a user to evaluate and display results of multi-year agronomic experiments on the computer (Uehara and Tsuji 1993).

The works of the early pioneers have continuously developed during the years. So, for example, the Wageningen University with C.T. de Wit trained many agricultural system modelers and developed a number of crop models, which are still in use today (Penning de Vries *et al.* 1991; Bouman *et al.* 1996; van Ittersum *et al.* 2003). Also, some of the early work of Duncan and Ritchie has influenced, generated and contributed to the DSSAT group of crop models (IBSNAT 1984; Tsuji *et al.* 1998; Uehara and Tsuji 1998; Jones *et al.* 2003; Hoogenboom *et al.* 2012).

Notable, government-funded initiatives, which are still widely used globally today, were, for example, the 1980 US Soil and Water Conservation Act that led to development the EPIC model (Williams *et al.* 1983, 1989), the IBSNAT project, funded from USAID, which led to the formation of the DSSAT suite of crop models (CERES and CROPGRO were combined) (Jones 1993; Boote *et al.* 1998, 2010; Jones *et al.* 2003; Hoogenboom *et al.* 2012), and, funded by the Dutch government from 1984, the Systems Analysis of Rice Production (SARP) project that resulted in the development of the ORYZA rice crop model (Penning de Vries *et al.* 1991; Bouman *et al.* 2001).

In the early 1990s, the establishment of the first fully financed, multidisciplinary crop modeling research group in Australia resulted in the development of the Agricultural Production Systems sIMulator (APSIM) (Jones *et al.* 2017*a*). Here started the fourth generation, from crop models to cropping systems models. The DSSAT model and many other crop models, or rater cropping systems models, were developed over the 1990–2000 period. DSSAT improved its functionality in cropping systems simulation and by 2003 it was defined as a modular cropping systems simulator (Jones *et al.* 2003). Further cropping system simulators are e.g. CropSyst (Stöckle *et al.* 2003) and STICS (Brisson *et al.* 2003). Still, there were the Dutch models in use (van Ittersum *et al.* 2003) but the Wageningen group did not go down the way of supporting a main cropping systems simulator as APSIM or DSSAT. However, the three groups sustained international connections through the International Consortium for Anti-microbial Stewardship in Agriculture (ICASA) Consortium (Keating and Thorburn 2018).

So far, still these models have to be relying on improving as the current models are mainly out of date (Rötter *et al.* 2011*b*). On the one hand, the mechanism of individual crop growth factors like nutrients dispersion, CO_2 diffusion, etc. are not yet included with the interaction of the environment, breeding programs, and microscale studies (Bhatia 2014). Here, the latest understanding of how crops respond to a changing climate as well as modern crop varieties and management practices need to be taken into account in the new models (Rötter *et al.* 2011*b*). On the other hand, the forces of shaping cropping systems model development and application should be intensifying. To have a better influence in real-world policy or practice settings, cropping systems models should be open in developments in data acquisition and model-data fusion and make so an important input to future agricultural productivity and sustainability (Keating and Thorburn 2018). Toward a 5th generation of agricultural system data, models and knowledge products, projects like the Agricultural Model Inter-comparison and Improvement Project (AgMIP) could play a key role, which is a major international endeavor combining climate, crop and economic modelling communities with state-of-the-art information technology. The aims are to develop the next generation of climate impact forecasts for the agricultural sector with the help of improved crop and economic models (Rosenzweig *et al.* 2013, Jones *et al.* 2017*b*). Latest developments try to establish modular, inter-transferable crop model compartments (e.g. on process level) using sophisticated higher open source “programming language levels” thus being transparent, following a concept that was already applied in the Wageningen school models in the 1980s (e.g. MACROS). Further the fast developments in molecular genetics, techniques in of determining functional plant traits etc. is going to establish multi-level models combining/integrating molecular, cell, and organ to whole plant simulation (González and Inzé 1015; Bardini *et al.* 2017).

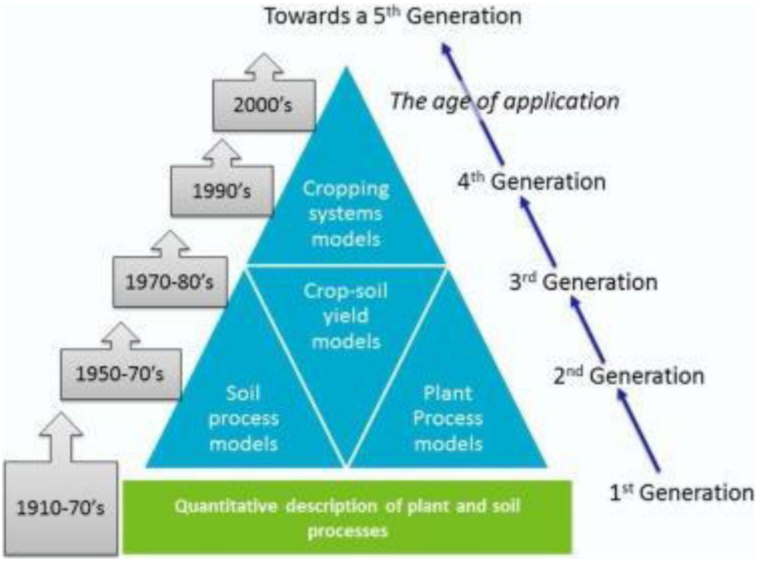

Figure 3. Representation of the development of cropping systems modelling: starting with the comprehension of the basic plant and soil processes to models for more integrated plant-soil interactions up to cropping and farming systems (source: Keating and Thorburn 2018)

3.1.3 Current limitations of crop growth simulation models

In Boote *et al.* (1996) it is well stated which application possibilities and limitations crop growth models have; furthermore, it is also indicated whether a model is appropriate for a certain purpose or whether the configuration of the model can be applied to other environmental conditions. Model limitations are, besides the model representation of the involved processes, the accuracy and availability of the input data, especially at regional scales. For example, Palosuo *et al.* (2011) simulated winter wheat in different European climates using eight crop growth models. The authors recognized that these crop models, which were performed at field scale, cannot be used for larger-scale applications without proper parameterization or ignoring essential factors about the model (Kasampalis *et al.* 2018). GIS and remote sensing, in particular, can help to obtain useful spatial information of certain parameters (e.g. Leaf Area Index) on larger areas and can contribute significantly to improve the performance of crop growth models (e.g. Thaler *et al.* 2012).

3.1.4 The Decision Support System for Agrotechnology Transfer (DSSAT)

The software application program DSSAT (Jones *et al.* 2001, 2003), which contains dynamic crop growth simulation models for over 40 crops, was applied in the current studies (Fig 4). These are process-based, management-oriented models, which simulate in diurnal running time effects of e.g. water and nitrogen on crop growth, weather, cultivar, crop management, soil, crop phenology, and yield. The CERES models run within the DSSAT (v4.0.2.0) framework (Hoogenboom *et al.* 1994; Tsuji *et al.* 1994, 1998) and CERES-Wheat Plant Growth Module (grain cereals wheat and barley) (Ritchie *et al.* 1984; Godwin *et al.* 1989) was used in the presented studies. This module is a widely used tool for the modelling of the yield components, water balance and other parameters within the soil-crop-atmosphere system (e.g. Jones *et al.* 2003; Eitzinger *et al.* 2004). The input requests for the CERES model comprises weather data, soil conditions, genotypes and crop management (Hunt *et al.* 2001).

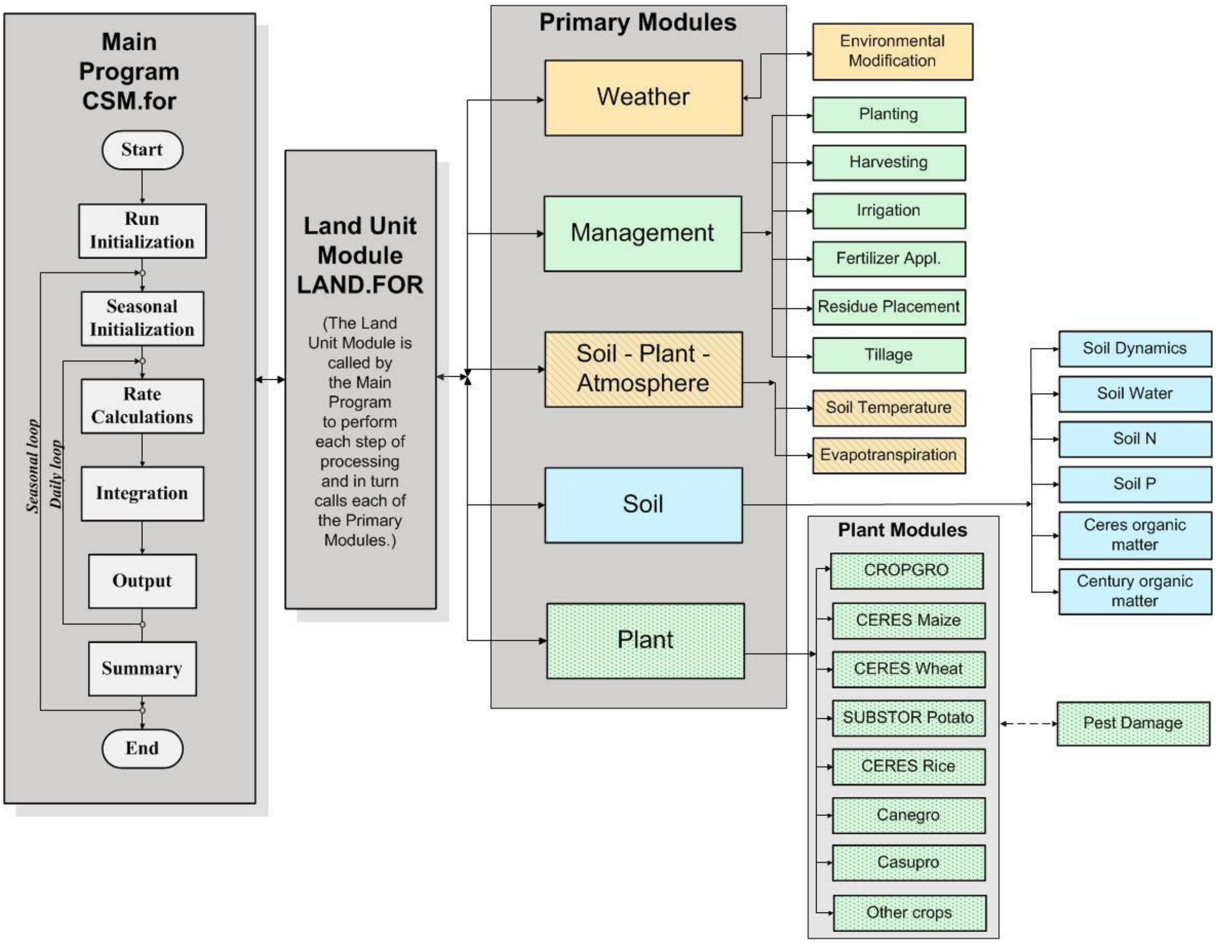

Figure 4. Schematic overview of the DSSAT Cropping System Model (sources: Jones et al. 2003; Hoogenboom et al. 2017)

3.2 Satellite Remote Sensing

In the last decades, satellite remote sensing has been developed as a powerful source of data for observing and monitoring the Earth's surface for a wide range of disciplines, including agriculture, hydrology, forestry, oceanography, weather, land use, environmental concerns, security purposes and military operations (Morris *et al.* 2005). The first use of the term “remote sensing” came from Ms. Evelyn Pruitt of the U.S. Office of Naval Research in the 1950s. Lillesand *et al.* (2004) described remote sensing as ‘the science and art of obtaining information about an object, area, or phenomenon through the analysis of data acquired by a device that is not in contact with the object, area or phenomenon under investigation’. One of the key objectives for remote sensing is the detection of various electromagnetic radiations (EMR) (Fig 5) by a sensor on a remote sensing platform (Tomlinson *et al.* 2011). EMR, which includes intensity, frequency spectrum polarization and time delay of the received energy, is characterized by its wavelength or frequency with the relationship $\nu = c/\lambda$ (c = speed of light in the medium [3.0×10^8 m s^{-1}], ν = frequency [cycles s^{-1} or hertz, Hz], λ = wavelength [m]) (Brown *et al.* 2007).

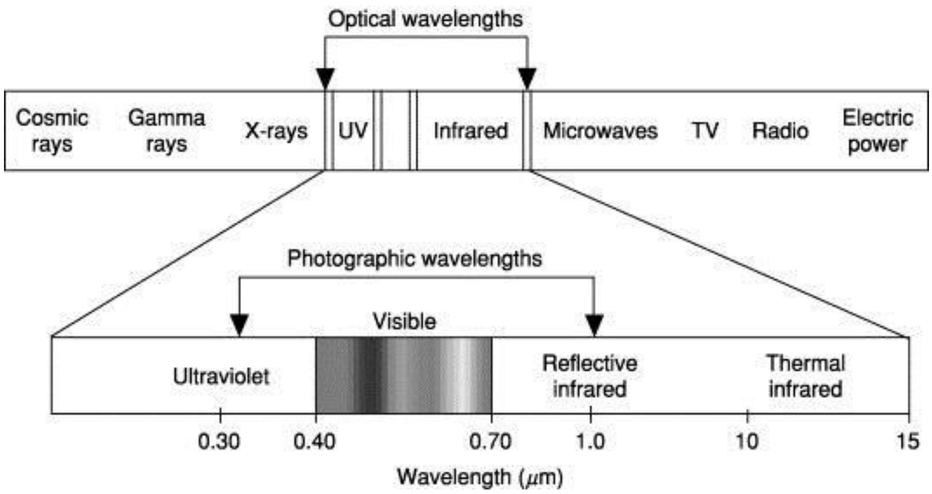

Figure 5. The wavelength ordered electromagnetic spectrum, which contains energy measurements within the ultraviolet, visible, reflective infrared, thermal infrared, and microwave ranges (source: Landgrebe 2003)

3.2.1 Brief history of remote sensing

Important events in the history of remote sensing are briefly summarized from the work by Campbell and Wynne (2011) in table 2. The technology of modern remote sensing lies in the beginnings of the practice of photography in the early 1800s. Several scientists conducted experiments with photosensitive chemicals, where e.g. 1839 Louse Daguerre (1789-1851) published his experiments. In 1858 Gaspard-Félix Tournachon (1829-1910) took the first aerial photographs of Paris from a hot air balloon (Campbell and Wynne 2011). The usage of kites in the 1880s and pigeons in the beginning of the 1900s was the next move, wherefrom cameras were carried at several hundred meters of altitude (Elachi and van Zyl 2006). During the First World War, cameras installed on airplanes delivered aerial views of large surface areas, which proved very valuable in military reconnaissance. Until the early 1960s, the aerial photograph was the standard instrument for photographing the surface from a vertical or oblique perspective. The remote sensing from aircraft was used more and more with the onset of the two world wars to spy on the enemy. In the beginning, the visible area of the spectrum was used. Then the development of sensors designed to see multiple spectrums including infrared and microwave bands was a further milestone in remote sensing. In this way, war planners were able to recognize and find before unseen intelligence (Campbell and Wynne 2011).

Satellite remote sensing can be observed from the early days of the space age of the Russian and American programs. At first, a dual method was used to image surfaces with different types of spacecraft sensors. In 1946, V-2 rockets, developed from Germany after World War II, were launched from New Mexico. Generally, these first space rockets never reached their orbit and included automated still or movie cameras, which shot photographs as the vehicle ascended.

In the early 1960s, the age of modern remote sensing was set with the launch of the Television Infrared Observation Satellite (TIROS-1). This satellite and its successors brought vidicon cameras into space and systematic monitoring of the weather and global environment from space was possible (Simonett *et al.* 1983). Satellite platforms, electro-optical (EO) sensor systems, and quantitative analytical tools for processing photographic and EO images are from now on available (Schott 2007).

Remote sensing has also been used from the outset to monitor and analyze agricultural activities. For example, aerial photography was utilized to conduct soil and crop surveys related to agricultural land in the USA and other parts of the world (Goodman 1959). With new advances in infrared photography introduced during the Second World War, remote sensing techniques developed a better understanding of crop status, water management as well as crop-soil conditions. Here, Robert Colwell of the University of California did pioneering work in this field in the 1950s. In the 1960s, new agricultural laboratories such as Purdue's were established (Nellis *et al.* 2009).

The first civilian earth observation satellite, LANDSAT-1, was launched in 1972. It was used, among other things, by the US government's Large Area Crop Inventory Experiment (LACIE) programme to estimate wheat production in large geographical areas; initially in the USA, then in Canada and the Soviet Union. LACIE's success resulted in a follow-up project in 1980 under the name AgRISTARS (Agriculture and Resources Inventory Surveys Through Aero-space Remote Sensing). The aim of this program was to expand LACIE and to cover the monitoring of other crops including rice, barley, cotton, maize, soybeans and wheat (Nellis *et al.* 2009). A summary of these programs can be found in Rundquist and Samson (1983), Bauer (1985) and Pinter *et al.* (2003); detailed information on historical developments in remote sensing and agricultural applications is available from Reeves (1975).

Table 2. Landmarks in the remote sensing history (source: Campbell and Wynne 2011)

1800	Discovery of infrared by Sir William Herschel
1839	Beginning of practice of photography
1847	Infrared spectrum shown by A. H. L. Fizeau and J. B. L. Foucault to share properties with visible light
1850–1860	Photography from balloons
1873	Theory of electromagnetic energy developed by James Clerk Maxwell
1909	Photography from airplanes
1914–1918	World War I: aerial reconnaissance
1920–1930	Development and initial applications of aerial photography and photogrammetry
1929–1939	Economic depression generates environmental crises that lead to governmental applications of aerial photography
1930–1940	Development of radars in Germany, United States, and United Kingdom
1939–1945	World War II: applications of nonvisible portions of electromagnetic spectrum; training of persons in acquisition and interpretation of airphotos
1950–1960	Military research and development
1956	Colwell's research on plant disease detection with infrared photography
1960–1970	First use of term *remote sensing*
	TIROS weather satellite
	Skylab remote sensing observations from space
1972	Launch of Landsat 1
1970–1980	Rapid advances in digital image processing
1980–1990	Landsat 4: new generation of Landsat sensors
1986	SPOT French Earth observation satellite
1980s	Development of hyperspectral sensors
1990s	Global remote sensing systems, lidars

Nowadays in Europe, on behalf of the joint initiative GMES (Global Monitoring for Environment and Security) of ESA and the European Commission, a series of next-generation Earth observation missions called SENTINEL has been developed, whereby the first satellite Sentinel-1A was launched on 3 April 2014. The aim of the SENTINEL programme is to replace the current older Earth observation missions that have retired, such as the ERS mission, or are nearing the end of their operational life. This will ensure continuity of data and avoid gaps in ongoing studies. These missions include a range of technologies, like radar and multi-spectral imaging instruments for monitoring atmosphere, land, and ocean (ESA 2019).

3.2.2 Basics of Satellite remote sensing

The properties of the observations and their applications are characterized by the physical features of a satellite remote sensing system. A satellite system is equipped with several components: sensors, a physical structure (i.e. bus), instruments to maintain the satellite's orientation and orbital position, data storage equipment, telemetry device to transmit the observations to Earth, the ground segment, which receives process, distributes the observations and derived parameters (Stewart 1985; Brown *et al.* 2007).

One way to differentiate the Earth observation satellite systems is to look at their orbits: there are two main orbits, called sun-synchronous (or polar) and geostationary orbits.

Satellites with polar or sun-synchronous orbits provide medium to high-resolution images of the entire Earth. They are mainly used for environmental monitoring, one example being LANDSAT (more information: https://landsat.gsfc.nasa.gov/). Polar or sun-synchronous orbits are located from 300 to 1400 km above the earth. Each satellite orbit lasts about 90 minutes and in the meantime, the Earth rotates a little further. The satellite observes different parts of the world in narrow bands (swaths). Days or weeks later, the satellite orbits the same area again. Consequently, the temporal resolution of these satellites is restricted in relation to geostationary satellites (Löffler *et al.* 2005; Albertz 2016).

Geostationary orbits at about 36 000 km above the earth. At this altitude, a satellite takes 24 hours to orbit around the Earth and it does synchronize with the rotation of the Earth. The satellites are at a right angle above the equator and so it seems that the satellite is stationary in the sky. Hence, the satellites observe the same segment of the earth's surface and the atmosphere. By reason of the high altitude of the orbit, the geometric resolution is very low and the smallest element, which can be recognized, is about 1 km^2 wide. One example of a geostationary satellite is METEOSAT (more information: https://www.eumetsat.int/website/home/index.html). Commonly, they were utilized to monitor and forecast the weather as well as for telecommunication and television broadcasting (Löffler *et al.* 2005; Albertz 2016).

Another way to distinguish between Earth observation satellites is to compare the sensors used. In most cases, there are passive sensors that measure reflected sunlight or thermal radiation, and active sensors that use their own radiation source. Active sensors emit artificial radiation to observe the earth's surface or atmospheric features in microwave scatterometers and altimeters, e.g. radar and laser scanners. Passive sensors detect solar radiation reflected from the earth and thermal radiation in the visible and infrared of the electromagnetic spectrum (Löffler *et al.* 2005; Albertz 2016).

3.2.3 Resolution

The resolution describes the ability to distinguish between objects both in space and time. The four main categories are spatial, temporal, spectral and radiometric resolution (Brown *et al.* 2007).

Looking at the spatial resolution, satellite sensors save data about objects in a grid form. Digital data are gathered from the covered area in the form of individual pixels, which are the smallest area unit in a digitized image. The size of the pixel differs depending on the sensor type and is responsible for the resolution of the image. The resolution measurement is the edge length of a pixel: the higher the resolution and the finer the raster, the greater the degree of visible detail on the earth's surface (Löffler *et al.* 2005; Albertz 2016).

The temporal resolution is based on the frequency at which the same place on earth is observed by the sensor. The re-visitation rate of a region is determined by several factors, e.g. the properties of the satellite orbitals, the field of view of the instrument, and the latitude of the observed area (Brown *et al.* 2007).

The spectral resolution includes the various satellite sensors, which differ in the number and bandwidth of their spectral channels and thus in their ability to observe discrete spectral ranges. Sensors are capable of a single wide panchromatic spectral band, which allows high-resolution observations. They are also capable to use multispectral and hyperspectral bands, which capture images in many spectral bands with medium to narrow bandwidth. A combination of both is also possible (Brown *et al.* 2007).

Radiometric resolution or quantization is the precision with which the observed measurements can be determined into discrete radiometric intervals. Whenever an image is scanned by a sensor, the sensitivity to the magnitude of the electromagnetic spectrum represents its radiometric resolution. The more finely the radiometric resolution of a sensor is, the more sensitive it is to detect small changes in reflected or emitted energy (Brown *et al.* 2007).

3.3 GIS and Remote Sensing combined with crop growth models

3.3.1 Interfacing crop growth models to GIS

GIS is a computer mapping and analysis tool where large datasets of spatial and non-spatial information can be integrated. It offers a digitized, spatially oriented database that can be evaluated with other spatially formatted data and information, such as satellites, maps, surveys, and other geo-referenced information sources. Different data sets can be overlaying digitally, enabling a joint spatial analysis of cartographic and statistical products. GIS can store a lot of spatial information and easily show the visual impact of changes in natural resources or policies on a large part of the region (Nagamani and Nethaji Mariappan 2017).

Crop growth models generate point output as input data are normally used from a specific field or location. The combination of different spatial inputs such as soil, weather or crop management with a GIS system can extend the scope of these simulation models to a wider scale. The aim of the combination of crop growth models and GIS is to perform spatial and temporal analyses simultaneously, as the behavior of crops on a regional scale has a spatial dimension and simulation models provide temporal performance. GIS can help in spatial visualization of results and their interpretation by spatial analysis of model results (Delécolle *et al.* 1992; Ewert *et al.* 2011; Dadhwal 2013).

Hartkamp *et al.* (1999) have suggested that "interface" and "interfacing" can be defined as generic terms for the concurrent use of GIS and crop growth models and "linking", "combining" and "integration" as appropriate terminology for the degree of the interface. These are the same terminology used by Burrough (1996) and Tim (1996) for loose, tight or embedded coupling. Although there is a continuum of linking and combination, the terms can be explained as follows (Dadhwal 2013):

- **linking:** Simple linking strategies utilize GIS for spatial representation of model results. One approach is the interpolation of model outputs. Different GIS functions like interpolation, overlay, slope, etc. can be used to create a database that contains model inputs and exports model outputs to the same database. The identifiers of raster cells or polygons are the input and output files for the data transfer between GIS and the model. Such an approach is not capable of realizing its full potential of the system and suffers from limitations due to dependence on GIS and model formats, incompatibility of operating environments and lack of use of GIS capabilities.

- **combining**: The combination processes data in the GIS and displays the model results. The model is configured with the GIS and the data is automatically exchanged using GIS package of macro language, interface programs, libraries of user-callable routines. This demands more complex programming and data management rather than simply linking.
- **integration**: Integration means that one system is integrated into the other. A model is either embedded in a GIS or a GIS system is part of a modeling system. This enables the automatic application of relational databases and statistical packages. Considerable knowledge, effort, and understanding of both instruments are here required (Dadhwal 2013).

3.3.2 Linking crop growth models with remote sensing data

Remote sensing data provide quantitative information on the actual state of crop conditions over large scale (Dadhwal 2013); whereas crop models can calculate the temporal dynamics of the plants, normally for local spots. Data assimilation methods, which include remote sensing data into existing crop growth model structures, can help to decrease the uncertainty of the model simulations and to increase the accuracy of the predicted models (Dorigo *et al.* 2007; Morel *et al.* 2014). In these frameworks it can be classified between (i) the driving variables that force the system; (ii) the system behaviour characterized by the state variables, (iii) the context between driving and state variables included the model parameters, and (iv) the outputs are the observable characteristics of the state variables (Delécolle *et al.* 1992). Some examples for used canopy state and driving variables can be found in table 3 of Dorigo *et al.* 2007.

Table 3. Canopy state and driving variables, which are derived from remote sensing data and applied in modelling studies for agroecosystems (source: Dorigo et al. 2007)

Biophysical parameter	Main indicator	Application	State (S) or driving (D)
Fraction of absorbed photosynthetically absorbed radiation (fAPAR)	Photosynthesis	Clevers (1997); Gobron et al. (2000)	S
Leaf Area Index (LAI)	Plant functioning	Bouman (1995); Doraiswamy et al. (2004); Mo et al. (2005); Moulin et al. (2003)	S
Fractional cover (fCOVER)	Plant development	Bouman (1995)	S
Chlorophyll and other pigments	Nitrogen stress/photosynthesis	Haboudane et al. (2002); Zhao et al. (2004)	S
Mineral content (K, P, Ca, Mg)	Crop quality	Mutanga et al. (2004)	S
Plant water content	Drought stress	Moran et al. (1994)	S
Above ground biomass/net primary production	Carbon storage; crop yield	Tucker et al. (1983)	S/D
Evapotranspiration	Drought stress	Bastiaanssen and Ali (2003); Hurtado et al. (1994)	D
Vegetation height	Plant development	Richardson et al. (1982)	S

Different methods have been used to link remote sensing data with agroecosystem models, mainly (Delécolle *et al.* 1992; Morel *et al.* 2014):

- **calibration method** (Fig 6a): the initial parameters of crop simulation models are adapted to the optimal configuration between the remote sensing data and the simulated state variables. So model parameters are re-initializing or re-calibrating by simulated and observed state variables (Moulin *et al.* 1998; Dorigo *et al.* 2007; Morel et al 2014). This approach has gained large attention in the scientific community by using optimised algorithms (Jin *et al.* 2018). Some examples of these different algorithms for calibration (Jin *et al.* 2018) are the simplex search algorithm (Guérif and Duke 1998; Launay and Guerif 2005; Ma *et al.* 2013), the Least Squares Method (LSM) (Zhao *et al.* 2013), the Maximum Likelihood Solution (MLS) (Dente *et al.* 2008), the Shuffled Complex Evolution (SCE-UA) (Shen *et al.* 2009; Jin *et al.* 2010; Ma *et al.* 2013), the Powell's conjugate direction method (PCDM) (Fang *et al.* 2008, 2011), the Very Fast Annealing Algorithm (VFSA) (Dong *et al.* 2013), and the Particle Swarm Optimization Algorithm (PSO) (Jin *et al.* 2015; Wang *et al.* 2014).
- **forcing method** (Fig 6b): the direct use of remote sensing inputs as a forcing variable, where leastwise one state variable has to be replaced or adjusted by remote sensing data. One example is the use of the estimated LAI from remote sensing data as a state variable and thus model input variable. In the works of e.g. Abou-Ismail (2004), Bouman (1995), Clevers *et al.* (2002), Hadria *et al.* (2006), Thorp *et al.* (2010) and Yao *et al.* (2015) estimated LAI of different remote sensing data were directly replaced in the crop growth model to improve the simulated LAI, biomass, yield, or crop transpiration. In general, in

the forcing method, the data assimilation of crop model and remote sensing data is simple to operate (Jin *et al.* 2018).

- **updating method** (Fig 6c): the constant updating of a state model variable (e.g. leaf area index, soil moisture) if continuously observation data are available. This method shows higher flexibility in comparison to others. A number of algorithms have hereby applied for assimilation of remote sensing data and crop models, e.g. Maas (1988), Clevers *et al.* (1994), Dente *et al.* (2008), Hadria *et al.* (2006). Nevertheless, this method requires a higher accuracy and quality from remote sensing data (Jongschaap 2006; Draper *et al.* 2012; Thorp *et al.* 2012; Li *et al.* 2015*b*).

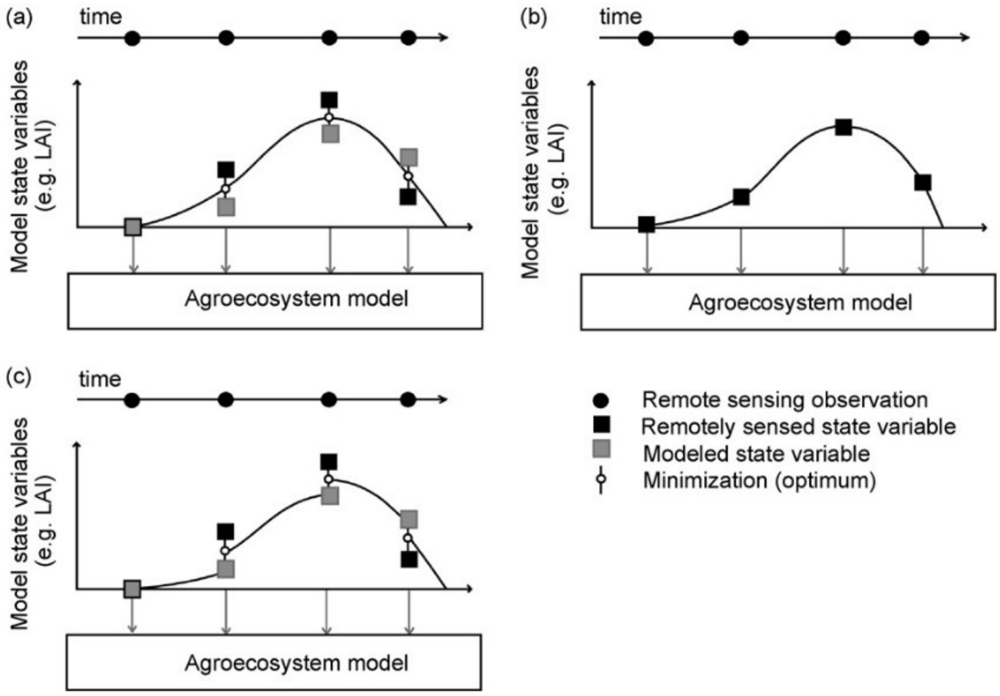

Figure 6. A schematic representation of the three methods to assimilate state variables from remote sensing data in crop growth models: (a) calibration, (b) forcing, and (c) updating method (source: Dorigo et al. 2007 adapted from Delécolle et al. 1992)

Remote sensing data can even be applied to assess and evaluate model outputs. For example, Thaler *et al.* 2018*b* compared soil moisture from crop growth models and ASCAT soil moisture data with in-situ measurements to investigate their performance.

3.4 Study area

One region and three sites in different climatic regions in Austria (Fig 7) were selected for these studies:

As a target region to study a changing climate, the Marchfeld area was chosen, which is in the north-eastern part of Austria. The region belongs to the Vienna Basin and is one of the most important crop production areas in Austria. At the same time, it is also one of the climatologically driest areas in the country. It is characterised by a semi-arid, continental climate where summers are hot and from time to time very dry, winters are in general cold with regularly strong frosts and limited snow cover. Furthermore, Marchfeld is marked by frequent wind, low air humidity and limited leaf wetness duration (Müller 1993). Main rainfed crops are cereals, other important crops, such as maize, vegetables, sugar beet or potatoes need to be irrigated in many years (Thaler *et al.* 2012).

The following three locations where selected for the analyses of different types of spatial precipitation data as crop model input:

- Groß-Enzersdorf (48°12'N, 16°33'E, 156 m a.s.l.) is located in the Marchfeld region and is characterized by a semi-arid, continental climate. The average annual temperature of 10.3°C and the mean annual rainfall of 516 mm were measured from 1981-2010.
- Hartberg (47°17', 15°58'E, 359 m a.s.l.) in Styria (SE Austria) is influenced by the Mediterranean and continental climates characterized by warm summers and mild winters. The mean annual temperature was 9.4°C and the precipitation sum over one year was 716 mm (1981–2010).
- As third location Kremsmünster (48°3'N, 14°8'E, 384 m a.s.l.) in Upper Austria was selected, which is marked by a central European transition climate, affected by the Atlantic climate. It is a humid region with a temperate climate. The mean temperature over a year was 9.1°C and the mean annual precipitation sum was 1003 mm (1981-2010).

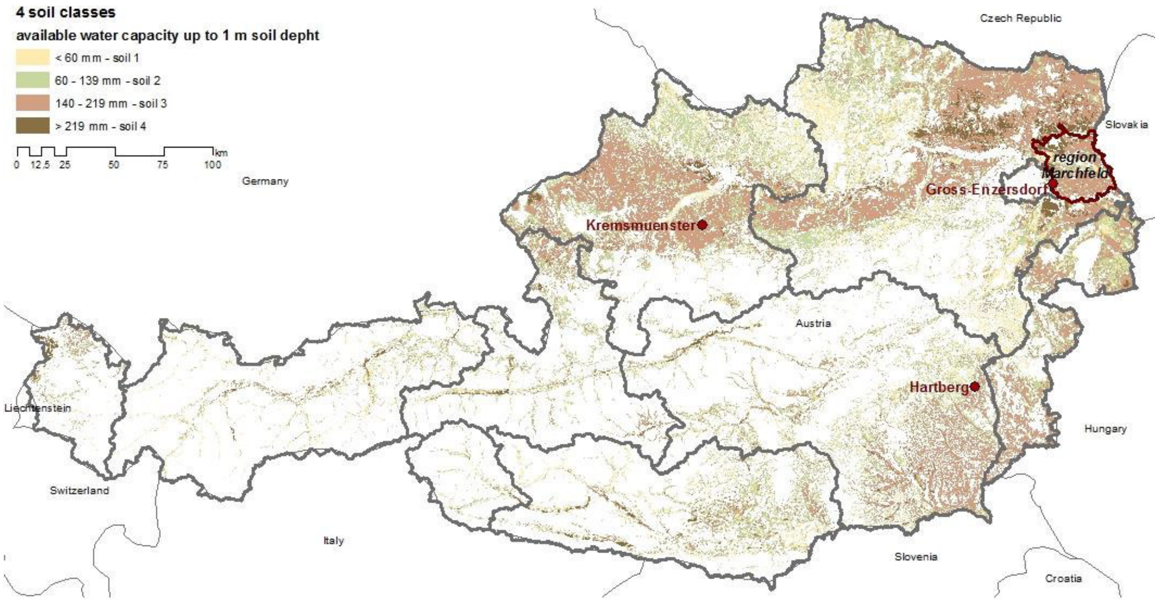

Figure 7. The four soil classes applied for the agricultural land use for Austria, the Marchfeld region and the three study sites

3.5 Input data of the crop model DSSAT

The minimum data set refers to a database necessary for the operation of the crop models and for the evaluation of crop model simulation and outputs.

3.5.1 Weather data

The basic daily weather information is the latitude and longitude of the weather station, maximum and minimum air temperature, solar radiation and precipitation (Jones *et al.* 2003; Hoogenboom *et al.* 2017). Here, weather data from the Austrian Met Service (ZAMG), different climate change scenarios and spatial precipitation data from satellite products were used.

In the first two studies, additional climate change scenarios were used. The stochastic weather generator (WG) M&Rfi generated a 100-year daily weather series (Dubrovsky 1997; Dubrovsky *et al.* 2000, 2004) for the baseline (1961–1990) and future scenarios (2021-2050). The climate change scenarios were modelled on the global circulation models (GCMs) ECHAM5, HadCM3 and NCAR PCM and on the Special Report on Emission Scenarios A1B (Nakicenovic and Swart 2000). The comparison of the results from three different GCMs allows to reduce the uncertainties in the climate scenarios. The final data sets used do not take into account changes in daily variability under future climate conditions. They assume that the variability under future climate conditions is the same as under the baseline conditions (Thaler *et al.* 2010, 2012).

In the third study, the following gridded precipitation data were used as forcing variables:

- The two high-resolution satellite precipitation data sets Tropical Rainfall Measurement Mission (TRMM) Multi-Satellite Precipitation Analysis (TMPA) and NOAA CPC MORPHing Technique (CMORPH) were applied. Precipitation estimates are based on calibrating and combining six passive microwave data of different satellite sensors and infrared data (only TMPA) of one satellite (Nayak and Villarini 2018). The end-product of TMPA is available for the ± 50° latitude band over a grid with a distance of 0.25° every 3 hours (Huffmann *et al.* 2018). CMORPH data are accessible with a horizontal resolution of 0.25°x0.25° from December 2002 until today on a 3-hour time basis for the ± 60° latitude band (Nayak and Villarini 2018). Neither TRMMRT nor CMORPH products used ground precipitation measurements to correct biases of satellite precipitation estimations. Their daily rainfall is the sum of rainfall estimates calculated within one day (Thaler *et al.* 2018*a*).
- Estimated rainfall on the assumption of satellite soil moisture dataset: The Advanced SCATterometer (ASCAT), a real-time radar, provides a surface soil moisture product (SM), with a spatial resolution of ~25 km (sampled at 12.5 km) on a daily basis (Wagner *et al.* 2013). The SM product represents a depth of 2-3 cm and lies between 0% (dry) and 100% (wet) with appropriate soil saturation. A Soil Water Index (SWI) can be used to obtain information about the root zone SM, which is a more robust product that can be used in deeper soil layers and has lower measurement noise (Wagner *et al.* 1999). Two approaches were applied to estimate the daily precipitation using these satellite SM observations:
    - An analytical relationship derived by reversing a soil-water balance equation to estimate precipitation accumulations from the SM time series called SM2RAIN (Brocca *et al.* 2013, 2014). Hereinafter referred to as $SM2R_{ASC}$.
    - A direct statistical relationship based on the measured rainfall and the SM of the ASCAT (Thaler *et al.* 2018*a*). Further referred to as RA_{ASC}.
- The Integrated Now-casting through Comprehensive Analysis (INCA) of the Austrian Met Service (ZAMG) is a numerical analysis and forecast tool of weather parameters in a very

high spatial (horizontal resolution of 1 km, vertical resolution of 200 m) and temporal resolution (4 h) (Karabatić *et al.* 2011; Haiden *et al.* 2014). The mean of all 1 km INCA pixels within one ASCAT resolution cell was computed to obtain a regional value corresponding to the ASCAT-based precipitation estimates (a Hamming window at a radius of approx. 23.7 km). The data set was referred to as $INCA_{23km}$.

3.5.2 Soil data

The desired crop model soil input contains soil classification (SCS), surface slope, color, permeability and drainage class. Upper and lower horizon depths in cm, soil texture information, bulk density, lower limit of plant extractable soil water, drained upper limit, saturated soil water content, pH value in water, initial water and N-content, organic carbon, aluminum saturation, and root abundance information is for example requested as model input for each individual soil layer set by the user (Jones *et al.* 2003; Hoogenboom *et al.* 2017). However, only soil texture information is the obligatory minimum input. The soil water holding limits are very critical and important, but if not available, the model will calculate them from soil texture information using pedotransfer functions, which are normally introducing uncertainty.

Table 4. Four soil classes according to the available water capacity for Austria (according to AG Boden 1994, source: Thaler et al. 2018a)

Soil classes	LL	DUL	SAT	area precentage in Austria (%)	available water capacity	Soil type
soil class 1	0	0.1	0.1	14.1	very low	loamy sand
soil class 2	0.1	0.2	0.3	33.7	low	sandy loam
soil class 3	0.2	0.4	0.5	47.5	moderate	sandy loam
soil class 4	0.2	0.4	0.5	4.7	high	loamy silt

LL = lower limit of plant extractable soil water; DUL = drained upper limit; SAT = saturated soil water content

In my study, the FAO-56 Penman-Monteith equation (Allen *et al.* 1998) was applied to estimate evapotranspiration and the effect of wind speed reductions. Four soil classes (termed herein as soil 1, soil 2, soil 3 and soil 4, respectively) were selected according to the total available water capacity (Tab 4, Fig 7). The digital Austrian soil map 1:25,000 include data on texture, pH value, humus content, etc. of each soil profile down to a depth of 1 m. Based on these data, Murer *et al.* (2004) calculated the physical soil properties of permanent wilt point, field capacity, saturation point and the available field capacity of the soil based on a pedotransfer function method in AG Boden (1994).

3.5.3 Genetic data

The genetic coefficients used in the CERES model present the specific growth and development of the selected crop cultivar (Tsuji *et al.* 1998; Alexandrov and Hoogenboom 2000). For the equalization of genetic coefficients, simulated outcomes were calibrated and validated with measured results from field trials. Winter wheat (*Triticum aestivum L.*) cultivar "Capo" (Rischbeck 2007; Thaler *et al.* 2012) and spring barley (*Hordeum vulgare L.*) cultivar "Magda" (Rischbeck 2007; Eitzinger *et al.* 2013*b*) were adjusted using agro technological, phenological, yield and weather data from the experimental site at Fuchensbigl, Marchfeld in Austria (48°12'N, 16°44'E, 157 m a.s.l.). The estimated genetic coefficients of the validated wheat and barley applied in the model simulations are provided in table 5.

Table 5. Estimated genetic coefficients of winter wheat (cultivar Capo) (source: Rischbeck 2007; Thaler et al. 2012) and spring barley (cultivar Magda) (source: Rischbeck 2007) used in the crop model simulation

Genotype	**P1V** (%/day)	**P1D** (%/day)	**P5** (°C/day)	**G1** (#/g)	**G2** (g/m² day)	**G3** (g)	**PHINT** (°C/day)
CAPO	60	90	560	28	42	1.33	95
MAGDA	0	0	420	22	40	1.00	75

P1D = photoperiod sensitivity coefficient; P1V = vernalization sensitivity coefficient; P5 = thermal time from the onset of linear fill to maturity (8 °C day); G1 = kernel number per unit stem and/spike weight at anthesis; G2 = potential kernel growth rate; G3 = tiller death coefficient: standard stem and/spike weight when elongation ceases; PHINT = thermal time between the appearance of leaf tips (8 °C day) (Jones *et al.* 2003)

3.5.4 Management data

Planting date, planting density and depth, row spacing, crop variety, irrigation and fertilizer schedules and practices are some of the most important input for crop management information (Jones *et al.* 2003; Hoogenboom *et al.* 2017). In the first two studies different management strategies were analyzed:

- rain-fed farming and automatic irrigation
- automatically adapted sowing dates and predefined dates
- with and without the enrichment of CO_2 according to the emission scenario
- ploughed soil and minimum tillage
- wind speed reduction due to hedges

- additional soil moisture owing to snow banks on hedgerows
- fix N fertilization according to the guidelines of the Austrian Agri-environmental Programme ÖPUL
- harvest at maturity

In the third study rain-fed farming, including N fertilization, fix sowing date, harvest at maturity and ploughed soil condition was simulated.

In all simulation studies yield losses, provoked by pest and diseases, were not included or considered.

3.6 Simulation and model performance analysis

In the first two simulation studies present climate (1961-1990) and usual crop management in the region Marchfeld as baseline was applied: winter wheat and spring barley were drilled in 12 cm spaced rows at a depth of 3 cm; the sowing density was set with 350 kernels m^{-2}. The application of two (spring barley) and three (winter wheat) fertilizer treatments was simulated; the amount that farmers presently use in this area. For spring barley 40 kg ha^{-1} N at the beginning and at the end of April was applied. Fertilization at 3 x 40 kg ha^{-1} N at tillering, steam elongation or jointing and booting was set for winter wheat. The baseline simulation contains rain-fed farming, automatically adapted sowing dates, ploughed soil and contemporary cultivars (Tab 5).

Modified scenarios were run including solar radiation, temperature, and precipitation databases, accordingly to each of the climate change scenarios. Simulations were carried out with and without the direct effects of increased atmospheric CO_2 levels. The atmospheric CO_2 concentrations were assumed to be 360 ppm for the current climate (1961-1991) and 452 ppm for the future climate in 2035 (2021-2050) according to the SRES-A1B emission scenario. Furthermore, different alternatives in crop management were simulated and evaluated (see above 2.5.4 Management data).

The third study examined the impact of different precipitation input data on simulated yields and their performances. Hereby a set of statistical parameters was calculated: the root-mean-square error (*RMSE*) was taken as a measure of the average differences between the model estimates and measurements. *RMSE* indicates the standard deviation by which the model prediction error occurred. A smaller value indicates better model performance.

$$RMSE = \sqrt{\frac{1}{N}\sum_{i=1}^{N}(S_\mathrm{i} - O_\mathrm{i})^2} \tag{1}$$

where *S* is simulated values and *O* observed ones.

Mean absolute error (*MAE*) calculates the absolute error between simulated and observed values.

$$MAE = \sqrt{\frac{1}{N}\sum_{i=1}^{N}|S_\mathrm{i} - O_\mathrm{i}|} \tag{2}$$

Singh *et al.* (2004) state that in the case where the *RMSE* and *MAE* values are below half the standard deviation of the measured data, they may be regarded as low and both are appropriate for model evaluation. Both statistic parameters indicate an error in the units of the constituent of interest and values of 0 indicate a perfect fit (Moriasi *et al.* 2007).

The percent bias (*PBias*) measures the average tendency of the simulated values to be larger or smaller as their observed ones. Low *PBias* values indicate a more precise model simulation, where the optimal value is 0.0. Positive values show overestimation bias, while negative values indicate model underestimation one. The result is given in percentage (%) (Sorooshian *et al.* 1993; Yapo *et al.* 1996*).*

$$PBias = 100\,\frac{\sum_{i=1}^{N}(S_\mathrm{i} - O_\mathrm{i})}{\sum_{i=1}^{N} O_\mathrm{i}} \tag{3}$$

The index of agreement (*d*) was developed by Willmott (1981) and can be seen as a generic indicator of modelling efficiency and presents the ratio between the mean square error and the “potential error” (Willmott 1984). The latter error can be quantified by the sum of the squared absolute values of the distance from the predicted values to the average of the observation and the distances from the observed values to the mean of the observation. *d* ranges from [0,1], which values near 1 indicating high simulation quality (Willmott 1981, 1984; Willmott *et al.* 1985; Legates and McCabe 1999). However, *d* is because of the squared differences very sensitive to extreme values (Legates and McCabe 1999; Moriasi *et al.* 2007).

$$d = 1 - \frac{\sum_{i=1}^{N}(O_i - S_i)^2}{\sum_{i=1}^{N}(|S_i - \bar{O}| + |O_i - \bar{O}|)^2} \tag{4}$$

For comparison, the r^2 regression statistics (least-squares coefficient of determination) were also computed, although they do not take into account model bias (Palousuo *et al.* 2011). In this context, it should be mentioned that *r* and r^2 are oversensitive to extreme values (outliers) and not sensitive to additive and proportional variations in model predictions and measured data (Legates and McCabe 1999).

Uncertainty is represented by a distribution of simulated model results, whereas the error presents the difference of observed and predicted values, applied to cases where true values are available (Wallach *et al.* 2006). Bias means an average (over sites or years, etc.) over- or underestimates by the models (illustrated by the *PBias*).

4 Results

4.1 Consequences of climate change in the Marchfeld, Austria

4.1.1 Climate change effects

The seasonal temperatures until 2035 (2021-2050) in Marchfeld show a clear increasing trend (Fig 8): the highest rises can be expected in the summer and winter months. August shows a temperature increase of up to 3.8°C (HadCM3) followed by the two months December and January up to 2.9°C (ECHAM5) (not shown). HadCM3 turns out to be the warmest scenario, while NCAR PCM is the scenario with the lowest temperature increase (Fig 8 year).

For the selected study area, ECHAM5 and HadCM3 forecast a decrease in annual precipitation between 11% (HadCM3) and 17% (ECHAM5), while NCAR PCM for 2035 forecast an increase by 5% in relation to the baseline (Fig 8). Whereas from November to March a higher rainfall can be expected, especially in the NCAR PCM scenarios, precipitation deficits are predicted from April to October. On a monthly scale, the months of July and August in ECHAM5 and HadCM3 show more than 70% less rainfall as in the baseline (not shown) (Thaler *et al.* 2012).

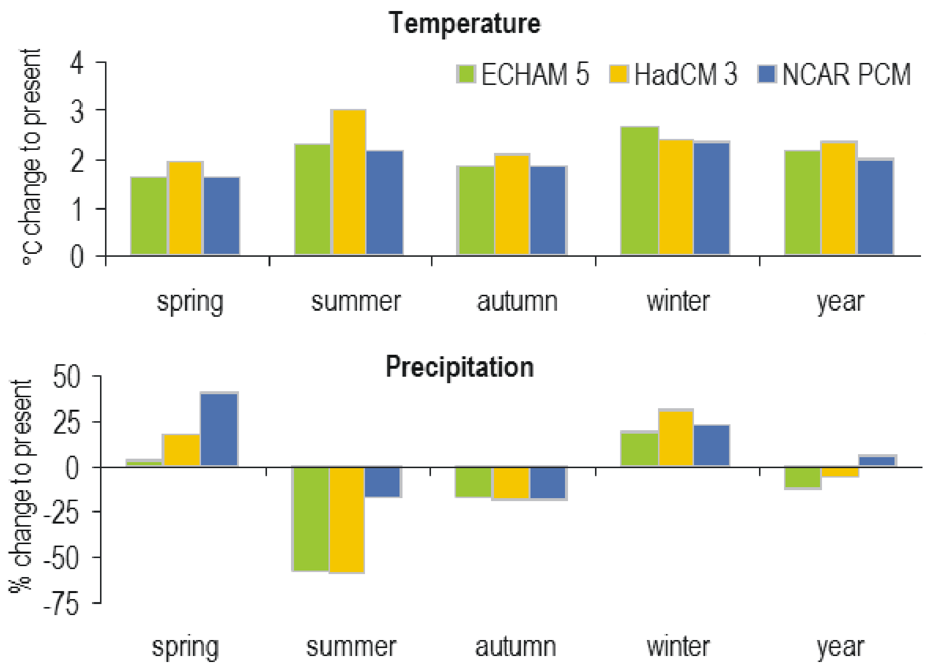

Figure 8. Changes of temperature (°C) as well as precipitation (%) in 2035 (2021-2050) in respect to present conditions (1961-1990) according to the SRES-A1B scenario (source: Thaler et al. 2009)

4.1.2 Climate change impacts on winter wheat and spring barley yield

The effects of the changing weather conditions under ECHAM and HadCM show a decline or stagnation of winter wheat (Fig 9a) and spring barley (Fig 9b) yields until 2035, where spring barley generally shows more stable yields. The decline in yield can be explained by a shortened vegetation period of the simulated crops (due to higher temperatures) and a reduction in precipitation during the vegetation period (especially May and June). In Marchfeld, even the additional effect of CO_2 fertilisation (combined effect) could not completely offset the decline in yields. The yield reduction is much more pronounced on sandy and shallow soils (soil 1 and 2) with low water storage capacity. Only NCAR presented a significant increase in winter wheat and spring barley yields, especially for soil 3 and 4. According to the simulations, the interannual yield variability of both crops increases in 2035, which leads to higher economic risks for farmers (Thaler *et al.* 2012; Eitzinger *et al.* 2013*b*).

(a)

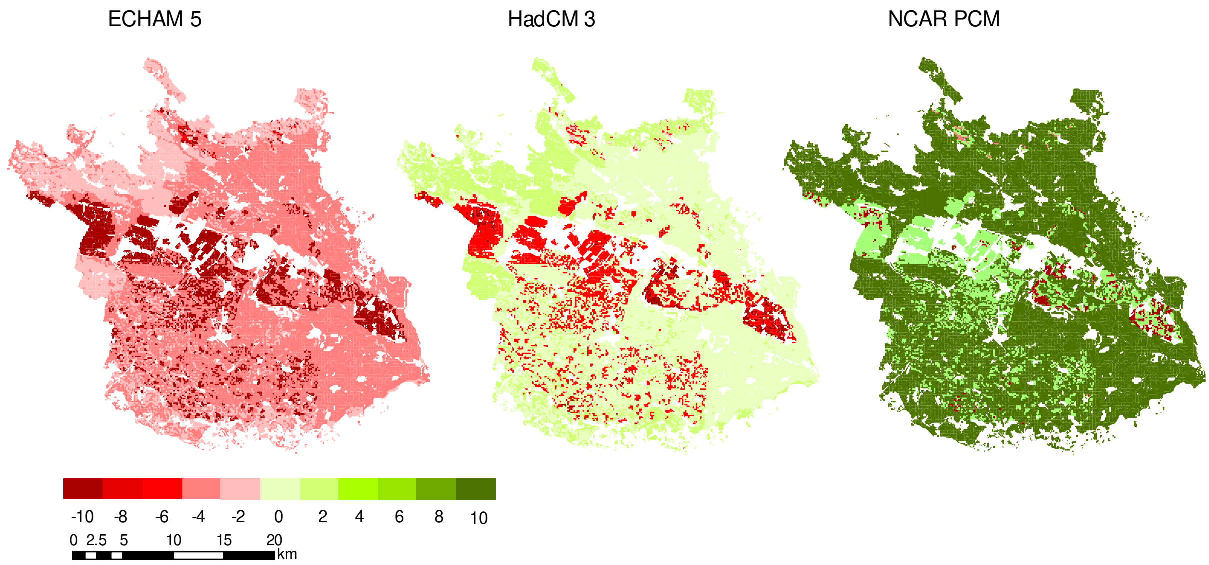

(b)

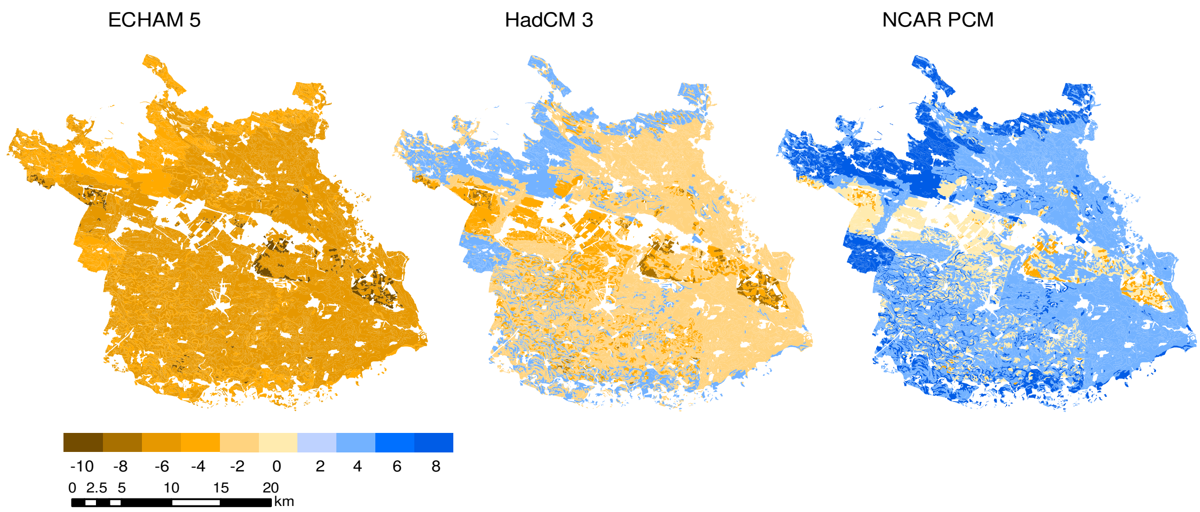

Figure 9. Relative change (%) in winter wheat (a) and spring barley yield (b) compared to baseline (1961-1990) and climate scenarios 2035s conditions (2021-2050) (source: Thaler et al. 2009)

4.1.3 Technical adaptation strategies in response to a changing climate

A set of agronomic adaptation strategies can be suggested to mitigate or prevent the negative impacts of a changing climate. Generally, these strategies differ between short-term and long-term adaptation. The first solutions concern water saving e.g. the changes in planting dates or cultivars, changes in external inputs such as irrigation and techniques for soil water conservation. Long-term adaption often involves profound structural changes to overcome the new disadvantages and includes e.g. change in land use, breeding and biotechnology applications, crop substitution and in farming systems (Alexandrov *et al.* 2002).

A change in planting dates in the future has already been considered in the crop simulations, as farmers already adapt to it autonomously. It can be interpreted as a free choice which can be made at the farm level. On the other hand, a major shift in sowing dates could compromise the agro-technical management of other crops that grow during the rest of the year (Alexandrov and Hoogenboom 2000). This aspect is not so relevant for the Marchfeld region: the sowing date for winter wheat would be later in autumn and more time would be available for other varieties and only intermediate crops are grown before spring barley.

By replacing in the 2035 scenario simulation ploughing with minimal tillage and direct cultivation, winter wheat yields of up to 3% (area-weighted average NCAR PCM) and spring barley yield of up to 4 % are in average enhanced (area-weighted average HadCM3). Especially on sandy and shallow soils (soil 1), minimum tillage can increase the yield potential by up to 10% for winter wheat and up to 6 % for spring barley (Fig 10) (Thaler *et al.* 2012; Eitzinger *et al.* 2013*b*).

(a)

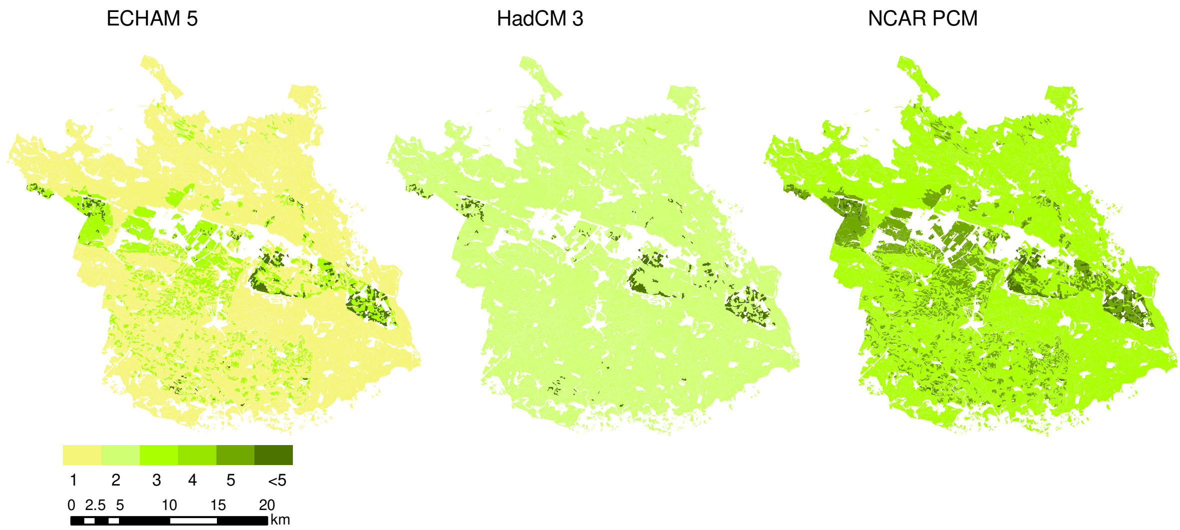

(b)

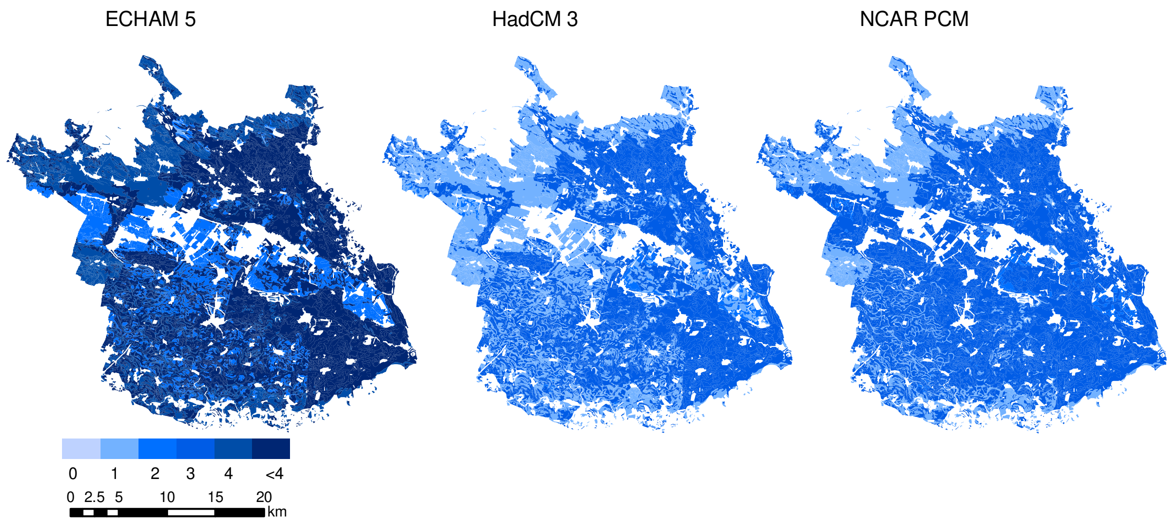

Figure 10. Relative change (%) of winter wheat yield (a) and spring barley yield (b) in 2035 (2021-2050) when ploughing would be replaced by minimum tillage in the Marchfeld region (source: Thaler et al. 2009)

Further technical adaptation structures were simulated in a next step only with winter wheat.

The effect of landscape structures such as hedgerows on wind reduction shows a positive effect on winter wheat yields through a reduction of evaporation losses. The ECHAM5 scenario shows the highest increases and the NCAR-PCM scenario the lowest. Soils 3 and 4, in particular, would benefit from a hedge with ploughing (Fig 11). In contrast to ploughing, a combination of minimum tillage with hedgerows would have the greatest impact on soils 1 and 2 with the lowest plant available water storage capacity. A yield increase between 4% (NCAR PCM) and 4.4% (ECHAM5) was simulated (for the area-weighted average) compared to reference management (not shown). In addition, a lower N leaching rate and a higher standard deviation were simulated (Thaler *et al.* 2012).

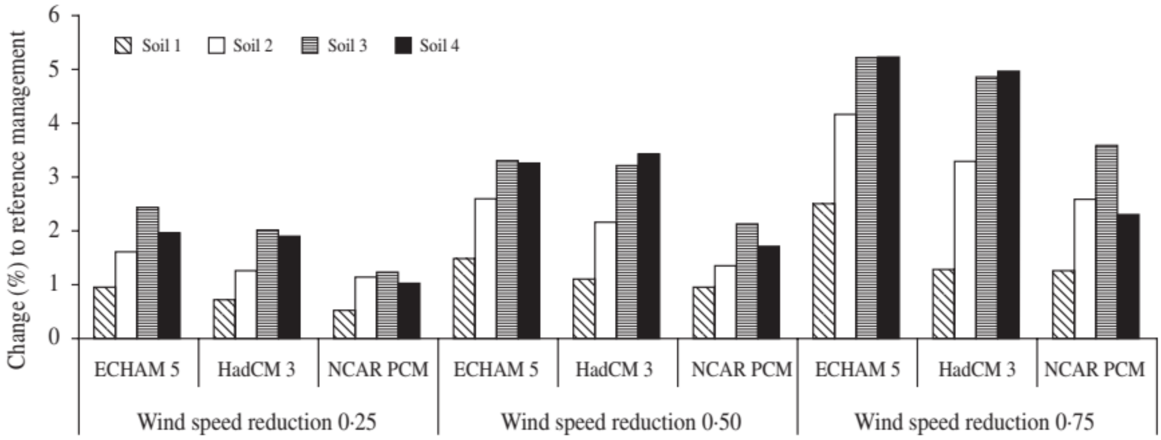

Figure 11. Relative changes (%) of winter wheat yield in 2035 (2021-2050) with average wind speed decreases of 25%, 50% and 75% due to hedges on ploughed fields compared to reference management (1961-1990) (source: Thaler et al. 2012)

The yield effect of an additional snow accumulation effect near hedgerows in connection with a wind speed reduction of 50% was simulated in a further step (only minimum tillage). In this scenario, the additional water input at the beginning of the crop growing period after snowmelt was taken into account. The results indicated a yield increase of 9% with ECHAM5 and 6% with HadCM3 (area-weighted average) in relation to the reference management. However, under these conditions, NCAR PCM predicted a yield loss of 1%, because this scenario predicts precipitation increases in spring (therefore lowering solar radiation and biomass accumulation) in contrast to the other scenarios. The results also show that the highest yield increase (and the lowest decrease, in the case of NCAR PCM) was simulated for soils 3 and 4 (Thaler *et al.* 2012).

Table 6. Changes of water demand (absolute in mm) across the various climate and management scenarios (2021-2050) against the baseline (1961-1990)

Management/Soil class	Plough	Minimum tillage	Plough+wind speed reduction 50%	Minimum tillage+wind speed reduction 50%	Minimum tillage+wind speed reduction 50%+snow retention
ECHAM 5					
Soil 1	11	12	2	4	-6
Soil 2	34	37	28	28	17
Soil 3	39	37	30	29	20
Soil 4	36	39	29	32	16
area-weighted average	*37*	*37*	*29*	*29*	*18*
HadCM3					
Soil 1	9	14	2	7	-3
Soil 2	33	34	27	29	20
Soil 3	38	37	31	29	21
Soil 4	33	39	29	30	19
area-weighted average	*36*	*37*	*29*	*29*	*20*
NCAR					
Soil 1	-8	-8	-14	-16	-27
Soil 2	2	4	-3	-5	-11
Soil 3	6	9	0	-3	-8
Soil 4	7	11	4	2	-7
area-weighted average	*6*	*8*	*0*	*-2*	*-8*

In order to answer the question of future water demand, the simulation option "automatic when required" for irrigation and water management was activated in the model. This new option was used to simulate the initial conditions as well as various climate and management scenarios. The ECHAM5 and HadCM3 scenarios led to similar results regarding the additional water demand: the highest additional water quantity due to climate change (up to 39 mm more water during the crop growing period) would be required for soils 3 and 4 (Tab 6). In the baseline scenario, soil 1 already showed relatively low yield potentials and a high water demand; additional irrigation would also not lead to better results due to the low water storage capacity connected with high leaching risk. Thus, soils with very low water storage capacity need only slightly more or less water in the applied climate scenarios to achieve a similar yield and irrigation is not a strong limiting factor rather than the low soil water storage capacity itself already under baseline conditions. An additional amount of 37 mm water (area-weighted average) during the crop growing period would be required to maintain the potential yield level according to ECHAM5 and HadCM3 in both tillage scenarios. Since the growing period of winter wheat would be shorter by about >10 days and about 7-8 months long due to higher temperatures, an average value of up to 37 mm more water demand is a considerable amount. NCAR PCM, the wettest scenario, predicted the lowest water demand of the future: 6 mm more for ploughed conditions and 8 mm more for minimum tillage. Hedges helped to reduce water requirements when wind speeds were expected to be reduced by 50 %, and additional snow cover would make the effect even more pronounced (Tab 6) (Thaler *et al.* 2012).

4.2 Influence of various spatial precipitation input data on the results of the crop model

4.2.1 Comparison of the different precipitation dataset

The two SM-based products $SM2R_{ASC}$ and RA_{ASC}, as well as the two satellite rainfall data sets TRMMRT and CMORPH were evaluated against $INCA_{23km}$ (benchmark) with respect to precipitation estimation (daily: Tab 7, monthly: Fig 12).

Table 7. Statistical characteristics (MAE, RMSE and r²) of daily rainfall differences $INCA_{23km}$ (benchmark) versus $SM2R_{ASC}$, RA_{ASC}, TRMMRT, CMORPH for the period March to July 2007-2015 in Groß-Enzersdorf, Hartberg and Kremsmünster (source: Thaler et al. 2018a)

	Groß-Enzersdorf				**Hartberg**				**Kremsmünster**			
	$SM2R_{ASC}$	RA_{ASC}	TRMMRT	CMORPH	$SM2R_{ASC}$	RA_{ASC}	TRMMRT	CMORPH	$SM2R_{ASC}$	RA_{ASC}	TRMMRT	CMORPH
MAE	1.67	2.31	1.86	1.75	2.8	2.97	2.37	2.11	3.04	3.69	2.88	2.75
RMSE	3.72	4.03	4.71	4.75	5.02	5.66	5.68	5.33	5.37	5.78	5.94	5.73
r^2	0.45	0.32	0.41	0.42	0.3	0.19	0.47	0.52	0.34	0.23	0.36	0.37

The lowest r^2 can be observed in RA_{ASC} daily and monthly precipitation data. However, RA_{ASC} is remarkable by high values at low precipitation periods and lower values in very humid months (Fig 12). The other three approaches, for the most part, show a good r^2 (up to 0.52 daily and 0.68 monthly) with $INCA_{23km}$. An exception is $SM2R_{ASC}$ in Kremsmünster, where it exhibits high differences and weak monthly performance results (r^2 = 0.18 and RMSE = 60mm). The two SM-based products have a low RMSE in Groß-Enzersdorf; at the other two locations, the RMSE differences between SM-based products and satellite precipitation data are noticeably lower (Tab 7, Fig 12).

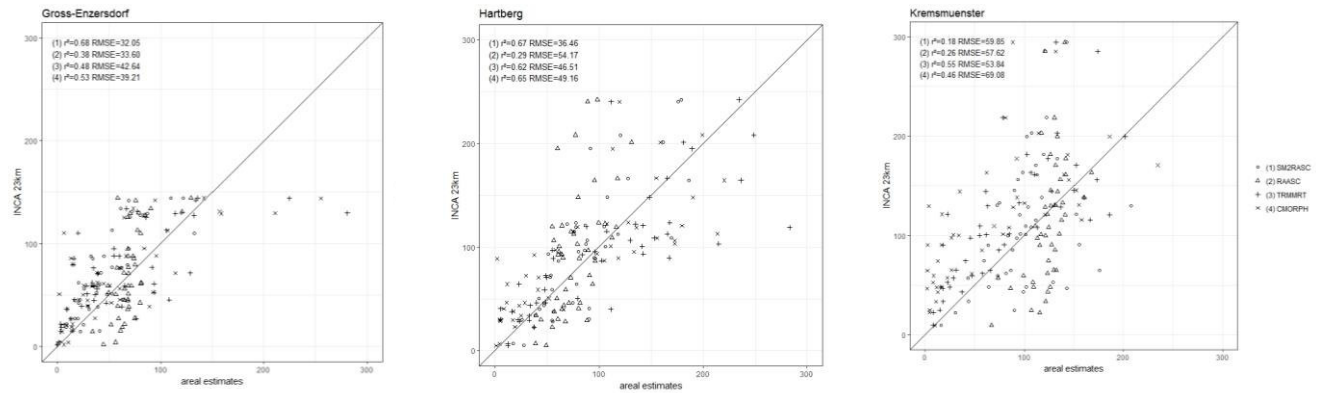

Figure 12. Monthly precipitation variations $INCA_{23km}$ (benchmark) versus $SM2R_{ASC}$, RA_{ASC}, TRMMRT, CMORPH for the period March to July 2007-2015 in (a) Groß-Enzersdorf, (b) Hartberg, (c) Kremsmünster (source: Thaler et al. 2018a)

4.2.2 Crop model response

The four different forcing variables of crop model precipitation input (2 SM-based products $SM2R_{ASC}$ and RA_{ASC}, 2 satellite precipitation data TRMMRT and CMORPH) were applied for simulating the yields of spring barley and winter wheat. These results were then evaluated against the benchmark ($INCA_{23km}$).

A detailed comparison of winter wheat and spring barley yields, estimated with $INCA_{23km}$ input data (benchmark), showed that none of the other precipitation data lead to a good fit to the simulated yields from the benchmark in all years (Tab 8). The analyses were performed for all soil types together (soils 1-4) and individually (soil 1, soil 2, soil 3, soil 4).

Table 8. Mean yield (kg/ha) with $INCA_{23km}$ input data and comparative statistics (RMSE, PBias, d, and r²) of model performance in simulated crop yield using $SM2R_{ASC}$, RA_{ASC}, TRMMRT and CMORPH precipitation inputs against $INCA_{23km}$ inputs for the three study areas: (a) winter wheat (b) spring barley (source: Thaler et al. 2018a)

(a) winter wheat

	Groß-Enzersdorf					**Hartberg**					**Kremsmünster**				
	soil 1-4	soil 1	soil 2	soil 3	soil 4	*soil 1-4*	soil 1	soil 2	soil 3	soil 4	*soil 1-4*	soil 1	soil 2	soil 3	soil 4
Mean yield (kg/ha) with $INCA_{23km}$ input data															
	5751	3276	5395	7290	7045	*5954*	3982	5982	7218	6633	*5523*	4226	5508	6355	6002
$SM2R_{ASC}$ - $INCA_{23km}$															
MAE	*838*	962	936	1035	419	*368*	546	319	353	251	*141*	272	35	145	111
RMSE	*1011*	1029	1060	1223	646	*516*	634	411	558	430	*223*	378	48	180	144
PBias %	*-13.1*	-19.5	-17.3	-14.2	-5.7	*-3.8*	-5.4	-2.9	-4.3	-3.1	*-1*	1.5	-0.5	-2.3	-1.9
d	*0.93*	0.82	0.71	0.61	0.69	*0.96*	0.82	0.71	0.78	0.85	*0.99*	0.95	1	0.91	0.95
r²	*0.87*	0.77	0.68	0.71	0.74	*0.89*	0.5	0.26	0.62	0.72	*0.95*	0.93	0.99	0.89	0.92
RA_{ASC} - $INCA_{23km}$															
MAE	*498*	826	698	351	116	*320*	804	215	88	174	*209*	397	60	190	188
RMSE	*818*	1221	961	493	141	*504*	929	303	110	223	*372*	660	65	245	228
PBias %	*5.6*	17	8.3	3.1	0.8	*-0.4*	-1.3	-1.3	-0.1	0.7	*-1*	4.2	-0.5	-3	-3.1
d	*0.94*	0.7	0.51	0.73	0.96	*0.96*	0.4	0.88	0.98	0.93	*0.95*	0.79	0.99	0.83	0.87
r²	*0.84*	0.52	0.01	0.43	0.87	*0.86*	0.01	0.69	0.95	0.77	*0.88*	0.5	0.97	0.75	0.86
TRMMRT - $INCA_{23km}$															
MAE	*568*	984	616	406	265	*136*	234	92	129	89	*241*	535	220	89	122
RMSE	*909*	1430	836	582	470	*194*	300	129	181	106	*426*	725	416	102	135
PBias %	*-4.2*	-14.3	-4.7	-2.3	-1.3	*-0.9*	-1.1	-0.3	-1.6	-0.7	*-2.3*	-12.1	-3.3	0.8	2
d	*0.94*	0.7	0.68	0.86	0.79	*0.99*	0.96	0.98	0.96	0.98	*0.96*	0.83	0.78	0.98	0.96
r²	*0.8*	0.25	0.19	0.79	0.79	*0.98*	0.85	0.92	0.92	0.97	*0.89*	0.68	0.59	0.95	0.97
CMORPH - $INCA_{23km}$															
MAE	*917*	1600	932	762	377	*496*	1318	288	276	102	*741*	1984	657	154	169
RMSE	*1253*	1853	1022	1081	794	*805*	1462	386	539	138	*1174*	2151	888	251	178
PBias %	*-12.6*	-35.5	-17.3	-8.2	-3.1	*-6.9*	-30.9	-4.8	-2.2	0.3	*-11.5*	-46.9	-11.7	-1.4	2.8
d	*0.9*	0.5	0.71	0.71	0.65	*0.93*	0.5	0.84	0.78	0.97	*0.81*	0.43	0.43	0.9	0.93
r²	*0.78*	0.1	0.74	0.73	0.76	*0.9*	0.32	0.75	0.52	0.91	*0.77*	0.23	0.12	0.84	0.97

(b) spring barley

	Groß-Enzersdorf					**Hartberg**					**Kremsmünster**				
	soil 1-4	soil 1	soil 2	soil 3	soil 4	*soil 1-4*	soil 1	soil 2	soil 3	soil 4	*soil 1-4*	soil 1	soil 2	soil 3	soil 4
Mean yield (kg/ha) with $INCA_{23km}$ input data															
	4727	3118	4444	5644	5701	*5111*	4056	5078	5779	5532	*4451*	3654	4451	4890	4810
$SM2R_{ASC}$ - $INCA_{23km}$															
MAE	*512*	719	532	488	307	*215*	352	270	127	111	*144*	237	58	139	142
RMSE	*633*	803	618	655	384	*369*	582	396	168	149	*220*	319	64	214	203
PBias %	*-9.1*	-23	-10.8	-7.8	-1.6	*-3.2*	-7.6	-4.6	-1.2	-0.7	*-0.9*	3.5	-0.5	-2.8	-2.9
d	*0.94*	0.75	0.69	0.69	0.67	*0.95*	0.49	0.71	0.98	0.97	*0.95*	0.72	0.98	0.86	0.87
r²	*0.89*	0.76	0.49	0.35	0.18	*0.87*	0.26	0.43	0.93	0.89	*0.87*	0.31	0.95	0.69	0.73
RA_{ASC} - $INCA_{23km}$															
MAE	*374*	449	525	318	202	*235*	509	148	149	136	*219*	304	102	222	246
RMSE	*544*	679	691	427	250	*343*	615	198	157	173	*275*	355	126	276	290
PBias %	*7*	12.2	11.5	4.9	2.5	*-1.7*	-11.4	-0.8	0.7	2	*-3.2*	-0.3	-2.1	-4.5	-5.1
d	*0.94*	0.67	0.47	0.76	0.87	*0.96*	0.39	0.94	0.98	0.96	*0.93*	0.45	0.93	0.78	0.77
r²	*0.86*	0.41	0.04	0.52	0.68	*0.92*	0.12	0.83	0.93	0.91	*0.84*	0.07	0.88	0.68	0.7
TRMMRT - $INCA_{23km}$															
MAE	*385*	556	466	310	209	*135*	101	161	170	111	*254*	401	220	206	189
RMSE	*506*	691	593	351	267	*174*	131	206	201	147	*340*	515	334	215	197
PBias %	*6.3*	10.8	7.9	5.2	3.6	*-1.8*	-1.2	-2.1	-1.8	-1.8	*0.3*	-3.6	-2.1	2.5	3.4
d	*0.95*	0.81	0.68	0.86	0.86	*0.99*	0.94	0.94	0.97	0.97	*0.93*	0.5	0.67	0.89	0.91
r²	*0.88*	0.51	0.33	0.83	0.76	*0.96*	0.8	0.84	0.91	0.94	*0.79*	0.14	0.18	0.78	0.93
CMORPH - $INCA_{23km}$															
MAE	*350*	537	259	296	309	*166*	272	160	146	85	*405*	581	497	286	255
RMSE	*431*	599	327	361	386	*277*	428	275	193	109	*602*	904	670	333	265
PBias %	*-2.7*	-14.8	-2.2	-0.8	1.8	*-0.9*	-4.3	-1.6	0.9	0.5	*-3.1*	-11.9	-9.6	1	5.3
d	*0.97*	0.83	0.88	0.85	0.68	*0.97*	0.55	0.9	0.97	0.98	*0.82*	0.25	0.34	0.75	0.82
r²	*0.92*	0.73	0.68	0.53	0.17	*0.91*	0.15	0.71	0.9	0.95	*0.62*	0.04	0.01	0.37	0.93

The yield variation of the two crops, winter wheat and spring barley, due to different precipitation input data shows similar behavior.

In Groß-Enzersdorf, the driest location, the various types of precipitation inputs caused the greatest deviations in simulated crop grain yield, with sandy soils (soil 1: $RMSE_{winter\ barley}$ up to 1800 kg/ha and $RMSE_{spring\ barley}$ > 600kg/ha) being more sensitive than moderately finely structured soils with higher plant available water storage capacity (soil 3 and 4) (Tab 8). $SM2R_{ASC}$ precipitation inputs generally lead to the highest MAE (soil 1-4 = 512 kg/ha) and RMSE (soil 1-4 = 633 kg/ha) values for spring barley, while CMORPH had the lowest (soil 1-4 = 431 kg/ha). It is also noticeable that $SM2R_{ASC}$ and CMORPH precipitation inputs underestimate the barley yield (negative PBias), while RA_{ASC} and TRMMRT input data shows a positive PBias. For winter wheat, $SM2R_{ASC}$, TRMMRT, and CMORPH based precipitation inputs largely underestimate yields, while RA_{ASC} presents positive PBias. All in all, RA_{ASC} shows the strongest performances with high d (soil 1-4 = 0.94) and r^2 values (soil 1-4 = 0.84), respectively and the lowest RMSE (soil 1-4 = 818 kg/ha) (Tab 8) (Thaler *et al.* 2018*a*).

In the more humid areas Hartberg and Kremsmünster, lower yield differences were simulated for all precipitation inputs – in particular for soils 3 and 4. It can be seen that the RMSE values at these two sites are about half as high as in Groß-Enzersdorf. TRMMRT precipitation inputs lead to very low MAE and RMSE values of crop grain yield in Hartberg (soil 1-4: $MAE_{winter\ wheat}$ = 136 kg/ha; $RMSE_{winter\ wheat}$ = 194 kg/ha; $MAE_{spring\ barley}$ = 135 kg/ha; $RMSE_{spring\ barley}$ = 174 kg/ha) and the highest r^2 (soil 1-4: $r^2_{winter\ wheat}$ = 98%; $r^2_{spring\ barley}$ = 96%) as well as d (soil 1-4: d = 0.99) (Tab 8). CMORPH, on the other hand, shows the greatest difficulties in yield simulation, especially in Kremsmünster for spring barley. All four precipitation data showed a yield underestimation (negative PBias) for winter wheat (all soils) and for spring barley soil 1 and 2, while soil 3 and 4 did not show such a clear trend (Thaler *et al.* 2018*a*). One reason is that other yield-limiting factors than water availability dominates in the more humid conditions.

5 Discussion and conclusion

The execution of agricultural field experiments is time-consuming and cost-intensive. They require considerable investment in infrastructure and organization. These resources are not always available for various reasons. Computer-aided simulation models for crop growth have therefore been developed since the 1960s from very simple descriptive models to complex process-based models. With their help, field experiments cannot be replaced, but they can be reduced or an extended set of variables can be analysed. The models are interdisciplinary and integrate a comprehensive knowledge of crop physiological and physical-ecological processes.

Therefore, crop growth simulation models are increasingly used as tools to assess regional impacts on crop production and related adaptation options under different environmental conditions, such as climate change and management options. The impact model results are strongly influenced by the results of climate models (climate scenarios used as input) in terms of quality, spatial representation, and uncertainty. In agriculture and food production, dynamic crop models have established themselves as tools for estimating e.g. the impacts of climate change on different scales (White *et al.* 2011). For example, in the report of Eitzinger *et al.* 2013*b*, a large-scale study for Central Europe reveals significant regional variations in the effects of changing climate on crop yields, as simulated by crop growth models. Similar to the climate models, the crop models themselves also can provide distinctly to the uncertainty in predicting the effects of a changing climate on crop yields (Angulo *et al.* 2013; Asseng *et al.* 2013; Eitzinger *et al.* 2013*a*). Nevertheless, the transferability of uncertainties in the selection of crop models to other regions with higher spatial heterogeneity under weather conditions as well as different soil and plant management data requires a stronger assessment (Angulo *et al.* 2013). The spatial resolution of daily weather data and other inputs on crop models (e.g. soil properties) is a central topic for regional climate change impact assessments and the development of adaptation options, where different scales can be considered depending on the application (Zhao *et al.* 2015). In particular, representative weather data with high spatial resolution are required at the local level, as is necessary for the development of custom farm-based adaptation possibilities in agriculture (APCC 2014), in order to reduce uncertainties through the modelling chain to the agro-economic level

(Schönhart *et al.* 2014). Rezaei *et al.* (2015*c*) reported that an aggregation of weather and soil input data led to lower spatial variability and lower severity of simulated stress events, especially for regions with high heterogeneity in weather and soil conditions. This confirms that climate-induced stress events in crops are more sensitive to spatial resolution (due to small-scale orographic effects) than mean climatic conditions.

Initially, the crop models have to be calibrated using measured accurate data sets to reduce parameter uncertainty related to the biophysical conditions of application (Asseng *et al.* 2013; Rötter *et al.* 2011*b*; Yin *et al.* 2017). Earlier studies have demonstrated that model calibration with appropriate observation data can enhance the accuracy of model predictions (e.g. Asseng *et al.* 2013). In our studies, we used data of winter wheat and spring barley from experimental sites to calibrate and validate both cultivars (Rischbeck 2007; Thaler *et al.* 2012; Eitzinger *et al.* 2013*a*), which subsequently were used for further analyses.

In the first two studies, an ensemble of climate change scenarios was used to point out local crop growth-limiting factors and potential crop yield changes in the Marchfeld region. With the help of the ensemble, it was possible to cover the most probable range of expected upcoming impacts.

For both winter wheat and spring barley, it is clear that shorter growing seasons due to higher temperatures until 2035 will lead to yield losses for currently used crop cultivars under the applied climate change scenarios (with the exception of the NCAR scenario, which involves an increase in precipitation). Thus, a decline in spring and summer precipitation in the climate scenarios is also a main yield reduction factor for this semi-arid region. Due to the limited availability of crop water, the yield reductions would be even more pronounced without the assumed CO_2 fertilizer effect (Amthor 2001). However, the degree of this last mention effect is uncertain from the estimates of the crop model and differs between crops and varieties (Tubiello *et al.* 1999; Tubiello and Ewert 2002; Wolf *et al.* 2002; Kersebaum and Nendel 2014). Additionally, the effects of direct heat stress are expected to create further yield risks and is only partially integrated into the models (Semenov and Shewry 2011), while others such as ozone effects on stomata function are not considered, such as in DSSAT.

The Marchfeld study showed that, due to the increased water demand, additional irrigation of about 30-40 mm would be necessary to maintain the current yield under the drier scenarios as these crops are not irrigated under the current conditions. However, additional water input may increase the risk of nitrate leaching rates (e.g. by uncertain precipitation forecasts), especially on sandy soils, which reduces the positive effects on yield. An adaptation method that could be used to improve the available soil water storage capacity is to change the tillage method (in the present study a change from ploughing to minimum tillage was investigated), which leads to higher simulated soil water contents and yields due to higher soil water capacity with minimum tillage. Hedges (by their windbreak effect leading to reduced evaporation rates) would also have a positive effect on soil water content (Thaler *et al.* 2012; Eitzinger *et al.* 2013*b*).

More recent climate change models, e.g. the ÖKS15, show a much lower precipitation reduction in spring and early summer in Austria and it can be assumed that yields of winter wheat and spring barley will also increase in the semi-arid regions of Austria due to higher atmospheric CO_2 and temperatures as well as more humid soil conditions in the spring months (Chimani *et al.* 2019). However, summer crops such as maize are differently affected as the reduction in summer precipitation and higher temperatures are clearly indicated in the ÖKS scenarios as well. It is expected that the yields from grain maize will decrease if there is no adaptation with the help of e.g. later ripening cultivars and irrigation.

For regional studies, crop models require spatially and temporally detailed input data of weather, soil, crop cultivation, and cultivars, which are usually difficult to obtain in good quality for larger areas (Angulo *et al.* 2013). Since weather data are restricted to a limited number of meteorological stations covering a region, it is important to assess the necessary weather inputs for the relevant simulation size (Faivre *et al.* 2004). The focus of the third study was therefore on deriving daily precipitation data from alternative sources, as these are the most important uncertain parameters for crop growth. Crop models (mimicking crops grown under water limiting conditions) are very sensitive to soil water, as soil moisture is a potential limiting factor for different processes of plant growth and harvest (see above yield effects of climate change). Here, satellite rainfall estimations can be a useful tool as alternative to ground-based measurements, which offers global coverage data and information in regions lacking data from other sources.

In the semi-arid region Groß-Enzersdorf winter wheat and spring barley simulations are very sensitive to various precipitation model inputs, particularly in light textured (sandy) soils.

This is because the availability of soil water under drought-prone conditions is a more dominant limiting growth factor. Thus, small differences in the amount of precipitation can strongly influence the simulated yield. Also, a missing precipitation event in a critical development phase can lead to crop failure or reduction (Thaler *et al.* 2018*a*).

In the more humid locations, Hartberg and Kremsmünster all four alternatives (remote sensing based) precipitation inputs led to good results. Crop drought stress does not occur so often and can be observed especially on sandy soils. A distortion of the precipitation sum is not so decisive here; a prediction of the event is much more important. Winter wheat and spring barley show similar yield forecasts at both locations (Thaler *et al.* 2018*a*).

The weakest results at all three sites and for both crops were determined using CMORPH based precipitation input data. The general underestimation of precipitation by CMORPH is reliable with the results of Stampoulis and Anagnostou (2012), who evaluated the quality of this product for Europe.

A closer look at the estimated precipitation of SM shows that $SM2R_{ASC}$ and RA_{ASC} perform well in this research, notably on light soils at the more humid sites of Kremsmünster and Hartberg versus the two satellite precipitation data. Here, for example, the use of information on the spatial-temporal variability of topsoil moisture could improve the spatial yield simulation of crops compared to the use of single point information for individual weather stations for a given area. Consequently, estimates from SM data ($SM2R_{ASC}$, RA_{ASC}) for agricultural applications in regions may be alternative when the precipitation data are adapted to their local climatic conditions and other weather data are not available. In addition, a remote sensing product need not at all be "better" than the crop growth model. Consideration should be given to whether the data provide added value or new information. Even if, for example, the r^2 values are lower than for models, clever data assimilation techniques can be made to use the data (see e.g. Draper *et al.* 2012).

The Sentinel 1 mission, launched in 2014, offers new perspectives with the use of Synthetic Aperture Radars (SAR). High-resolution radar images are routinely available at a scale of 20 meters, with a high frequency of revisits of 3-6 days and excellent radiometric accuracy. The TU Vienna developed SSM (Surface Soil Moisture) retrieval on a scale of 1 km with a temporal revisit time of 3 to 8 days (depending on location) (Bauer-Marschallinger *et al.* 2017).

Since the 25 km derived precipitation data of SM products have already delivered partly good results, the new high resolutions of SM data offer a new possibility for linking with crop growth models.

Improved spatial information on land surface characteristics is required to enhance performance related to spatial applications and assessments, for example, to better take into consideration the spatial variability of natural production conditions (e.g. soils, water availability, microclimate, etc.). Here, satellite data, the resolution of which is becoming more and more accurate (see Sentinel) and the use of complementary data sets from remote sensing sources, play a decisive role. This information combined with crop growth models, preferentially crop growth ensembles, have a great potential to reduce model uncertainties and can create an important contribution to agricultural applications and decision support tools, especially under water-limit production conditions, which encounter more and more frequently in Austria.

6 References

Abou-Ismail, O. (2004). Rice yield estimation by integrating remote sensing with rice growth simulation model. *Pedosphere* **14**, 519-526.

AG Boden (1994). *Bodenkundliche Kartieranleitung. 4.te Auflage*. Bundesanstalt für Geowissenschaften und Rohstoffe: Hannover, Germany.

Albertz, J. (2016). *Einführung in die Fernerkundung. Grundlagen der Interpretation von Luft- & Satellitenbildern, 5.te Auflage*. wbg Academic: Darmstadt, Germany.

Alexandrov, V.A. and Hoogenboom, G. (2000). The impact of climate variability and change on crop yield in Bulgaria. *Agricultural and Forest Meteorology* **104**, 315-327.

Alexandrov, V.A., Eitzinger, J., Cajic, V. and Oberforster, M. (2002). Potential impact of climate change on selected agricultural crops in north-eastern Austria. *Global Change Biology* **8**, 372-389.

Allen, R.G., Pereira, L.S., Raes, D. and Smith, M. (1998). *Crop Evapotranspiration: Guidelines for Computing Crop Water Requirements*. FAO Irrigation and Drainage Paper 56. FAO: Rome, Italy.

Amthor, J.S. (2001). Effects of atmospheric CO_2 concentration on wheat yield: review of results from experiments using various approaches to control CO_2 concentration. *Field Crops Research* **73**, 1-34.

Angulo, C., Gaiser, T., Rötter, R.P., Borgesen, C.D., Hlavinka, P., Trnka, M. and Ewert, F. (2014). 'Fingerprints' of four crop models as affected by soil input data aggregation. *European Journal of Agronomy* **61**, 35-48.

APCC (2014). *Österreichischer Sachstandsbericht Klimawandel 2014 (AAR14). Austrian Panel on Climate Change (APCC).* Verlag der Österreichischen Akademie der Wissenschaften: Wien, Austria.

Asseng, S., Ewert, F., Rosenzweig, C., Jones, J.W., Hatfield, J.L., Ruane, A., Boote, K.J., Thorburn, P., Rötter, R.P., Cammarano, D., Brisson, N., Basso, B., Martre, P., Aggarwal, P.K., Angulo, C., Bertuzzi, P., Biernath, C., Challinor, A., Doltra, J., Gayler, S., Goldberg, R., Grant, R., Heng, L., Hooker, J., Hunt, T., Ingwersen, J., Izaurralde, C., Kersebaum, K.C., Müller, C., Naresh Kumar, S., Nendel, C., O'Leary, G., Olesen, J.E., Osborne, T.M., Palosuo, T., Priesack, E., Ripoche, D., Semenov, M., Shcherbak, I., Steduto, P., Stöckle, C., Stratonovitch, P., Streck, T., Supit, I., Tao, F.L., Travasso, M., Waha, K., Wallach, D., White, J., Williams, J.R. and Wolf, J. (2013). Uncertainty in simulating wheat yields under climate change. *Nature Climate Change* **3**, 827-832.

Asseng, S., Ewert, F., Martre, P., Rötter, R.P., Lobell, D.B., Cammarano, D., Kimball, B.A., Ottman, M.J., Wall, G.W., White, J.W., Reynolds, M.P., Alderman, P.D., Prasad, P.V.V., Aggarwal, P.K., Anothai, J., Basso, B., Biernath, C., Challinor, A., De Sanctis, G., Doltra, J., Fereres, E., Garcia-Vila, M., Gayler, S., Hoogenboom, G., Hunt, T., Izaurralde, C., Jabloun, M., Jones, C.D., Kersebaum, K.C., Koehler, A.-K., Müller, C., Naresh Kumar, S., Nendel, C., O'Leary, G., Olesen, J.E., Palosuo, T., Priesack, E., Eyshi Rezaei, E., Ruane, A.C., Semenov, M., Shcherbak, I., Steduto, P., Stöckle, C., Stratonovitch, P., Streck, T., Supit, I., Tao, F., Thorburn, P., Waha, K., Wang, E., Wallach, D., Wolf, J., Zhao, Z. and Zhu, Y. (2015). Rising heat reduces global wheat production. *Nature Climate Change* **5**, 143-147.

Bardini, R., Politano, G., Benso, A. and Di Carlo, S. (2017). Multi-level and hybrid modelling approaches for systems biology. *Computational and Structural Biotechnology Journal* **15**, 396-402.

Batchelor, W.D., Jones, J.W. and Boote, K.J. (1993). Extending the use of crop models to study pest damage. *Transactions of the American Society of Agricultural Engineers* **36**, 551-558.

Barlow, K.M., Christy, B.P., O'Leary, G.J., Riffkin, P.A. and Nuttall J.G. (2015). Simulating the impact of extreme heat and frost events on wheat crop production: a review. *Field Crops Research* **171**, 109-119.

Bastiaanssen, W.G.M. and Ali, S. (2003). A new crop yield forecasting model based on satellite measurements applied across the Indus Basin, Pakistan. *Agriculture, Ecosystems & Environment* **94**, 321–340.

Battisti, R., Parker, P.S., Sentelhas, P.C. and Nendel, C. (2017). Gauging the sources of uncertainty in soybean yield simulations using the MONICA model. *Agricultural Systems* **155**, 9-18.

Bauer, M.E. (1985). Spectralinputs to crop identification and condition assessment. *Proc. IEEE* **73**, 1071–1085.

Bauer-Marschallinger, B., Cao, S., Schaufler, S. Paulik, C., Naeimi, V. and Wagner, W. (2017). *1km Soil Moisture from Downsampled Sentinel-1 SAR Data: Harnessing Assets and Overcoming Obstacles*. 19th EGU General Assembly, EGU2017, proceedings from the conference held 23-28 April, 2017 in Vienna, Austria.

Bhatia, A. (2014). Crop Growth Simulation Modeling. In Basu, S. and Kumar N. (Eds.). *Modelling and Simulation of Diffusive Processes. Simulation Foundations, Methods and Applications*. Springer International Publishing: Switzerland, 315-332.

Blackman, V.H. (1919). The compound interest law and plant growth. *Annals of Botany* **33**, 353-360.

BMNT - Bundesministerium für Nachhaltigkeit und Tourismus (2018). Grüne Bericht Österreich. Available: https://gruenerbericht.at/cm4/jdownload/category/2-gr-bericht-terreich (01.04.2019).

Boote, K.J., Jones, J.W., Mishoe, J.W. and Berger, R.D. (1983). Coupling pests to crop growth simulators to predict yield reductions. *Phytopathology* **73**, 1581-1587.

Boote, K.J., Jones, J.W., Mishoe, J.W. and Wilkerson, G.G. (1986). Modeling growth and yield of groundnut. *Agrometeorology of Groundnut: Proceedings of an International Symposium*, 21–26 Aug 1985, ICRISAT Sahelian Center, Niamey, Niger. ICRISAT, Patancheru, A.P. 502 324, India, 243–254.

Boote, K.J., Jones, J.W. and Pickering, N.B. (1996). Potential uses and limitations of crop models. *Agronomy Journal* **88**, 704–716.

Boote, K.J., Jones, J.W., Hoogenboom, G. and Pickering, N.B. (1998). The CROPGRO model for grain legumes. In Tsuji, G.Y., Hoogenboom, G. and Thornton, P.K. (Eds.). *Understanding Options for Agricultural Production*. Kluwer Academic Publishers: Dordrecht, The Netherlands, 99-128.

Boote, K.J., Allen Jr., L.H., Vara Prasad, P.V. and Jones, J.W. (2010). Testing effects of climate change in crop models. In Hillel, D. and Rosenzweig, C. (Eds.). *Handbook of Climate Change and Agroecosystems*. Imperial College Press: London, UK, 109-129.

Bouman, B.A.M. (1995). Crop modelling and remote sensing for yield prediction. *NJAS Wageningen J. Life Sci.* **43**, 143-161.

Bouman, B.A.M., van Keulen, H., van Laar, H.H. and Rabbinge, R. (1996). The 'school of de wit' crop growth simulation models: a pedigree and historical overview. *Agricultural Systems* **52**, 171-198.

Bouman, B.A.M., Kropff, M.J., Tuong, T.P., Woperies, M.C.S. and van Laar, H.H. (2001). *ORYZA 2000: Modeling Lowland Rice*. International Rice Research Institute and Wageningen University and Research Center: Wageningen, The Netherlands.

Brisson, N., Gary, C., Justes, E., Roche, R., Mary, B., Ripoche, D., Zimmer, D., Sierra, J., Bertuzzi, P., Burger, P., Bussiére, F., Cabidoche, Y.-M., Cellier, P., Debaeke, P., Gaudillére, J.-P., Hénault, C., Maraux, F., Seguin, B. and Sinoquet, H. (2003). An overview of the crop model STICS. *European Journal of Agronomy* **18**, 309-332.

Brocca, L., Moramarco, T., Melone, F. and Wagner, W. (2013). A new method for rainfall estimation through soil moisture observations. *Geophysical Research Letters* **40**, 853-858.

Brocca, L., Ciabatta, L., Massari, C., Moramarco, T., Hahn, S., Hasenauer, S., Kidd, R., Dorigo, W., Wagner, W. and Levizzani, V. (2014). Soil as a natural rain gauge: Estimating global rainfall from satellite soil moisture data. *Journal of Geophysical Research Atmospheres* **119**, 5128-5141.

Brouwer, R. and Wit, C.T. de (1968). *A simulation model of plant growth with special attention to root growth and its consequences*. IBS: Wageningen, The Netherlands.

Brown C.W., Connor L.N., Lillibridge J.L., Nalli N.R. and Legeckis R.V. (2007). An Introduction to Satellite Sensors, Observations and Techniques. In: Miller R.L., Del Castillo C.E. and Mckee B.A. (Eds.). *Remote Sensing of Coastal Aquatic Environments. Remote Sensing and Digital Image Processing, vol 7*. Springer: Dordrecht, The Netherlands, 21-50.

Burrough, P.A. (1996). Environmental modelling with geographical information system. In Stein, A., Penning de Vries, F.W.T. and Schotman, P.J. (Eds.). *Models in Action, Quantitative Approaches in Systems Analysis*. No 6, AB-DLO: Wageningen, The Netherlands, 56-59.

Campbell, J.B. and Wynne, R.H. (2011). *Introduction to Remote Sensing, Fifth Edition*. The Guilford Press: New York, USA.

Challinor, A. (2011). Agriculture: forecasting food. *Nature Climate Change* **1**, 103-104.

Challinor, A.J., Watson, J., Lobell, D.B., Howden, S.M., Smith, D.R. and Chetri, N. (2014). A meta-analysis of crop yield under climate change and adaptation. *Nature Climate Change* **4**, 287-291.

Chenu, K., Porter, J.R., Martre, P., Basso, B., Chapman, S.C., Ewert, F., Bindi, M. and Asseng, S. (2017). Contribution of Crop Models to Adaptation in Wheat. *Trends in Plant Science* **22**, 472-490.

Chimani, B., Matulla, C., Eitzinger, J., Gorgas-Schellander, T., Hiebl, J., Hofstätter, M., Kubu, G., Maraun, D., Mendlik, T. and Thaler, S. (2019). *Guideline zur Nutzung der ÖKS15-Klimawandelsimulationen sowie der entsprechenden gegitterten Beobachtungsdatensätze*. Ergebnisse des ACRP-Projektes „STARC-Impact“ (“Supporting the Austrian Research Community in using recent Climate Change Projections for Climate Impact Studies“, KR15AC8K12604): Vienna, Austria.

Clevers, J., Büker, C., Van Leeuwen, H. and Bouman, B. (1994). A framework for monitoring crop growth by combining directional and spectral remote sensing information. *Remote Sensing of Environment* **50**, 161-170.

Clevers, J.G.P.W. (1997). A simplified approach for yield prediction of sugar beet based on optical remote sensing data. *Remote Sensing of Environment* **61**, 221–228.

Clevers, J., Vonder, O., Jongschaap, R., Desprats, J.F., King, C., Prévot, L. and Bruguier, N. (2002). Using SPOT data for calibrating a wheat growth model under mediterranean conditions. *Agronomie* **22**, 687-694.

Dadhwal, V.K. (2003). *Crop growth and productivity monitoring and simulation using remote sensing and GIS.* Satellite Remote Sensing and GIS Applications in Agricultural Meteorology, Proceedings of a Training Workshop held 7-11 July 2003 in Dehra Dun, India, 263-289.

Dente, L., Satalino, G., Mattia, F. and Rinaldi, M. (2008). Assimilation of leaf area index derived from ASAR and MERIS data into CERES-Wheat model to map wheat yield. *Remote Sensing of Environment* **112**, 1395-1407.

de Wit, A.J.W., Boogaard, H.L. and van Diepen, C.A. (2005). Spatial resolution of precipitation and radiation: the effect on regional crop yield forecasts. *Agricultural and Forest Meteorology* **135**, 156-168.

de Wit, C.T. (1958). *Transpiration and Crop Yields*. Versl. Landbouwk. Onderz. 64. 6. Inst Biol. Chem. Res. Fid Crops and Hbge: Wageningen, The Netherlands.

de Wit, C.T. (1965). *Photosynthesis of leaf canopies*. Agricultural Research Report No. 663 PUDOC: Wageningen, The Netherlands.

de Wit, C.T. (1967). *Photosynthesis: its relationship to overpopulation*. IMC-symposium Chicago, l966: Harvesting the Sun Ac.Press: New York, USA, 315-320.

de Wit, C.T. (1970). Dynamic concepts in biology. *Proceedings International Biological Program/Plant Production Technical Meeting, Prediction and management of photosynthetic productivity*, Trebon, PUDOC: Wageningen, The Netherlands, 17-23.

de Wit, C.T., Brouwer, R. and Penning de Vries, F.W.T. (1970). *The simulation of photosynthetic systems*. Proceedings of the IBP/PP technical meeting, Trebon, 14-21 September 1969. PUDOC: Wageningen, The Netherlands, 47-70.

de Wit, C.T. and Goudriaan, J. (1978). *Simulation of assimilation, respiration and transpiration of crops*. Simulation monograph. PUDOC: Wageningen, The Netherlands.

Delécolle, R. Maas, S. J. Guérif, M. and Baret, F. (1992). Remote sensing and crop production models: present trends. *ISPRS Journal of Photogrammetry and Remote Sensing* **47**, 145-161.

Dong, Y., Zhao, C., Yang, G., Chen, L., Wang, J. and Feng, H. (2013). Integrating a very fast simulated annealing optimization algorithm for crop leaf area index variational assimilation. *Mathematical and Computer Modelling* **58**, 877-885.

Doraiswamy, P.C., Hatfield, J.L., Jackson, T.J., Akhmedov, B., Prueger, J. and Stern, A. (2004). Crop condition and yield simulations using Landsat and MODIS. *Remote Sensing of Environment* **92**, 548–559.

Dorigo, W.A., Zurita-Milla, R., de Wit, A.J., Brazile, J., Singh, R. and Schaepman, M.E. (2007). A review on reflective remote sensing and data assimilation techniques for enhanced agroecosystem modeling. *International Journal of Applied Earth Observation and Geoinformation* **9**, 165–193.

Draper, C.S., Reichle, R.H., De Lannoy, G.J.M. and Liu, Q. (2012). Assimilation of passive and active microwave soil moisture retrievals. *Geophysical Research Letters* **39**, L04401.

Dubrovski, M. (1997). Creating daily weather series with use of the weather generator. *Environmetrics* **8**, 409–424.

Dubrovsky, M., Zalud, Z. and Stastna, M. (2000). Sensitivity of CERES-Maize yields to statistical structure of daily weather series. *Climatic Change* **46**, 447–472.

Dubrovsky, M., Buchtele, J. and Zalud, Z. (2004). Highfrequency and low-frequency variability in stochastic daily weather generator and its effect on agricultural and hydrologic modelling. *Climatic Change* **63**, 145–179.

Dubrovsky, M., Svoboda, M.D., Trnka, M., Hayes, M.J., Wilhite, D.A., Zalud, Z. and Hlavinka, P. (2008). Application of relative drought indices in assessing climate-change impacts on drought conditions in Czechia. *Theoretical and Applied Climatology* **96**, 155–171.

Duncan, W.G., Loomis, R.S., Williams, W.A. and Hanau, R. (1967). A model for simulating photosynthesis in plant communities. *Hilgardia* **38**, 181-205.

Duncan, W.G. (1972). SIMCOT: a simulation of cotton growth and yield. In Murphy, C.M. (Ed.). *Proceedings of a Workshop for Modeling Tree Growth*, Duke University: Durham, North Carolina, USA, 115-118.

Eitzinger, J., Trnka, M., Hösch, J., Zalud, Z. and Dubrovsky, M. (2004). Comparison of CERES, WOFOST and SWAP models in simulating soil water content during growing season under different soil conditions. *Ecological Modelling* **171**, 223–246.

Eitzinger, J., Formayer, H., Thaler, S., Trnka, M., Zdenek, Z. and Alexandrov, V. (2008). Results and uncertainties of climate change impact research in agricultural crop production in Central Europe. *Die Bodenkultur* **59**, 131–147.

Eitzinger, J., Thaler, S., Schmid, E., Strauss, F., Ferrise, R., Moriondo, M., Bindi, M., Palosuo, T., Rotter, R., Kersebaum, K.C., Olesen, J.E., Patil, R.H., Saylan, L., Caldag, B. and Caylak, O. (2013*a*). Sensitivities of crop models to extreme weather conditions during flowering period demonstrated for maize and winter wheat in Austria. *The Journal of Agricultural Science* **151**, 813–835.

Eitzinger, J., Trnka, M., Semerádová, D., Thaler, S., Svobodová, E., Hlavinka, P., Siska, B., Takác, J., Malatinská, L., Nováková, M., Dubrovsky, M. and Zalud, Z. (2013*b*). Regional climate change impacts on agricultural crop production in Central and Eastern Europe—hotspots, regional differences and common trends. *The Journal of Agricultural Science* **151**, 787-812.

Elachi, C. and van Zyl, J. (2006). *Introduction to the Physics and Techniques of Remote Sensing. Second Edition*. John Wiley & Sons, Inc.: Hoboken, Ney Jersey, USA.

ESA (2019). Sentinel Online. Available: https://sentinel.esa.int/web/sentinel/home (01.04.2019).

Evans, G.C. (1972). *The Quantitative Analysis of Plant Growth*. Blackwell Scientific Publications, Oxford, UK.

Ewert, F., van Ittersum, M.K., Heckelei, T., Therond, O., Bezlepkina, I. and Andersen, E. (2011). Scale changes and model linking methods for integrated assessment of agri-environmental systems. *Agriculture, Ecosystems & Environment* **142**, 6-17.

Fang, H., Liang, S., Hoogenboom, G., Teasdale, J. and Cavigelli, M. (2008) Corn-yield estimation through assimilation of remotely sensed data into the CSM-CERES-Maize model. *International Journal of Remote Sensing* **29**, 3011-3032.

Fang, H., Liang, S. and Hoogenboom, G. (2011). Integration of MODIS LAI and vegetation index products with the CSM–CERES–maize model for corn yield estimation. *International Journal of Remote Sensing* **32**, 1039-1065.

Faivre, R., Leenhardt, D., Voltz, M., Benoît, M., Papy, F., Dedieu, G. and Wallach, D. (2004). Spatialising crop models. *Agronomie* **24**, 205-217.

Fisher, R.A. (1921). Some remarks on the methods formulated in a recent article on the quantitative analysis of plant growth. *Annals of Applied Biology* **7**, 367-372.

Gobron, N., Pinty, B., Verstraete, M.M. and Widlowski, J.-L. (2000). Advanced vegetation indices optimized for up-coming sensors—design, performance, and applications. *IEEE Transactions on Geoscience and Remote Sensing* **38**, 2489-2505.

Godwin, D.C., Ritchie, J.T., Singh, U. and Hunt, L. (1989). *A User's Guide to CERES Wheat-v2.10*. International Fertilizer Development Center: Muscle Schoals, Al, USA.

González, N. and Inzé, D. (2015). Molecular systems governing leaf growth: from genes to networks. *Journal of Experimental Botany* **66**, 1045-1054.

Goodman, M.A. (1959). Technique for the identification of farm crops on aerial photographs. *Photogrammetric Engineering* **25**, 131–137.

Goudriaan, J. (1977). *Crop micrometeorology: a simulation study*. Simulation Monograph. PUDOC: Wageningen, The Netherlands.

Gowda, P.T., Satyareddi, S.A. and Manjunath, S.B. (2013). Crop Growth Modeling: A Rewiev. *Research & Reviews: Journal of Agriculture and Allied Sciences* **2**, 1-11.

Grant, R.F., Kimball, B.A., Conley, M.M., White, J.W., Wall, G.W. and Ottman, M.J. (2011). Controlled warming effects on wheat growth and yield: field measurements and modeling. *Agronomy Journal* **103**, 1742-1754.

Gregory, F.G. (1917). Physiological conditions in cucumber houses. *3rd Ann .Rep. Exptl. Res. Stn. Cheshunt*, 19-28.

Guérif, M. and Duke, C. (1998). Calibration of the SUCROS emergence and early growth module for sugar beet using optical remote sensing data assimilation. *European Journal of Agronomy* **9**, 127-136.

Haboudane, D., Miller, J.R., Tremblay, N., Zarco-Tejada, P.J. and Dextraze, L. (2002). Integrated narrow-band vegetation indices for prediction of crop chlorophyll content for application to precision agriculture. *Remote Sensing of Environment* **81**, 416–426.

Hadria, R., Duchemin, B.I., Lahrouni, A., Khabba, S., Er Raki, S., Dedieu, G., Chehbouni, A. and Olioso, A. (2006). Monitoring of irrigated wheat in a semi-arid climate using crop modelling and remote sensing data: impact of satellite revisit time frequency. *International Journal of Remote Sensing* **27**, 1093-1117.

Haiden, T., Kann A. and Pistotnik, G. (2014). Nowcasting with INCA During SNOW-V_{10}. *Pure and Applied Geophysics* **171**, 231-242.

Hall, A.E. (2018). *Crop Responses to Environment. Adaptation to Global Climate Change, Second Edition*. CRC Press: Boca Raton, FL, USA.

Hartkamp, D.A., White, J.W. and Hoogenboom, G. (1999). Interfacing geographic information systems with agronomic modeling: A review. *Agronomy Journal* **91**, 761-772.

Hathfield J. L. (1979). Canopy temperatures: the usefulness and reliability of remote measurements. *Agronomy Journal* **71**, 889-892.

Heath, O.V.S. and Gregory, F.G. (1938). The constancy of the mean net assimilation rate and its ecological importance. *Annals of Botany* **2**, 811-818.

Hedhly, A. (2011). Sensitivity of flowering plant gametophytes to temperature fluctuations. *Environmental and Experimental Botany* **74**, 9–16.

Hodson, D. and White, J. (2010). GIS and crop simulation modelling applications in climate change research. In Reynolds, M.P. (Ed.). *Climate change and crop production*. CABI Publishers: Wallingford, UK.

Hoogenboom, G., White, J.W., Jones, J.W. and Boote, K.J. (1994). BEANGRO: A process-oriented dry bean model with a versatile user interface. *Agronomy Journal* **86**, 182-190.

Hoogenboom, G., Jones, J.W., Wilkens, P.W., Porter, C.H., Boote, K.J., Hunt, L.A., Singh, U., Lizaso, J.L., White, J.W., Uryasev, O., Royce, F.S., Ogoshi, R., Gijsman, A.J., Tsuji, G.Y. and Koo, J. (2012). *Decision Support System for Agrotechnology Transfer (DSSAT) Version 4.5* [CD-ROM]. University of Hawaii: Honolulu, Hawaii, USA.

Hoogenboom, G., Porter, C.H., Shelia, V., Boote, K.J., Singh, U., White, J.W., Hunt, L.A., Ogoshi, R., Lizaso, J.I., Koo, J., Asseng, S., Singels, A., Moreno, L.P. and Jones, J.W. (2017). *Decision Support System for Agrotechnology Transfer (DSSAT) Version 4.7 (https://DSSAT.net).* DSSAT Foundation: Gainesville, Florida, USA.

Huang, J., Tian, L., Liang, S., Ma, H., Becker-Reshef, I., Huang, Y., Su, W., Zhang, X., Zhu, D. and Wu, W. (2015). Improving winter wheat yield estimation by assimilation of the leaf area index from Landsat TM and MODIS data into the WOFOST model. *Agricultural and Forest Meteorology* **204**, 106–121.

Huffman, G.J., Adler, R.F., Bolvin, D.T., Gu, G., Nelkin, E.J., Bowman, K.P., Hong, Y., Stocker, E.F. and Wolff, D.B. (2007). The TRMM Multisatellite Precipitation Analysis (TMPA): Quasi-Global, Multiyear, Combined-Sensor Precipitation Estimates at Fine Scales. *Journal of Hydrometeorology* **8**, 38-55.

Hunt, R. (1982). *Plant Growth Curves*. Edward Arnold: London, UK.

Hunt, L.A., White, J.W. and Hoogenboom, G. (2001). Agronomic data: advances in documentation and protocols for exchange and use. *Agricultural Systems* **70**, 477–492.

Hurtado, E., Artigao, M.M. and Caselles, V. (1994). Estimating maize (Zea mays) evapotranspiration from NOAA-AVHRR thermal data in the Albacete area, Spain. *International Journal of Remote Sensing* **15**, 2023–2037.

IPCC (2014). *Climate Change 2014: Impacts, Adaptation, and Vulnerability. Part A: Global and Sectoral Aspects. Contribution of Working Group II to the Fifth Assessment Report of the Intergovernmental Panel on Climate Change*. Cambridge University Press: Cambridge, United Kingdom and New York, NY, USA.

IBSNAT (1984). Experimental design and data collection procedures for IBSNAT. The Minimum Data Set for Systems Analysis and Crop Simulation (first ed), IBSNAT Technical Report no 1. Available: https://pdf.usaid.gov/pdf_docs/PNABK919.pdf (01.04.2019).

Jin, H., Wang, J., Bo, Y., Chen, G. and Xue, H. (2010). Data assimilation of MODIS and TM observations into CERES-maize model to estimate regional maize yield, SPIE optical engineering + applications. *Int. Soc. Opt. Photon.*, 780908-780908-10.

Jin, X.L., Yang, G.J., Xu, X.G., Yang, H., Feng, H., Li, Z.H., Shen J.X., Lan, Y.B. and Zhao, C.J. (2015). Combined multi-temporal optical and radar parameters for estimating LAI and biomass in winter wheat using H J and RADARSAR-2 data. *Remote Sensing* **7**, 13251-13272.

Jin, X., Kumar, L., Li, Z., Feng, H., Xu, X., Yang, G. and Wang, J. (2018). A review of data assimilation of remote sensing and crop models. *European Journal of Agronomy* **92**, 141-152.

Jones, C.A. and Kiniry, J.R. (1986). *CERES-Maize: A Simulation Model of Maize Growth and Development*. Texas A&M University Press, College Station: Texas, USA.

Jones, J.W. (1993). Decision support systems for agricultural development. In Penning de Vries, F., Teng, P. and Metselaar, K. (Eds.). *Systems Approaches for Agricultural Development*. Kluwer Academic Press: Boston, USA, 459-471.

Jones, J.W., Keating, B.A. and Porter, C.H. (2001). Approaches to modular model development. *Agricultural Systems* **70**, 241-443.

Jones, J.W., Hoogenboom, G., Porter, C.H., Boote, K.J., Batchelor, W.D., Hunt, L.A., Wilkens, P.W., Singh, U., Gijsman, A.J. and Ritchie, J.T. (2003). DSSAT Cropping System Model. *European Journal of Agronomy* **18**, 235-265.

Jones, J.W., Antle, J.M., Basso, B., Boote, K.J., Conant, R.T., Foster, I, Godfray, C.J., Herrero, M., Howitt, R.E., Janssen, S., Keating, B.A., Munoz-Carpena, R., Porter, C.H., Rosenzweig, C. and Wheeler, T.R. (2017*a*). Brief history of agricultural systems modeling. *Agricultural Systems* **155**, 240-254.

Jones, J.W., Antle, J.M., Basso, B., Boote, K.J., Conant, R.T., Foster, I., Charles, H., Godfray, J., Herrero, M., Howitt, R.E., Janssen, S., Keating, B.A., Munoz-Carpena, R., Porter, C.H., Rosenzweig, C. and Wheeler, T.R. (2017*b*). Toward a new generation of agricultural system data, models, and knowledge products: state of agricultural systems science. *Agricultural Systems* **155**, 269-288.

Jongschaap, R.E. (2006). Run-time calibration of simulation models by integrating remote sensing estimates of leaf area index and canopy nitrogen. *European Journal of Agronomy* **24**, 316-324.

Karabatic, A., Weber, R. and Haiden, T. (2011). Near real-time estimation of tropospheric water vapour content from ground based GNSS data and its potential contribution to weather now-casting in Austria. *Advances in Space Research* **4**, 1691–1703.

Kasampalis, D.A., Alexandritis, T.K., Deva, C., Challinor, A., Moshou, D. and Zalidis, G. (2018). Contribution of remote sensing on crop models: a review. *Journal of Imaging* **4**, 1-19.

Keating, B.A. and Thorburn, P.J. (2018). Modelling crops and cropping systems—Evolving purpose, practice and prospects. *European Journal of Agronomy* **100**, 163-176.

Kersebaum, K.C. and Nendel, C. (2014). Site-specific impacts of climate change on wheat production across regions of Germany using different CO_2 response functions. *European Journal of Agronomy* **52**, 22-32.

Kollas, C., Kersebaum, K.C., Nendel, C., Manevski, K., Müller, C., Palosuo, T., Armas-Herrera, C.M., Beaudoin, N., Bindi, M., Charfeddine, M., Conradt, T., Constantin, J., Eitzinger, J., Ewert, F., Ferrise, R., Gaiser, T., Garcia de Cortazar-Atauri, I., Giglio, L., Hlavinka, P., Hoffmann, H., Hoffmann, M.P., Launay, M., Manderscheid, R., Mary, B., Mirschel, W., Moriondo, M., Olesen, J.E., Öztürk, I., Pacholsky, A., Ripoche-Wachter, D., Roggero, P.P., Roncossek, S., Rötter, R.P., Ruget, F., Sharif, B., Taká, J., Trnka, M., Ventrella, D., Waha, K., Wegehenkel, M., Weigel, H.J. and Wu, L.H. (2015). Crop rotation modelling – a European model intercomparison. *European Journal of Agronomy* **70**, 98-111.

Landgrebe, D.A. (2003). *Signal Theory Methods in Multispectral Remote Sensing.* Wiley-Interscience: New Jersey, USA.

Launay, M. and Guerif, M. (2005). Assimilating remote sensing data into a crop model to improve predictive performance for spatial applications. *Agriculture Ecosystems & Environment* **111**, 321-339.

Legates, D.R. and McCabe Jr., G.J. (1999). Evaluating the Use of "Goodness-of-Fit" Measures in Hydrologic and Hydroclimatic Model Validation. *Water Resources Research* **35**, 233–241.

Li, T., Hasegawa, T., Yin, X., Zhu, Y., Boote, K., Adam, M., Bregaglio, S., Buis, S., Confalonieri, R., Fumoto, T., Gaydon, D., Marcaida, M., Nakagawa, H., Oriol, P., Ruane, A.C., Ruget, F., Singh, B., Singh, U., Tang, L., Tao, F., Wilkens, P., Yoshida, H., Zhang, Z. and Bouman, B. (2015*a*). Uncertainties in predicting rice yield by current crop models under a wide range of climatic conditions. *Global Change Biology* **21**, 1328-1341.

Li, Z., Jin, X., Zhao, C., Wang, J., Xu, X., Yang, G., Li, C. and Shen, J. (2015*b*). Estimating wheat yield and quality by coupling the DSSAT-CERES model and proximal remote sensing. *European Journal of Agronomy* **71**, 53-62.

Lillesand, T., Kiefer, R and Chipman, J. (2004). *Remote Sensing and Image Interpretation*. *5th Edition.* John Wiley: Chichester, USA.

Linnemann, H., de Hoogh, J., Keyzer, M.A. and van Heemst, H.D.J. (1979). *MOIRA, Model of International Relations in Agriculture*. Report of the Project Group, Food for a Doubling World Population: Amsterdam, The Netherlands.

Lobell, D.B., Schlenker, W. and Costa-Roberts, J. (2011). Climate trends and global crop production since 1980. *Science* **333**, 616-620.

Löffler, E., Honecker, U. and Stabel, E. (2005). *Geographie und Fernerkundung: Eine Einführung in die geographische Interpretation von Luftbildern und modernen Fernerkundungsdaten* (Studienbücher der Geographie), 3.te Auflage. Borntraeger: Berlin, Stuttgart, Germany.

Ma, G.N., Huang, J.X., Wu, W.B., Fan, J.L., Zou, J.Q. and Wu, S.J. (2013). Assimilation of MODIS-LAI into the WOFOST model for forecasting regional winter wheat yield. *Mathematical and Computer Modelling* **58**, 634-643.

Maas, S.J. (1988). Use of remotely-sensed information in agricultural crop growth models. *Ecological Modelling* **41**, 247-268.

Martre, P., Jamieson, P.D., Semenov, M.A., Zyskowski, R.F., Porter, J.R. and Triboi, E. (2006). Modelling protein content and composition in relation to crop nitrogen dynamics for wheat. *European Journal of Agronomy* **25**, 138-154.

Mo, X., Liu, S., Lin, Z., Xu, Y., Xiang, Y. and McVicar, T.R. (2005). Prediction of crop yield, water consumption and water use efficiency with a SVAT-crop growth model using remotely sensed data on the North China Plain. *Ecological Modelling* **183**, 301–322.

Moran, M.S., Clarke, T.R., Inoue, Y. and Vidal, A. (1994). Estimating crop water deficit using the relation between surface-air temperature and spectral vegetation index. *Remote Sensing of Environment* **49**, 246–263.

Morel, J., Begue, A., Todoroff, P., Martine, J., Lebourgeois, V. and Petit, M. (2014). Coupling a sugarcane crop model with the remotely sensed time series of fIPAR to optimise the yield estimation. *European Journal of Agronomy* **61**, 60–68.

Moriasi, D.N., Arnold, J.G., Van Liew, M.W., Bingner, R.L., Harmel, R.D. and Veith, T.L. (2007). Model evaluation guidelines for systematic quantification of accuracy in watershed simulations. *Transactions of the ASABE* **50**, 885-900.

Morris, D.K., Johannsen, C.J., Brouder, S.M. and Steinhardt, G.C. (2005). Remote Sensing|Organic Matter. In Daniel Hillel (Ed.). *Encyclopedia of Soils in the Environment*. Elsevier, Columbia University: New York, USA, 385-392.

Moulin, S., Bondeau, A. and Delécolle, R. (1998). Combining agricultural crop models and satellite observations: From field to regional scales. *International Journal of Remote Sensing* **19**, 1021–1036.

Moulin, S., Zurita-Milla, R., Guérif, M. and Baret, F. (2003). *Characterizing the spatial and temporal variability of biophysical variables of a wheat crop using hyper-spectral measurements.* Proceedings of the International Geoscience and Remote Sensing Symposium (IGARSS), 2206–2208.

Müller, W. (1993). *Agroklimatische Kennzeichnung des Marchfelds.* Beiheft 3 zu den Jahrbüchern der Zentralanstalt für Meteorologie und Geodynamik. Eigenverlag: Wien, Austria.

Murer, E., Wagenhofer, J., Aigner, F. and Pfeffer, M. (2004). Die nutzbare Feldkapazität der mineralischen Böden der landwirtschaftlichen Nutzfläche Österreichs. *Schriftenreihe BAW* **20**, 72-78.

Murthy, V.R.K. (2003). *Crop Growth Modeling and Its Applications in Agricultural Meteorology.* Proceedings of the Satellite Remote Sensing and GIS Applications in Agricultural Meteorology, Dehra Dun, India, 7–11 July 2003, World Meteorological Organisation: Dehra Dun, India, 235-261.

Mutanga, O., Skidmore, A.K. and Prins, H.H.T. (2004). Predicting in situ pasture quality in the Kruger National Park, South Africa, using continuum-removed absorption features. *Remote Sensing of Environment* **89**, 393–408.

Myers, S.S., Zanobetti, A., Kloog, I., Huybers, P., Leakey, A.D.B., Bloom, A.J., Carlisle, E., Dietterich, L.H., Fitzgerald, G., Hasegawa, T., Holbrook, N.M., Nelson, R.L., Ottman, M.J., Raboy, V., Sakai, H., Sartor, K.A., Schwartz, J., Seneweera, S., Tausz, M. and Usui, Y. (2014). Increasing CO_2 threatens human nutrition. *Nature* **510**, 139-142.

Nagamani, K. and Nethaji Mariappan, V. E. (2017). Remote sensing, GIS and crop simulation models – A review. *International Journal of Current Research in Biosciences and Plant Biology* **4**, 80-92.

Nakicenovic, N. and Swart, R. (2000). *Emissions Scenarios – A Special Report of Working Group III of the Intergovernmental Panel on Climate Change*. Cambridge University Press: Cambridge, UK.

Nayak, M.A. and Villarini, G. (2018). Remote sensing-based characterization of rainfall during atmospheric rivers over the central United States. *Journal of Hydrology* **556**, 1038-1049.

Nendel, C., Rötter, R.P., Thorburn, P.J., Boote, K.J. and Ewert, F. (2018). Editorial Introduction to the Special Issue “Modelling cropping systems under climate variability and change: impacts, risk and adaptation”. *Agricultural Systems* **159**, 139-143.

Nellis, M.D., Price, K.P. and Rundquist, D. (2009). Chapter 26: Remote Sensing of Cropland Agriculture. In Warner, T.A., Nellis, M.D. and Goody, G.M (Eds). *The SAGE Handbook of Remote Sensing*. SAGE Publications Ltd: London, UK, 368-380.

Oteng-Darko, P., Yeboah, S., Addy, S.N.T., Amponsah, S. and Owusu Danquah, E. (2013). Crop modeling: A tool for agricultural research–A review. *Journal of Agricultural Research and Development* **2**, 1-6.

Palosuo, T., Kersebaum, K.C., Angulo, C., Hlavinka, P., Moriondo, M., Olesen, J.E., Patil, R.H., Ruget, F., Rumbaur, C., Takac, J., Trnka, M., Bindi, M., Caldag, B., Ewert, F., Ferrise, R., Mirschel, W., Saylan, L., Siska, B. and Rötter, R. (2011). Simulation of winter wheat yield and its variability in different climates of Europe: A comparison of eight crop growth models. *European Journal of Agronomy* **35**, 103–114.

Penning de Vries, F.W.T, Brunsting, A.B. and van Laar, H.H. (1974). Products, requirements and efficiency of biological synthesis, a quantitative approach. *The Journal of Theoretical Biology* **45**, 339-377.

Penning de Vries, F.W.T., Jansen, D.M., ten Berge, H.F.M. and Bakema, A. (1989). *Simulation of ecophysiological processes of growth in several annual crops*. Purdoc: Wageningen, The Netherlands.

Penning de Vries, F.W.T., van Laar, H.H. and Kropff, M.J. (1991). *Simulation and systems analysis for rice production (SARP).* PUDOC: Waneningen, The Netherlands.

Palosuo, T., Kersebaum, K.C., Angulo, C., Hlavinka, P., Moriondo, M., Olesen, J.E., Patil, R.H., Ruget, F., Rumbaur, C., Takáč, J., Trnka, M., Bindi, M., Çaldağ, B., Ewert, F., Ferrise, R., Mirschel, W., Şaylan, L., Šiška, B. and Rötter, R. (2011). Simulation of winter wheat yield and its variability in different climates of Europe: a comparison of eight crop growth models. *European Journal of Agronomy* **35**, 103-114.

Pimentel, D. and Peshin, R. (2014). *Use and Benefit of Pesticides in Agricultural Pest Control, Integrated Pest Management, Pesticide Problems, Vol 3*. Springer Science+Business Media: Dordrecht, The Netherlands.

Pinter, P., Ritchie, J., Hatfield, J. and Hart, G. (2003). The Agricultural Research Service's remote sensing program: an example of interagency collaboration. *Photogrametric Engineering and Remote Sensing* **69**, 615–618.

Porter, J.R., Xie, L., Challinor, A.J., Cochrane, K., Howden, S.M., Iqbal, M.M., Lobell, D.B. and Travasso, M.I. (2014). Food security and food production systems. In Field, C.B., Barros, V.R., Dokken, D.J., Mach, K.J., Mastrandrea, M.D., Bilir, T.E., Chatterjee, M., Ebi, K.L., Estrada, Y.O., Genova, R.C., Girma, B., Kissel, E.S., Levy, A.N., MacCracken, S., Mastrandrea, P.R. and White, L.L. (Eds.). *Climate Change 2014: Impacts, Adaptation, and Vulnerability. Part A: Global and Sectoral Aspects. Contribution of Working Group II to the Fifth Assessment Report of the Intergovernmental Panel on Climate Change*. Cambridge University Press: Cambridge, United Kingdom and New York, NY, USA, 485-533.

Prasad, P.V.V. and Djanaguiraman, M. (2014). Response of floret fertility and individual grain weight of wheat to high temperature stress: sensitive stages and thresholds for temperature and duration. *Functional Plant Biology* **41**, 1261-1269.

Prasad, P.V.V., Djanaguiraman, M., Perumal, R. and Ciampitti, I.A. (2015). Impact of high temperature stress on floret fertility and individual grain weight of grain sorghum: sensitive stages and thresholds for temperature and duration. *Frontiers in Plant Science* **6**, 1-11.

Prasad, P.V.V., Bheemanahalli, R. and Jagadish, S.V.K. (2017). Field crops and the fear of heat stress-opportunities: challenges and future directions. *Field Crops Research* **200**, 114-121.

Razzaghi, F., Zhou, Z., Andersen, M.N. and Plauborg, F. (2017). Simulation of potato yield in temperate condition by the AquaCrop model. *Agricultural Water Management* **191**, 113-123.

Reeves, R. (1975). *Manual of Remote Sensing*. American Society of Photogrammetry: Falls Church, Virginia, USA.

Rezaei, E.E., Siebert, S. and Ewert, F. (2015*a*). Intensity of heat stress in winter wheat – phenology compensates for the adverse effect of global warming. *Environmental Research Letters* **10**, 1-8.

Rezaei, E.E., Webber, H., Gaiser, T., Naab, J. and Ewert, F. (2015*b*). Heat stress in cereals: mechanisms and modelling. *European Journal of Agronomy* **64**, 98-113.

Rezaei, E.E., Siebert, S. and Ewert, F. (2015*c*). Impact of data resolution on heat and drought stress simulated for winter wheat in Germany. *European Journal of Agronomy* **65**, 69-82.

Richardson, A.J., Wiegand, C.L., Arkin, G.F., Nixon, P.R. and Gerbermann, A.H. (1982). Remotely-sensed spectral indicators of sorghum development and their use in growth modelling. *Agricultural Meteorology* **26**, 11–23.

Rischbeck, P.M. (2007). *Der Einfluss von Klimaänderung, Bodenbearbeitung und Saattermin auf den Wasserhaus halt und das Ertragspotential von Getreide im Marchfeld*. Ph.D. Thesis, University of Natural Resources and Life Sciences: Vienna, Austria.

Ritchie, J.T. and Otter S. (1984). Description and performance of CERES-wheat: a user-oriented wheat yield model. A.R.S. Wheat Yield Project (Ed.). *ARS-38, National Technical Information Service*. Springfield: Missouri, USA, 159-175.

Ritchie, J.T., Godwin, D.C. and Otter, S. (1984). *CERES-Wheat: A user oriented wheat yield model*. *Preliminary documentation*. AGRISTARS Publication: East Lansing, Michigan, USA.

Rosenzweig, C., Jones, J.W., Hatfield, J.L., Ruane, A.C., Boote, K.J., Thorburn, P., Antle, J.M., Nelson, G.C., Porter, C., Janssen, S., Asseng, S., Basso, B., Ewert, F., Wallach, D., Baigorria, G. and Winter, J.M. (2013). The Agricultural Model Intercomparison and Improvement Project (AgMIP): protocols and pilot studies. *Agricultural and Forest Meteorology* **170**, 166-182.

Rötter, R.P., Palosuo, T., Pirttioja, N.K., Dubrovsky, M., Salo, T., Fronzek, S., Aikasalo, R., Ristolainen, A. and Carter T.R. (2011*a*). What would happen to barley production in Finland if global warming exceeded 4°C? A model-based assessment. *European Journal of Agronomy* **35**, 205-214.

Rötter, R.P., Carter, T.R., Olesen, J.E. and Port, J.R. (2011*b*).Crop-climate models need an overhaul. *Nature Climate Change* **1**, 175-177.

Rötter, R.P., Palosuo, T., Kersebaum, K.C., Angulo, C., Bindi, M., Ewert, F., Ferrise, R., Hlavinka, P., Moriondo, M., Nendel, C., Olesen, J.E., Patil, R.H., Ruget, F., Takáč, J. and Trnka, M. (2012). Simulation of spring barley yield in different climatic zones of Northern and Central Europe: a comparison of nine crop models. *Field Crops Research* **133**, 23-36.

Rundquist, D. and Samson, S. (1983). Application of remote sensing in agricultural analysis. Chapter 15. In Richason, Jr., B. (Ed.). *Introduction to Remote Sensing of the Environment.* Kendall/Hunt Publishing Company: Dubuque, Iowa, USA, 317–337.

Saini, H.S., Sedgley, M. and Aspinall, D. (1983). Effect of heat stress during floral development on pollen tube growth and ovary anatomy in wheat (Triticum aestivum L.). *Functional Plant Biology* **10**, 137-144.

Sayago, S., Ovando, G. and Bocco, M. (2017). Landsat images and crop model for evaluating water stress of rainfed soybean. *Remote Sensing of Environment* **198**, 30-39.

Schönhart, M., Mitter, H., Schmid, E., Heinrich, G. and Gobiet, A. (2014). Integrated Analysis of Climate Change Impacts and Adaptation Measures in Austrian Agriculture. *GJAE* **63**, 156-176.

Schott, J.R. (2007). *Remote sensing: the image chain approach. 2nd ed.* Oxford University Press, Inc.: New York, USA.

Semenov, M.A. and Shewry, P.R. (2011). Modelling predicts that heat stress, not drought, will increase vulnerability of wheat in Europe. *Scientific Reports* **1**, Article number: 66.

Shen, S., Yang, S., Li, B., Tan, B., Li, Z. and Le Toan T. (2009). A scheme for regional rice yield estimation using ENVISAT ASAR data. *Sci. China Ser. D* **52**, 1183-1194.

Shi, W., Ishimaru, T., Gannaban, R.B., Oane, W. and Jagadish, S.V.K. (2015). Popular rice (Oryza sativa L.) cultivars show contrasting responses to heat stress at gametogenesis and anthesis. *Crop Science* **55**, 589-596.

Siebert, S. and Ewert, F. (2012). Spatio-temporal patterns of phenological development in Germany in relation to temperature and day length. *Agricultural and Forest Meteorology* **152**, 44-57.

Simonett, S. (1983). Chapter I. The development and principles of remote sensing. In Colwell, R.N. (Ed.). *Manual of remote sensing Vol. 1*. American Society of Photogrammetry and Remote Sensing: Falls Church, Virginia, USA, 1-35.

Singh, J., Knapp, H.V. and Demissie, M. (2004). *Hydrologic modeling of the Iroquois River watershed using HSPF and SWAT.* Illinois State Water Survey Contract Report 2004-08. Available: https://swat.tamu.edu/media/90101/singh.pdf (01.04.2019).

Singh, V., Nguyen, C.T., van-Oosterom, E.J., Chapman, S.C., Jordan, D.R. and Hammer, G.L. (2015). Sorghum genotypes differ in high temperature responses for seed set. *Field Crops Research* **171**, 32-40.

Soltani, A. and Sinclair, T.R. (2012). *Modeling Physiology of Crop Development, Growth and Yield.* CABI: Wallingford, Oxfordshire, UK and Cambridge, MA, USA.

Sorooshian, S., Duan, Q. and Gupta, V.K. (1993). Calibration of rainfall-runoff models: Application of global optimization to the Sacramento Soil Moisture Accounting Model. *Water Resources Research* **29**, 1185-1194.

Stampoulis, D. and Anagnostou, E.N. (2012). Evaluation of global satellite rainfall products over continental Europe. *Journal of Hydrometeorology* **13**, 588-603.

Stewart, R.H. (1985). *Methods of Satellite Oceanography*. University of California Press: Berkeley, USA.

Stöckle, C.O., Donatelli, M. and Nelson, R. (2003). CropSyst, a cropping systems simulation model. *European Journal of Agronomy* **18**, 289-307.

Stone, P.J. and Nicolas, M.E. (1995). Effect of timing of heat stress during grain filling on two wheat varieties differing in heat tolerance. 1. Grain growth. *The Australian Journal of Plant Physiology* **22**, 927-934.

Tashiro, T. and Wardlaw, I.F. (1990). The response of high temperature shock and humidity changes prior to and during early stages of grain development in wheat. *Functional Plant Biology* **17**, 551-561.

Teixeira, E.I., Fischer, G., van Velthuizen, H., Walter, C. and Ewert F. (2013). Global hot-spots of heat stress on agricultural crops due to climate change. *Agricultural and Forest Meteorology* **170**, 206-21.

Thaler, S., Eitzinger, J., Dubrovsky, M. and Trnka M. (2009). *Changes of water demand - possible adaptation of agricultural crops and management options to improve water use efficiency in the Marchfeld area.* EGU General Assembly 2009, 19-24 April 2009, Vienna, Austria.

Thaler, S., Eitzinger, J., Rischbeck, P., Dubrovsky, M. and Trnka, M. (2010). Vulnerability of crops to climate change in Northeastern Austria. *Bulgarian Journal of Meteorology and Hydrology* **15**, 50–61.

Thaler, S., Eitzinger, J., Trnka M. and Dubrovsky, M. (2012). Impacts of climate change and alternative adaptation options on winter wheat yield and water productivity in a dry climate in Central Europe. *The Journal of Agricultural Science* **150**, 537–555.

Thaler, S., Brocca, L., Ciabatta, L., Eitzinger, J., Hahn, S. and Wagner, W. (2018*a*). Effects of Different Spatial Precipitation Input Data on Crop Model Outputs under a Central European Climate. *Atmosphere* ***9***, 290.

Thaler, S., Eitzinger, J., Trnka, M., Možný, M., Hahn, S., Wagner, W. and Hlavinka, P. (2018*b*). The performance of Metop Advanced SCATterometer soil moisture data as a complementary source for the estimation of crop-soil water balance in Central Europe. *The Journal of Agricultural Science* **156**, 577-598.

Thorp, K.R., Hunsaker, D.J. and French, A.N. (2010). Assimilating leaf area index estimates from remote sensing into the simulations of a cropping systems model. *Trans. ASABE* **53**, 251-262.

Thorp, K.R., Wang, G., West, A.L., Moran, M.S., Bronson, K.F., White, J.W. and Mon, J. (2012). Estimating crop biophysical properties from remote sensing data by inverting linked radiative transfer and ecophysiological models. *Remote Sensing of Environment* **124**, 224-233.

Tim, U.S. (1996). Coupling vadose zone models with GIS: Emerging trends and potential bottlenecks. *Journal of Environmental Quality* **25**, 535-544.

Tomlinson, C.J., Chapman, L., Thornes, J.E. and Baker, C. (2011). Remote sensing land surface temperature for meteorology and climatology: a review. *Meteorological Applications* **18**, 296-306.

Trnka, M., Eitzinger, J., Dubrovsky, M., Semeradova, D., Stepanek, P., Hlavinka, P., Balek, J., Skalak, P., Farda, A., Formayer, H. and Zalud, Z. (2010). Is rainfed crop production in central Europe at risk? Using a regional climate model to produce high resolution agroclimatic information for decision makers. *The Journal of Agricultural Science* **148**, 639–656.

Trnka, M., Eitzinger, J., Semerádová, D., Hlavinka, P., Balek, J., Dubrovský, M., Kubu, G., Štepánek, P., Thaler, S., Možný, M. and Žalud, Z. (2011*a*). Expected changes in agroclimatic conditions in Central Europe. *Climatic Change* **108**, 261–289.

Trnka, M., Olesen, J.E., Kersebaum, K.-C., Skjelvag, A.O., Eitzinger, J., Seguin, B., Peltonen-Sainio, P., Rötter, R., Iglesias, A., Orlandini, S., Dubrowsky, M., Hlavinka, P., Balek, J., Eckersten, H., Cloppet, E., Calanca, P., Gobin, A., Vucetic, V., Nejedlik, P., Kumar, S., Lalic, B., Mestre, A., Rossi, F., Kozyra, J., Alexandrov, V., Semerádová, D. and Žalud, Z. (2011*b*). Agroclimatic conditions in Europe under climate change. *Global Change Biology* **17**, 2298–2318.

Trnka, M., Rötter, R.P., Ruiz-Ramos, M., Kersebaum, K.C., Olesen, J.E., Zalud, Z. and Semenov, M.A. (2014). Adverse weather conditions for European wheat production will become more frequent with climate change. *Nature Climate Change* **4**, 637-643.

Trnka, M., Brázdil, R., Balek, J., Semeradova, D., Hlavinka, P., Možný, M., Štěpánek, P., Dobrovolný, P., Zahradníček, P., Dubrovsky, M., Eitzinger, J., Fuchs, B., Svoboda, M., Hayes, M. and Žalud, Z. (2015*a*). Drivers of soil drying in the Czech Republic between 1961 and 2012. *International Journal of Climatology* **35**, 2664-2675.

Trnka, M., Brázdil, R., Možný, M., Štěpánek, P., Dobrovolný, P., Zahradníček, P., Balek, J., Semerádová, D., Dubrovský, M., Hlavinka, P., Eitzinger, J., Wardlow, B., Svoboda, M., Hayes, M. and Žalud, Z. (2015*b*). Soil moisture trends in the Czech Republic between 1961 and 2012. *International Journal of Climatology* **35**, 3733-3747.

Tsuji, G.Y., Uehara, G. and Balas, S. (1994). *Decision Support System for Agrotechnology Transfer (DSSAT) Version 3.* University of Hawaii: Honolulu, Hawaii, USA.

Tsuji, G.Y., Hoogenboom, G. and Thornton P.K. (1998). *Understanding Options for Agricultural Production.* Kluwer Academic Publishers: Springer, Dordrecht, The Netherlands.

Tubiello, F.N., Rosenzweig, C., Kimball, B.A., Pinter, P.J., Jr.,Wall, G.W., Hunsaker, D.J., Lamorte, R.L. and Garcia, R.L. (1999). Testing CERES-Wheat with FACE data: CO_2 and water interactions. *Agronomy Journal* **91**, 1856-1865.

Tubiello, F.N. and Ewert, F. (2002). Simulating the effects of elevated CO_2 on crops: approaches and applications for climate change. *European Journal of Agronomy* **18**, 57–74.

Tucker, C.J., Vanpraet, C., Boerwinkel, E. and Gaston, A. (1983). Satellite remote sensing of total dry matter production in the Senegalese Sahel. *Remote Sensing of Environment* **13**, 461–474.

Uehara, G. and Tsuji, G.Y. (1993). The IBSNAT project. In: Penning de Vries, F.P., Teng, P. and Metselaar K. (Eds.). *Systems approaches for agricultural development*. Springer: Dordrecht, The Netherlands, 505-513.

Uehara, G. and Tsuji, G.Y. (1998). Overview of IBSNAT. In Tsuji, G.Y., Hoogenboom, G. and Thornton, P.K. (Eds.). *Understanding Options for Agricultural Production*. Springer Science+Business Media: Dordrecht, The Netherlands, 1-7.

van Ittersum, M.K., Leffelaar, P.A., van Keulen, H., Kropff, M.J., Bastiaans, L. and Goudriaan J. (2003). On approaches and applications of the Wageningen crop models. *European Journal of Agronomy* **18**, 201-234.

Venus, J.C. and Causton, D.R. (1979). Plant growth analysis: the use of the Richards function as an alternative to polynomial exponentials. *Annals of Botany* **43**, 623-632.

Wagner, W., Lemoine G. and Rott, H. (1999). A method for estimating soil moisture from ERS scatterometer and soil data. *Remote Sensing of Environment* **70**, 191–207.

Wagner, W., Hahn, S., Kidd, R., Melzer, T., Bartalis, Z., Hasenauer, S., Figa, J., de Rosnay, P., Jann, A., Schneider, S., Komma, J., Kubu, G., Brugger, K., Aubrecht, C., Zuger, J., Gangkofner, U., Kienberger, S., Brocca, L., Wang, Y., Bloeschl, G., Eitzinger, J., Steinnocher, K., Zeil, P. and Rubel, F. (2013). The ASCAT soil moisture product: a review of its specifications, validation results, and emerging applications. *Meteorologische Zeitschrift* **22**, 5–33.

Wahid, A., Gelani, S., Ashraf, M. and Foolad, M.R. (2007). Heat tolerance in plants: An overview. *Environmental and Experimental Botany* **61**, 199-223.

Wallach, D., Makowski, D. and Jones, J.W. (2006). *Working with Dynamic Models. Evaluation, Analysis, Parameterization, and Applications*. Elsevier Science: Amsterdam, The Neterlands.

Wang, H. Zhu, Y. Li, W. Cao, W. and Tian Y. (2014). Integrating remotely sensed leaf area index and leaf nitrogen accumulation with RiceGrow model based on particle swarm optimization algorithm for rice grain yield assessment. *Journal of Applied Remote Sensing* **8**, 083674-1-16.

Wardlaw, I.F. and Moncur, L. (1995). The response of wheat to high temperature following anthesis. I. The rate and duration of kernel filling. *Functional Plant Biology* **22**, 391-397.

West, C., Briggs, G.E. and Kidd, F. (1920). Methods and significant relations in the quantitative analysis of plant growth. *New Phytologist* **19**, 200-207.

Wheeler, T. and von Braun, J. (2013). Climate change impacts on global food security. *Science* **41**, 508-513.

White, J.W., Hoogenboom, G., Kimball, B.A. and Wall, G.W. (2011). Methodologies for simulating impacts of climate change on crop production. *Field Crops Research* **124**, 357-368.

Wilkerson, G.G., Jones, J.W., Boote, K.J., Ingram, K.T. and Mishoe, J.W. (1983). Modeling soybean growth for crop management. *Transactions of the American Society of Agricultural Engineers* **26**, 63-73.

Williams, J.R., Renard, K.G. and Dyke P.T. (1983). EPIC: a new method for assessing erosion's effect on soil productivity. *Journal of Soil and Water Conservation* **38**, 381-383.

Williams, J.R., Jones, C.A., Kiniry, J.R. and Spanel, D.A. (1989). The EPIC crop growth model. *Transactions of the American Society of Agricultural Engineers* **32**, 497-511.

Williams, R.F. (1946). The physiology of plant growth with special reference to the concept of net assimilation rate. *Annals of Botany* **10**, 41-72.

Willmott, C.J. (1981). On the validation of models. *Physical Geography* **2**, 184-194.

Willmott, C.J. (1984). On the evaluation of model performance in physical geography. In Gaile, G.L. and Willmott, C.J. (Eds.). *Spatial Statistics and Models*. Springer Science+Business Media: Dordrecht, The Netherlands, 443-460.

Willmott, C.J., Ackleson, S.G., Davis, R.E., Feddema, J.J., Klink, K.M., Legates, D.R., O'Donnell, J. and Rowe, C.M. (1985). Statistics for the Evaluation and Comparison of Models. *Journal of Geophysical Research* **90**, 8995-9005.

Wolf, J., van Oijen, M. and Kempenaar, C. (2002). Analysis of the experimental variability in wheat responses to elevated CO_2 and temperature. *Agriculture, Ecosystems and Environment* **93,** 227-247.

Yao, F., Tang, Y., Wang, P. and Zhang, J. (2015). Estimation of maize yield by using a process-based model and remote sensing data in the Northeast China Plain. *Phys. Chem. Earth Parts A/B/C* **87**, 142-152.

Yapo, P.O., Gupta, H.V. and Sorooshian, S. (1996). Automatic calibration of conceptual rainfall-runoff models: sensitivity to calibration data. *Journal of Hydrology* **181**, 23-48.

Yin, X., Goudriaan, J., Lantinga, E.A., Vos, J. and Spiertz, H.J. (2003). A flexible sigmoid function of determinate growth. *Annals of Botany* **91**, 1-11.

Yin, X., Kersebaum, K.C., Kollas, C., Baby, S., Beaudoin, N., Manevski, K., Palosuo, T., Nendel, C., Wu, L., Hoffmann, M., Hoffmann, H., Sharif, B., Armas-Herrera, C.M., Bindi, M., Charfeddine, M., Conradt, T., Constantin, J., Ewert, F., Ferrise, R., Gaiser, T., de Cortazar-Atauri, I.G., Giglio, L., Hlavinka, P., Lana, M., Launay, M., Louarn, G., Manderscheid, R., Mary, B., Mirschel, W., Moriondo, M., Öztürk, I., Pacholski, A., Ripoche-Wachter, D., Rötter, R.P., Ruget, F., Trnka, M., Ventrella, D., Weigel, H.-J. and Olesen, J.E. (2017). Multi-model uncertainty analysis in predicting grain N for crop rotations in Europe. *European Journal of Agronomy* **84**, 152-165.

Zhang, Y., Yao, Y., Lin, Y. and Xiang, L. (2016). Satellite characterization of terrestrial drought over Xinjiang Uygur autonomous region of China over past three decades. *Environmental Earth Sciences* **75**, 1-13.

Zhao, C., Liu, L., Wang, J., Huang, W., Song, X., Li, C. and Wang, Z. (2004). *Methods and application of remote sensing to forecast wheat grain quality*. Proceedings of International Geoscience and Remote Sensing Symposium (IGARSS), 4008–4010.

Zhao, G., Siebert, S., Enders, A., Rezaei, E.E., Yan, C. and Ewert F. (2015). Demand for multi-scale weather data for regional crop modeling. *Agricultural and Forest Meteorology* **200**, 156-171.

Zhao, Y., Chen, S. and Shen, S. (2013). Assimilating remote sensing information with crop model using Ensemble Kalman Filter for improving LAI monitoring and yield estimation. *Ecological Modelling* **270**, 30-42.

7 Full list of publications

Thaler, S., Eitzinger, J., Trnka, M., Možný, M., Hahn, S., Wagner, W. and Hlavinka, P. (2018). The performance of Metop Advanced SCATterometer soil moisture data as a complementary source for the estimation of crop-soil water balance in Central Europe. *The Journal of Agricultural Science* **156**, 577-598.

Lalić, B., Firanj Sremac, A., Eitzinger, J., Stričević, R., Thaler, S., Maksimović, I. and Dekić, L. (2018). Seasonal forecasting of green water components and crop yield of summer crops in Serbia and Austria. *The Journal of Agricultural Science* **156**, 658-672.

Thaler, S., Brocca, L., Ciabatta, L., Eitzinger, J., Hahn, S. and Wagner, W. (2018). Effects of Different Spatial Precipitation Input Data on Crop Model Outputs under a Central European Climate. *Atmosphere* ***9***, 290.

Thaler, S., Gobin, A. and Eitzinger, J. (2017). Water Footprint of main crops in Austria. *Die Bodenkultur* **68**, 1–15.

Ebrahimi, E., Manschadi, A.M., Neugschwandtner, R.W., Eitzinger, J., Thaler, S. and Kaul, H.P. (2016). Assessing the impact of climate change on crop management in winter wheat - a case study for Eastern Austria. *The Journal of Agricultural Science* **154**, 1153-1170.

Lalic, B., Eitzinger, J., Thaler, S., Vucetic, V., Nejedlik, P., Eckersten, H., Jacimovic, G. and Nikolic-Djoric, E. (2014). Can Agrometeorological Indices of Adverse Weather Conditions Help to Improve Yield Prediction by Crop Models? *Atmosphere* **5**, 1020-1041.

Eitzinger, J., Thaler, S., Schmid, E., Strauss, F., Ferrise, R., Moriondo, M., Bindi, M., Palosuo, T., Rötter, R., Kersebaum, K.C., Olesen, J.E., Patil, R.H., Saylan, S., Caldac, B. and Caylak, O. (2013). Sensitivities of crop models to extreme weather conditions during flowering period demonstrated for maize and winter wheat in Austria. *The Journal of Agricultural Science* **151**, 813-835.

Eitzinger, J., Trnka, M., Semerádová, D., Thaler, S., Svobodová, E., Hlavinka, P., Siska, B., Takáč, J., Malatinská, L., Nováková, M., Dubrovský, M. and Zalud, Z. (2013). Regional climate change impacts on agricultural crop production in Central and Eastern Europe – hotspots, regional differences and common trends. *The Journal of Agricultural Science* **151**, 787-812.

Lalic, B., Eitzinger, J., Mihailovica, D.T., Thaler, S. and Jancic, M. (2013). Climate change impacts on winter wheat yield change – which climatic parameters are crucial in Pannonian lowland? *The Journal of Agricultural Science* **151**, 757-774.

Thaler, S., Eitzinger, J., Trnka, M. and Dubrovsky, M. (2012). Impacts of climate change and alternative adaptation options on winter wheat yield and water productivity in a dry climate in Central Europe. *The Journal of Agricultural Science* **150**, 537-555.

Trnka, M., Eitzinger, J., Semeradova, D., Hlavinka, P., Balek, J., Dubrovsky, M., Kubu, G., Stepanek, P., Thaler, S., Mozny, M. and Zalud, Z. (2011). Expected changes in agroclimatic conditions in Central Europe. *Climate Change* **108**, 261-289.

Hlavinka, P., Eitzinger, J., Smutny, V., Thaler, S., Zhalud, Z., Rischbeck, P. and Kren, J. (2010): Das Verhalten der Ertragsmodelle "CERES-Barely" und "CERES-Wheat" auf unterschiedlichen Böden und unter verschiedener Bodenbearbeitung in Mitteleuropa./The performance of CERES-Barley and CERES-Wheat under various soil conditions and tillage practices in Central Europe. *Die Bodenkultur* **61**, 9-21.

Thaler, S., Eitzinger, J., Rischbeck, P., Dubrovsky, M. and Trnka, M. (2010): Vulnerability of crops to climate change in Northeastern Austria. *Bulgarian Journal of Meteorology and Hydrology* **15**, 50-61.

Trnka, M., Eitzinger, J., Hlavinka, P., Dubrovsky, M., Semeradova, D., Stepanek, P., Thaler, S., Zalud, Z., Mozny, M. and Formayer, H. (2009). Climate-driven changes of production regions in Central Europe. *Plant Soil Environ* **55**, 257-266.

Eitzinger, J., Kubu, G., Thaler, S., Alexandrov, V., Utset, A., Mihailovic, D.T., Lalic, B., Trnka, M., Zalud, Z., Semeradova, D., Ventrella, D., Anastasiou, D. P., Medany, M., Attaher, S., Olejnik, J., Lesny, J., Nemeshko, N., Nikolaev, M., Simota, C. and Cojocaru, G. (2009): Adaptation of vulnerable regional agricultural systems in Europe to climate change - results from the ADAGIO project. *Advances in Science and Research* **3**, 133-135.

Eitzinger, J., Thaler, S., Orlandini, S., Nejedlik, P., Kazandjiev, V., Sivertsen, T.H. and Mihailovic, D. (2009): Applications of agroclimatic indices and process oriented crop simulation models in European agriculture. *Idojaras - quarterly journal of the Hungarian Meteorological Service* **113**, 1-12.

Eitzinger, J., Formayer, H., Thaler, S., Trnka, M., Zdenek, Z. and Alexandrov, V. (2008): Results and uncertainties of climate change impact research in agricultural crop production in Central Europe. *Die Bodenkultur* **59**, 1-4.

8 Appendix

The appendix contains three scientific publications in the original layout of the journals in which the papers were published.

Paper I

Thaler, S., Eitzinger, J., Trnka M. and Dubrovsky, M. (2012). Impacts of climate change and alternative adaptation options on winter wheat yield and water productivity in a dry climate in Central Europe. *The Journal of Agricultural Science* **150**, 537–555.

Paper II

Eitzinger, J., Trnka, M., Semerádová, D., Thaler, S., Svobodová, E., Hlavinka, P., Siska, B., Takác, J., Malatinská, L., Nováková, M., Dubrovsky, M. and Zalud, Z. (2013). Regional climate change impacts on agricultural crop production in Central and Eastern Europe—hotspots, regional differences and common trends. *The Journal of Agricultural Science* **151**, 787-812.

Paper III

Thaler, S., Brocca, L., Ciabatta, L., Eitzinger, J., Hahn, S. and Wagner, W. (2018). Effects of Different Spatial Precipitation Input Data on Crop Model Outputs under a Central European Climate. *Atmosphere* **9**, 290.

Journal of Agricultural Science (2012), **150**, 537–555.
doi:10.1017/S0021859612000093

CLIMATE CHANGE AND AGRICULTURE RESEARCH PAPER

Impacts of climate change and alternative adaptation options on winter wheat yield and water productivity in a dry climate in Central Europe

S. THALER[1]*, J. EITZINGER[1,2], M. TRNKA[2,3] AND M. DUBROVSKY[3,4]

[1] *Institute of Meteorology, University of Natural Resources and Applied Life Sciences, Vienna, Austria*
[2] *CzechGlobe – Center for Global Climate Change Impacts Studies, Poříčí 3b 603 00, Brno, Czech Republic*
[3] *Institute of Agrosystems and Bioclimatology, Mendel University Brno, Czech Republic*
[4] *Institute of Atmospheric Physics, Czech Academy of Sciences, Prague, Czech Republic*

(*Received 22 April 2011; revised 10 October 2011; accepted 16 January 2012; first published online 28 February 2012*)

SUMMARY

The main objective of the present crop simulation study was to determine the impact of climate change on the winter wheat production of a dry area situated in north-east Austria (Marchfeld region) based on the CERES-Wheat crop-growth simulation model associated with global circulation models (GCMs). The effects of some of the feasible regional- and farm-based adaptation measures (management options) on crop yield and water and nitrogen (N) balance under the climate scenarios were simulated. Climate scenarios were defined based on the ECHAM5, HadCM3 and NCAR PCM GCM simulations for future conditions (2021–50) as described in the Special Report on Emission Scenarios A1B (Nakicenovic & Swart 2000). The potential development, yield, water demand and soil N leaching were estimated for winter wheat and all of the defined climates (including rising CO_2 levels) and management scenarios (soil cultivation, windbreaks and irrigation).

The results showed that a warming of 2 °C in the air temperature would shorten the crop-growing period by up to 20 days and would decrease the potential winter wheat yield on nearly all of the soil types in the region. Particularly, high-yield reductions were projected for light-textured soils such as Parachernozems. A change from ploughing to minimum tillage within the future scenario would lead to an increase of up to 8% of the mean yield of winter wheat. This effect mainly resulted from improved water supply to the crop, associated with higher soil water storage capacity and decrease of unproductive water losses. Hedgerows, which reduce the wind speed, were predicted to have particularly positive effects on medium and moderately fine-textured soils such as Chernozems and Fluvisols. With both management changes, regional mean-yield level can be expected to be +4% in comparison with no management changes in the future conditions. Compared with the baseline period, water demand for the potential yield of winter wheat would require 6–37 mm more water per crop season (area-weighted average). The highest water demand would be on medium-textured soils, which make up the largest amount of area in the study region. Additionally, the effects of snow accumulation near hedgerows would further increase the yield, but would also lead to higher N leaching rates. However, specific management options, such as minimum tillage and hedgerows, could contribute towards reducing the increasing water demand.

INTRODUCTION

Changes in the mean and the variability of climatic parameters will have an essential influence on agricultural cropping systems, especially under water-limited production conditions, such as in the dry region of north-eastern Austria. For example, Dubrovsky *et al.* (2008) and Trnka *et al.* (2010*a*, 2011*a*, *b*) indicated that in dry agricultural areas of Central Europe, drought and periods of heat stress at particularly sensitive stages of development are expected to increase and will be limiting factors in crop production under future climate scenarios. Heat stress in plants is a complex function of the

* To whom all correspondence should be addressed. Email: Sabina.Thaler@boku.ac.at

temperature level and duration as well as the rate of temperature increase. The critical thresholds of temperature vary greatly with the developmental stages of crops and plants (Hall 2001). Water stress is often associated with (i) heat stress, as leaf temperature usually increases during stomata closure and (ii) a reduced transpirational cooling effect (Hathfield 1979). At the same time, the ongoing enrichment of atmospheric CO_2, which is expected to rise from a current 390 µmol/mol to *c*. 550 µmol/mol by the middle of the century (Solomon *et al*. 2007), enhances the photosynthetic rate and biomass accumulation. However, higher temperatures can provoke a notable shortening of the growth period, especially for annual crops, such as cereals with determinate growth, providing less time for carbon fixation and a reduction in biomass accumulation (Morison & Lawlor 1999). Therefore, the combination of increased CO_2 concentration with higher temperature does not necessarily result in a higher crop yield (Kristensen *et al*. 2011). Specific agricultural practices such as selecting earlier sowing dates or cultivars with a longer growth cycle contribute to preventing yield reductions and reducing water demand (Trnka *et al*. 2004*a*; Olesen *et al*. 2007, 2011; Kaukoranta & Hakala 2008). Additionally, limitations by other factors, such as water availability and the associated uptake of mineral nutrients, is expected to become increasingly important (Amthor 2001; Linke *et al*. 2005).

Several short- and long-term agronomic adaptation strategies are recommended to avoid or reduce the negative impact of climate change on the crop yield potential and develop eventual positive effects. Short-term adjustments at the farm level involve production techniques, such as changes in crop rotation and crop cultivars, changes in soil cultivation and tillage practices, a shift of sowing dates, adapted fertilization and crop protection measures (Tubiello *et al*. 2000; Chen & McCarl 2001; Alexandrov *et al*. 2002; Ghaffari *et al*. 2002; Trnka *et al*. 2004*b*; Patil *et al*. 2010; Davies *et al*. 2011; Seo 2011). These adjustments aim to optimize crop production without major system changes and can be developed and implemented independently at the farm level. Long-term adaptations, on the contrary, include major structural changes of farm production systems and need careful agro-economic planning and realization at a society level; these adaptations also involve a set of sectors and stakeholders, such as policy, research, water and land planning (Eitzinger *et al*. 2010; Olesen *et al*. 2011; Shahabfar & Eitzinger 2011). Some examples of long-term adjustments are changes in land use and landscape structure, breeding and biotechnology applications, crop substitution and changes in the farm production type (Alexandrov *et al*. 2002).

Various potential adaptations in farm practices for crop production aim to reduce the negative impacts of crop growth-limiting factors, such as water stress or heat, through changes in management aimed at more efficient use and/or decrease in the unproductive losses of production resources (e.g. water and soil). Both conservation and efficiency gains improve the local sustainability of production, reduce production risks and may concomitantly improve the resilience of the production system. A change in soil cultivation or tillage practices, for example, can have multiple effects, such as on the soil water storage and soil erosion caused by water and wind (Falloon & Betts 2010; Klik & Eitzinger 2010). Conservation tillage practices have several advantages over conventional tillage systems (i.e. based on ploughing) under various soil, climate and management conditions (Martínez *et al*. 2008), which among others include the preservation of soil and water resources, a reduction of energy input and costs and, therefore, an increase or stabilization of crop production (Osunbitan *et al*. 2005).

Hedges (hedgerows, windbreaks or shelterbelts) consist of trees or bushes forming elongated structures in the agricultural landscape. Their introduction in the landscape represents another important adaptation strategy in regions with water-limiting crop-growing conditions (Kuemmel 2003). Hedges reduce wind speed and, therefore, unproductive evaporative losses from the crop stand by a reduction in the advection of dry air. However, growing hedges may create a disadvantage to nearby crops by introducing competition for growth-limiting factors, such as water or light (Brenner *et al*. 1995; Cleugh *et al*. 1998). Increased snow retention near hedges may augment soil water storage, but it can also affect the soil nitrogen (N) balance (Rowe *et al*. 2005), delay field operations in spring time (Nuberg 1998), and cause fungal crop diseases (Brenner 1996; Nuberg 1998).

For the assessment and interpretation of the behaviour of agronomic systems under diverse environmental conditions, such as climate change and management options, mechanistic crop simulation models are suitable tools (Tsuji *et al*. 1998; Orlandini *et al*. 2008; Challinor 2011; Rötter *et al*. 2011). With the help of extensive spatial databases and analysis techniques supported by geographical information

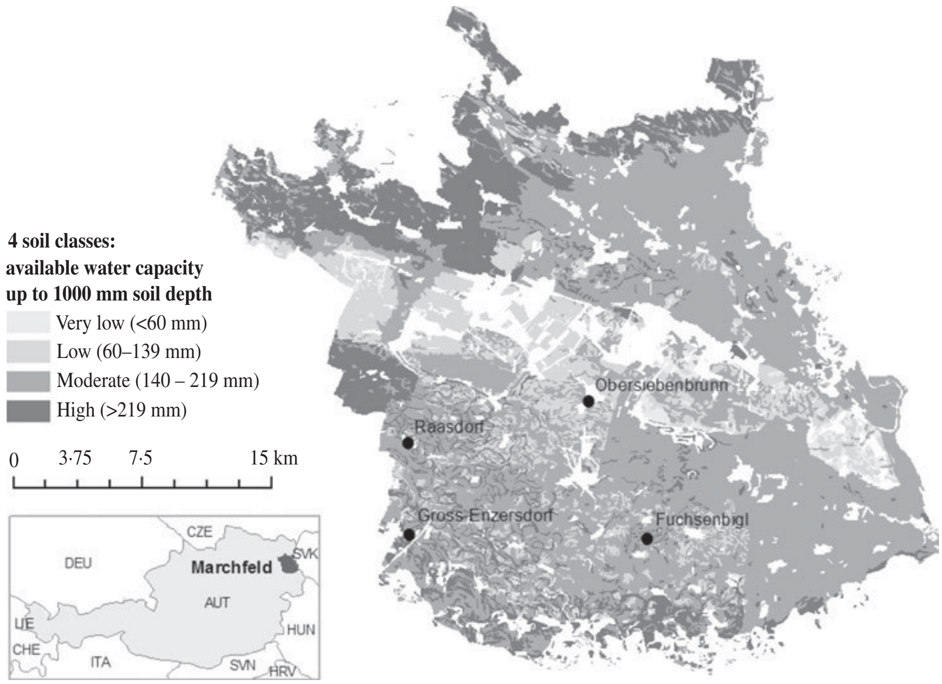

Fig. 1. The available water capacity of mineral soil classes in Marchfeld, Austria.

systems, the model outputs can be scaled up for regional planning (Uhlir & Carter 1994). Additionally, crop simulation models can help to find adequate adaptation strategies to avoid or reduce negative climate change effects on crop yield and exploit possible beneficial options (Alexandrov *et al.* 2002; Trnka *et al.* 2004*a*; Thaler *et al.* 2010; Iqbal *et al.* 2011). However, crop models are only a simplification of the complex soil-crop-atmosphere system. Uncertainties are thus abundant, such as the model representation of the involved processes and model inputs (Eitzinger *et al.* 2008; Challinor 2011; Rötter *et al.* 2011).

The present study contributes to the assessment of the regional-specific and multiple effects of farm-level climate change adaptation strategies in dry crop production regions of Central Europe for winter wheat production by use of crop simulation. Specifically, the main objectives of the paper include: (i) a determination of the impact of climate change and (ii) an evaluation of the possible adaptation strategies for current winter wheat production in north-eastern Austria under a changing climate. For this purpose, detailed input data were collected for the parameterization and validation of the crop growth model CERES-Wheat. The impact of different regionalized climate change and management scenarios for the period 2021–50 on simulated winter wheat phenology and yields was studied. Particular emphasis was put on the assessment of: (i) the range of potential future crop development and yields under different climate change scenarios and (ii) the effects of soil cultivation and hedges on crop yield-limiting factors (i.e., soil water and N balance) as adaptation options.

MATERIALS AND METHODS

Study region

The Marchfeld region (Fig. 1; 48°17′N, 16°38′E), located in the north-eastern part of Austria, is not only one of the major crop production areas but also one of the driest regions in the country. It is a plain of *c.* 900 km^2 with minor variations in elevation, ranging from 143 to 178 m a.s.l. The region is in the transition zone between the semi-humid Western-European climate and continental East-European one. Conditions are usually cold, with frequent hard frosts and limited snow cover in winter, and hot and periodically dry in summer (Müller 1993). According to the phytogeographical and climatological aspect Marchfeld is part of the Pannonicum, with high levels of sunshine, high average temperature during the growing period and low precipitation. The growing period (mean temperature >5 °C) lasts from the middle of March until middle of November, which means a growing period of *c*. 240 days (Cepuder & Schlederer 2002). Total precipitation of 550 mm and temperature of 9·9 °C characterize this semi-arid area (annual mean values 1961–90 weather station Groß-Enzersdorf 48°12′N, 16°33′E, 157 m a.s.l.). The mean annual potential evapotranspiration is 615 mm (1965–74 weather station Obersiebenbrunn 48°16′N, 16°41′E, 150 m a.s.l.) and was calculated with the Penman equation (Penman 1948, 1963). The annual water balance (precipitation – evapotranspiration according to Penman) is negative, with a value of −350 mm (Obersiebenbrunn 1969–74) (Müller 1993).

The main rain-fed crops are cereals in Marchfeld and other important crops, such as maize, vegetables, sugar beet or potatoes, need to be irrigated most years.

Model and data processing

The CERES-Wheat crop model (DSSAT 4.0.2.0) was selected for the present study. Palosuo *et al.* (2011) showed that CERES-Wheat performed well in comparison with real data and other models. It is a process-based, management-oriented model that simulates the daily time-step effects of the cultivar, crop management, weather, soil, water and N on crop growth, phenology and yield (Jones *et al.* 2001, 2003). The input requirements for CERES-Wheat include weather and soil conditions, plant characteristics and crop management (Hunt *et al.* 2001).

Weather data

The minimum weather input requests of the model are daily solar radiation, the maximum and minimum air temperature and precipitation (Singh *et al.* 2008). Since the target area is a flat, small region, the variability of climate due to topography is marginal and can be neglected, as the daily variability of the weather equates to the climatological mean. Therefore, a representative weather station at Groß-Enzersdorf was selected for the entire region.

Soil data

Soil inputs include the drainage and runoff coefficients, first-stage evaporation and soil albedo, water-holding capacity, soil texture, bulk density, organic carbon (C) content for each individual soil layer and the rooting preference coefficients at several depth increments. For the first simulated day, the model also requires information about the saturated and initial soil water and N contents (Singh *et al.* 2008). In the model, the FAO-56 Penman–Monteith equation (Allen *et al.* 1998) was used to calculate the evapotranspiration and effect of wind speed reductions. The CERES soil model was selected as the soil organic N sub-model (Godwin & Jones 1991; Godwin & Singh 1998), which among others has been evaluated in a wide range of studies (Kovács *et al.* 1995; Timsina *et al.* 1998; Singh *et al.* 2008).

The overall soil conditions in Marchfeld are characterized by high spatial variability, including soils with low to moderate water-storage capacity. The arable soils in this region have a humus-rich A-horizon with high variability in depth (from *c*. 300 to >1000 mm) and a sandy C-horizon underneath, followed by fluvial gravel from the former river bed of the Danube. The groundwater table is in this gravel body, 6 m below the surface. Gravels avoid capillary rise, therefore there is no groundwater impact in the rooting zone of the crops (Eitzinger *et al.* 2003). Four soil classes (termed herein as soil 1, soil 2, soil 3 and soil 4, respectively) were defined according to the total available water capacity from the digital Austrian Soil Map 1:25 000 (BFW 2007); they were calculated with the area-weighed mean values of physical and chemical soil properties (i.e. texture and organic C content; Fig. 1) (Rischbeck 2007). The first two soil classes have an available water capacity of up to 140 mm for a 1000-mm soil depth. They are mostly Parachernozems, which are characterized as loamy sand or sandy loam soils, comprising *c*. 0·17 of the target area. Soils 3 and 4 are Chernozems and Fluvisols, respectively, with an available water capacity >140 mm for a 1000-mm soil depth (soil 3: sandy loam, 0·61 of the Marchfeld area; soil 4: loamy silt, 0·22 of the area).

Crop characteristics of winter wheat

The genetic coefficients used in the model depict the specific growth and development of the relevant crop cultivar (Tsuji *et al.* 1998; Alexandrov & Hoogenboom 2000). Coefficients related to photoperiod sensitivity, duration of grain filling, conversion of mass to grain number, grain-filling rates, vernalization requirements, stem size and cold hardiness are essential information to run the model (Hunt *et al.* 1993).

For the calibration of the genetic coefficients, the experimental site at Fuchsenbigl in Marchfeld was chosen (48°11′N, 17°00′E, 149 m asl) using 17 years (1989–2005) of phenological and yield data of the crop cultivar Capo (Fig. 2). It is a well-established

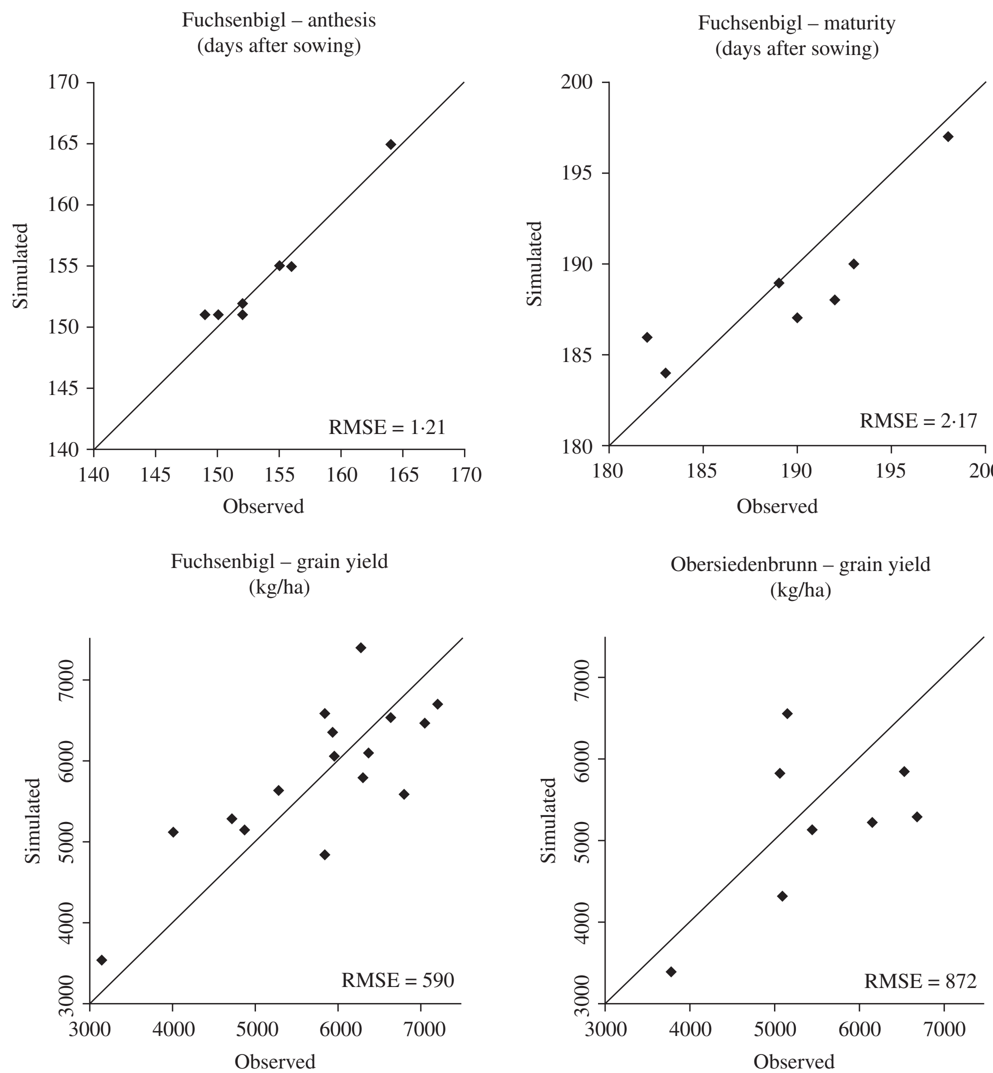

Fig. 2. Comparison between simulated and observed phenological and yield data of winter wheat cultivar CAPO in Fuchsenbigl and Obersiebenbrunn, Marchfeld.

cultivar, which is adapted to relatively dry and warm regions such as those found in eastern Austria (Oberforster & Werteker 2009). Nine years of observed winter wheat yield data from Obersiebenbrunn in the Marchfeld region were used for the model validation (Fig. 2) (Rischbeck 2007). The estimated genetic coefficients of the validated wheat used in the model simulations are presented in Table 1.

Crop management

The winter wheat simulations depending on the management scenarios (see below) were conducted for rain-fed farming, including N fertilization, automatically adapted sowing dates, with and without the enrichment of CO_2 according to the emission scenario, ploughed soil and minimum tillage, wind speed reduction due to hedges, additional soil moisture owing to snow banks on hedgerows and automatic irrigation without considering the potential yield losses caused by pest or diseases. Fertilization at 3×40 kg N/ha, the amount that farmers presently use in this area, at tillering, stem elongation or jointing and booting was simulated.

The effects of CO_2 on photosynthesis and water use were added to the CERES Wheat simulations. Internally in the model, the daily potential transpiration calculations were modified by the CO_2 concentration, due to the effects of CO_2 on stomatal conductivity (Peart *et al.* 1989). A multiplicative modification was made to daily canopy photosynthesis as described by Curry *et al.* (1990). An

Table 1. *Estimated genetic coefficients of winter wheat (cultivar Capo) used in the crop model simulation*

Genotype	P1V (%/day)	P1D (%/day)	P5 (°C/day)	G1 (#/g)	G2 (g/(m^2 day))	G3 (g)	PHINT (°C/day)
CAPO	60	90	560	28	42	1·33	95

P1D, photoperiod sensitivity coefficient (% reduction/h near threshold); P1V, vernalization sensitivity coefficient (%/day of unfulfilled vernalization); P5, thermal time from the onset of linear fill to maturity (8 °C day); G1, Kernel number per unit stem and/spike weight at anthesis (#/g); G2, potential kernel growth rate (mg/(kernel day)); G3, Tiller death coefficient. Standard stem and/spike weight when elongation ceases (g); PHINT, thermal time between the appearance of leaf tips (8 °C day) Jones *et al.* (2003).

atmospheric CO_2 level of 350 µmol/mol was set for the baseline. The future conditions were simulated with and without any CO_2 enrichment (458 µmol/mol according to the emission scenario) to obtain a range of possible impacts.

The automatic adapted sowing date was defined for a given day. This day was considered suitable for sowing from the model when the soil water content in the top layer of soil (the top 150 mm) was between 0·05 and 0·85 of the maximum soil water-holding capacity, while the soil temperature was between 8 and 15 °C. The automatic irrigation option implemented irrigation as a function of threshold parameters. These included the depth of the profile (300 mm), where soil moisture and threshold at which irrigation was triggered (defined 0·5 of max available) were controlled everyday. Once the soil water content at the top of the profile drops below this defined threshold, the automatic irrigation system adds water to raise the soil profile to the drained upper limit (Nijbroeka *et al.* 2003).

A 100-year daily weather series used as an input to the crop model was produced by the stochastic weather generator (WG) M&Rfi, which was developed from the earlier Met&Roll WG (Dubrovsky 1997; Dubrovsky *et al.* 2000, 2004). The weather series for the representative site were generated for the baseline period (1961–90) and 2021–50 (termed herein as the future scenario). When generating the weather series for the future climate, the WG parameters were modified according to the climate change scenarios. The climate change scenarios were constructed using a pattern scaling method (Dubrovsky *et al.* 2005), in which the scenario for a given future (specific climate sensitivity and emission scenario) was defined as a product of the change in global mean temperature by the standardized (accounting for 1 °C rise in global mean temperature) climate change scenarios. The standardized scenarios were based on the outputs from ECHAM5, HadCM3 and NCAR PCM global circulation models (GCMs). The change in global mean temperature was determined by simple climate model MAGICC 5·3 (Harvey *et al.* 1997; Hulme *et al.* 2000). The climate scenarios were based on the Special Report on Emission Scenarios A1B (Nakicenovic & Swart 2000) and moderate climate sensitivity (3 °C), which implies a change in global mean temperature of 1·28 °C (according to the MAGICC model). By comparing the results from three different GCMs it was possible to reduce uncertainties in the climate change scenarios. Maximum and minimum temperature as well as precipitation at baseline, and the changes with respect to the baseline period, are presented in Fig. 3. The final datasets that were used do not explicitly consider changes in the diurnal variability under future climate change conditions and assume that the variability under future climate is the same as under the baseline conditions.

The alternative management practices studied as selected adaptation strategies are described below.

Soil cultivation

Mouldboard plough with a ploughing depth of 250 mm was replaced by minimum tillage. The impacts on the soil physical properties: plant growth and yield were estimated in a 3-year field experiment comparing both conventional and minimum tillage in Raasdorf (48°15′N, 16°34′E, 156 m a.s.l.) from 2002 to 2004. Soil input data for ploughed and minimum tillage-scenarios were estimated by the model, where undisturbed soil or minimum tillage condition were determined from the values of the Austrian Soil Map (BFW 2007). For the ploughed soil, the first 250 mm soil layer was modified according to laboratory analyses of soil samples, as depicted in Table 2 (Rischbeck 2007). This two-tillage practice in the

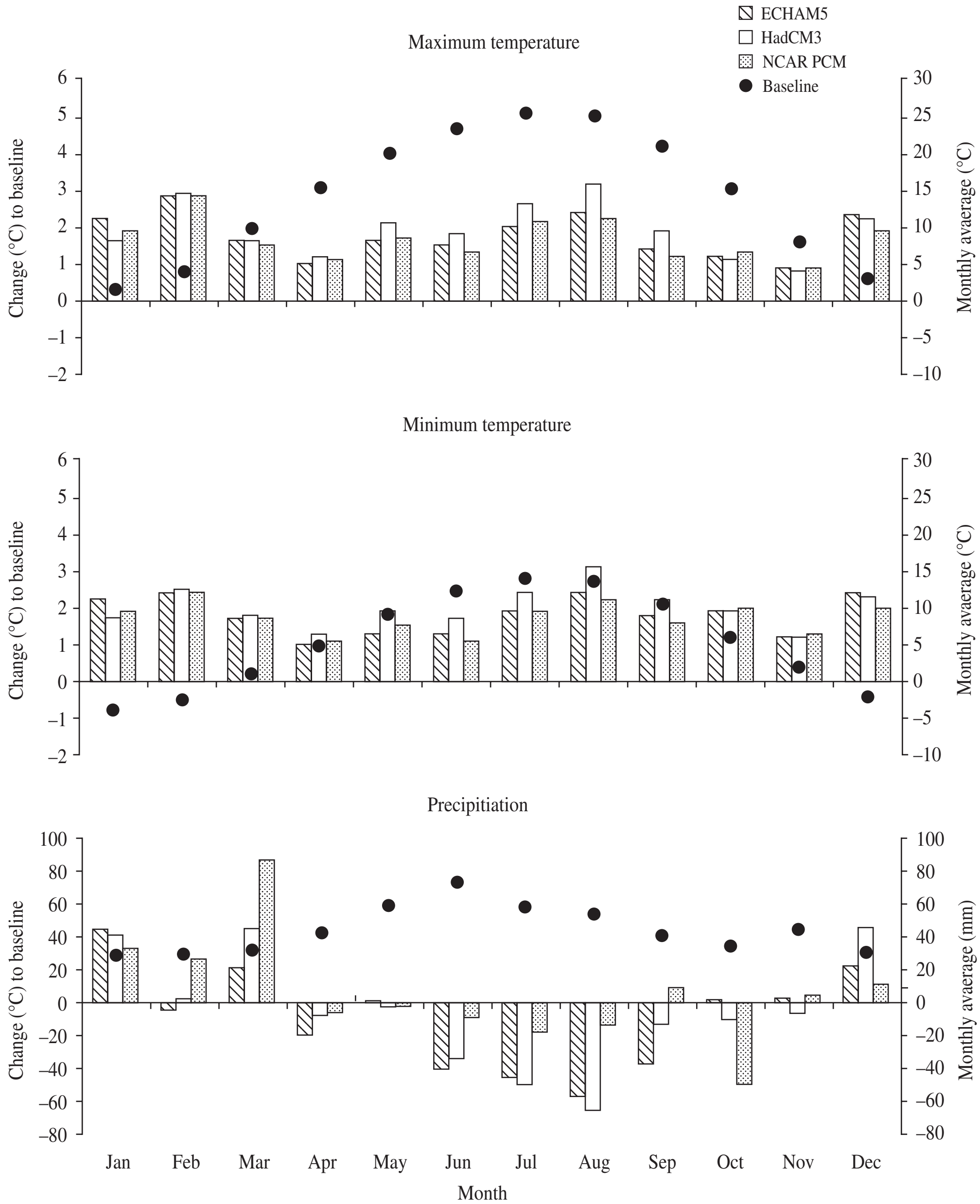

Fig. 3. Y (1): Changes of temperature (°C) and precipitation (%) for the three GCMs in the future scenario (2021–50), with respect to the baseline period. Y (2): Monthly average of the maximum and minimum temperature in °C as well as the precipitation in mm for the baseline period (1961–90).

target area with CERES-Wheat was validated by Hlavinka *et al.* (2010), who showed that the model is capable, to a certain extent, of mimicking the differences between conventional and minimum tillage.

Hedgerows

Winter wheat yields at various distances from a hedge were compared with unsheltered mid-field yield. Among other benefits, shelters reduce wind speed; therefore, wind speed reductions of 0·25, 0·50 and 0·75 were simulated, based on the study of Gerersdorfer *et al.* (2009).

Snow retention near hedges

The effect of windbreaks on snow near the hedgerows (snow banks) was considered in the simulation. Increased snow retention near hedges enhances the soil moisture after melting in the spring. Based on the snowMAUS model (Trnka *et al.* 2010*b*), information

Table 2. *Soil properties for the four soil classes under minimum tillage (400 mm soil depth) and modification factors of the first 250 mm layer of the soil data for the harrowed (0–50 mm) and ploughed (0–250 mm) soil in the DSSAT soil module (Rischbeck 2007)*

	Soil depth (mm)	Soil saturation (ml/ml)	Field capacity (ml/ml)	Wilting point (ml/ml)	Bulk density (g/cm^3)
Soil 1 minimum tillage	0–200	0·36	0·30	0·10	1·50
	200–400	0·13	0·07	0·03	1·95
Soil 2 minimum tillage	0–200	0·49	0·36	0·15	1·47
	200–400	0·44	0·33	0·15	1·47
Soil 3 minimum tillage	0–200	0·55	0·45	0·22	1·44
	200–400	0·49	0·41	0·21	1·42
Soil 4 minimum tillage	0–200	0·54	0·46	0·20	1·40
	200–400	0·46	0·41	0·18	1·42
Modification factors					
$f_{harrow} = Y_{harrow}/Y_{minimum\ tillage}$	0–50	1·15	0·83	0·84	0·85
$f_{plough} = Y_{plough}/Y_{minimum\ tillage}$	50–250	1·10	0·88	0·89	0·89

about the duration of snow cover and the snow-water equivalent (in mm) per year was available. During a field trial in Raasdorf in spring 2005, melting water equivalent to *c*. 158 mm was measured near a representative hedgerow (Gerersdorfer *et al.* 2009), a value that was 3·6 times higher than the one predicted by snowMAUS for the same year for unsheltered mid-field conditions. To simulate this additional soil moisture, the snow-water equivalent was added to the precipitation input at the beginning of the vegetation period, where the value of the 'volume of precipitation in term of snow melt per year' (snowMAUS) × 3·6/10 was used for the subsequent 10 days. The study region experiences prevailing winds from the north to the west (in more than 0·65 of cases per year), so that the accumulation of snow near hedgerows that are oriented from north to south is common.

Irrigation

To study the crop water demand under climate change scenarios, the automatic irrigation option of the crop model was selected.

The baseline period was simulated with rain-fed farming, including N fertilization and ploughed soil on unsheltered conditions. The reference management in the future scenario also included the CO_2 enrichment. For the evaluation and comparison of the model results of the different climate and management scenarios, the following outputs were used: yield (kg/ha), sowing, anthesis and maturity dates, nitrate (N) leached (kg/ha), applied irrigation (mm) and the water use efficiency (WUE) of the crops (WUE_{plant}) and cropping systems (WUE_{field}), which were calculated between two sowing dates as follows:

$$WUE_{plant}\ kg/(mm\ ha) = Yield/Transpiration \quad (1)$$

$$WUE_{field}\ kg/(mm\ ha) = Yield/Evapotranspiration \quad (2)$$

RESULTS

Impacts of climate change on winter wheat phenology

According to Alexandrov & Hoogenboom (2000) and Trnka *et al.* (2004*b*), the projected increases in temperature are expected to lead to shorter growing and reproductive seasons. The duration of the regular crop-growing season of winter wheat (the interval from sowing until physiological maturity area-weighted average) in the simulated future scenario was 17 (NCAR PCM), 18 (ECAM5) and 20 (HadCM3) days shorter than in the baseline period.

The analysis of these simulated future scenarios also suggested a delay to the sowing date of winter wheat by a maximum of 7 days (ECHAM5 and HadCM3), from 6 to 13 October. Anthesis would occur *c*. 10 (ECHAM5) to 11 days earlier (HadCM3 and NCAR PCM) and maturity between 11 (ECHAM5) and 13 days earlier (HadCM3) than in the baseline period (Fig. 4).

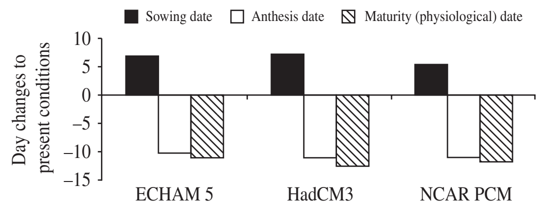

Fig. 4. Changes (in days) of the dates of sowing, anthesis and maturity of winter wheat (area-weighted average) in the future scenario, with respect to baseline conditions.

Impact of climate change on wheat production with unmodified management

Simulation of changes to future weather conditions without any associated CO_2 enrichment using the three GCMs would lead to a yield depression of winter wheat (except for soil 4 – NCAR PCM), especially for soil 1 and 2 in Marchfeld (Table 3*a*). A CO_2 level of 350 µmol/mol in future would account for a yield change of −18% using ECHAM5, −14% using HadCM3 and −3% using NCAR PCM (area-weighted average), whereas the WUE_{plant} would increase by between 4 and 6% and the WUE_{field} between −1 and 1% (area-weighted average) with respect to the baseline period. The interannual yield variability of winter wheat would increase for almost all soils (exception soil 1 – ECHAM5 and HadCM3). The yield decreases were caused by a shortened growing season and reductions in the precipitation during the crop-growing season.

For a CO_2 level of 458 µmol/mol, the future scenario simulations predicted lower yield losses or even yield increases in comparison with the ones without any CO_2 enrichment (*c*. +11% by area-weighted average), especially for soil 1 and 2. Yield losses (area-weighted average) of 7 and 4% were predicted by ECHAM5 and HadCM3 respectively, in comparison with the baseline period. The simulated CO_2-fertilizing effect could not offset the yield drop. On the contrary, an increase of +7% (area-weighted average) in winter wheat yield was predicted by NCAR PCM (Fig. 5 and Table 3*b*). This last GCM also forecasted an annual temperature increase of 2 °C and 3% additional precipitation for the region compared to the baseline period. This is the only scenario that showed higher precipitation than for the baseline period (Fig. 3).

The enhanced levels of atmospheric CO_2 were predicted to increase the WUE_{plant} by increasing the growth rates and decreasing the transpiration per leaf area unit (up to 19% area-weighted average), especially for soils with a low available water capacity. These soils showed the highest N leaching rates, which would be even higher without the CO_2 enrichment effect due to lower biomass accumulation and N uptake. At the same time WUE_{field} raised, especially in soils 3 and 4 (Table 3*b*).

In the last few decades, the N concentration in the groundwater at Marchfeld has increased to a critical level due to the intensive agricultural crop production practices. Agricultural fertilization is reported to be the main cause for the high concentration of N in the groundwater (Cepuder 1999). Depending on the amount and intensity of precipitation, the part of N that is not absorbed by the plants remains in the soil or is leached below the crop root zone. It stays in the soil during years with low precipitation and is leached downwards during years with heavy rainfall events.

A field trial, which included the winter wheat cultivar Capo, was carried out in Fuchsenbigl from 1999 to 2001 with conventional crop rotation, to investigate the groundwater quality in the pannonic region in Austria (Cepuder & Schlederer 2002). The lysimeter N leaching rates ranged from 2·2 to 16·8 kg/ha among three soils. The available water capacity of these soils was between 115 and 138 mm for a 900-mm soil depth, which is in the range of soils 2 and 3 in the present study.

Effects of management adaptation strategies on the winter wheat growth conditions (with CO_2 enrichment)

Replacement of ploughing by minimum tillage

In the climate change modelled scenario, the replacement of ploughing (reference management) by minimum tillage led to an increase in the mean yield for winter wheat of up to 2% (area-weighted average, NCAR PCM). Minimum tillage would potentially enhance the yield up to 8%, particularly for soil 1 (Table 4*a*). This positive effect mainly resulted from both improved water supply for the crops and a decrease of unproductive water losses. The relative change of soil water content would increase in soil 1 and 2 in ECHAM5 and HadCM3 and for all soil classes in NCAR PCM (Table 5). Additionally, minimum tillage induced lower N leaching potential in all soil classes (Table 4*a*).

Effects of hedges on winter wheat yield

The results of the previous simulation are representative of unsheltered conditions. The effects on the

Table 3. *Winter wheat yield mean (kg/ha) and* s.d., *WUE of crops (WUE_{plant}), cropping systems (WUE_{field}) (kg/ha per mm + s.d.) as well as nitrogen leached (kg/ha + s.d.) for the baseline and changes of winter wheat yield (%), WUE (%) and N leached (abs.) as well as s.d. (absolute value) (a) without and (b) with CO_2 enrichment in the future scenario* v. *the baseline*

	Baseline (CO_2 = 350 µmol/mol)							
	Yield		WUE_{plant}		WUE_{field}		N leached	
	kg/ha	s.d.	kg/ha per mm	s.d.	kg/ha per mm	s.d.	kg/ha	s.d.
Soil 1	3766	1107	33	5·1	8	2·1	46	27·6
Soil 2	5281	1222	30	4·1	11	1·7	12	16·1
Soil 3	6022	1665	32	3·3	12	2·3	3	11·4
Soil 4	5664	1473	31	3·8	11	2·0	1	4·9
Area-weighted average	*5790·7*		*31·4*		*11·2*		*4·8*	

	ECHAM5							
	Yield		WUE_{plant}		WUE_{field}		N leached	
	%	s.d.	%	s.d.	%	s.d.	Abs. change	s.d.
(a) CO_2 = 350 µmol/mol (without CO_2 enrichment)								
Soil 1	−31	1080	0·3	4·9	−15	2·4	27	56·8
Soil 2	−21	1716	8	4·2	−3	3·2	14	51·1
Soil 3	−18	2193	5	4·2	−2	3·9	21	65·5
Soil 4	−13	2229	9	5·0	4	3·9	6	24·4
Area-weighted average	*−17·7*		*6·4*		*−1·2*		*16·8*	
(b) CO_2 = 458 µmol/mol (with CO_2 enrichment)								
Soil 1	−19	1140	22	6·0	0·4	2·5	16	47·8
Soil 2	−12	1678	21	5·6	8	3·1	9	33·8
Soil 3	−7	2192	18	6·6	12	3·9	9	32·6
Soil 4	−4·1	2090	21	6·4	15	3·7	3	11·5
Area-weighted average	*−7·2*		*19·1*		*12·1*		*7·8*	

	HadCM3							
	Yield		WUE_{plant}		WUE_{field}		N leached	
	%	s.d.	%	s.d.	%	s.d.	Abs. change	s.d.
(a) CO_2 = 350 µmol/mol (without CO_2 enrichment)								
Soil 1	−28	1065	0·0	5·2	−13	2·3	24	35·3
Soil 2	−18	1590	7	4·3	−2	2·9	13	48·5
Soil 3	−14	2069	5	4·8	0·4	3·6	18	69·3
Soil 4	−9	2034	7	4·5	5	3·4	6	64·6
Area-weighted average	*−13·5*		*5·8*		*0·7*		*14·7*	
(b) CO_2 = 458 µmol/mol (with CO_2 enrichment)								
Soil 1	−17	1139	22	6·1	2	2·5	14	35·1
Soil 2	−9	1538	20	5·5	9	2·7	8	45·0
Soil 3	−4	2007	17	6·0	13	3·4	10	64·5
Soil 4	0·1	1906	20	6·0	16	3·2	4	58·3
Area-weighted average	*−3·9*		*18·0*		*12·8*		*8·5*	

	NCAR PCM							
	Yield		WUE_{plant}		WUE_{field}		N leached	
	%	s.d.	%	s.d.	%	s.d.	Abs. change	s.d.
(a) CO_2 = 350 µmol/mol (without CO_2 enrichment)								
Soil 1	−19	1166	−4	5·8	−16	2·2	24	45·5
Soil 2	−9	1567	5	5·3	−5	2·5	15	29·3
Soil 3	−3	1851	4	4·4	−0·7	2·9	20	44·9
Soil 4	2	1769	6	4·7	4	2·7	8	20·7
Area-weighted average	*−2·8*		*4·1*		*−0·7*		*16·7*	
(b) CO_2 = 458 µmol/mol (with CO_2 enrichment)								
Soil 1	−9	1255	18	6·2	−3	2·3	16	38·1
Soil 2	0·3	1609	18	4·8	6	2·2	12	23·7
Soil 3	8	1848	16	4·4	12	2·5	14	27·9
Soil 4	11	1724	18	4·4	14	2·3	7	15·4
Area-weighted average	*7·1*		*16·9*		*11·0*		*12·2*	

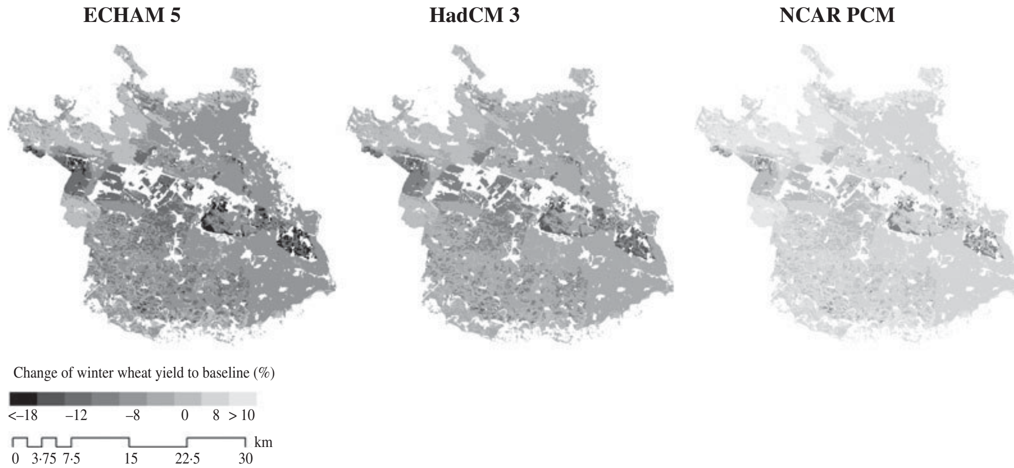

Fig. 5. Relative change (%) of winter wheat yield to baseline conditions for different GCMs with CO_2 enrichment on ploughed soil.

landscape of hedgerows that lie at right angles to the prevailing winds are as follows. The effects of wind speed reductions of 0·25, 0·50 and 0·75 under ploughed soil cultivation were simulated for the applied climate scenarios. As the results show (see Fig. 6 and Table 4*b* for wind reduction 0·50), wind speed reductions would raise winter wheat yield. For all cases, the ECHAM5 scenario showed the highest increases, and the NCAR PCM scenario showed the lowest ones. Furthermore, the highest yield raises were found on soils 3 and 4; whereas only minor effects for the two other soil classes.

In contrast to plough cultivation practices, a combination of minimum tillage with hedgerows (the results are shown only for a wind speed reduction of 0·50) would have the highest impact on soils 1 and 2. An increase in yield of between 4% (NCAR PCM) and 4·4% (ECHAM5) was predicted (for the area-weighted average) compared to the reference management. In addition, a lower N leaching rate and higher WUE_{plant} and WUE_{field} as well as s.d. was simulated (Table 4*c*).

The simulated yield effect of additional snow accumulation near hedgerows for the case of minimum tillage associated with a wind speed reduction of 0·50 is shown in Table 4*d*. Additional water input at the beginning of the vegetation period after the snow-melting period was considered in this scenario. The results showed a yield increase of 9% using ECHAM5 and 6% using HadCM3 (area-weighted average) with respect to the reference management. However, NCAR PCM projected a yield loss of 1% under these conditions. The results also show that the highest yield increase (and the lowest decrease, in the case of NCAR PCM) was simulated for soils 3 and 4. The WUE_{plant} and s.d. is lower, the WUE_{field} is between 3% and −3% and the N leaching would be *c.* 20–26 kg/ha (area-weighted average) higher than for the reference management.

Changing water demand for potential yields

To answer the question of water demand in the future and stabilize winter wheat yields in the studied area, the simulation option 'automatic when required' for irrigation and water management was activated in the model. Baseline conditions, and different climate and management scenarios were simulated with this new option.

The ECHAM5 and HadCM3 scenarios led to similar results concerning any additional water demand to maintain the potential winter wheat yield level. The highest extra amount of water due to climate change (up to 39 mm more water during the growing season) was required for soils 3 and 4 (Table 6). In the baseline scenario, soil 1 already showed relatively low potential yields and a high water demand, while any additional irrigation would not help to obtain better results. Under the applied climate scenarios, the soils with very low water-storage capacity only need slightly more or rather less water to achieve a similar yield than the currently one; thus, water is not predicted be a strong limiting factor in the climate scenarios considered in the present paper for these soils in the case of a winter wheat crop.

An additional amount of 37 mm of water (area-weighted average) during the growing season would be required for the maintenance of the potential yield level according to ECHAM5 and HadCM3 in both tillage scenarios. As the growing season of winter wheat would be >10 days shorter due to higher temperatures and *c*. 7–8 months long, a mean value of up to 37 mm more water required is a significant amount. The range of maximum and minimum water demand is higher under minimum tillage. NCAR PCM, the wettest scenario, predicted the lowest water requirement in the future: 6 mm more for ploughed conditions and 8 mm more for minimum tillage. At the same time, soils 1 and 2 both showed the maximum range with this GCM: this was >100 mm higher than with ECHAM5 or HadCM3. Hedges helped to reduce the water demand, when a wind speed reduction of 0·50 was assumed. ECHAM5 and HadCM3 predicted an additional 29 mm, while NCAR PCM predicted 0 mm under ploughed conditions and −2 mm under minimum tillage (the area-weighted average). Changes of +18 mm using ECHAM5, +20 mm using HadCM3 and −8 mm using NCAR PCM (the area-weighted average) were simulated by minimum tillage, a wind speed reduction of 0·50 and additional water input from melted snow banks. The S.D. was higher than for the baseline for all climate and management scenarios.

DISCUSSION

Climate change is predicted to lead to an increase of 2 °C in the mean air temperature with respect to the baseline period in north-eastern Austria (Fig. 3). The GCMs used in the present study forecast a change of annual precipitation of −15% using ECHAM5, −12% using HadCM3 and +3% using NCAR PCM; these methods predict a strong reduction in rainfall, particularly for the summer months. For the critical spring winter wheat growing period (April–June), ECHAM5 and HadCM3 show a significant reduction in rainfall for June, more than 30% in the scenarios considered in the present paper. Higher annual temperatures will extend the vegetation period, increase CO_2 concentrations, enhance plant growth and consequentially improve the vegetative cover. These advantages might be offset by the increased water stress experienced by specific annual crops, such as winter wheat, during summer and shorter growing periods. A high winter wheat yield loss under future conditions was simulated by ECHAM5 and HadCM3 due to additional crop water stress. However, under the NCAR PCM scenario a yield increase would be expected due to additional precipitation during the spring growing period of winter wheat. At the same time, the interannual yield variability of winter wheat would increase, which would lead to higher economic risks for farmers. The most vulnerable areas, where yield losses can be expected for drier spring conditions, are the regions with low soil water-storage capacity. In this particular case, the additional annual precipitation predicted by NCAR PCM or any additional irrigation would not help to increase the yield in the future.

A common uncertainty in climate change impact-simulation studies for crops is the CO_2-fertilizing effect, which can vary widely under different environmental conditions. For this reason, the simulations took into account the impact of climate change both with and without CO_2 enrichment. The CERES model uses constant multipliers for the daily total crop biomass under elevated CO_2, which are equally applied to both stressed and unstressed growth conditions (Tubiello *et al*. 2007). Free-air CO_2 enrichment experiments have shown a more complex picture. In fact, it is impossible to simulate in detail the high variability due to cultivars and environmental conditions, considering that many processes related to them are still unknown (Kartschall *et al*. 1995; Fuhrer 2003; Kersebaum *et al*. 2008). The present simulations without and with CO_2 enrichment show a high variation in the winter wheat yield, where the yield differences amount to *c*. 10% of the area-weighted average. Related to the interaction between the CO_2 effect and an improved WUE, higher N leaching was simulated in all scenarios, when no CO_2 enrichment was considered.

The only set of adaptations that does not consider irrigation and would lead to higher yields under any GCM (with CO_2 enrichment) compared to the baseline period (area-weighted average), were a combination of minimum tillage and hedgerows, inducing a wind reduction of 0·50 and snow retention. To maintain the baseline yield level, the minimum adaptation to implement is the combination of either minimum tillage and hedgerows (using HadCM3) or minimum tillage, hedgerows and snow retention (using ECHAM5). According to NCAR PCM, any CO_2 enrichment would increase the yield, and no adaptation would be necessary to maintain the baseline yield. Without any CO_2 enrichment, none of the adaptation sets could improve the baseline yield using ECHAM5 or HadCM3, whereas minimum tillage could maintain the yield level using NCAR PCM.

Table 4. *Changes of winter wheat yield (relative), WUE (relative) and N leaching (absolute) for the different climate and management change scenarios* v. *the reference management (=ploughed soil on unsheltered conditions) with CO_2 enrichment as well as* S.D. *(absolute value)*

	ECHAM5								HadCM3								NCAR PCM							
	Yield		WUE_{plant}		WUE_{field}		N leached		Yield		WUE_{plant}		WUE_{field}		N leached		Yield		WUE_{plant}		WUE_{field}		N leached	
	%	S.D.	%	S.D.	%	S.D.	Abs. change	S.D.	%	S.D.	%	S.D.	%	S.D.	Abs. change	S.D.	%	S.D.	%	S.D.	%	S.D.	Abs. change	S.D.
(a) Minimum tillage																								
Soil 1	6·7	1266	−0·5	6·2	4·8	2·8	−6	47·9	7·9	1218	−0·2	6·4	5·9	2·6	−6	37·4	8·1	1369	−0·7	6·1	6·2	2·3	−5·0	37·7
Soil 2	2·2	1808	1·1	6·4	1·5	3·4	−1	36·3	2·5	1665	0·7	6·1	1·7	3·0	−1	49·9	3·1	1730	1·1	5·3	2·2	2·4	−2·0	23·6
Soil 3	0·5	2371	1·7	5·9	0·6	4·2	0	34·7	0·9	2196	1·2	5·3	0·8	3·6	−2	70·5	1·5	1951	0·8	4·5	1·3	2·8	−1·0	30·1
Soil 4	−0·3	2248	1·0	7·0	0·1	4·1	−1	9·5	−0·6	2051	0·3	6·3	−0·3	3·5	−1	63·3	0·6	1818	0·0	5·0	0·7	2·5	−2·0	13·3
Area-weighted average	*0·7*		*1·4*		*0·7*		*−0·5*		*0·9*		*0·9*		*0·8*		*−1·7*		*1·7*		*0·6*		*1·4*		*−1·4*	
(b) Plough + wind speed reduction 0·50																								
Soil 1	1·5	1160	−1·6	6·0	2·8	2·7	−1	45·3	1·1	1106	−1·6	5·8	2·4	2·4	0	33·3	0·9	1246	−1·5	6·0	2·1	2·3	0·0	36·7
Soil 2	2·6	1585	−0·2	5·1	3·5	3·0	−1	27·4	2·2	1469	−0·5	4·9	3·1	2·6	0	42·1	1·3	1648	0·2	4·5	2·5	2·4	1·0	23·7
Soil 3	3·3	2064	0·3	5·6	4·0	3·7	−1	29·4	3·2	1872	0·3	4·8	3·9	3·2	0	60·0	2·1	1747	0·7	4·1	3·2	2·4	1·0	26·7
Soil 4	3·2	1959	0·3	5·6	3·9	3·5	1	11·7	3·4	1787	0·3	5·0	4·0	2·9	0	54·0	1·7	1621	0·8	4·2	2·8	2·2	1·0	16·7
Area-weighted average	*3·1*		*0·2*		*3·9*		*−0·6*		*3·1*		*0·1*		*3·8*		*0·0*		*1·9*		*0·6*		*3·0*		*1·0*	
(c) Minimum tillage + wind speed reduction 0·50																								
Soil 1	10·2	1221	−1·2	6·0	9·5	2·7	−8	42·2	9·1	1194	−1·6	6·2	8·5	2·6	−6	35·5	9·1	1387	−1·9	6·0	8·4	2·4	−5·0	36·0
Soil 2	5·2	1713	0·9	5·7	5·3	3·2	−2	31·7	4·8	1586	0·5	5·7	4·9	2·9	−1	47·3	5·4	1686	1·3	4·8	5·5	2·3	−1·0	23·4
Soil 3	4·4	2240	1·9	6·5	5·1	4·1	−1	30·0	4·1	2059	1·5	4·9	4·7	3·4	−1	66·3	4·1	1830	2·2	4·2	5·0	2·6	−1·0	28·0
Soil 4	3·3	2099	1·0	6·4	4·2	3·8	−1	10·6	3·1	1948	1·1	6·0	4·0	3·3	−1	59·1	2·5	1716	0·7	4·7	3·6	2·4	−1·0	14·9
Area-weighted average	*4·4*		*1·5*		*5·0*		*−1·3*		*4·1*		*1·2*		*4·6*		*−1·1*		*4·0*		*1·7*		*4·8*		*−1·1*	
(d) Minimum tillage + wind speed reduction 0·50 + snow retention																								
Soil 1	−1·0	1033	−4·8	5·3	−3·2	2·2	7	38·6	−3·4	1012	−4·0	5·7	−5·0	2·2	10	29·7	−2·8	1204	−3·5	6·0	−3·8	2·1	9·0	35·1
Soil 2	2·6	1288	−3·4	4·4	−1·3	2·3	16	31·4	−0·4	1306	−3·3	5·3	−3·2	2·4	20	35·4	−2·4	1465	−0·5	4·1	−3·6	2·0	21·0	31·8
Soil 3	9·8	1350	−3·0	3·4	3·4	2·2	21	35·4	6·6	1284	−3·1	3·5	1·2	2·1	25	40·8	−0·8	1452	−0·8	3·6	−2·3	2·0	29·0	40·2
Soil 4	11·8	1177	−2·4	3·2	4·7	2·0	19	25·8	9·3	1161	−1·8	3·4	3·3	1·9	22	34·0	−1·3	1403	−1·1	4·2	−2·6	1·9	23·0	29·2
Area-weighted average	*9·0*		*−3·0*		*2·9*		*19·6*		*6·0*		*−2·9*		*0·9*		*23·3*		*−1·2*		*−0·9*		*−2·6*		*26·1*	

Table 5. *Soil water content (=precipitation–runoff – drainage) on ploughed and minimum tillage soil (mean, s.d., max, min) in the future scenario as well as relative change (%) of soil water content if ploughing were to be replaced by minimum tillage, from sowing until harvest*

		ECHAM5	HadCM3	NCAR PCM	ECHAM5	HadCM3	NCAR PCM	ECHAM5	HadCM3	NCAR PCM
		Plough (mm)			Minimum tillage (mm)			Change of soil water content (%)		
Soil 1	Mean	275	280	288	282	285	292	2·4	2·0	1·7
	s.d.	45·9	45·9	45·0	48·0	47·1	47·0			
	Max	372	379	375	380	384	385			
	Min	159	172	170	162	173	170			
Soil 2	Mean	315	322	324	316	323	329	0·2	0·4	1·3
	s.d.	58·8	57·5	59·0	60·2	58·8	60·5			
	Max	446	446	460	454	456	464			
	Min	168	173	170	158	164	170			
Soil 3	Mean	332	341	342	332	340	348	−0·1	−0·4	1·9
	s.d.	70·5	70·0	84·7	69·5	69·4	71·7			
	Max	492	510	505	478	492	511			
	Min	158	164	−122	158	162	168			
Soil 4	Mean	337	347	355	335	345	357	−0·8	−0·3	0·6
	s.d.	73·2	73·6	75·9	71·8	72·1	74·6			
	Max	496	507	530	499	501	517			
	Min	158	164	173	157	162	173			
Area-weighted average								*−0·1*	*−0·3*	*1·5*

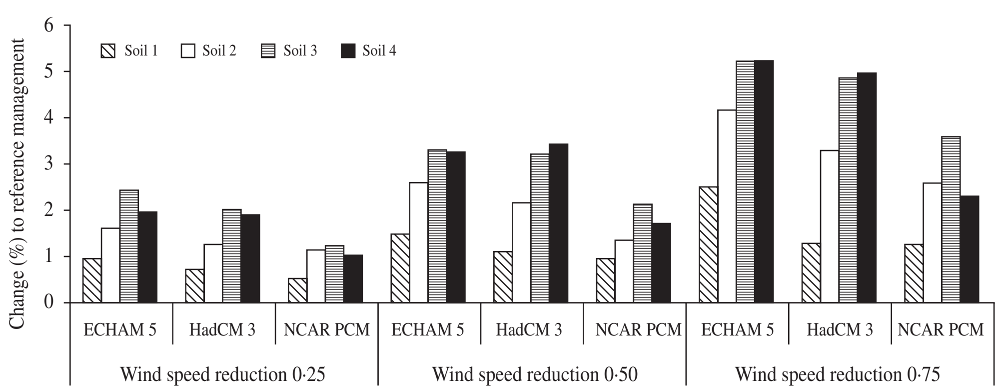

Fig. 6. Relative changes (%) of winter wheat yield in the future scenario with wind speed reductions of 0·25, 0·50 and 0·75 due to hedges on ploughed fields *v*. the reference management.

The set of adaptation applied in the first two GCMs can only help to reduce negative climate change effects.

The simulated multiple effects of potential adaptation options under climate scenarios, simulated for the next few decades for winter wheat, clarified several aspects that may be useful for decision makers to increase the resilience of winter wheat-dominated cropping systems in the semi-arid Marchfeld region. These aspects are summarized as follows. The introduction of minimum tillage improved crop water supply and decreased unproductive water losses due to a higher plant-available water-storage capacity in the soil, in particular for soils 1 and 2 where a change in tillage practices could help reduce yield losses in the near future. Additionally, higher soil water contents and WUE and reduced N leaching rates could be expected.

A change in the landscape structure, such as the introduction of windbreaks or hedges, influenced the microclimate of crops in neighbouring fields, mainly by slowing down the wind speed. Further effects were: an increased dew formation and leaf-wetness duration

Table 6. *Simulated winter wheat water demand (mm) for the baseline period (mean, S.D., max, min), changes of water demand (absolute) under the different climate and management scenarios* v. *baseline as well as S.D., max and min*

	Baseline											
	Mean	S.D. (mm)	Max	Min								
Soil 1	190	41·0	269	50								
Soil 2	112	36·7	170	0								
Soil 3	93	36·8	199	0								
Soil 4	80	38·6	177	0								
Area-weighted average	*94·5*	*37·3*	*191*	*1·0*								
	ECHAM5				HadCM3				NCAR PCM			
	Abs. change	S.D.	Max	Min	Abs. change	S.D.	Max	Min	Abs. change	S.D.	Max	Min
Plough												
Soil 1	11	41·9	317	75	9	43·5	316	75	−8	48·9	455	75
Soil 2	34	44·8	237	0	33	46·1	240	0	2	49·3	367	0
Soil 3	39	46·1	222	0	38	47·3	225	0	6	44·8	286	0
Soil 4	36	48·9	277	0	33	48·3	237	0	7	45·7	234	0
Area-weighted average	*37*	*46·5*	*238*	*1·4*	*36*	*47·3*	*232*	*1·4*	*6*	*45·7*	*290*	*1·4*
Minimum tillage												
Soil 1	12	43·7	328	60	14	45·2	321	56	−8	51·8	431	55
Soil 2	37	45·9	257	0	34	48·0	259	0	4	50·9	360	0
Soil 3	37	48·8	278	0	37	47·8	244	0	9	46·9	273	0
Soil 4	39	52·6	264	0	39	53·4	256	0	11	52·1	259	0
Area-weighted average	*37*	*49·1*	*273*	*1·1*	*37*	*49·0*	*250*	*1·1*	*8*	*48·8*	*286*	*1·0*
Plough + wind speed reduction 0·50												
Soil 1	2	41·7	294	76	2	41·9	294	50	−14	47·9	429	75
Soil 2	28	44·0	242	0	27	43·5	240	0	−3	47·3	361	0
Soil 3	30	46·1	217	0	31	47·9	223	0	0	45·7	286	0
Soil 4	29	48·1	240	0	29	50·4	273	0	4	46·1	199	0
Area-weighted average	*29*	*46·2*	*227*	*1·4*	*29*	*47·7*	*238*	*1·0*	*0*	*46·1*	*281*	*1·4*
Minimum tillage + wind speed reduction 0·50												
Soil 1	4	43·3	321	59	7	41·8	319	56	−16	47·9	398	56
Soil 2	28	43·7	249	0	29	43·6	234	0	−5	47·3	358	0
Soil 3	29	46·7	236	0	29	46·0	241	0	−3	46·8	274	0
Soil 4	32	51·9	260	0	30	52·3	263	0	2	49·0	221	0
Area-weighted average	*29*	*47·3*	*245*	*1·1*	29	*47·0*	*246*	*1·1*	*−2*	*47·4*	*277*	*1·1*
Minimum tillage + wind speed reduction 0·50 + snow retention												
Soil 1	−6	41·5	292	86	−3	41·8	291	56	−27	50·7	399	56
Soil 2	17	43·2	226	0	20	45·0	226	0	−11	44·0	324	0
Soil 3	20	46·3	238	0	21	46·9	279	0	−8	45·5	312	0
Soil 4	16	47·0	258	0	19	50·7	265	0	−7	46·3	216	0
Area-weighted average	*18*	*45·9*	*242*	*1·6*	*20*	*47·4*	*268*	*1·1*	*−8*	*45·5*	*294*	*1·1*

and a reduction of dry air advection, evapotranspiration, unproductive water loss and wind erosion (Cleugh *et al.* 1998; Mayus *et al.* 1999). All these effects are expected to result in an increase of crop yields under semi-arid climate. However, increased leaf-wetness duration may cause a higher incidence of crop diseases, an effect, which was not considered in the model.

The present simulations, which include different wind speed-reduction effects, confirm these often-reported positive effects. This is especially true for soils 3 and 4, which are the prevailing soil conditions in

Marchfeld. Higher winter wheat yield and soil water content associated with lower N leaching, were simulated here.

A combination of different adaptation options could further increase the positive effects on the winter wheat yield. For example, a yield increase of up to 4% (area-weighted average) and a lower N leaching rate (compared to the reference management) were simulated under the combination of minimum tillage with hedgerows considering a wind speed reduction of 0·50.

An additional effect of windbreaks could also have a positive impact on the crop yield through an improved soil water budget in the spring (Kuemmel 2003). In particular, this positive yield effect was due to an additional water input at the beginning of the vegetation period under the ECHAM5 and HadCM3 scenarios with reduced spring precipitation. Even though a higher yield was simulated in this case, negative side effects such as a higher N leaching rate and a lower WUE were also found. This demonstrates that a combination of several adaptation options does not necessarily provide positive effects but can also result in negative effects that need to be carefully evaluated under the specific local conditions (Olesen *et al.* 2011).

The water demand was projected to increase (under most of the future climate scenarios) in order to maintain similar yield levels compared to actual conditions. However, the present study has shown that the additional water demand could also be effectively reduced with adaptation strategies other than irrigation. Negative side effects should also be taken into account. This includes the N leaching rate, which could increase up to 300% on soil 4, with regard to the baseline conditions with optimum irrigation.

Transferring into practice the findings of this study requires further research and scientific efforts, and should be addressed especially in the field of crop and climate change modelling.

The contribution by Dr Trnka was supported by the Research Plan No. MSM6215648905, 'Biological and technological aspects of sustainability of controlled ecosystems and their adaptability to climate change' and KONTAKT project no. LH11010. The development of the climate-change scenarios (by M. Dubrovsky) were funded by the project IAA300420806, sponsored by the Grant Agency of Academy of Sciences of CR.

REFERENCES

Alexandrov, V. A., Eitzinger, J., Cajic, V. & Oberforster, M. (2002). Potential impact of climate change on selected agricultural crops in north-eastern Austria. *Global Change Biology* **8**, 372–389.

Alexandrov, V. A. & Hoogenboom, G. (2000). The impact of climate variability and change on crop yield in Bulgaria. *Agricultural and Forest Meteorology* **104**, 315–327.

Allen, R. G., Pereira, L. S., Raes, D. & Smith, M. (1998). *Crop Evapotranspiration: Guidelines for Computing Crop Water Requirements*. FAO Irrigation and Drainage Paper 56. Rome, Italy: FAO.

Amthor, J. S. (2001). Effects of atmospheric CO_2 concentration on wheat yield: review of results from experiments using various approaches to control CO_2 concentration. *Field Crops Research* **73**, 1–34.

Brenner, A. J. (1996). Microclimate modifications in agroforestry. In *Tree-Crop Interactions* (Eds C. K. Ong & P. Huxley), pp. 159–187. Oxon, UK: CAB International.

Brenner, A. J., Jarvis, P. G. & Van Den Beldt, R. (1995). Windbreak–crop interactions in the Sahel. 2. Crop response of millet in shelter. *Agricultural and Forest Meteorology* **75**, 235–262.

BFW – Bundesforschungs- und Ausbildungszentrum für Wald, Naturgefahren und Landschaft (2007). *Digitale Bodenkarte von Österreich*. Vienna: BFW.

Challinor, A. (2011). Forecasting food. *Nature Climate Change* **1**, 103–104.

Chen, C. C. & McCARL, B. A. (2001). An investigation of the relationship between pesticide usage and climate change. *Climatic Change* **50**, 475–487.

Cepuder, P. (1999). Zur Nitratproblematik in Ostösterreich, dem Tullner Feld, dem Marchfeld und dem nördlichen Burgenland. In *BAL – Bericht Nr. 8* (Ed. Bundesanstalt für Alpenländische Landwirtschaft), pp. 1–4. Gumpenstein, Austria: Eigenverlag.

Cepuder, P. & Schlederer, W. (2002). *Untersuchung der Grundwasserbelastung mit Nitrat unter Feldgemüsebau im pannonischen Klimaraum. Endbericht*. Vienna: Bundesministeriums für Land- und Forstwirtschaft.

Cleugh, H. A., Miller, J. & Bohm, M. (1998). Direct mechanical effects of wind on crops. *Agroforestry Systems* **41**, 85–112.

Curry, R. B., Peart, R. M., Jones, J. W., Boote, K. J. & Allen, L. H. (1990). Simulation as a tool for analyzing crop response to climate change. *Transactions of the American Society of Agricultural Engineers* **33**, 981–990.

Davies, W. J., Zhang, J., Yang, J. & Dodd, I. C. (2011). Novel crop science to improve yield and resource use efficiency in water-limited agriculture. *Journal of Agricultural Science, Cambridge* **149** (Suppl. 1), 123–131.

Dubrovsky, M. (1997). Creating daily weather series with use of the weather generator. *Environmetrics* **8**, 409–424.

Dubrovsky, M., Zalud, Z. & Stastna, M. (2000). Sensitivity of CERES-Maize yields to statistical structure of daily weather series. *Climatic Change* **46**, 447–472.

Dubrovsky, M., Buchtele, J. & Zalud, Z. (2004). High-frequency and low-frequency variability in stochastic daily weather generator and its effect on agricultural and hydrologic modelling. *Climatic Change* **63**, 145–179.

Dubrovsky, M., Nemesova, I. & Kalvova, J. (2005). Uncertainties in climate change scenarios for the Czech Republic. *Climate Research* **29**, 139–156.

Dubrovsky, M., Svoboda, M. D., Trnka, M., Hayes, M. J., Wilhite, D. A., Zalud, Z. & Hlavinka, P. (2008). Application of relative drought indices in assessing climate-change impacts on drought conditions in Czechia. *Theoretical and Applied Climatology* **96**, 155–171.

Eitzinger, J., Formayer, H., Thaler, S., Trnka, M., Zdenek, Z. & Alexandrov, V. (2008). Results and uncertainties of climate change impact research in agricultural crop production in Central Europe. *Die Bodenkultur* **59**, 131–147.

Eitzinger, J., Orlandini, S., Stefanski, R. & Naylor, R. E. L. (2010). Climate change and agriculture: introductory editorial. *Journal of Agricultural Science, Cambridge* **148**, 499–500.

Eitzinger, J., Stastná, M., Zalud, Z. & Dubrovsky, M. (2003). A simulation study of the effect of soil water balance and water stress on winter wheat production under different climate change scenarios. *Agricultural Water Management* **61**, 195–217.

Falloon, P. & Betts, R. (2010). Climate impacts on European agriculture and water management in the context of adaptation and mitigation – the importance of an integrated approach. *Science of the Total Environment* **408**, 5667–5687.

Fuhrer, J. (2003). Agroecosystem responses to combinations of elevated CO_2, ozone and global climate change. *Agriculture, Ecosystems and Environment* **97**, 1–20.

Gerersdorfer, T., Eitzinger, J. & Rischbeck, P. (2009). Simulation of crop yield near hedgerows under aspects of a changing climate – an Austrian attempt. In *Climate Variability, Modeling Tools and Agricultural Decision-Making* (Ed. A. Utset), pp. 321–330. Hauppauge, NY: Nova Science Publishers.

Ghaffari, A., Cook, H. F. & Lee, H. C. (2002). Climate change and winter wheat management: a modelling scenario for south-eastern England. *Climatic Change* **55**, 509–533.

Godwin, D. C. & Jones, C. A. (1991). Nitrogen dynamics in soil-plant systems. In *Modeling Plant and Soil Systems*. Agronomy Monograph No. 31 (Eds J. Hanks & J. T. Ritchie), pp. 287–321. Madison, WI: ASA, CSSA & SSSA.

Godwin, D. C. & Singh, U. (1998). Nitrogen balance and crop response to nitrogen in upland and lowland cropping systems. In *Understanding Options for Agricultural Production. System Approaches for Sustainable Agricultural Development* (Eds G. Y. Tsuji, G. Hoogenboom & P. K. Thornton), pp. 55–77. Dordrecht, The Netherlands: Kluwer Academic Publishers.

Hall, A. E. (2001). *Crop Responses to Environment*. Boca Raton, FL: CRC Press LLC.

Harvey, L. D. D., Gregory, J., Hoffert, M., Jain, A., Lal, M., Leemans, R., Raper, S. B. C., Wigley, T. M. L. & De Wolde, J. (1997). *An Introduction to Simple Climate Models used in the IPCC Second Assessment Report. IPCC Technical Paper 2* (Eds J. T. Houghton, L. G. Meira Filho, D. J. Griggs & M. Noguer). Geneva, Switzerland: IPCC.

Hathfield, J. L. (1979). Canopy temperatures: the usefulness and reliability of remote measurements. *Agronomy Journal* **71**, 889–892.

Hlavinka, P., Eitzinger, J., Smutny, V., Thaler, S., Zhalud, Z., Rischbeck, P. & Kren, J. (2010). The performance of CERES-Barley and CERES-Wheat under various soil conditions and tillage practices in Central Europe. *Bodenkultur* **61**, 9–21.

Hulme, M., Wigley, T. M. L., Barrow, E. M., Raper, S. C. B., Centella, A., Smith, S. & Chipanshi, A. C. (2000). *Using a Climate Scenario Generator for Vulnerability and Adaptation Assessments: Magicc and SCENGEN Version 2.4 Workbook*. Norwich, UK: Climatic Research Unit.

Hunt, L. A., Pararajasingham, S., Jones, J. W., Hoogenboom, G., Imamura, D. T. & Ogoshi, R. M. (1993). Gencalc: software to facilitate the use of crop models for analyzing field experiments. *Agronomy Journal* **85**, 1090–1094.

Hunt, L. A., White, J. W. & Hoogenboom, G. (2001). Agronomic data: advances in documentation and protocols for exchange and use. *Agricultural Systems* **70**, 477–492.

Iqbal, M. A., Eitzinger, J., Formayer, H., Hassan, A. & Heng, L. K. (2011). A simulation study for assessing yield optimization and potential for water reduction for summer-sown maize under different climate change scenarios. *Journal of Agricultural Science, Cambridge* **149**, 129–143.

Jones, J. W., Hoogenboom, G., Porter, C. H., Boote, K. J., Batchelor, W. D., Hunt, L. A., Wilkens, P. W., Singh, U., Gijsman, A. J. & Ritchie, J. T. (2003). The DSSAT cropping system model. *European Journal of Agronomy* **18**, 235–265.

Jones, J. W., Keating, B. A. & Porter, C. H. (2001). Approaches to modular model development. *Agricultural Systems* **70**, 421–443.

Kartschall, T., Grossman, S., Pinter, P. J., Garcia, R. L., Kimball, B. A., Wall, G. W., Hunsaker, D. J. & Lamorte, R. L. (1995). A simulation of phenology, growth, carbon dioxide exchange and yields under ambient atmosphere and free-air carbon dioxide enrichment (FACE) Maricopa, Arizona, for wheat. *Journal of Biogeography* **22**, 611–622.

Kaukoranta, T. & Hakala, K. (2008). Impact of spring warming on sowing times of cereal, potato and sugar beet in Finland. *Agricultural and Food Science* **17**, 165–176.

Kersebaum, K. C., Nendel, C., Mirschel, W., Manderscheid, R., Weigel, H.-J. & Wenkel, K.-O. (2008). Testing different CO2 response algorithms against a FACE crop rotation experiment and application for climate change impact assessment on different sites in Germany. In *Symposium on Climate Change and Variability – Agro-meteorological Monitoring and Coping Strategies for Agriculture, 3–6 June 2008, Oscarsborg, Norway. Book of Abstracts* (Eds T. H. Sivertsen, A. O. Skjelvåg, S. Orlandini, M. V. K. Sivakumar, J. Eitzinger, P. Nejedlik, V. Alexandrov, L. Toulios, P. Calanca, R. Stefanski, R. Motha, M. Gamedze, M. Trnka, W. Smith & J. Netland), p. 30. Ås, Norway: Bioforsk.

Klik, A. & Eitzinger, J. (2010). Impact of climate change on soil erosion and the efficiency of soil conservation practices in Austria. *Journal of Agricultural Science, Cambridge* **148**, 529–541.

KovácS, G. J., Németh, T. & Ritchie, J. T. (1995). Testing simulation models for the assessment of crop production and nitrate leaching in Hungary. *Agricultural Systems* **49**, 385–397.

Kristensen, K., Schelde, K. & Olesen, J. E. (2011). Winter wheat yield response to climate variability in Denmark. *Journal of Agricultural Science, Cambridge* **149**, 33–47.

Kuemmel, B. (2003). Theoretical investigation of the effects of field margin and hedges on crop yields. *Agriculture, Ecosystems and Environment* **95**, 387–392.

Linke, R., Pfundtner, E., Bolhar-Nordenkampf, H. R., Dersch, G. & Meister, M. (2005). Crops and climate change: influences of changed growth conditions on water relations and yield of different cultural crops. *Mitteilungen der Gesellschaft für Pflanzenbauwissenschaften* **17**, 313–314.

Martínez, E., Fuentes, J.-P., Silva, P., Valle, S. & Acevedo, E. (2008). Soil physical properties and wheat root growth as affected by no-tillage and conventional tillage systems in a Mediterranean environment of Chile. *Soil and Tillage Research* **99**, 232–244.

Mayus, M., Van Keulen, H. & Stroosnijder, L. (1999). A model of tree-crop competition for windbreak systems in the Sahel: description and evaluation. *Agroforestry Systems* **43**, 183–201.

Morison, J. I. L. & Lawlor, D. W. (1999). Interactions between increasing CO_2 concentration and temperature on plant growth. *Plant, Cell and Environment* **22**, 659–682.

Müller, W. (1993). *Agroklimatische Kennzeichnung des Marchfelds, Beiheft 3 zu den Jahrbüchern der Zentralanstalt für Meteorologie und Geodynamik*. Vienna: Eigenverlag.

Nakicenovic, N. & Swart, R. (2000). *Emissions Scenarios – A Special Report of Working Group III of the Intergovernmental Panel on Climate Change*. Cambridge: Cambridge University Press.

Nijbroeka, R., Hoogenboomb, G. & Jonesa, J. W. (2003). Optimizing irrigation management for a spatially variable soybean field. *Agricultural Systems* **76**, 359–377.

Nuberg, I. K. (1998). Effect of shelter on temperate crops: a review to define research for Australian conditions. *Agroforestry Systems* **41**, 3–34.

Oberforster, M. & Werteker, M. (2009). Relative Vorzüglichkeit verschiedener Weizensorten in Abhängigkeit von Ertrag, Qualität und Erzeugerpreisen. In *Werte – Wege – Wirkungen: Biolandbau im Spannungsfeld zwischen Ernährungssicherung, Markt und Klimawandel. Beiträge zur 10. Wissenschaftstagung zum Ökologischer Landbau, Zurich, 11–13 February 2009. Band 2: Tierhaltung, Agrarpolitik und Betriebswirtschaft, Märkte und Lebensmittel* (Eds H. von Jochen Mayer, T. Alföldi, F. Leiber, D. Dubois, P. Fried, F. Heckendorn, E. Hillmann, P. Klocke, A. Lüscher, S. Riedel, M. Stolze, F. Strasser, M. van der Heijden & H. Willer), pp. 302–305.

Olesen, J. E., Carter, T. R., Diaz-Ambrona, C. H., Fronzek, S., Heidmann, T., Hickler, T., Holt, T., Minguez, M. I., Morales, P., Palutikov, J., Quemada, M., Ruiz-Ramos, M., Rubæk, G., Sau, F., Smith, B. & Sykes, M. (2007). Uncertainties in projected impacts of climate change on European agriculture and ecosystems based on scenarios from regional climate models. *Climatic Change* **81** (Supp. 1), 123–143.

Olesen, J. E., Trnka, M., Kersebaum, K. C., Skjelvåg, A. O., Seguin, B., Peltonen-Sainio, P., Rossi, F., Kozyra, J. & Micale, F. (2011). Impacts and adaptation of European crop production systems to climate change. *European Journal of Agronomy* **34**, 96–112.

Orlandini, S., Nejedlik, P., Eitzinger, J., Alexandrov, V., Toulios, L., Calanca, P., Trnka, M. & Olesen, J. E. (2008). Impacts of climate change and variability on European agriculture: results of inventory analysis in COST 734 countries. *Annals of the New York Academy of Sciences* **1146**, 338–353.

Osunbitan, J. A., Oyedele, D. J. & Adekalu, K. O. (2005). Tillage effects on bulk density, hydraulic conductivity and strength of a loamy sand soil in southwestern Nigeria. *Soil and Tillage Research* **82**, 57–64.

Palosuo, T., Kersebaum, K. C., Angulo, C., Hlavinka, P., Moriondo, M., Olesen, J. E., Patil, R. H., Ruget, F., Rumbaur, C., Takac, J., Trnka, M., Bindi, M., Caldag, B., Ewert, F., Ferrise, R., Mirschel, W., Saylan, L., Siska, B. & Rötter, R. (2011). Simulation of winter wheat yield and its variability in different climates of Europe: a comparison of eight crop growth models. *European Journal of Agronomy* **35**, 103–114.

Patil, R. H., Laegdsmand, M., Olesen, J. E. & Porter, J. R. (2010). Growth and yield response of winter wheat to soil warming and rainfall patterns. *Journal of Agricultural Science, Cambridge* **148**, 553–566.

Peart, R. M., Jones, J. W., Curry, R. B., Boote, K. J. & Allen, L. H. (1989). Impact of climate change on crop yield in the southwestern USA: a simulation study. In *The Potential Effects of Global Climate Change on the United States*, Vol. 1 (Eds J. B. Smith & D. A. Tirpak), pp. 1–54. Washington, DC: USEPA.

Penman, H. L. (1948). Natural evaporation from open water, bare soil and grass. *Proceedings of the Royal Society of London A: Mathematical and Physical Sciences* **193**, 120–145.

Penman, H. L. (1963). *Vegetation and Hydrology*. Technical Communication No. 53. Harpenden, UK: Commonwealth Bureau of Soils.

Rischbeck, P. M. (2007). Der Einfluss von Klimaänderung, Bodenbearbeitung und Saattermin auf den Wasserhaus halt und das Ertragspotential von Getreide im Marchfeld. Ph.D. Thesis, University of Natural Resources and Life Sciences, Vienna, Austria.

Rötter, R. P., Carter, T. R., Olesen, J. E. & Porter, J. R. (2011). Crop-climate models need an overhaul. *Nature Climate Change* **1**, 175–177.

Rowe, E. C., Van Noordwijk, M., Suprayogo, D. & Cadisch, G. (2005). Nitrogen use efficiency of monoculture and hedgerow intercropping in the humid tropics. *Plant and Soil* **268**, 61–74.

SEO, S. N. (2011). A geographically scaled analysis of adaptation to climate change with spatial models using agricultural systems in Africa. *Journal of Agricultural Science, Cambridge* **149**, 437–449.

SHAHABFAR, A. & EITZINGER, J. (2011). Agricultural drought monitoring in semi-arid and arid areas using MODIS data. *Journal of Agricultural Science, Cambridge* **149**, 403–414.

SINGH, A. K., TRIPATHY, R. & CHOPRA, U. K. (2008). Evaluation of CERES-Wheat and CropSyst models for water–nitrogen interactions in wheat crop. *Agricultural Water Management* **95**, 776–786.

SOLOMON, S., QIN, D., MANNING, M., CHEN, Z., MARQUIS, M., AVERYT, K. B., TIGNOR, M. & MILLER, H. L. (2007). *Climate Change 2007. Working Group I: The Physical Science Basis*. Cambridge, UK: Cambridge University Press.

THALER, S., EITZINGER, J., RISCHBECK, P., DUBROVSKY, M. & TRNKA, M. (2010). Vulnerability of crops to climate change in Northeastern Austria. *Bulgarian Journal of Meteorology and Hydrology* **15**, 50–61.

TIMSINA, J., SINGH, U., BADARUDDIN, M. & MEISNER, C. (1998). Cultivar, nitrogen, and moisture effects on a rice–wheat sequence: experimentation and simulation. *Agronomy Journal* **90**, 119–130.

TRNKA, M., DUBROVSKY, M. & ZALUD, Z. (2004*a*). Climate change impacts and adaptation strategies in spring barley production in the Czech Republic. *Climatic Change* **64**, 227–255.

TRNKA, M., DUBROVSKY, M., SEMERÁDOVÁ, D. & ZALUD, Z. (2004*b*). Projections of uncertainties in climate change scenarios into expected winter wheat yields. *Theoretical and Applied Climatology* **77**, 229–249.

TRNKA, M., EITZINGER, J., DUBROVSKY, M., SEMERADOVA, D., STEPANEK, P., HLAVINKA, P., BALEK, J., SKALAK, P., FARDA, A., FORMAYER, H. & ZALUD, Z. (2010*a*). Is rainfed crop production in central Europe at risk? Using a regional climate model to produce high resolution agroclimatic information for decision makers. *Journal of Agricultural Science, Cambridge* **148**, 639–656.

TRNKA, M., EITZINGER, J., SEMERÁDOVÁ, D., HLAVINKA, P., BALEK, J., DUBROVSKÝ, M., KUBU, G., ŠTEPÁNEK, P., THALER, S., MOŽNÝ, M. & ŽALUD, Z. (2011*a*). Expected changes in agroclimatic conditions in Central Europe. *Climatic Change* **108**, 261–289.

TRNKA, M., KOCMANKOVA, E., BALEK, J., EITZINGER, J., RUGET, F., FORMAYER, H., HLAVINKA, P., SCHAUMBERGER, A., HORAKOVA, V., MOZNY, M. & ZALUD, Z. (2010*b*). Simple snow cover model for agrometeorological applications. *Agricultural and* Forest Meteorology **150**, 1115–1127.

TRNKA, M., OLESEN, J. E., KERSEBAUM, K.-C., SKJELVAG, A. O., EITZINGER, J., SEGUIN, B., PELTONEN-SAINIO, P., RÖTTER, R., IGLESIAS, A., ORLANDINI, S., DUBROWSKY, M., HLAVINKA, P., BALEK, J., ECKERSTEN, H., CLOPPET, E., CALANCA, P., GOBIN, A., VUCETIC, V., NEJEDLIK, P., KUMAR, S., LALIC, B., MESTRE, A., ROSSI, F., KOZYRA, J., ALEXANDROV, V., SEMERÁDOVÁ, D. & ŽALUD, Z. (2011*b*). Agroclimatic conditions in Europe under climate change. *Global Change Biology* **17**, 2298–2318.

TUBIELLO, F. N., AMTHOR, J. S., BOOTE, K. J., DONATELLI, M., EASTERLING, W., FISCHER, G., GIFFORD, R. M., HOWDEN, M., REILLY, J. & ROSENZWEIG, C. (2007). Crop response to elevated CO2 and world food supply. A comment on 'Food for Thought...' by Long *et al.*, Science 312:1918–1921, 2006. *European Journal of Agronomy* **26**, 215–223.

TUBIELLO, F. N., DONATELLI, M., ROSENZWEIG, C. & STOCKLE, C. O. (2000). Effects of climate change and elevated CO_2 on cropping systems: model predictions at two Italian locations. *European Journal of Agronomy* **13**, 179–189.

TSUJI, G., HOOGENBOOM, G. & THORNTON, P. (1998). *Understanding Options for Agricultural Production*. Dordrecht, The Netherlands: Kluwer Academic Publishers.

UHLIR, P. F. & CARTER, G. C. (1994). *Crop Modelling and Related Environmental Data, a Focus on Applications for Arid and Semiarid Regions in Developing Countries*. Paris, France: CODATA – Commission on Global Change Data.

Journal of Agricultural Science (2013), **151**, 787–812. © Cambridge University Press 2012
doi:10.1017/S0021859612000767

CLIMATE CHANGE AND AGRICULTURE RESEARCH PAPER

Regional climate change impacts on agricultural crop production in Central and Eastern Europe – hotspots, regional differences and common trends

J. EITZINGER[1,2]*, M. TRNKA[2,3], D. SEMERÁDOVÁ[2], S. THALER[1], E. SVOBODOVÁ[2,3], P. HLAVINKA[3], B. ŠIŠKA[4], J. TAKÁČ[5], L. MALATINSKÁ[4], M. NOVÁKOVÁ[5], M. DUBROVSKÝ[2,6] AND Z. ŽALUD[2,3]

[1] *Institute of Meteorology, University of Natural Resources and Life Sciences, Vienna, Austria*
[2] *CzechGlobe – Global Change Research Centre AS CR, v.v.i., 986/4a, 603 00 Brno, Czech Republic*
[3] *Institute of Agrosystems and Bioclimatology, Mendel University Brno, Czech Republic*
[4] *Department of Ecology, Slovak University of Agriculture, Nitra, Slovakia*
[5] *Soil Science and Conservation Research Institute, Bratislava, Slovakia*
[6] *Institute of Atmospheric Physics Czech Academy of Sciences, Prague, Czech Republic*

(*Received 7 March 2012; revised 28 June 2012; accepted 2 August 2012; first published online 9 October 2012*)

SUMMARY

The present study investigates regional climate change impacts on agricultural crop production in Central and Eastern Europe, including local case studies with different focuses in Austria, the Czech Republic and Slovakia. The area studied experiences a continental European climate and is characterized by strong climatic gradients, which may foster regional differences or trends in the impacts of climate change on agriculture. To study the regional aspects and variabilities of climate change impacts on agriculture, the effect of climate change on selected future agroclimatic conditions, crop yield and variability (including the effect of higher ambient CO_2 concentrations) and the most important yield limiting factors, such as water availability, nitrogen balance and the infestation risks posed by selected pests were studied. In general, the results predicted significant agroclimatic changes over the entire area during the 21st century, affecting agricultural crop production through various pathways. Simulated crop yield trends confirmed past regional studies but also revealed that yield-limiting factors may change from region to region. For example, pest pressures, as demonstrated by examining two pests, are likely to increase due to warmer conditions. In general, higher potentials for cereal yield increase are seen for wetter and cooler regions (i.e. uplands) than for the drier and warmer lowlands, where yield potentials will be increasingly limited by decreasing crop water availability and heat under most scenarios. In addition, yield variability will increase during the coming decades, but this may decrease towards the end of the 21st century. The present study contributes to the interpretation of previously conducted climate change impact and adaptation studies for agriculture and may prove useful in proposing future research in this field.

INTRODUCTION

In agriculture, projected climatic changes will affect crop yields, livestock management and the location of production in Europe (Olesen & Bindi 2002). Climate change will affect crop growing processes not only directly through changed agroclimatic conditions (Eitzinger *et al.* 2003; Trnka *et al.* 2011*a*, *b*) but also indirectly, e.g. by changing soil properties that affect soil water and nutrient balance (M. Trnka *et al.*, personal communication) or by changing pest, disease and weed occurrence (Porter *et al.* 1991), resulting in altered yield potentials that are crop-specific. Further, the increasing likelihood and severity of extreme weather events (especially heat waves, droughts and heavy precipitation) can considerably increase the risk of crop failure and enhance yield variability (Peltonen-Sainio *et al.* 2010; Semenov & Shewry 2011). In

* To whom all correspondence should be addressed. Email: josef.eitzinger@boku.ac.at

particular, climate change will cause significant changes in the quality and availability of water resources for crop irrigation (IPCC 2011; Iqbal *et al.* 2011; Thaler *et al.* 2012), affecting food production and security; in this scenario, the occurrence of extreme events such as droughts will play a crucial role.

In general, climate change impacts crop production in various and complex ways at different levels, different scales and depending on local natural crop growing limitations. The main impacts of changing climatic parameters and weather extremes on crops are well known, such as the impact of temperature on phenology and on various physiological processes that depend on temperature such as maintenance, which influences net biomass accumulation. Photosynthetic activity and water use efficiency can increase through the interaction of plant responses with increasing atmospheric CO_2 levels; however, a wide variation in these responses is expected between crops and environments (Fuhrer 2003). In addition, short- and long-term effects on crop growing conditions are reported, such as the direct impact of weather extremes or the influence of changing climate on soil conditions such as water holding capacity due to desertification processes. Although many results have already been obtained using, e.g. the application of ecosystem or crop models, many research questions remain; these questions are often related to processes or impacts that are insufficiently considered by single crop models or modelling approaches (Rötter *et al.* 2011). A related issue is that large-scale crop simulation studies do not consider the variability of region-specific conditions sufficiently (White *et al.* 2011), and there is a need for high-spatial resolution of inputs for the calibration of regional models (Eitzinger *et al.* 2008; Strauss *et al.* 2012). Therefore, considering regional aspects (including model calibration) in regional climate change impact studies is of increasingly high importance; the present study contributes directly to this topic.

The results of climate change impact and adaptation studies, therefore, often show considerably different results, depending on the spatial scale of regionalization. However, reliable recommendations are crucial for stakeholders for early risk recognition and the implementation of anticipatory adaptation strategies; precautionary adaptation is more effective and less costly than forced, last-minute or emergency adaptation (ANL 1994; EEA 2005, 2007; Eitzinger *et al.* 2007; Parry & Carter 1998). In this context, it is recommended that regional studies should be undertaken and recommendations developed for adaptations considering local conditions (environmental and socio-economic) (Reidsma *et al.* 2009).

The present study addressed these aspects using a regional and holistic approach by modelling various types of climate change impacts on crop production within the same region. The key results from Central and Eastern Europe, including local case studies with different focuses in Austria, the Czech Republic and Slovakia, are presented. The study domain experiences a continental European climate and is characterized by strong climatic gradients, which may foster regional differences or trends in climate change impacts on agriculture.

To study the regional aspects and variability of the effects of climate change on agriculture, the following objectives were addressed:

(1) The effect of climate change on selected future agroclimatic conditions;
(2) The effect of climate change (including the effect of higher ambient CO_2 concentration) on yield levels and variability;
(3) The effect of climate change on the most important yield-limiting factors, such as water availability, nitrogen balance and infestation risks posed by selected thermophile insects (pests);
(4) Assessment of potential adaptation options based on case study results.

MATERIALS AND METHODS

Agroclimatic indices

Agroclimatic indices describe the complex relations existing between climate and crops (their development and/or production) as well as the agrosystems in a simplified manner (Orlandini *et al.* 2008) and can be applied over large regions and with limited data input. To describe specific agroclimatic conditions over the Central European domain examined in the present study, seven agroclimatic indicators were used. The goal was to select a set of key indices that would be relevant for various aspects of crop production and complement the other tools applied (pest and crop models) to assess climate change impacts on crop production conditions.

The first indicator, the sum of effective global radiation (EGR), was calculated as the sum of global radiation during the period over which the mean air temperature was continuously above 5 °C

https://doi.org/10.1017/S0021859612000767

(and without snow cover (SC) or frost occurrence) and with sufficient soil water available for evapotranspiration. The soil profile necessary for calculating EGR was assumed to have a maximum rooting depth of 1·3 m and an available soil water holding capacity of 270 mm. The critical ratio between actual and potential evapotranspiration was chosen to be greater than 0·4, based on the settings used by Trnka *et al.* (2011*a*).

As the second indicator, the climatological water balance (CW) during the climatological spring (March–May) and summer (June–August) was calculated (i.e. difference between reference evapotranspiration (ET_r) and precipitation). This indicator reflects drought intensity during the most critical crop growing periods.

To assess wine-growing conditions, the Huglin index (HUG) was used to classify potential wine-growing regions in terms of the sum of temperatures required for grape development and ripening (Huglin 1978). The minimum requirement for grape wine is defined as a HUG value of *c*. 1500. The attribution of particular varieties to thermal conditions estimated using HUG was based on the study by Schultz *et al.* (2005) and should be treated as an approximation only.

For assessing agroclimatic winter conditions, three further indicators were used. The number of days with SC was estimated using the SnowMAUS model (Trnka *et al.* 2010*a*); this model estimates SC absence/presence using daily temperature and total precipitation. Potential frost risk (FR) for field crops was estimated as the number of days from September to April without SC and during which the minimum daily temperature (at 2 m above ground level) dropped below −10 °C (Trnka *et al.* 2010*a*). To estimate changes in the conditions relevant to the vernalization of winter wheat (V), the temperature thresholds derived from Petr & Hnilička (2002) were used to estimate the number of conducive days required for the vernalization of winter wheat. Vernalization days from October to April were accumulated from 3 to 6 °C daily mean temperature (estimated optimum range) and the accumulation was reduced or stopped when daily maximum, minimum or mean temperatures were beyond optimum ranges. Vernalization was cancelled when mean daily temperature rose above 20 °C for more than 2 days during the vernalization period (40 vernalization days).

As an indicator for field operation conditions (FOCs) during spring and autumn, the suitabilities of sowing windows (spring and autumn) and harvest (June) were estimated. A given day is considered suitable for sowing or harvest when the soil water content in the top 100 mm layer of soil is between 10 and 70% of the available soil water-holding capacity (this parameter was set at 20 mm for all soils in the present study). The thresholds of soil moisture that were used to define days suitable for sowing and harvesting were parameterized at 30 experimental stations in the Czech republic (1985–2005); these thresholds were stricter than those used by Rounsevell (1993) and Cooper *et al.* (1997) to avoid potential soil compaction, which is considered as unsustainable in the long term.

All agrometeorological parameters described above were calculated using the software package *AgriClim* (Trnka *et al.* 2011*a*). This software uses daily inputs of global radiation, maximum and minimum temperatures, precipitation, water vapour pressure and mean daily wind speed. To allow grid-to-grid comparability, the same soil profile was used at all sites, and spring barley was used as a reference crop. While calculating evapotranspiration under climate change scenarios (see below), an adjustment was made for increased CO_2 concentrations using the method proposed by Kruijt *et al.* (2008), which resulted in a decrease in reference evapotranspiration rates compared with runs that did not consider increases in CO_2 levels. The ambient CO_2 concentration in air for the time horizon of the study (i.e. 2050) was set at 536 ppm, and the baseline calculations were set at 360 ppm. The agroclimatic indicators noted above were calculated for 99 years and the growing seasons in each grid of the entire domain for the applied climate change scenarios representing 2050 (Table 1).

In most cases, the median value of the parameter and the 5th and 95th percentiles were analysed to determine 20-year extremes of the given agroclimatic index. To increase the spatial resolution of the interpolated outputs, the values in the 10 × 10 km grids were regridded at a 1 × 1 km resolution using co-kriging techniques with altitude used as an additional parameter.

Pest models

From the range of pests that could have been studied, two thermophile insects, the Colorado potato beetle (*Leptinotarsa decemlineata*, referred to as CPB) and the European corn borer (*Ostrinia nubilalis*, referred to as ECB), were selected. The CPB is one of the

https://doi.org/10.1017/S0021859612000767

Table 1. *Climate change (CC) signals of the climate change scenarios applied to the presented studies as a mean for the entire domain and for the regional case study regions related to the reference period*

Case study region	CC scenario	Atmospheric CO_2 concentration of CC scenario (ppm)	Reference period*	CC signal Temperature: Oct–Apr (°K)	CC signal Temperature: May–Sep (°K)	CC signal Precipitation: Oct–Apr (%)	CC signal Precipitation: May–Sep (%)
Central Europe/	ECHAM 5 SRES A2 2050	536	1961–90	+2·7	+2·6	+4·3	−22·6
whole	NCAR–PCM SRES A2 2050		1961–90	+2·6	+2·4	+5·3	−1·5
domain	HadCM 3 SRES A2 2050		1961–90	+2·7	+3·8	+7·1	−23·8
Czech Republic	ECHAM 5 SRES A2 2050		1961–90	+2·6	+2·3	+7·9	−14·1
	NCAR–PCM SRES A2 2050		1961–90	+2·6	+2·1	+6·3	+4·4
	HadCM 3 SRES A2 2050		1961–90	+2·6	+3·2	+9·5	−12·4
Marchfeld, Austria	ECHAM 5 SRES A2 2035	478	1961–90	+3·0	+2·0	+12·0	−43·0
	HadCM 3 SRES A2 2035	478	1961–90	+2·0	+3·0	+19·0	−40·0
	NCAR PCM SRES A2 2035	478	1961–90	+2·0	+2·0	+21·0	−9·0
Danubian/Zahorie	ARPEGE SRES A1B Time slice 2021–2050	440	1961–90	+1·7	+1·4	+5·0	+3·0
Lowlands, Slovakia	ARPEGE SRES A1B Time slice 2071–2100	660	1961–90	+3·3	+3·2	+12·0	−15·0

* The atmospheric CO_2 concentration of the reference period 1961–90 was set as 360 ppm for crop simulation.

most important insect pests of potato globally and is widespread in Europe (EPPO 2009). The ECB, as the most important pest of grain maize (Mason *et al.* 1996), has also been recorded to occur across all of Europe (Keszthelyi & Lengyel 2003; EPPO 2009) and the development of this pest is closely related to temperature.

The pest model CLIMEX (Sutherst & Maywald 1985; Sutherst *et al.* 2001) was applied in the study of these two pests. Knowing the climatological requirements of a given species, the model allows the suitability of a given area for the population growth of the pest in question to be assessed and determines the stress exposure due to unsuitable climatic conditions. These factors are expressed in terms of the Ecoclimatic index (EI), which describes the overall suitability of a climate for the establishment and long-term presence of a pest's population at a given location. Generally, EI lies in the range 0–100; EI = 0 indicates locations experiencing climate conditions that are unfavourable for long-term species occurrence, and EI > 25–30 represents a climate that is very suitable for species occurrence (Hoddle 2004). The observed occurrence data obtained from field observations in the Czech Republic constituted the base material for the validation of the pest model CLIMEX under recent climate conditions (Kocmánková *et al.* 2008). Following validation and calibration of the model outputs, the model was applied over the entire domain of the present study and for the applied climate change scenarios (Table 1).

Crop models

In recent years, process-oriented (mechanistic) crop models have been among the most frequently used tools in climate change impact studies (Audsley *et al.* 2006; White *et al.* 2011). To explore the effect of climate change in the various case study regions on crop yields and growth conditions (phenology and crop water stress), three crop models were applied: CERES-Barley (Otter-Nacke *et al.* 1991), CERES-Wheat (Ritchie & Otter 1985) and DAISY (Hansen *et al.* 1990, 1991; Abrahamsen & Hansen 2000; Hansen 2000). The CERES models operate within the Decision Support System for Agrotechnology Transfer (DSSAT) (Hoogenboom *et al.* 1994; Tsuji *et al.* 1994, 1998). All crop models considered the impact of enhanced atmospheric CO_2 concentration under the relevant climate scenarios (Table 1) for crop growth.

https://doi.org/10.1017/S0021859612000767

Table 2. *Main arable soil types of the study areas in the Czech Republic, Austria and Slovakia and their relation to the crop model inputs of soil properties that are relevant for soil water balance*

Study area	Soil	Soil type	Available soil water capacity (mm) and related soil depth (m)	Study area (proportion)
Czech Republic				
Whole CR	Cambisols	Loam	180 (1·3 m)	0·210
Whole CR	Cambisols	Sandy loam	180 (1·3 m)	0·173
Whole CR	Haplic luvisols	Loam	220 (1·3 m)	0·096
Whole CR	Stagnosols	Loam	220 (1·3 m)	0·091
Whole CR	Chernozem	Loam	260 (1·3 m)	0·089
Whole CR	Gleysols	Loam	180 (1·3 m)	0·054
Whole CR	Albic luvisols	Loam	220 (1·3 m)	0·049
Whole CR	Fluvisosl	Loam	220 (1·3 m)	0·047
Whole CR	Chernozem	Clay-loam	260 (1·3 m)	0·021
Austria				
Marchfeld – soil 1	Parachernozems	Sandy loam	52 (1·0 m)	0·019
Marchfeld – soil 2	Parachernozems	Sandy loam	129 (1·0 m)	0·147
Marchfeld – soil 3	Chernozems and fluvisols	Sandy loam	204 (1·0 m)	0·613
Marchfeld – soil 4	Chernozems and fluvisols	Loamy silt	248 (1·0 m)	0·219
Marchfeld – soil 5	Colluvial chernozem	Sandy loam	371 (1·5 m)	0·002
Slovakia				
Danubian lowland-site A	Haplic chernozem	Loamy	280 (1·2 m)	0·143
Danubian lowland-Site B	Haplic fluvisol	Loamy	290 (1·2 m)	0·132
Danubian lowland-Site C	Haplic luvisol	Loamy	240 (1·2 m)	0·200
Danubian lowland-Site D	Calcaric chernozem	Loamy	250 (1·2 m)	0·110
Záhorie lowland-Site E	Mollic fluvisol	Sandy loam	220 (1·2 m)	0·184
Záhorie lowland-Site F	Regosol	Sandy loam	200 (1·2 m)	0·063

Crop model and simulation setup – a case study in the Czech Republic

Experimental data used for model evaluation were derived from field trials of the State Institute for Agricultural Supervision and Testing (SIAST). The CERES-Barley calibration was based on 50 experimental seasons at four sites; during calibration, the crop parameters of spring barley cultivar 'Akcent' were determined. The evaluation of the model used independent data sets from 13 experimental sites over 155 experimental seasons. The simulated values of the anthesis and maturity dates fit well with the observations. Despite the large variability of the experimental data, few simulated yields (<0·05) differed by more than 25% from the observations. In most seasons (0·90), the difference between simulated and observed grain yields was smaller than 20%, and 0·80 of the yields were simulated with a bias of < 800 kg/ha. CERES-Barley was able to explain 65–74% of the variability of key developmental stages and almost 70% of the yield variability. Calibration of the CERES-Wheat model for winter wheat cultivar 'Hana' has been described previously (Trnka *et al.* 2004*a*) and shows very similar results to those for spring barley described above.

The simulation of mean potential yields scaled up from 1 km grids to the district level (areas of *c.* 1000 km^2) showed that attainable yields are over 40% higher than observed yields. This was, however, expected, as the model assumes optimum growing conditions without any yield-limiting factors. Both crop models also show a consistent performance under varying conditions within individual districts and are able to explain almost two thirds of the inter-regional variability.

Crop model simulations accounted for autonomous adaptation of the sowing date, which was simulated based on soil temperature and workability. Medium fertilizing intensity (a nitrogen dosage of 60 kg/ha for spring barley and 100 kg/ha for winter wheat) and a leguminous pre-crop were considered as further conditions. The main soil type characteristics over the Czech domain used for the simulations are shown in Table 2.

https://doi.org/10.1017/S0021859612000767

For a spatial analysis, each crop model was run for each climate scenario for all 125 weather stations using 400 soil type groups in 1600 soil polygons. The native resolution of the soil map was 1 : 500 000 (Tomášek 2007).

Crop model and simulation setup – Austrian case study

The region of Marchfeld (48°17′N, 16°38′E, *c*. 1000 km^2, in the north-east of Austria) was chosen to simulate the effects of climate change on winter wheat and spring barley using CERES-Wheat and CERES-Barley. Marchfeld is a major crop production area and one of the warmest and driest regions in the country. The groundwater table in the Marchfeld region is very deep; crops have no access to groundwater and there is no capillary rise from groundwater to the rooting zone. The main soil types in Marchfeld are Parachernozems, Chernozems and Fluvisols, which are characterized by a high-spatial variability and include soils with low to moderate water-storage capacity. To simulate crop yields in the Marchfeld region, five soil classes were created; these were based on the 1 : 25 000-scale Austrian digital soil map (BFW 2007) and the amount of available water capacity of the individual soil classes (Table 2) in conjunction with pseudo-transfer function (Murer *et al*. 2004). Soil-layer-specific model input parameters of soil physical properties represent the dominant type of soil cultivation in Marchfeld, which is ploughing. In addition, area-weighted mean values of physical and chemical soil properties (i.e. texture and humus content) were calculated for these soil classes (Rischbeck 2007) (Table 2). Two different tillage operations (ploughing and minimum tillage) were simulated to analyse the effect of soil cultivation on soil water balance under the climate change scenarios. For this purpose, undisturbed soil or minimum tillage conditions were determined from the values of the Austrian soil map (BFW 2007). For ploughed soil, selected soil input parameters (bulk density, soil saturation, field capacity and wilting point) were modified based on field experiment results (Thaler *et al*. 2012).

To validate the two CERES models, simulated outcomes were compared with measured results obtained from field trials. The CERES wheat model for winter wheat was calibrated for the winter wheat cultivar 'Capo' using agrotechnological, phenological, yield and weather data from an experimental site at Fuchsenbigl, Marchfeld (48°12′N, 16°44′E, 157 m a.s.l.) during 1989–2005. The difference between the simulated and observed dates of anthesis and the physiological maturity of winter wheat for calibration varied from 0 to 4 days. Simulated grain yields mostly agreed with the measured data ($R^2 = 0{\cdot}61$; root-mean-square error (RMSE) = 590 kg/ha), and the deviation in annual yield predictions was less than 20% (Thaler *et al*. 2012).

The CERES barley model for spring barley was calibrated in the same way and verified for the periods 1989–95, 1998 and 2001/02 using data for the cultivar 'Magda'. The difference between the simulated and observed dates of anthesis and physiological maturity varied from 0 to 7 days, and the simulated yield was within 20% of the measured values for each year ($R^2 = 0{\cdot}57$; RMSE = 623 kg/ha).

Long-term weather data from the representative weather station Groß-Enzersdorf (48°12′N, 16°33′E, 157 m a.s.l.) were used as data for the reference period and for creating the climate scenarios (Table 1); this methodology is the same as that used for the Czech Republic case study.

Crop model and simulation setup – Slovakian case study

In the present study, the effects of climate change on spring barley, winter wheat and maize in two crop production regions of Slovakia were simulated using the crop model DAISY. Crop modules of spring barley, winter wheat and maize were calibrated and validated using long-term data (1973–2006) obtained from the experimental station at the Research Institute of Irrigation near Bratislava (48°10′N, 17°12′E, 131 m a.s.l.). Yield data of various cultivars that did not differ significantly in growing period length and potential yield under the specific environmental conditions (Patil *et al*. 2010; Hakala *et al*. 2012) were used for this purpose. Comparisons of measured and simulated dry matter production, crop nitrogen uptake and soil inorganic nitrogen content proved good performance of the crop model (Takáč & Šiška 2011). Simulated winter wheat grain yields mostly agreed with the measured yields ($R^2 = 0{\cdot}81$, RMSE = 924 kg/ha, coefficient of variation (CV) (RMSE) = 0·15). Simulated spring barley yields also showed generally good agreement with the measured yields ($R^2 = 0{\cdot}77$, RMSE = 759 kg/ha, CV (RMSE) = 0·15). The mean deviation from predicted grain yields of spring barley and winter wheat was 12%. Measured and simulated

https://doi.org/10.1017/S0021859612000767

maize yields were in good agreement ($R^2 = 0{\cdot}94$, RMSE = 834 kg/ha, CV (RMSE) = 0·11).

The mean deviation in predicted maize grain yields from observed yields was 9%. The differences between simulated and observed dates of maturity of all three crops were all less than 7 days.

Representative soil profiles of the Danubian and Záhorie lowlands were defined according to texture, humus content and C/N ratio. The database of the Soil Science and Conservation Research Institute in Bratislava (17741 soil samples) was used for creation of soil characteristics in a 10 × 10 km grid. Based on soil parameters, soils were classified as shown in Table 2. Various crop rotations and management practices (including irrigation and fertilization) were considered while preparing representative datasets for yield simulations. Crop rotation involved the dominant crops in the Danubian and Záhorie lowlands (winter wheat, spring barley, sugar beet, maize, potato, winter rape and pea). Fertilization rates of 150 kg N/ha for winter wheat and 160 kg N/ha + 40 t farmyard manure/ha for maize were applied during the crop simulation. Maize was also fertilized in the autumn, before the growing season. Soil trafficability, which is limited by topsoil water content and soil temperature, was considered for field operations such as the simulated sowing date.

The crop model was run for the regions of the Záhorie and Danubian Lowlands with two different climatic datasets for 1971–2000 and two climate scenarios for the periods 2021–51 and 2071–2100 (Table 1).

Climate scenarios

Climate change scenarios for Central Europe (whole domain) and the case study regions in the Czech Republic and Austria (Table 1) were developed via a 'pattern-scaling' technique (Santer *et al.* 1990) and then applied to modify the parameters of the weather generator. The pattern-scaling technique defines a climate change scenario based on the product of the standardized scenario and the change in global mean temperature. The standardized scenarios, which relate the responses of climatic characteristics to a 1 °C rise in global mean temperature (ΔT_G), were determined by applying a regression method (Dubrovský *et al.* 2005) to the 2000–99 period, which was obtained from three global climate models (GCMs) from the IPCC Fourth Assessment Report (Solomon *et al.* 2007). The three GCMs used (Table 1) include ECHAM5/MPI-OM, HadCM3 and NCAR-PCM, hereafter referred to as ECHAM, HadCM and NCAR, respectively. The climate scenarios of the whole domain and the Czech Republic were calculated for an increase in global mean temperatures by 2·1 °C until 2050, specifically for a time-slice centred at *c.* 2050 (Hulme *et al.* 2000). This assumed the A2 emission scenario (SRES) and high climate sensitivities (i.e. an equilibrium change in global mean surface temperature following a doubling of the atmospheric equivalent CO_2 concentration, $T_{G,2} \times CO_2$). The scenarios of the Austrian case study were calculated accordingly for 2035 (time slice 2021–50), based on the SRES-A2 scenario. To create the daily model weather input data for the climate change scenarios, the authors applied a method originally developed by Semenov & Porter (1995) and adapted by Žalud & Dubrovský (2002). A weather generator was parameterized on observed weather data (1961–2001) and used to generate daily weather data for the climate scenarios.

The climate scenarios applied for the case study in Slovakia (Table 1) included data generated by the ALADIN climate model (Farda *et al.* 2007) and the measured climatic data for the particular locality. The climate scenarios applied are based on the ARPEGE climate model (Lopez *et al.* 2000) for two intervals (2021–51 and 2071–2100).

RESULTS

The results illustrate general agricultural production conditions based on agroclimatic indices for the domain of Central–Eastern Europe (Fig. 1), and this information is complemented with three regional case studies (Fig. 1(*a*)) that focus on simulated climate change impacts on crop yields. When combined, these results should allow for the development of recommendations for regional adaptation options for the various production regions that consider regional differences in production conditions (soils, climate and crop management) as well as the development and shifts of the overall climatic conditions under the applied climate scenarios.

The effect of climate change on agroclimatic conditions in Central–Eastern Europe

The following section presents the results of the applied agroclimatic indices for the entire domain of Central and Eastern Europe.

https://doi.org/10.1017/S0021859612000767

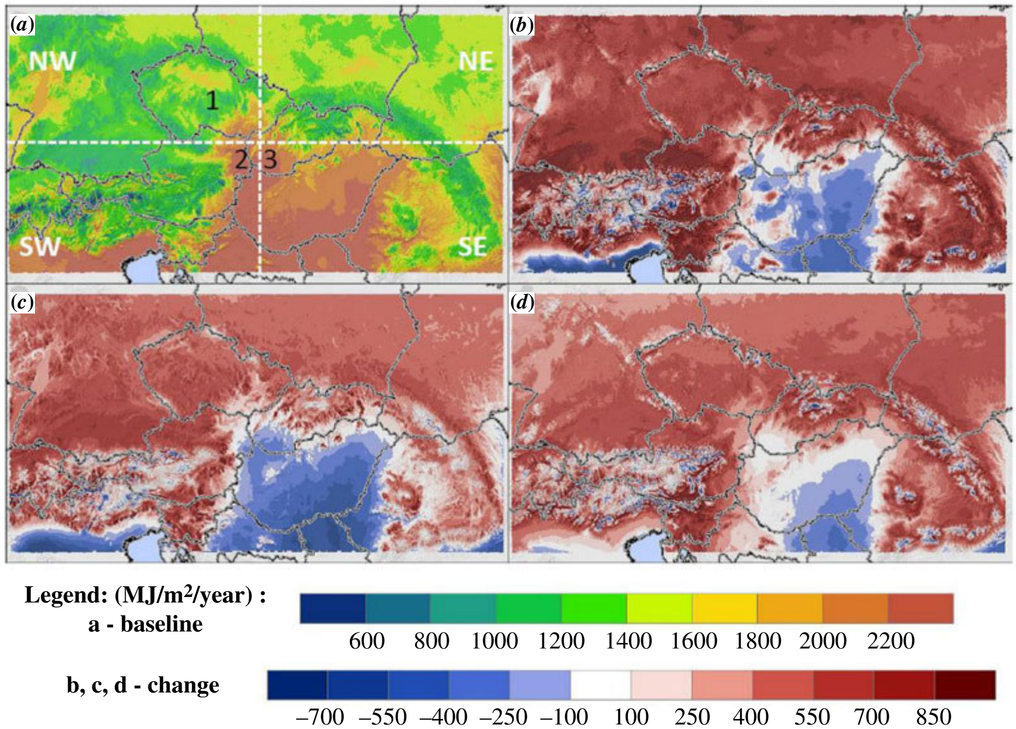

Fig. 1 (*Colour online*). The sum of EGR in Central-Eastern Europe for *a*) the baseline period (1961–90) and for an increase in global mean temperatures by 2·1 °C until 2050 under three standardized scenarios based on the HadCM, ECHAM and NCAR GCMs (*b–d*). The numbers in (*a*) show the location of the case study regions in the Czech Republic (1 – includes the entire country), Austria (2) and Slovakia (3). The white lines show the division of the region into four quadrants.

Based on the applied climate scenarios (Table 1), the annual sum of EGR would rise via increases in the duration of the potential growing period (i.e. with mean air temperatures continuously above 5 °C). In addition, EGR would be affected in some cases by the increase in global radiation that occurs due to reduced cloudiness associated with decreased precipitation, especially during the summer months. Although these changes may increase crop production potential, the decrease in precipitation would also increase the probability of water deficit, leading to a lower overall value of this key parameter. Under present conditions, the southern and southeastern areas of the domain exhibited the highest EGR values (Fig. 1(*a*)), indicating the potential productivity of rainfed agriculture. The western and northern parts of the domain would benefit most from the changed climate conditions, with areas in Germany, Poland, parts of Austria, Slovakia and the Czech Republic showing a sustained increase in the values of this parameter (Fig. 1(*b–d*)). The largest decreases are to be expected within the Pannonian lowland, which includes almost all of Hungary, northern Serbia and Croatia, as well as parts of southern Slovakia, eastern Austria and western parts of Romania. The most marked changes (both positive and negative in regard to growing conditions) within the regions are to be expected under HadCM-driven scenarios; NCAR-based results indicate a much lower rate of change. The overall spatial pattern of these changes remained the same, regardless of the scenario used.

Regarding drought intensity, the spatial patterns of the 20-year extremes of CW balance during spring (MAM) and summer (JJA) months (results not shown in the figures) showed the highest water deficit in the Pannonian region and the lowest water deficit in the Alps and mountain regions in general. The climate change scenarios (in particular, the HadCM-based scenario) demonstrated an increase in the present spatial gradients during spring (i.e. dry areas becoming drier and wet areas wetter), but significant changes are to be expected over the entire region during the summer months. The magnitude of the changes exhibited a southeast gradient, in which the arable land in the Czech Republic would be affected least and Hungary and Slovenia would experience the most marked increase in drought intensity. However, a slight easing of the 20-year drought intensity was seen

https://doi.org/10.1017/S0021859612000767

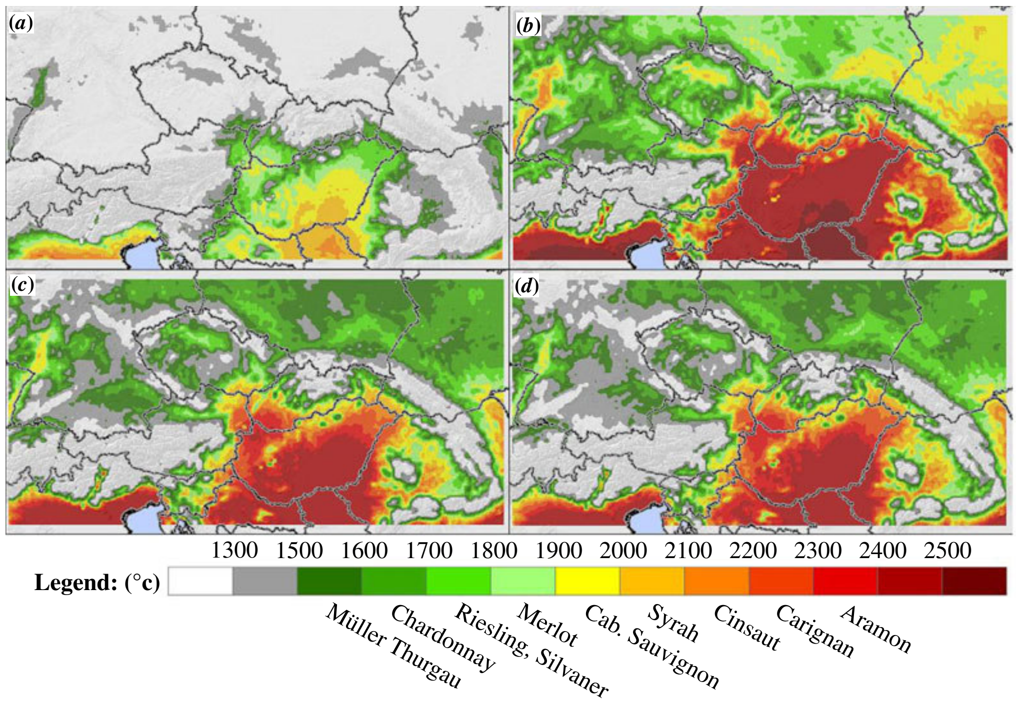

Fig. 2 (*Colour online*). Value of the HUGLIN index, which serves as a proxy for wine growing suitability in Central-Eastern Europe, for (*a*) the baseline period (1961–90) and for an increase in global mean temperatures by 2·1 °C until 2050 under three standardized scenarios based on the HadCM, ECHAM and NCAR GCMs (*b*–*d*).

in the Czech Republic, Austria, Slovakia and Slovenia under the NCAR scenario, leaving only the arable lands in Hungary worse off.

The HUG indicated a significant increase across the entire domain as a direct consequence of the expected temperature increase based on the climate projections used. Figure 2 illustrates that the present mean HUG value would not allow for permanent successful production of grapes across most of the domain except in areas already established as wine-growing regions. Very good thermal conditions for wine growing were found especially in the southeastern part of the domain. Under the climate scenarios studied, the area with wine-growing potential would increase substantially, providing HUG values sufficient for wine production across most of the region with the exception of mountainous areas. It must be stressed that HUG only considers temperature requirements during the summer period, and this is not the sole factor in wine production (Dalla Marta *et al*. 2010). Other limitations such as amount of precipitation, soil conditions and small-scale local climatic variations based on terrain effects (such as the effects of slope on temperature or cold air lake conditions) were not considered in the present paper. The results clearly showed that the present wine-growing regions in Central Europe will generally experience much warmer conditions, and this may force the use of cultivars other than those grown currently. The results also indicated that wine growing may be possible even in northern latitudes where wine production is currently infeasible for climatic reasons.

Agroclimatic conditions during winter will change significantly, including such factors as the number of days with SC. Figure 3(*a*) and (*b*) indicates that by 2050, more than 0·8 of the domain will have an average SC of less than 50 days, and in one-third of the domain, SC will be less than 25 days. Despite less frequent SC, the risk of severe frost to field crops (FR) resulting from low temperatures (air temperature less than −10 °C) is likely to decrease (Fig. 3(*c*) and (*d*)) across most of the domain. However, the reduction of SC, which protects winter crops effectively against frost damage, could partly overcome this positive effect. The occurrence of late FR (especially radiative frost) is unlikely to be altered much. However, perennial crops such as orchards will tend to start their growing season earlier and will consequently lose their frost tolerance earlier (Arora & Rowland 2011).

An increase of winter temperatures will inevitably influence the vernalization conditions (V) for winter wheat (results not shown in the figures) but the

https://doi.org/10.1017/S0021859612000767

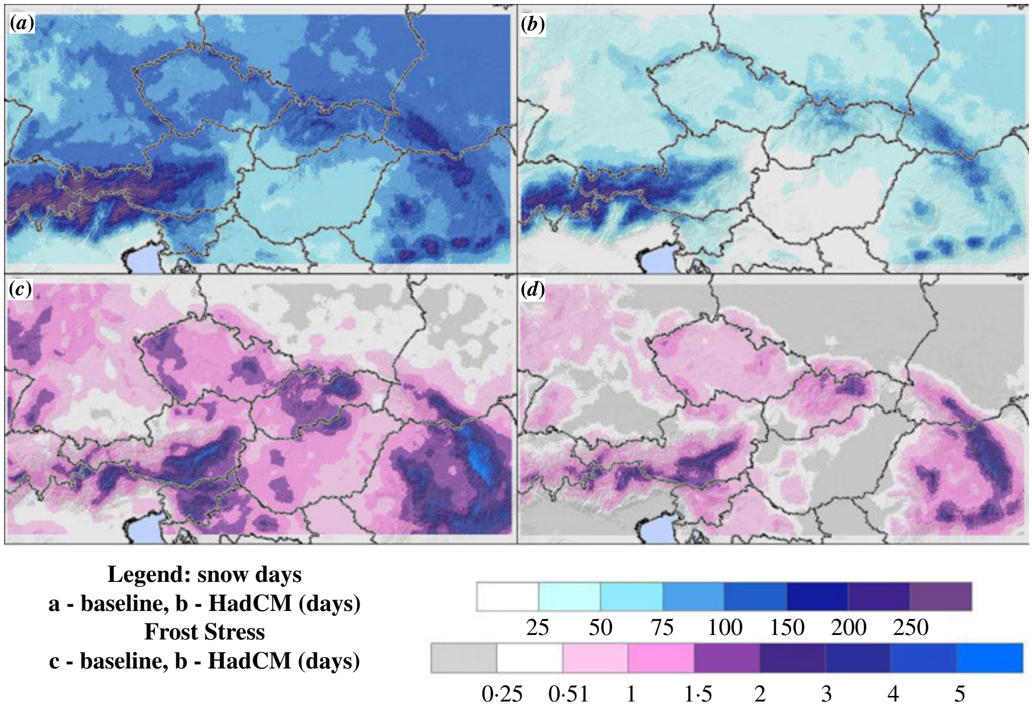

Fig. 3 (*Colour online*). (*a*) The mean number of days with SC in Central–Eastern Europe for the baseline period (1961–90); (*b*) the expected change of the number of snow days based on an increase in global mean temperatures by 2·1 °C until 2050 based on the HadCM standardized scenario; (*c*) the number of days at high risk of frost damage with a 20-year return period for the baseline period and (*d*) the expected change of FR based on an increase of global mean temperatures by 2·1 °C until 2050 under the HadCM standardized scenario.

expected change does not exceed critical levels that hinder the vernalization. With the exceptions of the Pannonian basin and Rhine valley, an increase in the mean value of V is expected mainly due to an increase in the number of days with the optimum temperature for vernalization. The majority of the presently used cultivars of winter wheat or winter barley require at least 40 vernalization days, and in most cases, they require 50–60 vernalization days (Petr & Hnilička 2002). In light of the present results, the vernalization season will be sufficiently long in most years. The expected change would only prevent vernalization for most of the presently grown winter wheat cultivars in extremely warm winters.

Agroclimatic conditions during spring and autumn for field operations (FOCs), (results not shown in the figures) will be altered in that the growing season will start earlier, and this will be accompanied by changes in the proportion of days suitable for sowing in spring. However, the three GCM-based predictions showed little agreement regarding the proportion of suitable sowing days during early spring. The NCAR-based projections showed a slight decrease in the number of suitable days in the centre and north and increases in the south of the domain. The ECHAM-based results showed an overall increase in early spring sowing suitability. However, HadCM differed from the other two predictions in that it predicted a substantial drop in the number of suitable days for sowing in spring in most of the Czech Republic, Bavaria, northern and eastern Austria and in some regions of Hungary and Romania. This particular result was caused by the predicted increases, compared with the present, in precipitation during March and April according to the HadCM model. At the same time, FOC increased sharply in spring in northern Italy, eastern Hungary and in parts of Saxony that are within the domain.

The increase of FOCs during the autumn (25 September–25 November) was very pronounced. The positive development mainly affected areas with low suitability under present conditions (mountainous areas of Austria, Italy, Slovenia, the Czech Republic, Poland and Slovakia), whereas areas in the south-eastern part of the domain (Hungary, eastern Austria, northern Serbia and Croatia) showed no change or a slight decrease. According to all three projections (ECHAM, HadCM and NCAR), increases in the suitable days are to be expected mainly due to an

https://doi.org/10.1017/S0021859612000767

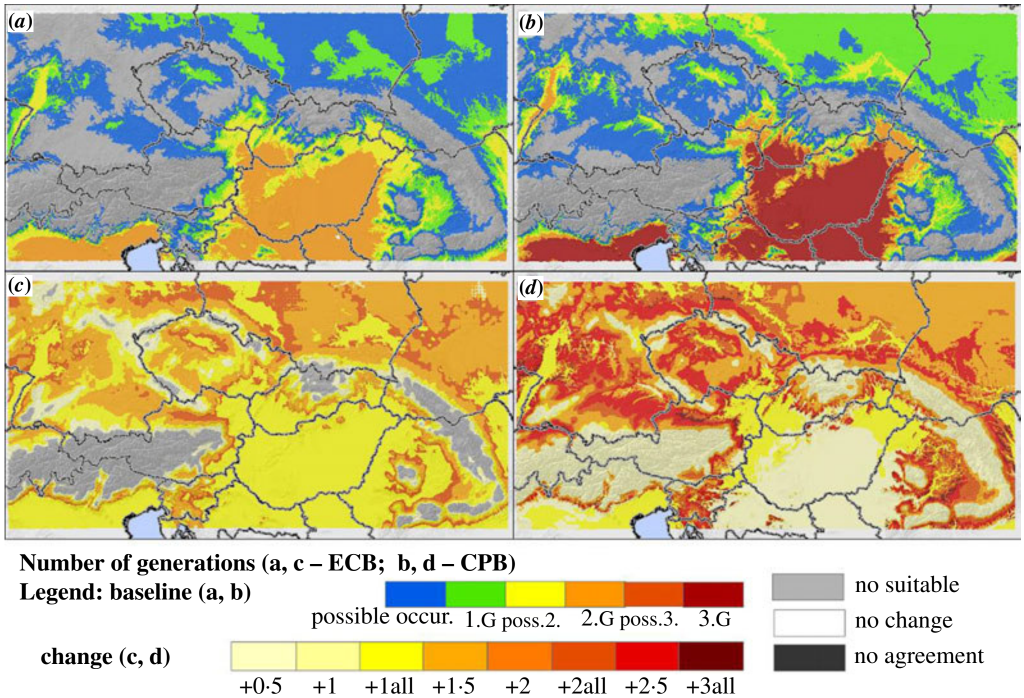

Fig. 4 (*Colour online*). Suitability of the EI for (*a*) the ECB and (*b*) the CPB in Central–Eastern Europe for the baseline (1961–90) period. (*c*) and (*d*) illustrate the likely shift in the number of generations of the pests as a composite of three standardized scenarios (HadCM, NCAR and ECHAM) for 2050. The blank areas indicate no change in the number of generations, grey areas are not suitable for pest occurrence, and dark grey pixels indicate disagreement in the trend between the various models. The intensity of the colour expresses the degree of the agreement between the various models.

increase in the growing season (thus causing a prolongation of the sowing window) and a drop in precipitation in September and partly also in October and November.

The earlier start of the growing season and the higher rate of phenological development will lead to earlier harvest dates for crops in general (this effect, however, partly can be mitigated by growing later ripening cultivars). For cereals, FOCs for harvest were analysed for June, when the main cereal harvest will take place under expected climate scenario conditions (Alexandrov *et al*. 2002). According to the NCAR-based scenario, the harvest suitability in June is likely to remain the same or decrease slightly over the main production areas; however, the results obtained using the ECHAM-based scenario indicate increases in the harvesting window, especially in southern parts of the domain. The HadCM-based results indicated a relatively sharp drop (on average by >10%) in the number of suitable harvest days in June, especially across most of the Czech Republic, parts of northern and eastern Austria and almost all of Bavaria, with improvements over northern Italy, most of Hungary and southern Poland.

The effect of climate change on the infestation pressure of two indicator pest species in Central–Eastern Europe

European corn borer

The model indicated the presence of one or two generations of ECB (Fig. 4(*a*)) under the reference climate conditions (1960–90). Two generations are found in the southern part of the domain, in areas that are more climatically favourable for development of the ECB, i.e. Hungary, the northern parts of Croatia, Serbia and Italy, and the eastern part of Romania. Under future climate conditions in which temperature increases and a prolonged warm season are expected, the area of pest occurrence is expected to expand (Fig. 4(*c*)). At the same time, the emergence of bivoltine populations and a further increase to a third generation in the warmest areas is indicated. The results showed that the pest would, for example, colonize areas recently unoccupied by univoltine populations, up to an altitude of *c*. 800 m. The ratio of arable land that is endangered by an increase in the number of generations shows the decrease in the pest's univoltine areas due to an increase in the bivoltine population

https://doi.org/10.1017/S0021859612000767

Table 3. *The ratio of arable land occupied by a particular number of generations of the CPB and the ECB under current and expected climate conditions according to the HadCM, NCAR and ECHAM scenarios in 2050 (Table 1) over the entire Central European domain*

	CPB	ECB
	First and partial second generation	First generation
1961–90	34·8	9·5
ECHAM 2050	7·0	3·4
NCAR 2050	6·8	4·8
HadCM 2050	1·4	0·9
	Second generation	Partial Second generation
1961–90	8·4	8·8
ECHAM 2050	16·8	36·8
NCAR 2050	11·4	28·2
HadCM 2050	10·8	8·9
	Third generation	Second generation
1961–90	5·1	25·1
ECHAM 2050	30·5	44·8
NCAR 2050	25·8	46·4
HadCM 2050	16·9	86·0
	Fourth generation	Third generation
1961–90	0·4	0·2
ECHAM 2050	2·9	13·1
NCAR 2050	6·7	17·8
HadCM 2050	1·8	3·8

and the risk of three generations in some regions (Table 3).

Colorado potato beetle

Under baseline climate conditions (1961–90), the simulated values of the EI predicted one to four generations of CPB over the domain (Fig. 4(*b*)). Simulations of baseline climate conditions indicated that 0·35 of arable land is threatened by one complete generation of the CPB, 0·08 by two generations and 0·05 by three generations (Table 3). The results of the simulations for the applied climate scenarios exhibited an apparent trend of a widening of the pests' climatic niche and increase in the number of generations based on the temperature increase (Fig. 4(*d*)). Similar to the results obtained regarding the ECB, the occurrence of at least one CPB generation is expected to increase in the northern part of the domain up to an altitude of 800 m. In addition, there was a marked increase of approximately two generations in the lowlands, and three generations are expected to occur, but rarely. The overall decrease in the area established by the univoltine population was caused by a shift towards higher number of populations (Table 3). The bivoltine population would therefore occupy 0·17 of arable land, whereas the area occupied by a third generation increases to 0·31 (ECHAM). However, a marked decrease in climates favourable to CPB development under ECHAM is simulated in northern Serbia (the Vojvodina region), where the significant temperature increases under ECHAM exceeds the high-temperature limitation for the development of the pest and a subsequent decrease to approximately one generation.

The effect of climate change on cereal crop production and crop growing conditions in Central–Eastern Europe

Various factors and regional conditions can alter the response of crop production potential to climate change, as demonstrated by the examination of three regional case studies over the domain using crop models. The simulated yield estimates did not account for the influence of pests/diseases, changes in soil workability and extreme events (e.g. hail, heat waves, prolonged drought and floods); therefore, the results should be treated together with outcomes of agro-climatic indicators, e.g. those presented above.

The effect of climate change on spatial cereal production conditions in the Czech Republic

In the first case study, the effects of climate change prior to 2050 were simulated for three scenarios (Table 1) on winter wheat and spring barley for all arable lands of the Czech Republic.

The highest yields of winter wheat and spring barley in the baseline climate (1961–90) were simulated at lower altitudes in the Czech Republic (Fig. 5(*a*) and (*d*)). Apart from the effect of climate, this result was also determined by the good soil conditions present at *c.* 250 m a.s.l. (lowlands), where arable land was composed of chernozem (0·43), fluvisols, phaeozems, haplic Luvisols, cambisols and regosols. The increase in air temperature under all climate scenarios is expected to lead to the shortening of the growing period of both simulated crops (data not shown), as confirmed by many related studies.

In general, the changed climate conditions prior to 2050 are expected to lead to a moderate decrease in the yield of winter wheat when the effect of CO_2

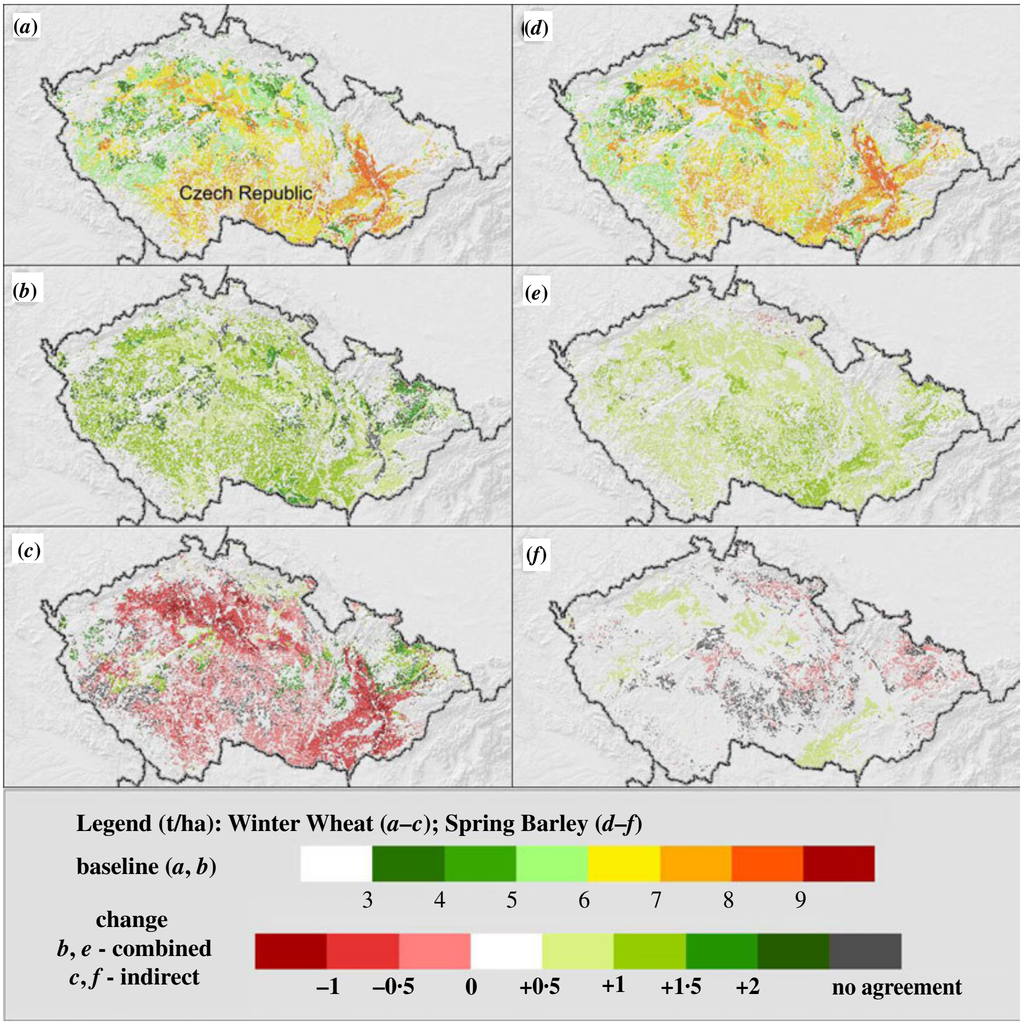

Fig. 5 (*Colour online*). Mean yield levels (t/ha) of (*a*) spring barley and (*d*) winter wheat during the baseline period (1961–90) in the Czech Republic (78864 km^2). Maps (*b*) and (*e*) show the change in yield (t/ha) resulting from climate change and effect of increased ambient CO_2, and maps (*c*) and (*f*) only show the effect of changed climate conditions. Set of maps showing combined and indirect effects are based on composites of three standardized scenarios (HadCM, NCAR and ECHAM) for 2050. The blank areas indicate no change compared to the present conditions, grey depicts areas where estimates based on three scenarios do not agree on the sign of the change, green depicts increased yield, and red indicated decreased yields. The results indicated in red and green represent the average results of all three scenarios.

fertilization is not considered (indirect effect); this effect would be greatest in the lowland and midland areas (Fig. 5(*c*)). For spring barley, the impact on yield was equally great because the negative effect of a shortened growing period was outbalanced by the earlier sowing dates (Fig. 5(*f*)). Generally, sites in regions that experience low air temperatures at present would be less negatively or positively affected by the indirect effect (mainly due to the increase of temperatures) of climatic change, as would lowland areas with deep fertile soils. In addition, the potentially positive effect of increased CO_2 concentration on crop yields (combined effect) (Trnka *et al*. 2004*b*) would lead to an overall increase in the yields of winter wheat (Fig. 5(*b*)) and spring barley (Fig. 5(*e*)), especially in areas that currently experience lower annual temperatures (e.g. upland regions).

Assessment of the potential impacts and adaptation options for cereals in a semi-arid region of Austria

In the Marchfeld lowland region (in the north-east of Austria), the changes in winter wheat and spring barley yields were simulated for 2035 relative to the baseline conditions using the same methodologies (crop

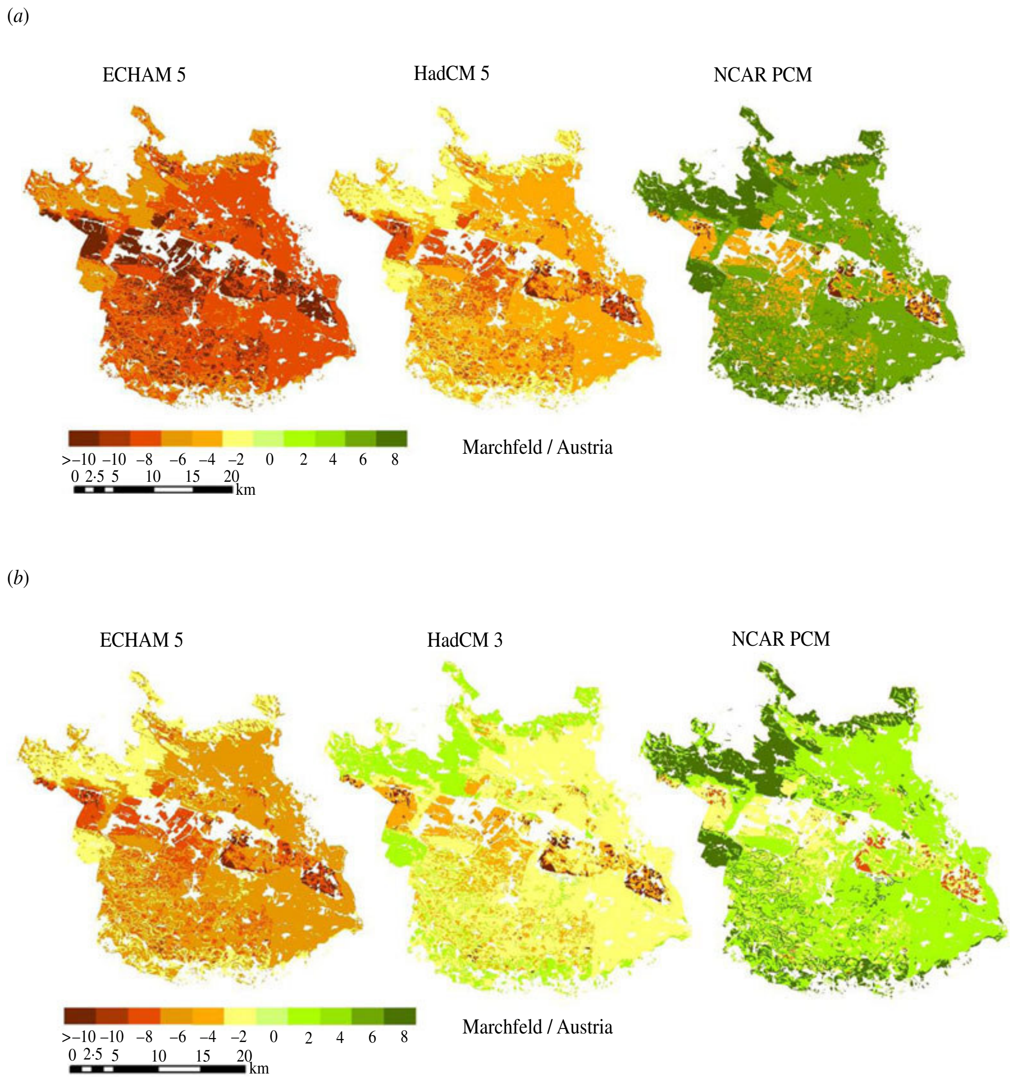

Fig. 6 (*Colour online*). Relative change (%) in the yields of (*a*) winter wheat and (*b*) spring barley for various climate scenarios for 2035 (Table 1) in the Marchfeld region (1000 km^2) in comparison with those observed under baseline conditions (1961–90).

models and climate scenarios) as those used in the Czech case study.

In accordance with the results of the Czech case study for lowland regions, the impact of the changed weather conditions under ECHAM and HadCM was the decrease or a stagnation in the yields of winter wheat and spring barley until 2035, at which time spring barley exhibits more stable yields. The decrease in yield was caused primarily by a shortened growing season of the simulated cultivars and by reductions in precipitation during the growing season. In Marchfeld, even the additional effect of CO_2 fertilization (combined effect) could not fully offset the decrease in yields. The decrease in yield would be more distinct for both crops studied on soils with low water storage capacity (Table 2, Fig. 6). Only NCAR presented a significant increase of winter wheat and spring barley yields, especially on soil classes 3–4 (Table 2) with better soil water storage capacity (Fig. 6). As mentioned above, winter wheat yields differed more among the three climate scenarios than spring barley yields; this result was probably caused by the positive and greater effect of the simulated earlier sowing dates for spring barley under the climate scenarios.

The interannual yield variability of these two crops is expected to increase for almost all soils, leading to increased economic risk for farmers. Without the positive effect of CO_2 fertilization, the mean yield would decrease more, especially on sandy soils (see the results of the Czech Republic case study above).

https://doi.org/10.1017/S0021859612000767

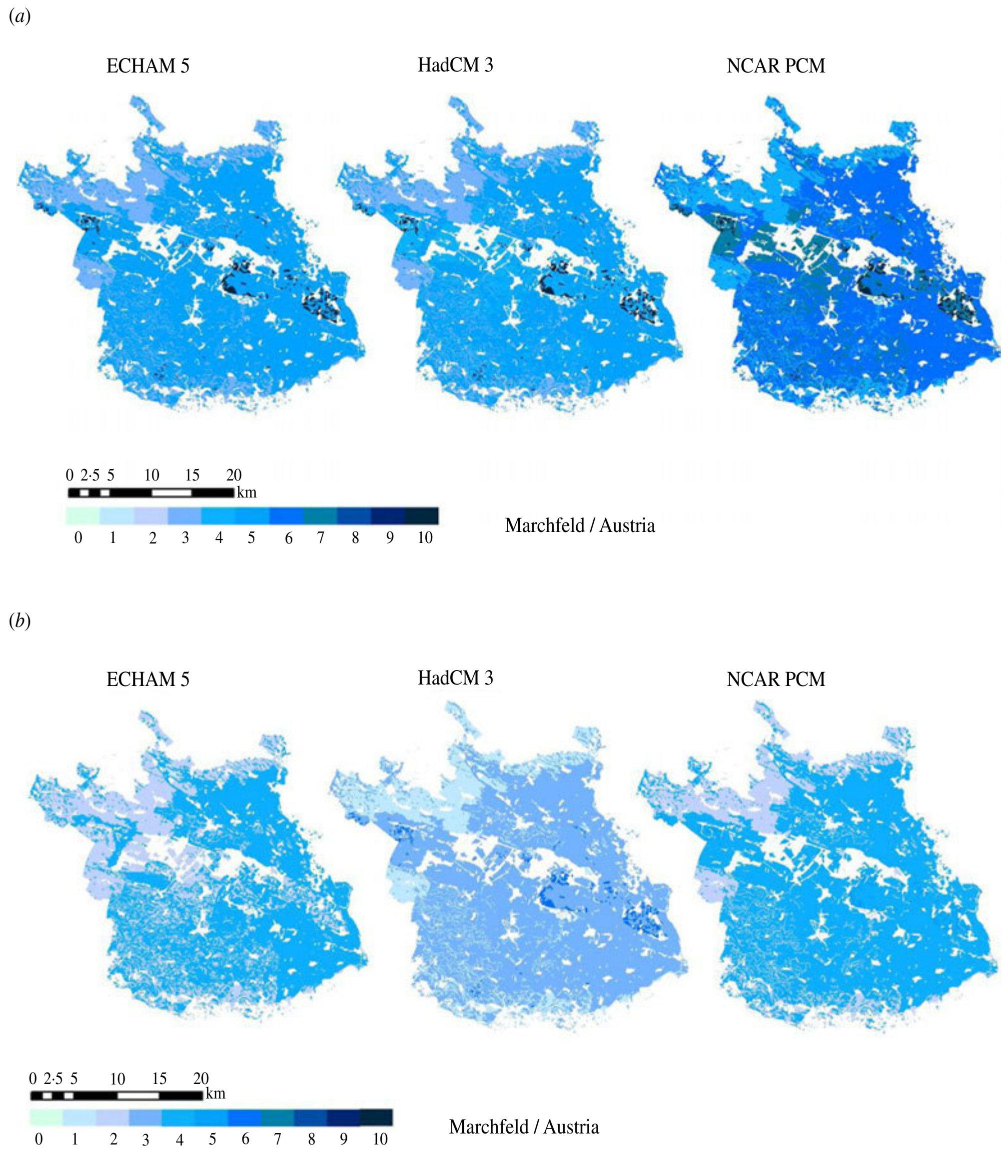

Fig. 7 (*Colour online*). Relative change (%) in the yields of (*a*) winter wheat and (*b*) spring barley yield if ploughing were replaced by minimum tillage in the Marchfeld region (1000 km^2) in 2035 for the various scenarios.

The effect of climate change on crop water demand and the effect of soil cultivation changes on crop yield and water balance were investigated for the Marchfeld region to evaluate potential adaptation effects. The effects of replacing ploughing by the use of minimum tillage on the simulated yield of winter wheat and spring barley are shown in Fig. 7. The results for the 2035 scenarios showed that such altered cultivation would lead to an increase in the mean yield for both crops; this effect was more pronounced for winter wheat and the NCAR scenario. In general, replacing ploughing with minimum tillage under the 2035 scenarios resulted in an increase of the mean yields of winter wheat (up to 10%) and of spring barley (up to 6%). Especially on sandy soils with low water storage capacity (soil classes 1–2), minimum tillage enhanced the yield potential significantly.

This effect was mainly due to improved water supply for the crops and a decrease in unproductive water losses, resulting in higher water use efficiency. If ploughing were replaced by minimum tillage in 2035 for the three climate scenarios, an increase of up to 2·3% vol. was seen in the simulated mean soil water content for the winter wheat growing season and up to 4% vol. in the simulated mean soil water content for the spring barley growing season on sandy soils (Table 4). This result may be due to the greater (*c*. 12%)

https://doi.org/10.1017/S0021859612000767

Table 4. *Simulated relative change of mean soil water content during winter wheat and spring barley growing periods in the Marchfeld region under climate change scenarios in 2035, if ploughing were to be replaced by minimum tillage*

	Marchfeld (area weighted)	Soil 1*	Soil 2*	Soil 3*	Soil 4*	Soil 5*
	Mean change of soil water content (winter wheat) (%)					
ECHAM	+0·6	+2·3	+1·1	+0·6	0	+1·0
HadCM	+0·5	+2·3	+1·1	+0·4	+0·2	+1·4
NCAR	+0·9	+2·2	+1·5	+0·7	+0·8	+1·9
	Mean change of soil water content (spring barley) (%)					
ECHAM	+3·7	+3·2	+3·7	+3·8	+3·3	+1·8
HadCM	+1·0	+4·0	+1·7	+1·0	+0·4	+0·7
NCAR	+1·1	+3·4	+2·5	+0·9	+0·3	+1·5

* Soil classes as defined in Table 2.

Table 5. *Absolute changes of water demand (mm per growing season) required to maintain optimum yield levels of winter wheat and spring barley in the Marchfeld region under climate change scenarios in 2035 with respect to present conditions*

	Marchfeld (area weighted)	Soil 1*	Soil 2*	Soil 3*	Soil 4*	Soil 5*
	Mean change of water demand (winter wheat) (mm)					
ECHAM	+30	−10	25	33	29	14
HadCM	+33	−10	30	36	31	14
NCAR	−3	−30	−10	0	−3	−11
	Mean change of water demand (spring barley) (mm)					
ECHAM	+39	29	36	38	44	31
HadCM	+42	26	40	41	46	32
NCAR	+11	−2	7	13	11	5

* Soil classes as defined in Table 2.

available water storage capacity of the top 250 mm of soils under minimum tillage *v.* ploughing (Thaler *et al.* 2012). The main effective adaptation options for agricultural crop production in semi-arid regions are related to irrigation. Regarding the crop water demand required in the coming decades to maintain optimum yields of winter wheat and spring barley in Marchfeld, the irrigation option 'automatic when required' was used in the simulations for baseline and climate scenarios, respectively. In this context, the effect of nitrate leaching was also considered (in the simulation, nitrogen balance was assumed).

The ECHAM and HadCM scenarios generally led to similar results for potential change of water demand of winter wheat (Table 5). Maintaining optimal yield of winter wheat would require more water (e.g. provided by irrigation) per year (up to 33 mm for the area-weighted average) in 2035, except under the wetter NCAR scenario. Soils with low water storage capacity (sandy soils) showed relatively low yields even at present, and additional water input (irrigation) would reduce yields under all three climate scenarios due to strong increases in nitrate leaching (Table 6). Under the NCAR scenario, even less irrigation would be necessary in almost all soil classes to obtain the same winter wheat yields as those obtained under the baseline scenario (Table 5).

The results showed mostly increased water demand for spring barley for all soils and scenarios (although these are less pronounced under the NCAR scenario); this demand was greater than for winter wheat (Table 5). The nitrate leaching for spring barley was 29 kg/ha, almost twice as much as for winter wheat in the baseline period. The absolute increases in nitrate leaching rates in the climate change scenarios and with optimized irrigation (Table 5) are, in most cases, lower than for winter wheat (Table 6).

https://doi.org/10.1017/S0021859612000767

Table 6. *Changes of nitrate leaching (kg/ha per growing season) for winter wheat and spring barley in the Marchfeld region under climate change scenarios in 2035 that will occur when the change of water demand (as change in irrigation) of Table 5 is applied*

Winter wheat	Marchfeld (area weighted)	Soil 1*	Soil 2*	Soil 3*	Soil 4*	Soil 5*
Present (kg/ha)	15	41	21	15	9	36
	Mean change of nitrate leaching to present conditions (kg/ha)					
ECHAM	+10	+22	+11	+12	+6	+17
HadCM	+13	+24	+14	+15	+8	+21
NCAR	+18	+24	+16	+21	+12	+25
Spring barley						
Present (kg/ha)	29	42	24	33	19	47
	Mean change of nitrate leaching to present conditions (kg/ha)					
ECHAM	+7	+3	+5	+8	+6	+12
HadCM	+11	+6	+9	+13	+9	+16
NCAR	+19	+8	+14	+20	+21	+20

* Soil classes as defined in Table 2.

The effects of climate change on crop growth and yield in the lowlands of Slovakia

The effects of the climate change scenarios for 2021–50 and 2071–2100 (Table 1) on the simulated crop growth and yield of spring barley, winter wheat and maize were estimated and analysed for the main cropping regions of the Danubian and Záhorie lowlands in Slovakia (Fig. 8).

As expected, the physiological maturity of all simulated crops (spring barley, winter wheat and maize) grown on different soil types was accelerated under all three scenarios. Owing to the increased air temperature, spring barley, winter wheat and maize reached maturity on average *c.* 6, 17 and 17 days earlier, respectively during 2071–2100 compared with the baseline of 1971–2000 (results not shown).

The combined effect of changing climate (including the CO_2 fertilization effect) would lead to increasing grain yields of spring barley and winter wheat, especially towards the time horizon of 2021–50. This trend, however, would be stabilized for 2071–2100 over almost the entire area of Western Slovakia. The highest positive yield effects for winter wheat and spring barley were simulated for Haplic Chernozems on Danubian lowlands in Western Slovakia. Unlike the Marchfeld case study, the fertilizing effect of increased concentrations of CO_2 could more than compensate for any decrease in cereal yield in this case, probably due to lower temperature increases and precipitation changes in the climate change scenario applied for Slovakia (Table 1).

Maize yields tended to decline significantly compared with winter wheat and spring barley under the climate scenarios tested. The highest decrease in rainfed maize yields was found during 2071–2100 for the entire case study region (Fig. 8). This was because maize, as a crop grown during summer, was more affected by drought, and the fertilizing effect of increasing CO_2 concentrations is small for C4 crops.

The interannual yield variability of simulated crop yields is influenced mainly by the frequency of extreme weather such as drought and heat waves, although these effects are often not sufficiently considered by crop models (Eitzinger *et al.* 2004; Rötter *et al.* 2011). The present results for the Slovakian case study demonstrated that the interannual variability of yields (indicated as upper and lower quartiles in Fig. 8) in regions with high available water storage capacity was relatively small. However, simulated yields were highly variable in sandy loams, luvisols and fluvisols over the entirety of western Slovakia. Similar relationships were reported from Marchfeld in Austria (Thaler *et al.* 2012).

The interannual yield variability of spring barley and winter wheat, as indicated by the 90% percentile, showed a decreasing trend especially for the 2021–50 periods, except at a few sites. However, in all cases, the differences between the absolute extreme yield levels increased towards 2071. Spring barley generally exhibited lower interannual yield variability than winter wheat and lower differences in the mean yields between the climate scenarios tested (in agreement with the Austrian case study).

https://doi.org/10.1017/S0021859612000767

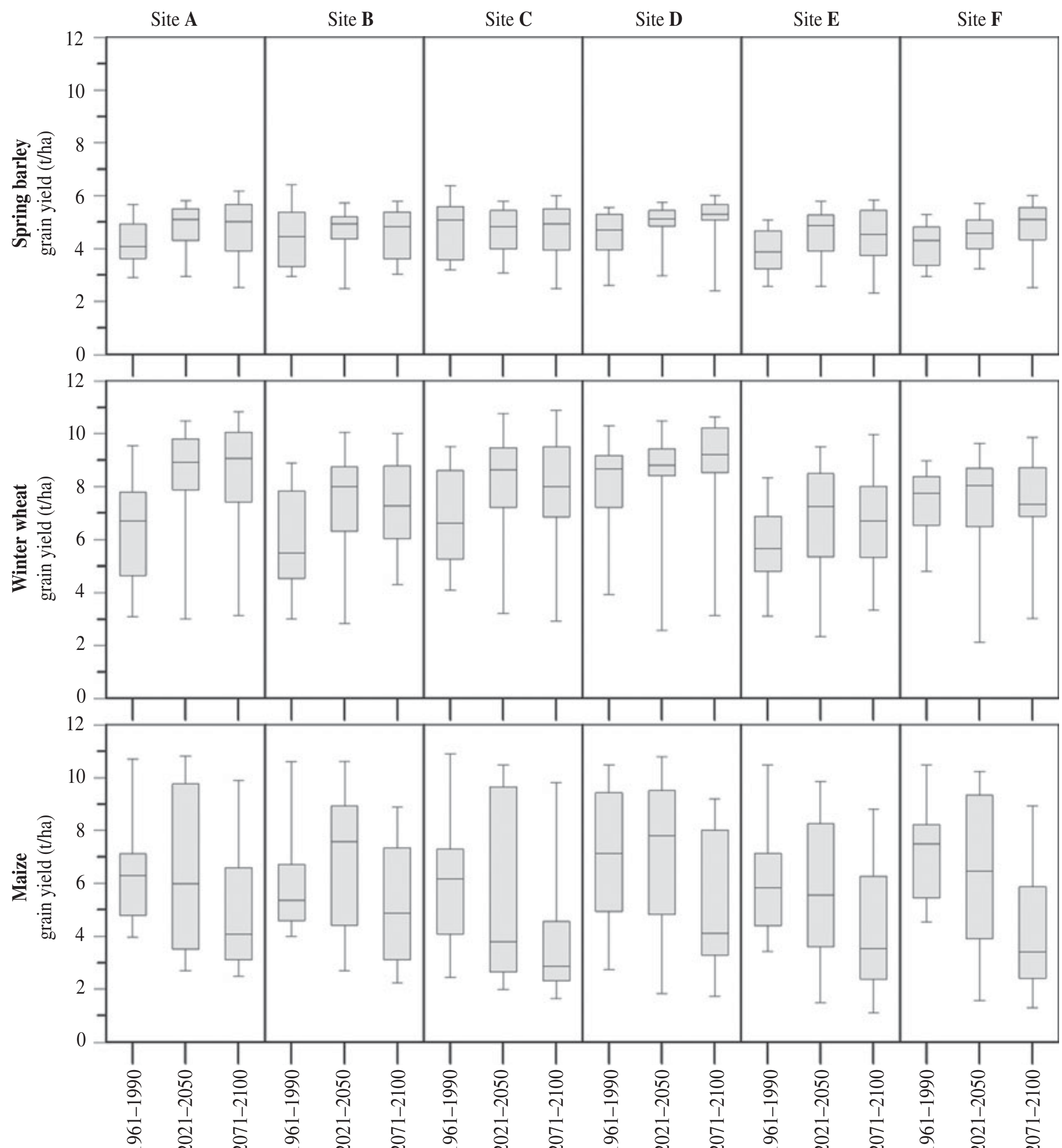

Fig. 8. Grain yields of spring barley, winter wheat and maize for different soils on the Danubian and Záhorie lowlands (Table 2) and the time intervals 1971–2000, 2021–50 and 2071–2100 (statistical distribution: lines represent the simulated full yield range, and columns represent the upper and lower quartiles; the medium yield level is also shown).

Simulated rainfed grain maize yields (representing ripening group FAO310) were affected by increasing temperatures and droughts during summer, as can be seen from the significantly higher interannual yield variabilities especially for 2021–50 and from the strongly decreasing mean yields towards 2071–2100. The simulations clearly showed that the risk for maize cultivation around this ripening group will increase in almost all regions. However, an increase of precipitation during 2021–50 will positively influence the mean yield of grain maize on average (except for the Nitra region). Owing to the lower fertilizing effect of CO_2 on C4 crops, the decrease in maize yields will be greater than that of other cereals, especially in warmer regions. Grain maize is often considered to have increased yield potential due to its heat resistance in the agro-climatic conditions of Slovakia. However, as the present study shows, this could be only exploited with later ripening cultivars and irrigation.

DISCUSSION

Common trends in the effects of climate change in Central and South-eastern Europe

Potential crop yield changes under various climate scenarios are affected by the interaction between

https://doi.org/10.1017/S0021859612000767

climate and other local crop growth-limiting factors. Climate change signals together with increased CO_2 concentrations influence biomass accumulation directly with respect to the genetically determined optimal conditions for the growth and yield of specific cultivars. However, additional parameters that affect crop yield occur on different time scales; these include pest, disease and weed pressures or the damaging effects of extreme weather events such as hail, floods and heavy precipitation. Agroclimatic conditions also affect crop management options and the suitability of crops for specific regions (Trnka *et al.* 2011*a*, *b*). These additional factors affect crop yields both directly (the plant) and indirectly (e.g. via soil conditions and crop management) and should be considered in long-term and holistic assessments of climate change impact studies, including the related uncertainties (Eitzinger *et al.* 2008; Trnka *et al.* 2009). The present study, therefore, used an extended set of parameters for the assessment of Central European crop yield potentials under various climate change conditions (Table 7).

The results showed that most parts of Austria, the Czech Republic, Germany, Poland, Romania, Slovakia, Ukraine and Switzerland exhibited an increase in the mean production potential for the 21st century as a whole (based on the EGR and number of effective growing days). The Pannonian and Mediterranean climatic regions in Hungary, Serbia, Slovenia and Italy were exceptions; in these regions, increases in water deficit will increasingly limit rainfed agriculture. An increase in the severity of the 20-year drought intensity and a more substantial water deficit during the critical part of the growing season are very likely over the central and western parts of the domain. Sowing conditions during spring could deteriorate due to increasing soil wetness, which might further support the preference given to winter crops. Harvest conditions in June (which will become the main harvest period) will generally not improve beyond the current level. In general, it is concluded that rainfed agriculture will face more climate-related risks, and extremely unfavourable years will occur under the applied climate scenarios; however, the overall conditions will probably lead to, on average, increasing yield potentials over the whole domain. This finding is in general agreement with previous studies that have been conducted for this region; however, none of these studies covered the entire domain of Central Europe (Alexandrov *et al.* 2002; Trnka *et al.* 2011*a*) or applied aggregated scales (Trnka *et al.* 2011*b*).

However, based on the combined effects of changing agroclimatic conditions, several additional negative impacts on potential yields can be assumed, such as an increasing risk for soil erosion over the domain, e.g. due to reduced duration of SC and increasing winter precipitation. Overwintering conditions will also change. In winter cereals, for example, this change could affect risk of frost damage and disease pressure either positively or negatively (depending on the combination of SC, temperatures and frost impact). However, no significant negative impacts on the mean vernalization conditions of winter wheat were calculated over the domain with the assumed temperature thresholds.

Further yield-limiting factors include the increasing potential for damage from pests due to warmer conditions, especially from thermophile insects in most of the domain, as demonstrated by the findings related to the ECB and the CPB. Significant shifts in spatial occurrence can also be expected for weeds and diseases (Porter *et al.* 1991).

Spatial analysis conducted for winter wheat yields in the Czech case study concerning altitude suggested that cereal yields should increase especially in upland regions, where increasing temperatures will provide favourable conditions, rainfall will remain sufficient and soil conditions are relatively good. The spatial patterns of yield distribution for spring barley were similar for all altitude categories according to all three projections considered. Despite differences between individual regions, the simulated trend seemed to be slightly positive or without any significant change across the entire Czech Republic until 2050.

In the Austrian case study region of Marchfeld, factors that particularly limit crop yields were analysed, and these are comparable with those of the lowland conditions in the Czech Republic. It can be clearly seen for both winter wheat and spring barley that shorter growing periods (Porter & Gawith 1999) will lead to decreases in yield for currently grown cultivars under the applied climate change scenarios (except the NCAR scenario that includes increasing precipitation) until 2035. Therefore, the decrease in spring and summer precipitation in the climate scenarios is also a crucial factor for this semi-arid region. Owing to the limitation of crop water availability, the decreases in yields would be even more significant without the assumed CO_2 fertilizing effect (Amthor 2001). However, the degree of this effect is uncertain from crop model estimates and differs between crops and cultivars (Tubiello *et al.*

https://doi.org/10.1017/S0021859612000767

Table 7. *Overview of the estimated trends in factors for crop production over the Central and Eastern European domain under the various CC scenarios presented in Table 1*

Crop production factor	CC scenario and time horizon	Simulated region of the domain	Crops affected	Trend (+/0/−)	Comments
EGR	All 2050	North-west*	All	+	Especially south and south-eastern part of the domain affected negatively (i.e. Pannonian lowlands)
		North-east*		+	
		South-west*		−	
		South-east*		−	
Drought		North-west*	All	−/0	Enhanced regional differences over the domain with relation to orography; especially south and south-eastern part of the domain affected negatively; water deficit and heat stress during summer increases over the whole domain
		North-east*		+	
		South-west*		+	
		South-east*		+	
HUG index		All	Grapes	+	Improved wine growing conditions throughout the domain
Winter conditions		All	Winter crops and perennials	+/0	Overall improvement of winter conditions; little change for vernalization conditions and late FR; Potential of higher risks for diseases; increased soil erosion risk depending on region (orography)
Spring conditions		South-east*	All crops	+	Spring conditions improve or decrease depending on the region; autumn conditions and harvest conditions in June will mostly improve over the domain
		North-west*		−	
		North-east*		+	
		South-west*		−	
Nitrate leaching change (crop model)	All 2035	Austria – Marchfeld	Winter Wheat	+	Higher N-leaching especially on sandy soils and with irrigation
			Spring barley	+	Higher N-leaching especially on sandy soils and with irrigation
Pest pressure– Corn borer	All 2050	North-west*	Maize	+	More infestation of maize due to the newly presence of the pest in still not affected areas; additionally the increase of generation number in regions with long-term presence of the pest
		North-east*		+	Similar to north-west region
		South-west*		+	Modest growth of the number of generation
		South-east*		+	Similar to south-west region; In whole domain the shift of the pest coupled with the increase of generation number will likely affect economical losses caused by lower yield of maize and higher cost of the pest management
Pest pressure– Colorado beetle	All 2050	North-west*	Potato, tomato	+	In areas with potato cultures higher pest harmfulness due to the increase of generation number; total defoliation of plants with subsequent loss of yield can be expected
		North–east*		+	Similar to north-west
		South–west*		−	Croatia and the north of Italy – recession of the pest as a reaction to high temperature stress which potentially could decrease the costs of pest management if the plants would not be affected by drought
		South–east*		−	Serbia, Hungary – the same effect of high temperature stress as in south-west area

Crop yield (indirect effect)	SRES-A2 2050 ECHAM	Czech Republic – arable land	Winter wheat, winter barley, winter rye, winter rape	–	Lowlands mostly affected negatively
	SRES-A2 2050 HadCM			–	
	SRES-A2 2050 NCAR			–	
	All 2050		Spring barley, spring wheat, oat	–	Especially within drought-prone regions (e.g. Southern Moravia)
Crop yield (combined effect)	All 2050	Czech Republic – arable land	Winter barley, winter rye, winter rape	+	Especially regions within higher altitudes with quality soils will be affected positively
			spring barley, spring wheat, oat	+	Steady positive effect through all included altitudes
	All 2035	Austria–Marchfeld	Winter wheat	+	Soil type dependent (most enhanced yields on medium soils); additional water demand 30–40 mm
			Spring barley	0	Most limited on sandy soils; additional water demand
	SRES A1B ARPEGE 2021–2050 2071–2100	Slovakia – Danubian and Záhorie lowlands	Winter wheat	+	Soil type dependent (most stable yields on calcaric chernozems)
			Spring barley	+	Soil type dependent (most stable yields on calcaric chernozems); Higher yield variability in 2021–2050
			Grain maize	–	Drought periods during growing season will decrease yields on all evaluated soils; higher yield variability in 2021–2050

* Sector of the CECILIA domain (Fig. 1).

1999; Tubiello & Ewert 2002; Wolf *et al.* 2002; Nendel *et al.* 2009). In addition, the effects of direct heat stress and ozone will probably create additional yield risks (Semenov & Shewry 2011).

The Marchfeld study on winter wheat and spring barley showed that because of increased water demand, additional irrigation of *c.* 30–40 mm would be necessary to maintain current yield levels under the drier scenarios because these crops are not irrigated under current conditions. Additional water input can, however, increase nitrate leaching rates, especially on sandy soils, reducing positive effect on yield. Another example of an adaptation measure that could be used to improve crop water availability is alteration of the soil cultivation method (the present study examined a change from ploughing to minimum tillage), and this leads to higher simulated soil water contents and yields due to higher soil water storage capacity under minimum tillage. Based on the two crops studied for the semi-arid lowland region of Marchfeld in central Europe, several crop management factors have to be considered to adapt to new climatic conditions. Soil water and N-fertilization management techniques may play a crucial role in maintaining the production potential of cereals (Thaler *et al.* 2012).

Several studies focused on Europe have noted that climate change can affect interannual crop yield variability (Hlavinka *et al.* 2009; Peltonen-Sainio *et al.* 2010). This fact is confirmed for the present Slovakian case study region for different sites and soils, especially for maize. It revealed increasing maize yield variability towards the middle of the 21st century, followed by a later decrease. As indicated by the Marchfeld study results and the increasing drought frequencies under the various climate scenarios (see the agroclimatic indices), extreme shortages of precipitation in some years will depress crop yields, especially on sandy loam and loamy soils (luvisols, fluvisols and chernozems). However, under good soil conditions, the direct CO_2 fertilizing effect may lead to lower yield variability and increasing mean crop yields. Grain maize yields are also expected to decrease for almost all evaluated time horizons if there is no adaptation using later-ripening cultivars and irrigation (Vučetić 2011).

Although several risks and trends can already be described for crop yield potentials for the main areas of the studied domain under climate change conditions (Table 7), it is noted that the current local soil and climate conditions can vary significantly within small areas; changing precipitation levels and temperatures

https://doi.org/10.1017/S0021859612000767

can therefore have variable effects relative to each other on locally grown crops and cultivars.

Recommended adaptation options

Farmers must and will respond to the changing growing conditions by altering their production techniques (Olesen & Bindi 2002; Reidsma *et al.* 2009). The major climate change impacts of the present study are related to changes in the seasonal water balance for crops accompanied with increased temperatures; under future climate scenarios, increasing drought and heat stress during summer and wetter and warmer conditions during winter can be expected.

Specific recommendations for adaptation can therefore be related to altered production techniques that affect the water balance/demand of crops, the effective use of water and soil resources (EEA 2005), adapted crop timing and selection, and altered pest/disease/weed management.

Rainfed summer crops such as maize and spring crops, particularly in the lowlands of the domains (e.g. the Pannonian region), will lose production potential unless their management is altered (Trnka *et al.* 2010*b*). Therefore, the growing of winter crops and the consequent use of intermediate crops can be recommended to reduce yield risks that leading to lower mean yields and higher interannual yield variability. Moreover, vegetation cover during winter will protect against soil erosion resulting from warmer winters with less SC and higher precipitation. This will be especially important for crops grown on hilly terrain and erosive soils over the domain (Klik & Eitzinger 2010).

Several measures for reducing unproductive evaporation will be increasingly crucial for rainfed crops. A number of management options are available for improving water availability and water use efficiency including irrigation, soil cultivation, fertilization, crop rotation and others (Latiri-Souki *et al.* 1998; Connor 2004; Tennakoon & Hulugalle 2006; Zhang *et al.* 2006; Hsiao *et al.* 2007). For example, permanent soil cover (mulch) established during periods without crop cover (preferably in connection with reduced soil cultivation methods or direct drilling) can reduce evaporation and nitrate leaching (Thaler *et al.* 2012). Mulching also contributes to reduced soil erosion, surface leakage and crust formation (thereby reducing runoff). Windbreaks such as hedgerows can reduce unproductive water losses, especially in the Pannonian Lowlands, which experience high wind loads (Müller 1993). Flexible fertilization schemes, especially for nitrogen, should reflect seasonal shifts of rainfall and rainfall intensity. For example, applying precision farming methods (e.g. considering real-time crop demand, reduced and more frequent applications, using slow-release fertilizers, etc.) can help farmers to adapt to the new conditions.

The present results have shown that crops, especially in the warm and dry lowland regions (the Danubian lowlands and vast regions of the Pannonian area of south-eastern Europe) will need more water to maintain their production potential. With regard to irrigation, efficient management of regional irrigation water resources, improvements in the water use efficiency of irrigation systems and the introduction and application of efficient irrigation methods such as deficit irrigation are recommended.

Owing to the increasing temperatures, growing degree days (GDDs) will increase throughout the domain, leading to longer vegetation seasons and shortened crop growing periods. Simultaneously, the number of heat extremes and heat stress days for crops will increase significantly, and this has been identified as an important yield-limiting factor for cereals (drought stress is another) (Semenov & Shewry 2011). Therefore, selection (and breeding) of adapted cultivars with respect to the higher expected GDD demand and for drought and heat tolerance will be important for all regions of the domain.

Other measures that can be used to adapt to longer vegetation periods are shifting sowing dates or changing the crops planted to those that are adapted to higher temperatures and exhibit heat tolerance (e.g. millet, maize, soybeans or sunflowers). Land use, especially in highlands with permanent grasslands, could be increasingly forced towards fodder crops or other farming types such as the planting of orchards or vineyards (Trnka *et al.* 2011*a*). Where this is not possible, a decrease in grassland production potential can be expected (such as in the highlands of the Czech Republic or northern and south-eastern parts of Austria).

As demonstrated in the present study, thermophile pests could spread considerably (and increase their populations by breeding more often within one season) under the future climate scenarios; this may be exacerbated by increases in the areas being devoted to the host crops (e.g. maize). This development will require efficient and better crop protection methods in future decades over the domain. In addition to technical measures such as adapted crop rotations,

https://doi.org/10.1017/S0021859612000767

the use of new genetic cultivars, adapted soil cultivation and monitoring and forecasting systems will be crucial for early warning to allow efficient crop protection.

International cooperation and data for this study were provided through support of the 6th FP EU projects CECILIA (Central and Eastern Europe Climate Change Impact and Vulnerability Assessment (www.cecilia-eu.org)), ADAGIO (Adaptation of Agriculture in European Regions at Environmental Risk under Climate Change) SSPE-CT-2006-044210 and CLIMSAVE (Climate Change Integrated Assessment Methodology for Cross-Sectoral Adaptation and Vulnerability in Europe) no. 244031, OPVK project Partnership in Climate Research and Adaptation Strategies (no.: CZ.1·07/2·4·00/31·0056) and COST 734 action.

REFERENCES

Abrahamsen, P. & Hansen, S. (2000). Daisy: an open soil–crop–atmosphere system model. *Environmental Modelling and Software* **15**, 313–330.

Alexandrov, V., Eitzinger, J., Cajic, V. & Oberforster, M. (2002). Potential impact of climate change on selected agricultural crops in north-eastern Austria. *Global Change Biology* **8**, 372–389.

ARGONNE NATIONAL LABORATORY (ANL) (1994). *Guidance for Vulnerability and Adaptation Assessments*. Illinois, USA: USCSP.

Arora, R. & Rowland, L. J. (2011). Physiological research on winter-hardiness: deacclimation resistance, reacclimation ability, photoprotection strategies, and a cold acclimation protocol design. *Hortscience* **46**, 1070–1078.

Audsley, E., Pearn, K. R., Simota, C., Cojocaru, G., Koutsidou, E., Rounsevell, M. D. A., Trnka, M. & Alexandrov, V. (2006). What can scenario modelling tell us about future European scale land use, and what not? *Environmental Science and Policy* **9**, 148–162.

Amthor, J. S. (2001). Effects of atmospheric CO_2 concentration on wheat yield: review of results from experiments using various approaches to control CO_2 concentration. *Field Crops Research* **73**, 1–34.

BFW – Bundesforschungs- und Ausbildungszentrum für Wald, Naturgefahren und Landschaft (2007). *Digitale Bodenkarte von Österreich*. Vienna: BFW.

Connor, D. J. (2004). Designing cropping systems for efficient use of limited water in southern Australia. *European Journal of Agronomy* **21**, 419–431.

Cooper, G., Mcgechan, M. B. & Vinten, A. J. A. (1997). The influence of a changed climate on soil workability and available workdays in Scotland. *Journal of Agriculture Engineering Research* **68**, 253–269.

Dalla Marta, A., Grifoni, D., Mancini, M., Storchi, P., Zipoli, G. & Orlandini, S. (2010). Analysis of the relationships between climate variability and grapevine phenology in the Nobile di Montepulciano wine production area. *Journal of Agricultural Science, Cambridge* **148**, 657–666.

Dubrovský, M., Nemešová, I. & Kalvová, J. (2005). Uncertainties in climate change scenarios for the Czech Republic. *Climate Research* **29**, 139–156.

EPPO (2009). *EPPO Plant Quarantine Data Retrieval System*. PQR- version 4.6. Paris, France: EPPO. Available from: www.eppo.org/DATABASES/pqr/pqr.htm (verified 14 October 2009).

European Environmental Agency (EEA) (2005). Vulnerability and adaptation to climate change in Europe. *EEA Technical Report No. 7*. Copenhagen: EEA.

European Environmental Agency (EEA) (2007). Climate change: the cost of inaction and the cost of adaptation. *EEA Technical Report No. 13*. Copenhagen: EEA.

Eitzinger, J., Stastná, M., Zalud, Z. & Dubrovský, M. (2003). A simulation study of the effect of soil water balance and water stress on winter wheat production under different climate change scenarios. *Agricultural Water Management* **61**, 195–217.

Eitzinger, J., Trnka, M., Hösch, J., Žalud, Z. & Dubrovský, M. (2004). Comparison of CERES, WOFOST and SWAP models in simulating soil water content during growing season under different soil conditions. *Ecological Modelling* **171**, 223–246.

Eitzinger, J., Utset, A. & Alexandrov, V. (2007). Methods for assessing climate change impacts and adaptation measures in agriculture – the ADAGIO project. *Georgikon for Agriculture* **15**, 1–9.

Eitzinger, J., Formayer, H., Thaler, S., Trnka, M., Zdenek, Z. & Alexandrov, V. (2008). Results and uncertainties of climate change impact research in agricultural crop production in Central Europe. *Bodenkultur* **59**, 131–147.

Farda, A., Štepánek, P., Halenka, T., Skalák, P. & Belda, M. (2007). Model ALADIN in climate mode forced with ERA-40 reanalysis (coarse resolution experiment). *Meteorological Journal* **10**, 123–130.

Fuhrer, J. (2003). Agroecosystem responses to combinations of elevated CO2, ozone and global climate change. *Agriculture, Ecosystems and Environment* **97**, 1–20.

Hakala, K., Jauhiainen, L., Himanen, S. J., Rötter, R., Salo, T. & Kahiluoto, H. (2012). Sensitivity of barley varieties to weather in Finland. *Journal of Agricultural Science, Cambridge* **150**, 145–160.

Hansen, S. (2000). *DAISY, a Flexible Soil – Plant – Atmosphere System Model. Equation Section 1*. Copenhagen: The Royal Veterinary and Agricultural University.

Hansen, S., Jensen, H. E., Nielsen, N. E. & Svendsen, H. (1990). *DAISY – A Soil Plant System Model. Danish Simulation Model for Transformation and Transport of Energy and Matter in the Soil-Plant-Atmosphere System*. Copenhagen: National Agency for Environmental Protection.

Hansen, S., Jensen, H. E., Nielsen, N. E. & Svendsen, H. (1991). Simulation of nitrogen dynamics and biomass production in winter wheat using the Danish simulation model DAISY. *Fertilizer Research* **27**, 245–259.

Hlavinka, P., Trnka, M., Semerádová, D., Dubrovský, M., Zalud, Z. & Mozny, M. (2009). Effect of drought on yield variability of key crops in Czech Republic. *Agricultural and Forest Meteorology* **149**, 431–442.

Hoddle, M. S. (2004). The potential adventive geographic range of glassy-winged sharpshooter, Homalodisca coagulata and the grape pathogen Xylella fastidiosa: implications for California and other grape growing regions of the world. *Crop Protection* **23**, 691–699.

Hoogenboom, G., Jones, J. W., Wilkens, P. W., Batchelor, W. D., Bowen, W. T., Hunt, L. A., Pickering, N. B., Singh, U., Godwin, D. C., Bear, B., Boote, K. J., Ritchie, J. T. & White, J. W. (1994). *Crop models, DSSAT Version 3.0*. International Benchmark sites Network for Agrotechnology Transfer. Honolulu, USA: University of Hawaii.

Hsiao, T. C., Steduto, P. & Fereres, E. (2007). A systematic and quantitative approach to improve water use efficiency in agriculture. *Irrigation Science* **25**, 209–231.

Huglin, P. (1978). Nouveau mode d'évaluation des possibilités héliothermique d'un milieu viticole. *Comptes Rendus Académie d'Agriculture* **1978**, 1117–1126.

Hulme, M., Wigley, T. M. L., Barrow, E. M., Raper, S. C. B., Centella, A., Smith, S. & Chipanshi, A. C. (2000). *Using a Climate Scenario Generator for Vulnerability and Adaptation Assessments: MAGICC and SCENGEN Version 2.4 Workbook*. Norwich, UK: Climatic Research Unit.

Iqbal, M. A., Eitzinger, J., Formayer, H., Hassan, A. & Heng, L. K. (2011). A simulation study for assessing yield optimization and potential for water reduction for summer-sown maize under different climate change scenarios. *Journal of Agricultural Science, Cambridge* **149**, 129–143.

IPCC (2011). Summary for policymakers. In *Intergovernmental Panel on Climate Change Special Report on Managing the Risks of Extreme Events and Disasters to Advance Climate Change Adaptation* (Eds C. B. Field, V. Barros, T. F. Stocker, D. Qin, D. J. Dokken, K. L. Ebi, M. D. Mastrandrea, K. J. Mach, G.-K. Plattner, S. K. Allen, M. Tignor & P. M. Midgley), pp. 3–24. Cambridge, UK: Cambridge University Press.

Keszthelyi, S. & Lengyel, Z. (2003). Flight of the ECB (*Ostrinia nubilalis* Hbn.) as followed by light and pheromone traps in Várdaadn balatonmagyaród 2002. *Journal of Central European Agriculture* **4**, 55–64.

Klik, A. & Eitzinger, J. (2010). Impact of climate change on soil erosion and the efficiency of soil conservation practices in Austria. *Journal of Agricultural Science, Cambridge* **148**, 529–541.

Kocmánková, E., Trnka, M., Zalud, Z., Semeradova, D., Dubrovsky, M., Muska, F. & Mozny, M. (2008). The comparison of mapping methods of European corn borer (*Ostrinia nubilalis*) potential distribution. *Plant Protection Science* **44**, 49–56.

Kruijt, B., Witte, J. P. M., Jacobs, C. M. J. & Kroon, T. (2008). Effects of rising atmospheric CO_2 on evapotranspiration and soil moisture: a practical approach for the Netherlands. *Journal of Hydrology* **349**, 257–267.

Latiri-Souki, A. K., Nortcliff, S. & Lawlor, D. W. (1998). Nitrogen fertilizer can increase dry matter, grain production and radiation and water use efficiencies for durum wheat under semi-arid conditions. *European Journal of Agronomy* **9**, 21–34.

Lopez, P., Schmith, T. & Kaas, E. (2000). Sensitivity of the Northern Hemisphere circulation to North Atlantic SSTs in the ARPEGE climate AGCM. *Climate Dynamics* **16**, 535–547.

Mason, C. E., Rice, M. E., Calvin, D. D., Van Duyn, J. W., Showers, W. B., Hutchinson, W. D., Witkowski, J. F., Higgins, R. A., Onstad, D. W. & Dively, G. P. (1996). *European Corn Borer: Ecology and Management*. North Central Region Extension Publication no. 327. Ames, Iowa, USA: Iowa State University.

Murer, E., Wagenhofer, J., Aigner, F. & Pfeffer, M. (2004). Die nutzbare Feldkapazität der mineralischen Böden der landwirtschaftlichen Nutzfläche Österreichs. *Schriftenreihe BAW* **20**, 72–78.

Müller, W. (1993). *Agroklimatische Kennzeichnung des Marchfelds*. Beiheft 3 zu den Jahrbüchern der Zentralanstalt für Meteorologie und Geodynamik. Vienna, Austria: Eigenverlag.

Nendel, C., Kersebaum, K. C., Mirschel, W., Manderscheid, R., Weigel, H. J. & Wenkel, K. O. (2009). Testing different CO2 response algorithms against a FACE crop rotation experiment. *NJAS-Wageningen Journal of Life Sciences* **57**, 17–25.

Olesen, J. E. & Bindi, M. (2002). Consequences of climate change for European agricultural productivity, land use and policy. *European Journal of Agronomy* **16**, 239–262.

Orlandini, S., Nejedlik, P., Eitzinger, J., Alexandrov, V., Toulios, L., Calanca, P., Trnka, M. & Olesen, J. E. (2008). Impacts of climate change and variability on European agriculture: results of inventory analysis in COST 734 countries. *Annals of the New York Academy of Sciences* **1146**, 338–353.

Otter-Nacke, S., Ritchie, J. T., Godwin, D. C. & Singh, U. (1991). *A User's Guide to CERES Barley – V2·10*. Muscle Shoals, AL, USA: International Fertilizer Development Center Simulation manual, IFDC-SM-3.

Parry, M. & Carter, T. (1998). *Climate Impact and Adaptation Assessment*. London: Earthscan Publication Ltd.

Patil, R. H., Laegdsmand, M., Olesen, J. E. & Porter, J. R. (2010). Growth and yield response of winter wheat to soil warming and rainfall patterns. *Journal of Agricultural Science, Cambridge* **148**, 553–566.

Peltonen-Sainio, P., Jauhiainen, L., Trnka, M., Olesen, J. E., Calanca, P., Eckersten, H., Eitzinger, J., Gobin, A., Kersebaum, K. C., Kozyra, J., Kumar, S., Dalla Marta, A., Micale, F., Schaap, B., Seguin, B., Skjelvag, A. O. & Orlandini, S. (2010). Coincidence of variation in yield and climate in Europe. *Agriculture, Ecosystems and Environment* **139**, 483–489.

Petr, J. & Hnilička, F. (2002). Changes in requirements on vernalization of winter wheat varieties in the Czech Republic in 1950–2000. *Plant, Soil and Environment (Rostlinná Výroba)* **48**, 148–153.

Porter, J. R. & Gawith, M. (1999). Temperatures and the growth and development of wheat: a review. *European Journal of Agronomy* **10**, 23–36.

Porter, J. H., Parry, M. L. & Carter, T. R. (1991). The potential effects of climatic change on agricultural insect pests. *Agricultural and Forest Meteorology* **57**, 221–240.

Reidsma, P., Ewert, F., Lansink, A. O. & Leemans, R. (2009). Adaptation to climate change and climate variability in european agriculture: the importance of farm level responses. *European Journal of Agronomy* **32**, 91–102.

Rischbeck, P. M. (2007). *Der Einfluss von Klimaänderung, Bodenbearbeitung und Saattermin auf den Wasserhaushalt und das Ertragspotential von Getreide im Marchfeld*. Dissertation, Uiversität für Bodenkultur, Wien.

Ritchie, J. T. & Otter, S. (1985). Description and performance of CERES-Wheat: a user-oriented wheat yield model. In *ARS Wheat Yield Project* (Ed. W. O. Willis), pp. 159–175. ARS-38, US Department of Agriculture-Agricultural Research Service, Springfield, VA.

Rötter, R. P., Carter, T. R., Olesen, J. E. & Porter, J. R. (2011). Crop-climate models need an overhaul. *Nature Climate Change* **1**, 175–177.

Rounsevell, M. D. A. (1993). A review of soil workability models and their limitations in temperate regions. *Soil Use and Management* **9**, 15–21.

Santer, B. D., Wigley, T. M. L., Schlesinger, M. E. & Mitchell, J. F. B. (1990). Developing climate scenarios from equilibrium GCM results. *Report No. 47*. Hamburg: Max Planck Institut für Meteorologie.

Schultz, H. R., Hoppmann, D. & Hofmann, M. (2005). *Der Einfluss Klimatischer Veränderungen auf die Phänologische Entwicklung der Rebe, die Sorteneignung sowie Mostgewicht und Säurestruktur der Trauben*. Beitrag zum Integrierteen Klimaschutzprogramm des Landes Hessen (InKlim 2012) des Fachgebiets Weinbau der Forschungsanstalt Geisenheim. Wiesbaden, Germany: Hessisches Landesamt für Umwelt und Geologie. Available from: http://klimawandel.hlug.de/fileadmin/dokumente/klima/inklim/endberichte/weinbau.pdf (Accessed 18 September 2012).

Semenov, M. A. & Porter, J. R. (1995). Climatic variability and the modelling of crop yields. *Agricultural and Forest Meteorology* **73**, 265–283.

Semenov, M. A. & Shewry, P. R. (2011). Modelling predicts that heat stress, not drought, will increase vulnerability of wheat in Europe. *Scientific Reports* **1**, 66. doi:10.1038/srep00066.

Strauss, F., Schmid, E., Moltchanova, E., Formayer, H. & Wang, X. (2012). Modeling climate change and biophysical impacts of crop production in the Austrian Marchfeld region. *Climatic Change* **111**, 641–664.

Solomon, S., Qin, D., Manning, M., Chen, Z., Marquis, M., Averyt, K. B., Tignor, M. & Miller, H. L. (2007). *Contribution of Working Group I to the Fourth Assessment Report of the Intergovernmental Panel on Climate Change*. Cambridge, UK: Cambridge University Press.

Sutherst, R. W. & Maywald, G. F. (1985). A computerised system for matching climates in ecology. *Agriculture, Ecosystems and Environment* **13**, 281–299.

Sutherst, R. W., Maywald, G. F., Bottomley, W. & Bourne, A. (2001). CLIMEX v2 User's Guide. *CSIRO Entomology* **12–13**, 281–99.

Takáč, J. & Šiška, B. (2011). Calibration and Validation of DAISY Model In Conditions of the Slovak Republic (in Slovak with English abstract). *Proceedings of Soil Science and Conservation Research Institute* **33**, 161–172. Available from: http://www.vupop.sk/dokumenty/vedecke_prace_2011.pdf (Accessed 10 July 2012).

Tennakoon, S. B. & Hulugalle, N. R. (2006). Impact of crop rotation and minimum tillage on water use efficiency of irrigated cotton in a Vertisol. *Irrigation Science* **25**, 45–52.

Thaler, S., Eitzinger, J., Trnka, M. & Dubrovsky, M. (2012). Impacts of climate change and alternative adaptation options on winter wheat yield and water productivity in a dry climate in Central Europe. *The Journal of Agricultural Science* **150**, 537–555.

Tomášek, J. (2007). *Soils of the Czech Republic*. Prague: Czech Geological Service.

Trnka, M., Dubrovský, M., Semerádová, D. & Žalud, Z. (2004*a*). Projections of uncertainties in climate change scenarios into expected winter wheat yields. *Theoretical and Applied Climatology* **77**, 229–249.

Trnka, M., Dubrovský, M., & Žalud, Z. (2004*b*). Climate change impacts and adaptation strategies in spring barley production in the Czech Republic. *Climatic Change* **64**, 227–255.

Trnka, M., Eitzinger, J., Hlavinka, P., Dubrovský, M., Semeradova, D., Stepanek, P., Thaler, S., Zalud, Z., Mozny, M. & Formayer, H. (2009). Climate-driven changes of production regions in Central Europe. *Plant, Soil and Environment* **55**, 257–266.

Trnka, M., Kocmánková, E., Balek, J., Eitzinger, J., Ruget, F., Formayer, H., Hlavinka, P., Schaumberger, A., Horáková, V., Možný, M. & Zalud, Z. (2010*a*). Simple snow cover model for agrometeorological applications. *Agricultural and Forest Meteorology* **150**, 1115–1127.

Trnka, M., Eitzinger, J., Dubrovský, M., Semerádová, D., Štěpánek, P., Hlavinka, P., Balek, J., Skalák, P., Farda, A., Formayer, H. & Žalud, Z. (2010*b*). Is rainfed crop production in central Europe at risk? Using a regional climate model to produce high resolution agroclimatic information for decision makers. *Journal of Agricultural Science, Cambridge* **148**, 639–656.

Trnka, M., Eitzinger, J., Semeradova, D., Hlavinka, P., Balek, J., Dubrovsky, M., Kubu, G., Stepanek, P., Thaler, S., Mozny, M. & Zalud, Z. (2011*a*). Expected changes in agroclimatic conditions in Central Europe. *Climatic Change* **108**, 261–289.

Trnka, M., Olesen, J. E., Kersebaum, K. C., Skjelvag, A. O., Eitzinger, J., Seguin, B., Peltonen-Sainio, P., Rötter, R., Iglesias, A., Orlandini, S., Dubrovsky, M., Hlavinka, P., Balek, J., Eckersten, H., Cloppet, E., Calanca, P., Gobin, A., Vucetic, V., Nejedlik, P., Kumar, S., Lalic, B., Mestre, A., Rossi, F., Kozyra, J., Alexandrov, V., Semeradova, D. & Zalud, Z. (2011*b*). Agroclimatic conditions in Europe under climate change. *Global Change Biology* **17**, 2298–2318.

Tsuji, G. Y., Uehara, G. & Balas, S. (1994). *DSSAT v3*. Honolulu, Hawaii, USA: University of Hawaii.

Tsuji, G. Y., Hoogenboom, G. & Thorton, P. K. (1998). *Understanding Options for Agricultural Production*. Kluwer Academic, Dodrecht, The Netherlands.

Tubiello, F. N. & Ewert, F. (2002). Simulating the effects of elevated CO_2 on crops: approaches and applications for climate change. *European Journal of Agronomy* **18**, 57–74.

Tubiello, F. N., Rosenzweig, C., Kimball, B. A., Pinter, P. J., Wall, G. W., Husanker, D. J., Lamorte, R. L. & Garcia, R. L. (1999). Testing CERES-Wheat with free-air carbon dioxide enrichment (FACE) experiment data: CO_2 and water interactions. *Agronomy Journal* **91**, 247–255.

Vučetić, V. (2011). Modelling of maize production in Croatia: present and future climate. *Journal of Agricultural Science, Cambridge* **149**, 145–157.

White, J. W., Hoogenboom, G., Kimball, B. A. & Wall, G. W. (2011). Methodologies for simulating impacts of climate change on crop production. *Field Crops Research* **124**, 357–368.

Wolf, J., Van Oijen, M. & Kempenaar, C. (2002). Analysis of the experimental variability in wheat responses to elevated CO_2 and temperature. *Agriculture, Ecosystems and Environment* **93**, 227–247.

Žalud, Z. & Dubrovský, M. (2002). Modelling climate change impacts on maize growth and development in the Czech Republic. *Theoretical and Applied Climatology* **72**(1–2), 85–102.

Zhang, B., Li, F. M., Huang, G., Cheng, Z. Y. & Zhang, Y. (2006). Yield performance of spring wheat improved by regulated deficit irrigation in an arid area. *Agricultural Water Management* **79**, 28–42.

atmosphere

MDPI

Article

Effects of Different Spatial Precipitation Input Data on Crop Model Outputs under a Central European Climate

Sabina Thaler [1,2,*], Luca Brocca [3], Luca Ciabatta [3], Josef Eitzinger [1], Sebastian Hahn [4] and Wolfgang Wagner [4]

[1] Institute of Meteorology, University of Natural Resources and Life Sciences (BOKU), Gregor-Mendel-Straße 33, 1180 Vienna, Austria; josef.eitzinger@boku.ac.at
[2] CzechGlobe—Global Change Research Institute CAS, Belidla 986, 4a, 603 00 Brno, Czech Republic
[3] Research Institute for Geo-Hydrological Protection, National Research Council, Via della Madonna Alta 126, 06128 Perugia, Italy; luca.brocca@irpi.cnr.it (L.B.); luca.ciabatta@irpi.cnr.it (L.C.)
[4] Department of Geodesy and Geoinformation, Vienna University of Technology (TU Wien), Gußhausstraße 27–29, 1040 Vienna, Austria; sebastian.hahn@geo.tuwien.ac.at (S.H.); wolfgang.wagner@geo.tuwien.ac.at (W.W.)
* Correspondence: sabina.thaler@boku.ac.at; Tel.: +43-1-47654-81420

Received: 30 May 2018; Accepted: 23 July 2018; Published: 26 July 2018

check for updates

Abstract: Crop simulation models, which are mainly being utilized as tools to assess the consequences of a changing climate and different management strategies on crop production at the field scale, are increasingly being used in a distributed model at the regional scale. Spatial data analysis and modelling in combination with geographic information systems (GIS) integrates information from soil, climate, and topography data into a larger area, providing a basis for spatial and temporal analysis. In the current study, the crop growth model Decision Support System for Agrotechnology Transfer (DSSAT) was used to evaluate five gridded precipitation input data at three locations in Austria. The precipitation data sets consist of the INtegrated Calibration and Application Tool (INCA) from the Meteorological Service Austria, two satellite precipitation data sources—Multisatellite Precipitation Analysis (TMPA) and Climate Prediction Center MORPHing (CMORPH)—and two rainfall estimates based on satellite soil moisture data. The latter were obtained through the application of the SM2RAIN algorithm ($SM2R_{ASC}$) and a regression analysis (RA_{ASC}) applied to the Metop-A/B Advanced SCATtermonter (ASCAT) soil moisture product during a 9-year period from 2007–2015. For the evaluation, the effect on winter wheat and spring barley yield, caused by different precipitation inputs, at a spatial resolution of around 25 km was used. The highest variance was obtained for the driest area with light-textured soils; TMPA and two soil moisture-based products show very good results in the more humid areas. The poorest performances at all three locations and for both crops were found with the CMORPH input data.

Keywords: DSSAT; INCA; ASCAT soil moisture; SM2RAIN; satellite precipitation data

1. Introduction

The behavior of crops under environmental conditions and cultivation practices can be analyzed with the useful tool and technique of crop growth models. Depending on their purpose, the models differ in their approaches and complexity, with consequences for the required type and amount of input data. Consisting of one or more mathematical equations, descriptive or empirical models define the behavior of a system or part of a system in a simple manner [1], such as agrometeorological indices. These can be an efficient tool to relate various crop responses to environmental observations if the extent of the measurements or of data availability is limited. Explanatory (or process-oriented) crop models comprise quantitative descriptions of the mechanisms and processes that cause the behavior of a system [1]. These are based on bio-physical plant processes, simulating the diurnal effects of changes in the environment on plant growth as well as development. The core processes of such crop models are all methods which aim to assess potential changes in plant production, e.g., phenology, photosynthesis, dry matter production. Environments with limited water and nutrition are included by using soil water balance modules including transpiration and nutrient (e.g., nitrogen, phosphor, and potassium) transformations in the soil as well as remobilization within the plants [2].

The main aim of a crop simulation model is to assess the consequences of climatic conditions and individual management behavior on plant production at the field scale. In a further step the results can be implemented in a distributed model at the regional scale. Limitations usually occur on the availability and quality of used data. Weak quality input data is often the main source of uncertainty in simulated outputs; e.g., caused by spatial representative problems or measurement errors. In addition, challenges arise at the regional scale in which model input parameters must be collected at dispersed point features such as weather stations [3] and produce outputs for local spots (for example, soil pits). Spatial data analysis and modelling in combination with geographical information systems (GIS) can help to integrate information from crop model outputs into a larger area [4,5]. For example, soil, climate, and topographical data provide the interface of these two technologies and are at the same time the basis for spatial and temporal analysis. An increasingly promising approach for monitoring crop growth or grain yield over large regions more accurately is the additional use of remote sensing data for spatial crop growth model applications. The linkage between crop simulation models with remote sensing and modelling techniques has been already applied in various examples, such as regional crop forecasting [6–8], agro-ecological zoning [9–11], crop suitability assessments [12–14], yield gap analysis [15,16], and in precision agriculture applications [17,18].

Data assimilation methods that incorporate remote sensing data into existing crop growth modelling frameworks might help to reduce uncertainty of the model simulations and to increase the evidence of the predicted models [19,20]. In such frameworks, one needs to distinguish between (i) driving variables (which constrain the system); (ii) state variables (which characterize the system behavior); (iii) model parameters (which establish the relation between driving and state variables); and (iv) output variables (observable functions of the state variables) [4]. Several methods have been developed and used to combine remote sensing data into agroecosystem models, mainly [4,20]: (i) the direct use of remote sensing inputs as a forcing variable, where at least one state variable must be replaced by measured data. A key challenge is the precondition of model calibration [4,21]; (ii) crop simulation models must re-initialize or re-calibrate using simulated and observed state variables [19–21]. This approach has gained attention in the scientific community by using optimize algorithms. Nevertheless, this method increases the amount of computation resources [20,22–26]; (iii) the continuous updating of a state variable of the model (for example, leaf area index) is only possible if data observation is ongoing. This method shows a higher flexibility in comparison to the others. However, this methodological approach requires a higher accuracy of data quality from remote sensing [27–30].

A key advantage of using remotely sensed information is to provide quantitative information on actual state of crop conditions over a large scale [2]; whereabouts crop models can assess the temporal dynamics of the plants. Even in the early use of crop model applications, Wiegand et al. [31] and Richardson et al. [32] recommended the use of remotely sensed information to enhance crop model outputs. Satellite rainfall as a model input was studied by Reynolds et al. [33], who used rainfall estimation images for regional yield prediction with a resolution of 7.6 km obtained from the geostationary Meteosar-5 satellite for Africa; Ovando et al. [34] evaluated soybean yield estimations using satellite precipitation input data in a crop growth model.

This paper analyses how different types of spatial precipitation data, taken as the input, influence a crop model application. Finding site-representative precipitation estimates is of importance, as rainfall patterns during the growing season play a key role in crop growth and development conditions. Similar importance is reported for other applications, such as the assessment of drought events, adaptive behavior and response to a warmer climate, weather forecasting, agriculture, and disease prevention [35,36]. In the current study, the dynamic crop growth and yield model Decision Support System for Agrotechnology Transfer (DSSAT v.4.0.2.0) [37] for wheat and barley was applied at three case study sites in Austria, characterized by different climate and soil conditions. Precipitation input data were used on the one hand as a reference from weather station-based measurements (point location) and on the other hand were compared to different types of spatial precipitation data: the data from the INtegrated Calibration and Application Tool (INCA) from the Meteorological Service Austria (1 km grid spatial resolution as well as a 25 km raster mean value), two satellite precipitation data sources—Multisatellite Precipitation Analysis (TMPA) and Climate Prediction Center MORPHing (CMORPH) with a $0.25 \times 0.25°$ spatial resolution—a new soil moisture (SM)-derived rainfall dataset obtained through the application of the SM2RAIN algorithm [38,39] to the Metop-A/B Advanced SCATtermonter (ASCAT) soil moisture product (25 km spatial resolution) and a simple regression analysis of satellite SM data from Metop ASCAT (25 km spatial resolution). First, the performance of the different precipitation data was assessed for the three reference locations (weather station sites at each case study area). The second purpose of this study was to evaluate the consequences of the different types of precipitation data as crop model inputs, considering simulated spring barley and winter wheat yield at different soil types in the three study areas. The main aim was to test and compare whether the satellite-based precipitation data are suitable sources as input data for crop models and to identify their limitations in comparison to INCA. INCA data sets, with their high spatial resolution of 1 km, are already used as crop model inputs in Austria (for example, for the operational drought monitoring system in Austria and in research studies); however, INCA data are relatively expensive, so a survey of acceptable alternatives is of interest for several applications. Further, it is also of interest to determine under which circumstances and to which degree errors in precipitation data are propagated into final crop model results (simulated crop yield). Precipitation is the main uncertain limiting crop growth parameter over the area of interest; thus, information regarding under which conditions this important weather input parameter could be replaced by alternative spatial sources is essential.

2. Materials and Methods

2.1. Study Areas

Three sites in different climatic regions in Austria were chosen for this study (Figure 1). Groß-Enzersdorf (48°12′ N, 16°33′ E, 156 m a.s.l.) in Lower Austria is located in eastern Austria and is influenced by a semi-arid, continental climate whereabouts summers are hot and intermittently dry; winters are most of the time cold with strong frosts and rarely snow cover. The annual mean temperature in Groß-Enzersdorf from 1981–2010 was 10.3 °C and the mean annual precipitation sum was 516 mm.

Hartberg (47°17′, 15°58′ E, 359 m a.s.l.) in Styria is located in the south-eastern part of Austria and is characterized by both Mediterranean and continental climates with warm summers and mild winters. The mean average temperature was 9.4 °C and the annual precipitation sum was 716 mm (1981–2010).

Kremsmünster (48°3′ N, 14°8′ E, 384 m a.s.l.) in Upper Austria was chosen as the third site and is characterized by a central-European transition climate influenced by the Atlantic climate. It is a humid area with a moderate climate. The mean average temperature was 9.1 °C and the mean annual precipitation sum was 1003 mm (1981–2010).

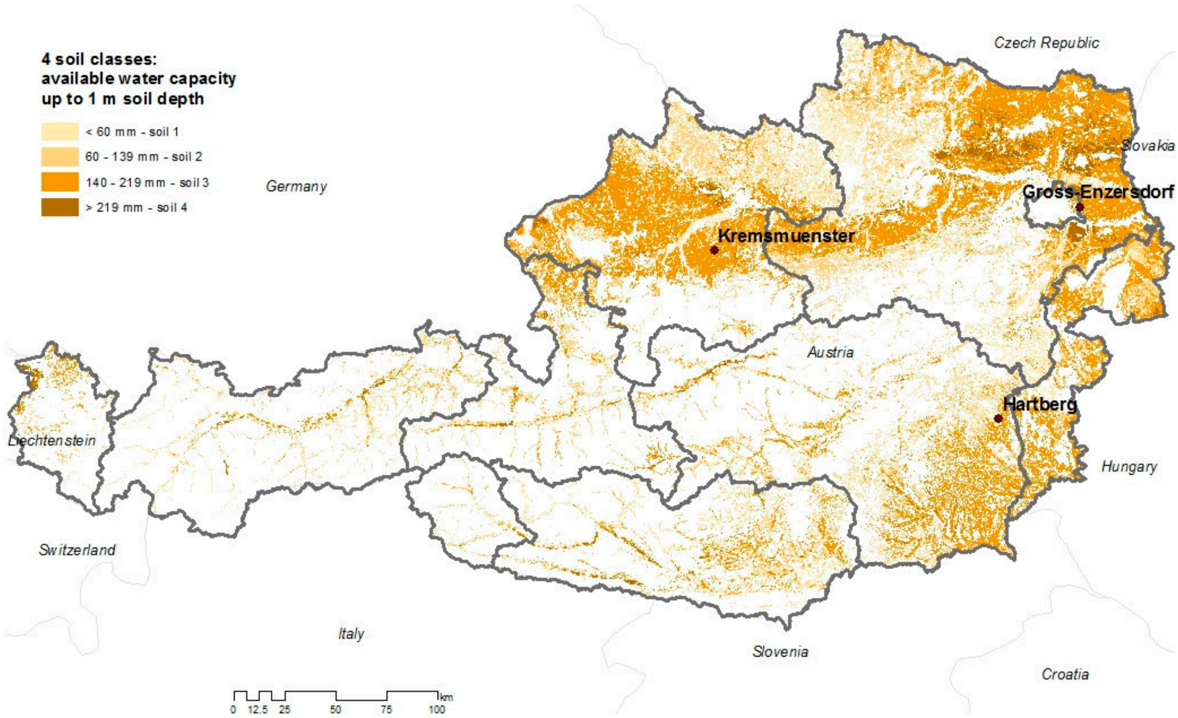

Figure 1. The four applied soil classes for agricultural land use for Austria and the three study sites.

These three locations, characterized by different climates, and four soil classes (Table 1, Figure 1) used in the study represent the main arable cropping areas in Austria, which occupies about 25% of the total area of Austria, quite well. We note that a high resolution and qualitative soil map is available only for the agricultural areas of Austria. Grasslands were not covered by this study.

Table 1. Four soil classes according to the available water capacity for Austria.

Soil Classes	LL	DUL	SAT	Area Percentage in Austria (%)	Available Water Capacity	Soil Type
soil class 1	0	0.1	0.1	14.1	very low	loamy sand
soil class 2	0.1	0.2	0.3	33.7	low	sandy loam
soil class 3	0.2	0.4	0.5	47.5	moderate	sandy loam
soil class 4	0.2	0.4	0.5	4.7	high	loamy silt

LL = lower limit of plant extractable soil water; DUL = drained upper limit; SAT = saturated soil water content.

2.2. Crop Growth Model

The DSSAT 4.0.2.0 crop model is a mechanistic or process-based, management-oriented model [37,40] and the input requirements comprehend daily weather data, soil conditions, plant characteristics, and crop management [41].

The minimum daily weather inputs for DSSAT are global solar radiation, maximum, and minimum air temperature, and precipitation [42]. These data were available from the Austrian Met Service (ZAMG) for the three weather stations Groß-Enzersdorf, Hartberg, and Kremsmünster.

Soil inputs include the soil water contents (volumetric fraction) for the lower limit of plant water availability (LL), and for the drain upper limit (DUL), where capillary forces are higher than gravity ones, and for field saturation (SAT) [42]. In the model, the FAO-56 Penman–Monteith equation [43] was used to calculate the evapotranspiration. Four different soil classes (termed here in as soil 1, soil 2, soil 3, and soil 4, respectively) were calculated from the total available water capacity (Table 1, Figure 1).

As there was no observed crop yield for all three sites available, two well calibrated crops for eastern Austria, the winter wheat cultivar "Capo" [44] and spring barley cultivar "Magda" [45], were used in this study. The simulation was set for rain-fed farming, including N fertilization (spring barley: 2 × 40 kg N/ha, 1 × 25 kg P/ha and 1 × 170 kg K/ha; winter wheat 2 × 52 kg N/ha, 1 × 26 kg P/ha and 1 × 100 K/ha), fix sowing date, harvest at maturity, and ploughed soil condition, without considering a potential yield loss provoked by pest or diseases. The sowing dates were mean values from different experimental sites of the Austrian Agency for Health and Food Safety (AGES) and were set as fixed for spring barley on March 19 in Groß-Enzersdorf and on March 24 in Hartberg as well as in Kremsmünster. For winter wheat, the dates were set on October 1 at all three locations.

2.3. Precipitation Datasets

Different spatial precipitation crop model input data were used during the 9-year period from 2007 to 2015 (Table 2): precipitation data were obtained from a nowcasting model (INCA), satellite precipitation data and rainfall estimations from SM data. All datasets were completed in the investigated period.

Table 2. Spatial precipitation input datasets in this study.

Name	Abbreviation	Short Description	Spatial Resolution	Input Data	Temporal Resolution	Reference	Available
(1) forecasting system							
Integrated Nowcasting through Comprehensive Analysis	INCA	observation-based analysis and forecasting system	1 km horizontal resolution and 200 m vertical resolution	Surface sensor observations, weather radar, satellite data, topographic data and forecast models	hourly	Haiden et al. [46]	Commercially available: www.zamg.ac.at
(2) satellite precipitation data							
Multi-satellite Precipitation Analysis	TRMMRT	Tropical rainfall Measuring Mission (~40S–40N and ~50S–50N)	0.25° × 0.25°	satellite microwave and IR; gauge (for calibration)	Sub-daily, daily, monthly	Huffmann et al. [47]	Freely available: https://pmm.nasa.gov/TRMM
Climate Prediction Center MORPHing	CMORPH	High resolution precipitation (60S–60N)	0.25° × 0.25°	satellite microwave	Sub-daily, daily	Joyce, R. J. et al. [48]	Freely available: http://www.cpc.ncep.noaa.gov/products/janowiak/cmorph_description.html
(3) Estimated rainfall based on satellite soil moisture dataset							
	$SM2R_{ASC}$	analytical relationship by inverting a soil–water balance equation from soil moisture time series	25 km (sampled at 12.5 km)	ASCAT—Metop's Advanced Scatterometer	daily	Brocca et al. [38,39]	Available upon request, SM-Data: http://hsaf.meteoam.it/
	RA_{ASC}	exponential regression analyses of soil moisture values and precipitation	25 km (sampled at 12.5 km)	ASCAT—Metop's Advanced Scatterometer	daily		Constructed in this study SM-Data: http://hsaf.meteoam.it/

2.3.1. Integrated Now-Casting through Comprehensive Analysis (INCA)

INCA, a system of the Austrian Meteorological Agency (ZAMG), produces analyses and forecasts of weather parameters in a very high spatial and temporal resolution [46]. The goal of the INCA system is to provide a high-resolution weather forecast information at 1 × 1 km resolution from 6 h until 14 days. Furthermore, INCA should be more suitable for mountain landscapes, where especially attention is given to the behavior of orographic effects. The database includes topography information, more than 200 ground meteorological stations, weather radar, satellite data, and forecast models. Analyses and nowcasts are updated and produced at 1 h intervals on a horizontal resolution of 1 km and a vertical resolution of 200 m [49]. As model inputs, the INCA data at a 1 km resolution ($INCA_{1km}$) were used. Additionally, the average of all 1 km INCA pixels within one ASCAT resolution cell was calculated to obtain a regional value commensurate with the ASCAT-based precipitation estimates. To simulate the ASCAT resolution cell, a Hamming window with a radius of about 23.7 km was used ($INCA_{23km}$).

2.3.2. Satellite Precipitation Data

In the current study, two high-resolution satellite precipitation data sets were additionally used: the Tropical Rainfall Measurement Mission (TRMM), Multi-satellite Precipitation Analysis (TMPA) [47], and the NOAA CPC MORPHing Technique (CMORPH) [48].

The National Aeronautics and Space Administration (NASA) in cooperation with the Japan Aerospace Exploration Agency (JAXA) developed TMPA [50], a system where the estimates are reached by calibrating and merging passive microwave data and ~10 µm band infra-red (IR) data from multiple satellite sensors [51]. Six passive microwave radiometers (PMW) named the TRMM Microwave Imager (TMI), Special Sensor Microwave/Imager (SSM/I), Advanced Microwave Scanning Radiometer-EOS (AMSR-E), Advanced Microwave Sounding Unit-B (AMSU-B), Special Sensor Microwave Imager/Sounder (SSMIS), and Microwave Humidity Sounder (MHS) are utilized for rainfall estimates [50]. The IR data are accessible from the international constellation of Geosynchronous Earth Orbit (GEO) satellites [51] and contain rainfall estimates at a high spatial-temporal resolution. The product is available for the ±50° latitude band over a grid with a 0.25° spacing every 3 h [47]. In the current study, the TMPA 3B42 in real-time (RT) product, version 7, is used. Detailed information about the TMPA product can be found in Huffman et al. [47]. TMPA is hereafter referred to as TRMMRT.

CMORPH technology is developed from the NOAA/Climate Prediction Center (NOAA/CPC) and their data are available at a 0.25° × 0.25° horizontal resolution from December 2002 to the present on a 3-hourl basis [51] for the ±60° latitude band. Rainfall estimates are obtained from the same PMW radiometers (AMSU-B, SSM/I, TMI, and AMSR-E) used for retrieving TRMM rainfall estimates [48]. The dataset obtained through CMORPH v1 is hereafter referred to as CMORPH.

Both TRMMRT and CMORPH products did not use ground rainfall observations to correct satellite precipitation estimates. Diurnal accumulated precipitation was calculated by adding up rainfall estimates within one day.

2.3.3. Estimated Rainfall Based on Satellite SM Dataset

The Advanced SCATterometer (ASCAT) is a real-aperture radar instrument operating in the C-band (5.255 GHz) using vertical transmit and vertical receive (VV) polarization. ASCAT is part of the payload of a series of three Metop satellites. At the moment, Metop-A and Metop-B share the same sun-synchronous polar orbit. They were launched in October 2006 and September 2012, respectively. The last Metop satellite, Metop-C, is foreseen to be launched in October 2018, also carrying an identical ASCAT instrument [52,53]. ASCAT provides a surface soil moisture (SM) product characterized by a ~25 km (sampled at 12.5 km) and daily spatial-temporal resolution [54]. The SM product corresponds to a depth of 2–3 cm and ranges between 0% (dry) and 100% (wet) presenting the relative soil saturation [55]. A Soil Water Index (SWI) can be used to get root-zone SM information, which is a more robust product applicable for deeper soil layers and presents lower measurement noise [54].

Two approaches to estimate daily precipitation by using these satellite SM observations were used in this study, as follows:

1. An analytical relationship derived by inverting a soil–water balance equation for estimating rainfall accumulations from SM time series named SM2RAIN [38,39]. This method estimates rainfall by exploiting the knowledge about the changes in time of the amount of water stored in the soil [56]. A detailed description of the method can be found in Brocca et al. [38]. The method has been applied to several SM products and validated at different spatial/temporal scales. In the current study, the dataset obtained through the application of SM2RAIN to the ASCAT SM product was named as SM2R$_{ASC}$ [56].
2. A direct statistical relationship between measured precipitation and the SM of the ASCAT. To estimate the daily accumulated precipitation (rainfall), the difference in ASCAT soil moisture between two consecutive days was calculated. As soon as more than one daily ASCAT SM value was available, the daily mean was used for the calculation. The daily SM differences were applied in five intervals from −100 until 100 mm, where the mean measured precipitation was added. An exponential regression analysis of these SM values (dependent variable) with the average precipitation (independent variable) in each class and each location was carried out (Figure 2). Subsequently daily precipitations were calculated with the three equations and further named as RA$_{ASC}$. The analyses were done for the months March until October for the period 2007–2015.

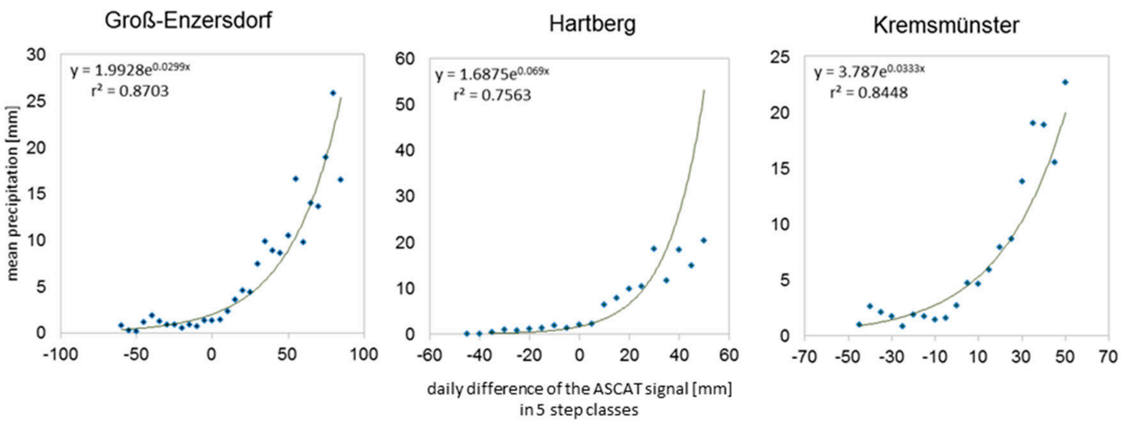

Figure 2. Scatterplot of daily difference of the Advanced SCATterometer (ASCAT) signal (in 5 step classes in mm) and the average precipitation [mm] as well as their exponential regression equation and r^2—March–October 2007–2015.

2.4. Methods Used for the Evaluation of Model Performance

Initially, a comparison of the precipitation datasets was carried out in order to evaluate the differences of the INCA$_{1km}$ in reference to the measured station data (point location). The analysis was done by calculating the least-squares coefficient of determination (r^2), the root mean square error (*RMSE*), and the mean absolute error (*MAE*) between the daily and monthly precipitation sums.

To obtain a regional value, INCA$_{1km}$ was aggregated to one ASCAT resolution cell (INCA$_{23km}$). Then, an evaluation of the two SM-based products and the two satellite precipitation data with INCA$_{23km}$ (benchmark) at the 25 km scale was carried out.

In a last step, the crop model simulations were carried out over a 9-year period covering 2007–2015 for five different daily precipitation model inputs; as references, daily precipitation data from INCA$_{23km}$ were used. Furthermore, SM2R$_{ASC}$, RA$_{ASC}$, TRMMRT, and CMORPH were used as forcing variables, respectively (Figure 3). These rain data were utilized only for the months March until October, as satellite soil moisture retrievals are influenced by the presence of snow and frozen surfaces [57]. From November until February, $INCA_{23km}$ rainfall data was used. To assess and compare model performance, a set of statistical parameters was calculated: the mean absolute error (*MAE*), the root mean square error (*RMSE*), the percent bias (*PBias*), the index of agreement (*d*), and the least-squares coefficient of determination (r^2).

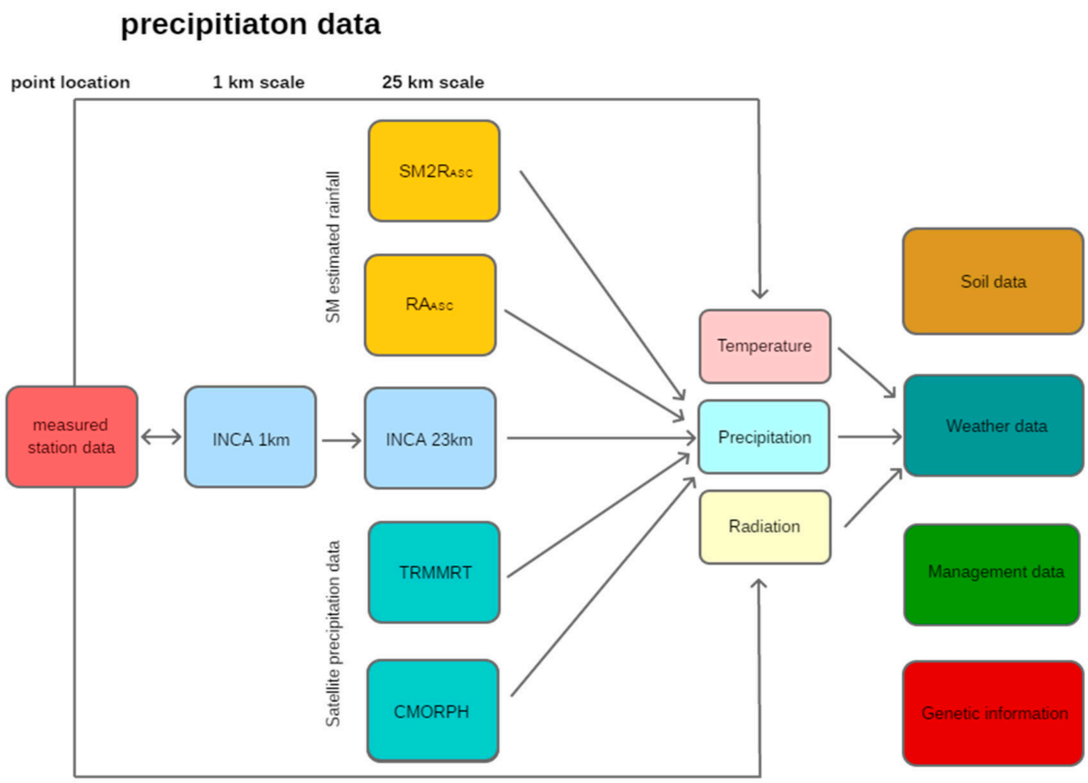

Figure 3. Simple flowchart of the methods used for the evaluation of model performances. SM: soil moisture; INCA: Integrated Now-casting through Comprehensive Analysis; TRMMRT: Multi-satellite Precipitation Analysis; CMORPH: Climate Prediction Center MORPHing.

3. Results

3.1. Rainfall Datasets Comparison

The daily and monthly precipitation differences between point-measured (ZAMG) and areal estimates from $INCA_{1km}$ for the months March until July and years 2007–2015 are shown in Table 3. For the evaluation, only five months per year were considered, as they include the main growing period of the two simulated crops, spring barley and winter wheat. Trends during the growing season period (March until July) were estimated on a monthly scale to get the temporal variability of the product performance by calculating r^2, *RMSE*, and *MAE*. $INCA_{1km}$ performs very well with an r^2 greater than 0.69 (diurnal) and 0.89 (by the month), respectively, as well as a daily *RMSE* < 4 mm and monthly *RMSE* < 18 mm. The daily *MAE* is between 0.7 and 1.4 mm, the monthly one between 8.5 and 17.7 mm. It should be kept in mind that $INCA_{1km}$ also integrates the ground measurements to estimate the gridded precipitation values.

To evaluate values in the same spatial resolution, and due to the good accordance of $INCA_{1km}$ and ZAMG precipitation values, INCA data were next aggregated to the 25 km scale. The aggregated $INCA_{23km}$ presents in all three locations a higher precipitation sum (monthly and daily) and is particularly pronounced in the first three months of the study in all three locations (except Groß-Enzersdorf in April and Kremsmünster in March) (Table 4).

Table 3. Statistical parameters of rainfall differences between point-measured (ZAMG) (as reference) and $INCA_{1km}$ for the months March until July 2007–2015.

	Groß-Enzersdorf	**Hartberg**	**Kremsmünser**
Daily based			
r^2	0.8	0.69	0.82
RMSE	2.38 mm	3.71 mm	2.95 mm
MAE	0.7 mm	1.37 mm	1.26 mm
Monthly based			
r^2	0.96	0.89	0.96
RMSE	8.49 mm	17.69 mm	12.31 mm
MAE	4.13 mm	12.12 mm	6.64 mm

In a next step, the two SM-based products $SM2R_{ASC}$, and RA_{ASC}, as well as the two satellite precipitation datasets TRMMRT and CMORPH, were compared with $INCA_{23km}$ (benchmark) in terms of rainfall estimation (daily: Table 5, monthly: Figure 4).

The lowest r^2 can be seen in the RA_{ASC} daily and monthly precipitation data. RA_{ASC} is characterized by high values during low precipitation periods and by lower values in very humid months (Figure 4). The other three approaches show—for the most part—a good coefficient of determination (up to 0.52 daily and 0.68 monthly) with $INCA_{23km}$. One exception is $SM2R_{ASC}$ in Kremsmünster, where it shows high deviations and presents weak monthly performance results (r^2 = 0.18 and *RMSE* = 60 mm). The two SM-based products present a low root-mean-square error in Groß-Enzersdorf; in the other two locations *RMSE* differences between SM-based products and satellite precipitation data are smaller (Table 5, Figure 4).

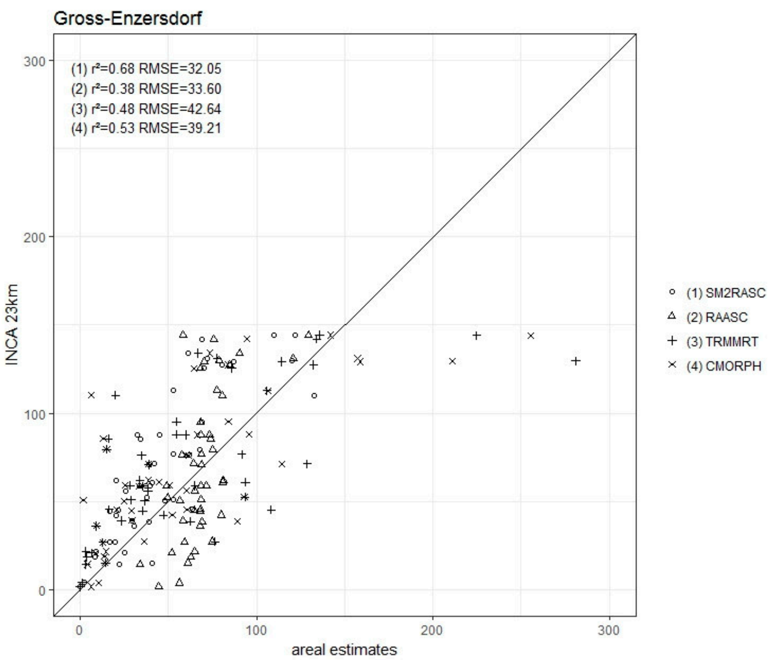

(**a**)

Figure 4. *Cont.*

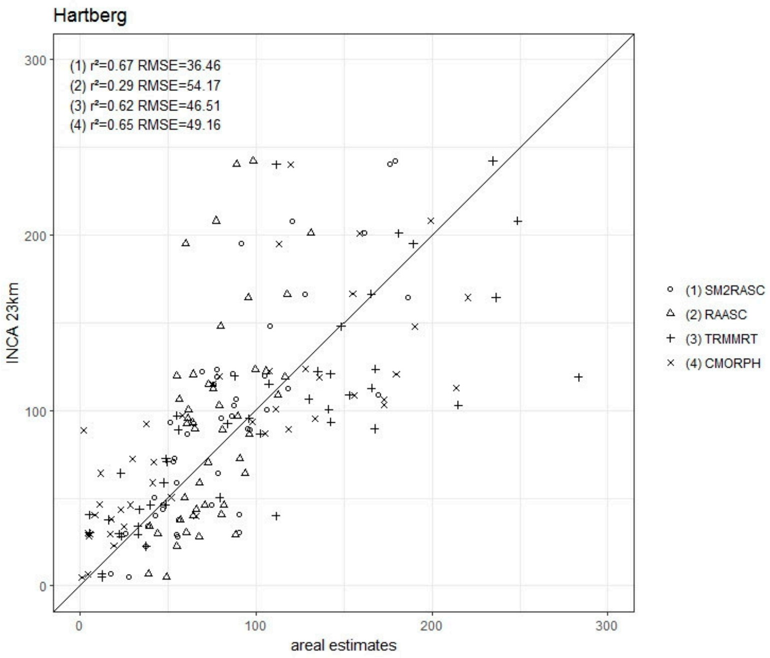

(**b**)

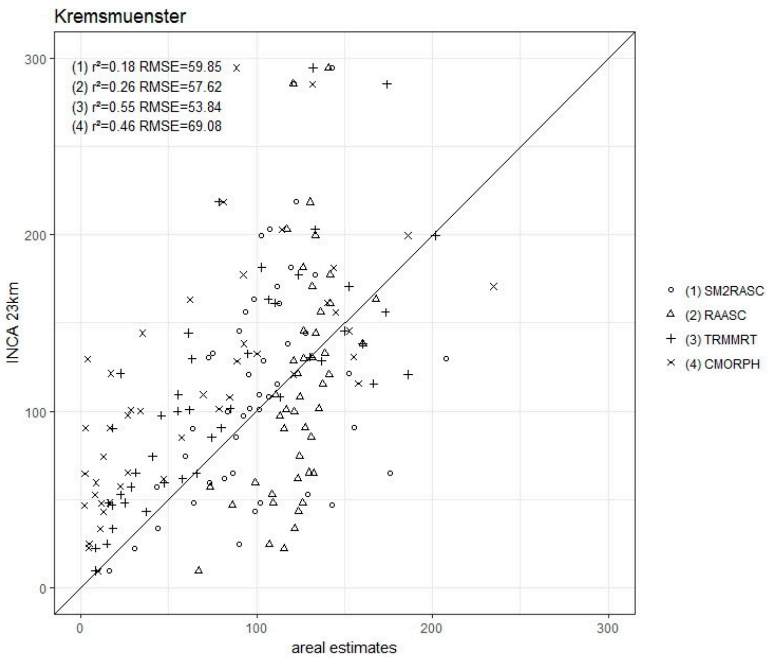

(**c**)

Figure 4. Monthly rainfall differences between $INCA_{23km}$ and $SM2R_{ASC}$, RA_{ASC}, TRMMRT and CMORPH, respectively, for the period March until July 2007–2015 in (**a**) Groß-Enzersdorf; (**b**) Hartberg; (**c**) Kremsmünster.

The number of rain days alone was not considered in this study as a main crucial factor for crop water balance in Austria, as factors such as actual evapotranspiration affecting soil water balance are omitted. More important is the soil available water capacity for the plants and its dynamics on a daily basis, which is used in this study as the best estimator of crop water stress available; e.g., [43].

Table 4. Monthly precipitation sums and mean differences of rainfall (monthly and daily) between $INCA_{1km}$ and $INCA_{23km}$ for the months March until July 2007–2015.

	Groß-Enzersdorf				**Hartberg**				**Kremsmünster**			
	Prec. (mm) $INCA_{1km}$	**Prec. (mm) $INCA_{23km}$**	**Mean diff. mo. (%)**	**Mean diff. d. (%)**	**Prec. (mm) $INCA_{1km}$**	**Prec. (mm) $INCA_{23km}$**	**Mean diff. mo. (%)**	**Mean diff. d. (%)**	**Prec. (mm) $INCA_{1km}$**	**Prec. (mm) $INCA_{23km}$**	**Mean diff. mo. (%)**	**Mean diff. d. (%)**
March	304	446	46	0.5	322	393	22	0.3	615	680	11	0.2
April	300	332	11	0.1	323	398	23	0.3	376	489	30	0.4
May	600	767	28	0.6	892	1113	25	0.8	1075	1318	23	0.9
June	678	804	18	0.5	1005	1139	13	0.5	1284	1382	8	0.4
July	693	770	11	0.3	1025	1175	15	0.5	1058	1246	18	0.7

Prec. = precipitation, diff. = difference, mo. = monthly, d. = daily.

Table 5. Statistical parameters of daily rainfall differences between $INCA_{23km}$ (benchmark) and $SM2R_{ASC}$, RA_{ASC}, TRMMRT as well as CMORPH for the months March until July 2007–2015.

	Groß-Enzersdorf				**Hartberg**				**Kremsmünster**			
	$SM2R_{ASC}$	**RA_{ASC}**	**TRMMRT**	**CMORPH**	**$SM2R_{ASC}$**	**RA_{ASC}**	**TRMMRT**	**CMORPH**	**$SM2R_{ASC}$**	**RA_{ASC}**	**TRMMRT**	**CMORPH**
MAE	1.67	2.31	1.86	1.75	2.8	2.97	2.37	2.11	3.04	3.69	2.88	2.75
RMSE	3.72	4.03	4.71	4.75	5.02	5.66	5.68	5.33	5.37	5.78	5.94	5.73
r^2	0.45	0.32	0.41	0.42	0.3	0.19	0.47	0.52	0.34	0.23	0.36	0.37

3.2. Crop Model Performance

The influence of four different forcing variables (2 SM-based products $SM2R_{ASC}$ and RA_{ASC}, 2 satellite precipitation data TRMMRT, and CMORPH) were used as an input on the DSSAT model in order to evaluate their impact on spring barley and winter wheat yield estimations in comparison to the benchmark ($INCA_{23km}$).

3.2.1. Spring Barley

The growing season for spring barley reaches from March until July. The sowing date was set as fixed (see Section 2.2) and the 9-year mean flowering was simulated between 5 and 9 June and mean maturity from 30 June (Groß-Enzersdorf) until 5 July (Kremsmünster). The mean spring barely yield over all soil classes (soils 1–4) was simulated in Groß-Enzersdorf with around 4700 kg/ha, in Hartberg around 5100 kg/ha, and in Kremsmünster 4400 kg/ha (Table 6).

A detailed comparison of the spring barley yield, estimated with $INCA_{23km}$ input (benchmark), showed that none of the other grid precipitation inputs perfectly reproduced the simulated yields in all years (Figure 5, Table 6). The analyses were carried out for all soil types together (soils 1–4) as well as separately (soil 1, soil 2, soil 3, and soil 4).

In the semi-arid area of Groß-Enzersdorf, the different types of precipitation inputs caused the highest deviations, where mainly light-textured soils (soil classes 1 and 2 with mostly *RMSE* > 600 kg/ha) are more sensitive than moderately fine-textured soils (soil classes 3 and 4) (Figure 4, Table 3). $SM2R_{ASC}$ generally presented the highest *MAE* (soil 1–4 = 512 kg/ha) and *RMSE* values (soil 1–4 = 633 kg/ha), whereas CMORPH showed the lowest one (soil 1–4 = 431 kg/ha). It is also noticeable that $SM2R_{ASC}$ and CMORPH underestimated the barley yield (negative *PBias*), where RA_{ASC} and TRMMRT input data demonstrated a positive *PBias* (Table 3).

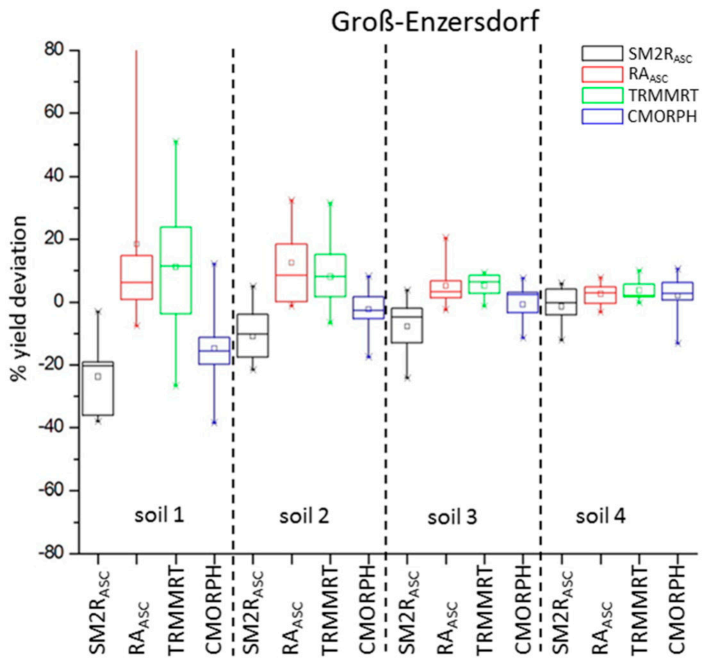

(**a**)

Figure 5. *Cont.*

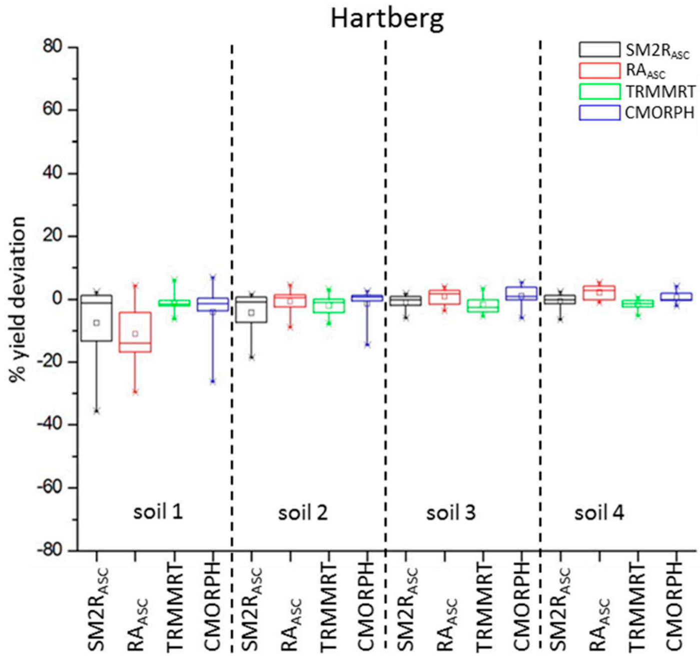

(**b**)

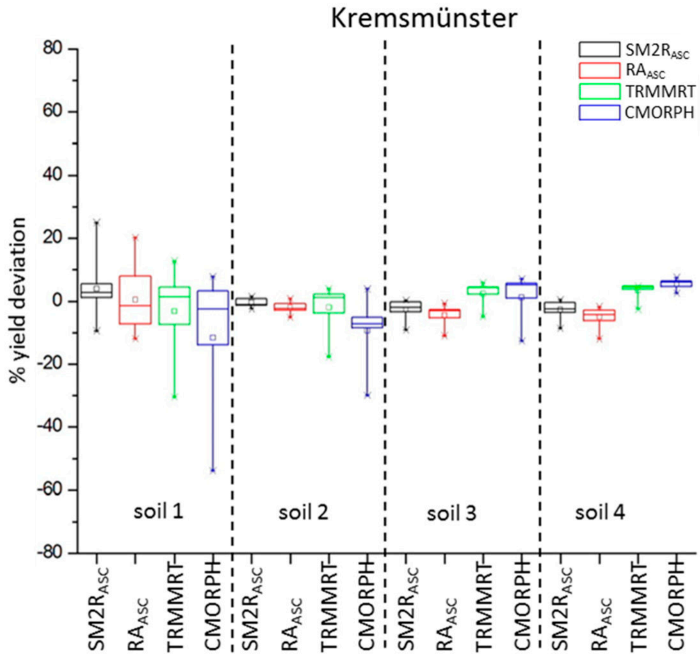

(**c**)

Figure 5. Boxplots of the relative differences [%] of spring barley yield $INCA_{23km}$ vs. $SM2R_{ASC}$ (black line), RA_{ASC} (red line), TRMMRT (green line) and CMORPH (blue line) precipitation inputs in (**a**) Groß-Enzersdorf; (**b**) Hartberg and (**c**) Kremsmünster 2007–2015. The box lines represent the 25th, 50th and 75th percentiles, while the whiskers present the max and min values.

Table 6. Mean yield (kg/ha) with $INCA_{23km}$ input data and comparative statistics (*MAE*, *RMSE*, *PBias*, *d* and r^2) of model performance in simulated crop yield using $SM2R_{ASC}$, RA_{ASC}, TRMMRT, and CMORPH precipitation inputs against $INCA_{23km}$ inputs for the three study areas—spring barley.

	Groß-Enzersdorf					**Hartberg**					**Kremsmünster**				
	Soil 1–4	**Soil 1**	**Soil 2**	**Soil 3**	**Soil 4**	***Soil 1–4***	**Soil 1**	**Soil 2**	**Soil 3**	**Soil 4**	***Soil 1–4***	**Soil 1**	**Soil 2**	**Soil 3**	**Soil 4**
Mean yield (kg/ha) with $INCA_{23km}$ input data															
	4727	3118	4444	5644	5701	*5111*	4056	5078	5779	5532	*4451*	3654	4451	4890	4810
$SM2R_{ASC}$—$INCA_{23km}$															
MAE	*512*	719	532	488	307	*215*	352	270	127	111	*144*	237	58	139	142
RMSE	*633*	803	618	655	384	*369*	582	396	168	149	*220*	319	64	214	203
PBias %	*−9.10*	−23	−10.8	−7.8	−1.6	*−3.2*	−7.6	−4.6	−1.2	−0.7	*−0.9*	3.5	−0.5	−2.8	−2.9
d	*0.94*	0.75	0.69	0.69	0.67	*0.95*	0.49	0.71	0.98	0.97	*0.95*	0.72	0.98	0.86	0.87
r^2	*0.89*	0.76	0.49	0.35	0.18	*0.87*	0.26	0.43	0.93	0.89	*0.87*	0.31	0.95	0.69	0.73
RA_{ASC}—$INCA_{23km}$															
MAE	*374*	449	525	318	202	*235*	509	148	149	136	*219*	304	102	222	246
RMSE	*544*	679	691	427	250	*343*	615	198	157	173	*275*	355	126	276	290
PBias %	*7*	12.2	11.5	4.9	2.5	*−1.7*	−11.4	−0.8	0.7	2	*−3.2*	−0.3	−2.1	−4.5	−5.1
d	*0.94*	0.67	0.47	0.76	0.87	*0.96*	0.39	0.94	0.98	0.96	*0.93*	0.45	0.93	0.78	0.77
r^2	*0.86*	0.41	0.04	0.52	0.68	*0.92*	0.12	0.83	0.93	0.91	*0.84*	0.07	0.88	0.68	0.7
TRMMRT—$INCA_{23km}$															
MAE	*385*	556	466	310	209	*135*	101	161	170	111	*254*	401	220	206	189
RMSE	*506*	691	593	351	267	*174*	131	206	201	147	*340*	515	334	215	197
PBias %	*6.3*	10.8	7.9	5.2	3.6	*−1.8*	−1.2	−2.1	−1.8	−1.8	*0.3*	−3.6	−2.1	2.5	3.4
d	*0.95*	0.81	0.68	0.86	0.86	*0.99*	0.94	0.94	0.97	0.97	*0.93*	0.5	0.67	0.89	0.91
r^2	*0.88*	0.51	0.33	0.83	0.76	*0.96*	0.8	0.84	0.91	0.94	*0.79*	0.14	0.18	0.78	0.93
CMORPH—$INCA_{23km}$															
MAE	*350*	537	259	296	309	*166*	272	160	146	85	*405*	581	497	286	255
RMSE	*431*	599	327	361	386	*277*	428	275	193	109	*602*	904	670	333	265
PBias %	*−2.7*	−14.8	−2.2	−0.8	1.8	*−0.9*	−4.3	−1.6	0.9	0.5	*−3.1*	−11.9	−9.6	1	5.3
d	*0.97*	0.83	0.88	0.85	0.68	*0.97*	0.55	0.9	0.97	0.98	*0.82*	0.25	0.34	0.75	0.82
r^2	*0.92*	0.73	0.68	0.53	0.17	*0.91*	0.15	0.71	0.9	0.95	*0.62*	0.04	0.01	0.37	0.93

Lower yield differences were found in the more humid areas of Hartberg and Kremsmünster with all precipitation inputs—especially for soils 3 and 4 (Figure 4). It can be notice, that the *RMSE* values in these two locations are about less than half that in Groß-Enzersdorf. Above all, TRMMRT presents very low *MAE* and *RMSE* values in Hartberg (*MAE*: soil 1–4 = 135 kg/ha; *RMSE*: soil 1–4 = 174 kg/ha) and the highest r^2 (soil 1–4 = 99%) as well as *d* (soil 1–4 = 96%). CMORPH, on the other hand, shows difficulties to simulate yield in Kremsmünster, which is characterized by the highest *RMSE* (soil 1–4 = 602 kg/ha) and the weakest coefficient of determination (soil 1–4 = 82%) as well as index of agreement (soil 1–4 = 62%) (Table 3). The light-textured soils result in all simulations in a negative *PBias*; soils 3 and 4 do not show such a clear trend.

3.2.2. Winter Wheat

The winter wheat phenological season spans from October until July, including a dormant period during winter. The sowing date was set as fixed on October 1 and the 9-year mean flowering date was simulated between 27 and 30 May, with mean maturity between 28 June and 3 July. The mean yield for all soil types together (soils 1–4) was simulated between 5500 kg/ha in Kremsmünster and 5900 kg/ha in Hartberg (Table 7).

The variation of winter wheat yields, as a result of different precipitation input data, illustrated a similar behavior to the spring barley simulations.

Groß-Enzersdorf presented the highest winter wheat yield deviations (Figure 5)—especially for soil classes 1 and 2, with *RMSE* values up to 1800 kg/ha. The outlier in soil 1 was caused in year 2011, where $INCA_{23km}$ input data simulated yield failure. $SM2R_{ASC}$, TRMMRT, and CMORPH mainly underestimated yield, whereas RA_{ASC} presented a positive *PBias* (Figure 5, Table 4). All in all, RA_{ASC} showed the strongest performances, with the lowest *RMSE* (soil 1–4 = 818 kg/ha) and a high *d* (soil 1–4 = 0.94) as well as r^2 (soil 1–4 = 0.84).

In the two locations Hartberg and Kremsmünster, lower deviations can be seen (Figure 6). Notable are the TRMMRT input data, which simulated winter wheat yield in Hartberg (*RMSE* soil 1–4 = 194 kg/ha; *d* > 95%) and $SM2R_{ASC}$ in Kremsmünster (*RMSE* soil 1–4 = 223 kg/ha, *d* > 95%) very well (Table 4). CMORPH input data caused the highest deviations and the poorest performances. All four rainfall input data showed a yield underestimation (negative *PBias*) (Table 4).

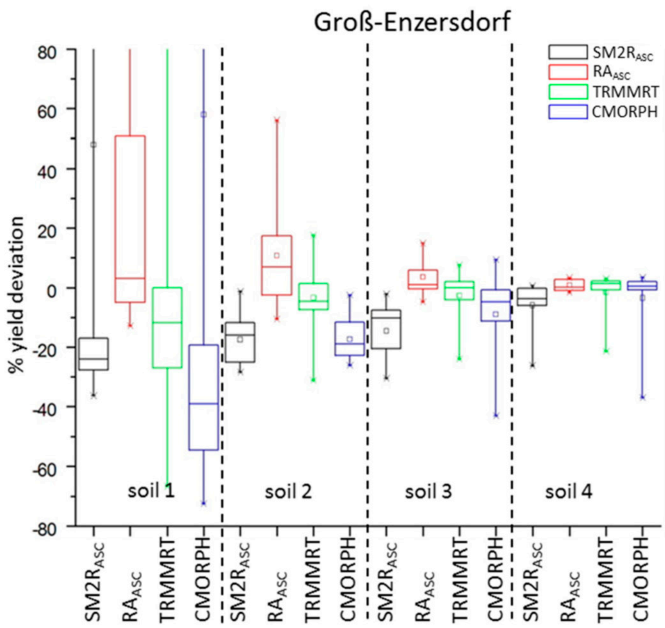

(**a**)

Figure 6. *Cont.*

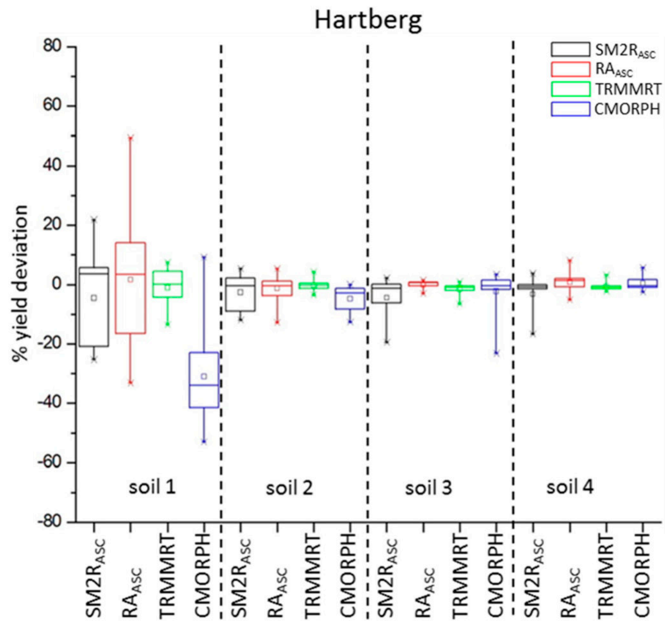

(**b**)

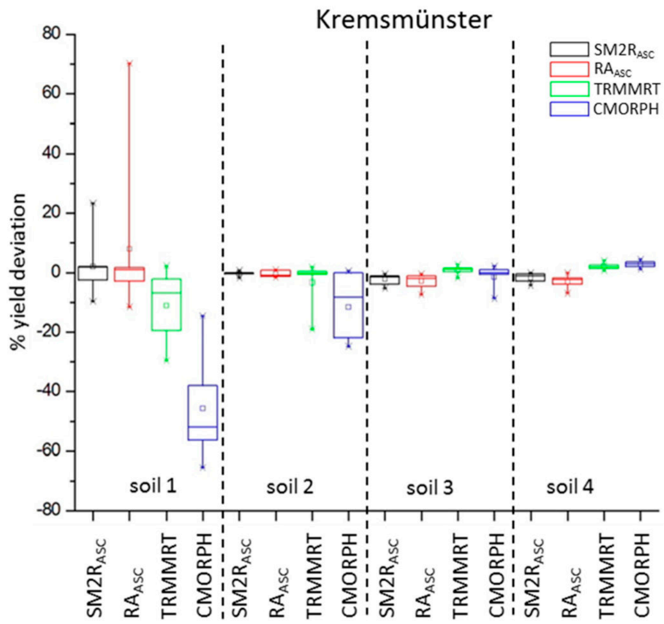

(**c**)

Figure 6. Boxplots of the relative differences [%] of winter wheat yield $INCA_{23km}$ vs. $SM2R_{ASC}$ (black line), RA_{ASC} (red line), TRMMRT (green line) and CMORPH (blue line) precipitation inputs in (**a**) Groß-Enzersdorf, (**b**) Hartberg and (**c**) Kremsmünster 2007–2015. The box lines represent the 25th, 50th and 75th percentiles, while the whiskers present the max and min values.

Table 7. Mean yield (kg/ha) with $INCA_{23km}$ input data and comparative statistics (*RMSE*, *PBias*, *d* and r^2) of model performance in simulated crop yield using $SM2R_{ASC}$, RA_{ASC}, TRMMRT and CMORPH precipitation inputs against $INCA_{23km}$ inputs for the three study areas—winter wheat.

	Groß-Enzersdorf					**Hartberg**					**Kremsmünster**				
	Soil 1–4	**Soil 1**	**Soil 2**	**Soil 3**	**Soil 4**	***Soil 1–4***	**Soil 1**	**Soil 2**	**Soil 3**	**Soil 4**	***Soil 1–4***	**Soil 1**	**Soil 2**	**Soil 3**	**Soil 4**
Mean yield (kg/ha) with $INCA_{23km}$ input data															
	5751	3276	5395	7290	7045	*5954*	3982	5982	7218	6633	*5523*	4226	5508	6355	6002
$SM2R_{ASC}$—$INCA_{23km}$															
MAE	*838*	962	936	1035	419	*368*	546	319	353	251	*141*	272	35	145	111
RMSE	*1011*	1029	1060	1223	646	*516*	634	411	558	430	*223*	378	48	180	144
PBias %	*−13.1*	−19.5	−17.3	−14.2	−5.7	*−3.8*	−5.4	−2.9	−4.3	−3.1	*−1*	1.5	−0.5	−2.3	−1.9
d	*0.93*	0.82	0.71	0.61	0.69	*0.96*	0.82	0.71	0.78	0.85	*0.99*	0.95	1	0.91	0.95
r^2	*0.87*	0.77	0.68	0.71	0.74	*0.89*	0.5	0.26	0.62	0.72	*0.95*	0.93	0.99	0.89	0.92
RA_{ASC}—$INCA_{23km}$															
MAE	*498*	826	698	351	116	*320*	804	215	88	174	*209*	397	60	190	188
RMSE	*818*	1221	961	493	141	*504*	929	303	110	223	*372*	660	65	245	228
PBias %	*5.6*	17	8.3	3.1	0.8	*−0.4*	−1.3	−1.3	−0.1	0.7	*−1*	4.2	−0.5	−3	−3.1
d	*0.94*	0.7	0.51	0.73	0.96	*0.96*	0.4	0.88	0.98	0.93	*0.95*	0.79	0.99	0.83	0.87
r^2	*0.84*	0.52	0.01	0.43	0.87	*0.86*	0.01	0.69	0.95	0.77	*0.88*	0.5	0.97	0.75	0.86
TRMMRT—$INCA_{23km}$															
MAE	*568*	984	616	406	265	*136*	234	92	129	89	*241*	535	220	89	122
RMSE	*909*	1430	836	582	470	*194*	300	129	181	106	*426*	725	416	102	135
PBias %	*−4.2*	−14.3	−4.7	−2.3	−1.3	*−0.9*	−1.1	−0.3	−1.6	−0.7	*−2.3*	−12.1	−3.3	0.8	2
d	*0.94*	0.7	0.68	0.86	0.79	*0.99*	0.96	0.98	0.96	0.98	*0.96*	0.83	0.78	0.98	0.96
r^2	*0.8*	0.25	0.19	0.79	0.79	*0.98*	0.85	0.92	0.92	0.97	*0.89*	0.68	0.59	0.95	0.97
CMORPH—$INCA_{23km}$															
MAE	*917*	1600	932	762	377	*496*	1318	288	276	102	*741*	1984	657	154	169
RMSE	*1253*	1853	1022	1081	794	*805*	1462	386	539	138	*1174*	2151	888	251	178
PBias %	*−12.6*	−35.5	−17.3	−8.2	−3.1	*−6.9*	−30.9	−4.8	−2.2	0.3	*−11.5*	−46.9	−11.7	−1.4	2.8
d	*0.9*	0.5	0.71	0.71	0.65	*0.93*	0.5	0.84	0.78	0.97	*0.81*	0.43	0.43	0.9	0.93
r^2	*0.78*	0.1	0.74	0.73	0.76	*0.9*	0.32	0.75	0.52	0.91	*0.77*	0.23	0.12	0.84	0.97

4. Discussion

Crop growth simulation models are increasingly being utilized as tools to assess the regional impact on crop production under different environmental conditions, such as changing climate and management options. These models need spatially and temporally detailed input data of weather, soil, crop management, and cultivar, which are usually difficult to get reliably for larger areas [58]. As observation data are merely available at a limited number of meteorological stations within a region, it is essential to estimate the required weather inputs for the related simulation-scale [59]. The focus of this study was set on daily precipitation data, as they are the main uncertain limiting crop growth parameter over the area of interest. Crop models are highly sensitive to soil water, as soil moisture is a limiting factor for different processes for crop growth and yield. A valued alternative to ground-based measurements can be satellite-rainfall estimate systems, which produce global coverage data and supply information in areas where data from other sources are unavailable [60]. The spatial and temporal resolution increased lately; e.g., the current NASA–JAXA joint Global Precipitation Measurement (GPM) mission makes available rainfall products in near-real time with a spatial sampling of 0.1° each 30 min, by utilizing different satellite sensors [61]. Satellite rainfall products which have been previously developed include the near-real-time TMPA 3B42RT [48]; the Precipitation Estimation from Remotely Sensed Information using Artificial Neural Networks (PERSIANN) [62]; CMORPH [49]; and the Climate Hazards Group InfraRed Precipitation with Station (CHIRPS) products [63]. Nevertheless, satellite rainfall estimations are not free of error [64,65]. One main reason is the inconsistent scan of rainfall patterns, which makes the reconstruction of the accumulated rainfall in longer temporal scales (e.g., daily accumulated rainfall) challenging [66]. Further, the estimation of light rainfall is generally underestimated especially over land by remote sensing analyses as a result of land surface emissivity [36,60,67].

Approaches to enhance the quality of satellite rainfall estimates, the use of satellite surface soil moisture (SSM) data has been utilized recently [38,39,68–71]. These methods analyze the intense correlation between SSM and rainfall to improve and/or estimate rainfall by using satellite surface SM data. Here, SM2RAIN [38] is the first method, which directly makes available rainfall estimates from SSM observations, whereas the other approaches are correction-based techniques [36,38,39,60,72–75]. In our study, we also added a new approach to estimate rainfall directly using the statistical relationship between measured precipitation and the SM of the ASCAT.

Meteorological station data are normally spatially irregular and can be interpolated to a regular grid. At this point, especially high-resolution gridded data sets can be used for impact studies. Examples are the EURO4M-APGD dataset for the Alps [76], the European E-OBS [77], and JRC's Agri4cast dataset (http://agri4cast.jrc.ec.europa.eu). These data were not analyzed in the current study. Here (e.g., for Austria), INCA data exists with a very high-resolution gridded data set; unfortunately, they are not freely available.

An important aspect of crop models is that they are sensitive to perturbations in precipitation. In Eitzinger et al. [78], the sensitivity of seven different crop models for winter wheat and maize to extreme heat and drought over a short but critical period of two weeks after the start of flowering in two locations in Austria was studied. It showed, that the models respond differently to climate stresses (according to references [79,80]), even though they mainly present similar trends in grain yields between different climatic situations. In Fronzek et al. [81], process-based wheat models were applied, and no single model property was found, which describe the combined yield response to temperature and precipitation perturbations.

The main objective of the current study was to test different types of spatial precipitation data as inputs for a crop model application in three locations in Austria with different soil types and climates. As INCA data are not freely available, a study of acceptable spatial alternatives is of interest for serval applications. Also, under which circumstances and to which degree errors in precipitation data are propagated into final crop model results are of interest. Therefore, the aggregated $INCA_{23km}$ presented in all three locations already a higher precipitation sum as $INCA_{1km}$ and were thus not free of errors.

All investigated grid-based types of precipitation data perform at their best as crop yield model inputs on moderately fine-textured soils and under humid conditions (Hartberg and Kremsmünster).

In the semi-arid region of Groß-Enzersdorf, winter wheat and spring barley simulations are very sensitive to different precipitation model inputs; especially in light-textured soils. This is due to the fact that soil water availability is a more dominant limiting growth factor under drought-prone conditions. Therefore, little differences in precipitation input can affect greatly the simulated yield (high *RMSE*, low d and r^2 values). Also, even one missing precipitation event in a critical development stage can cause a crop failure. In this region, the model reacts more sensitively for winter wheat than for spring barley. RA_{ASC} (winter wheat) and TRMMRT (winter wheat and spring barley) seem to be the best predictors for this location.

In the more humid places of Hartberg and Kremsmünster, all four precipitation inputs produced good agreements. Plant water stress does not occur often and can be observed mainly in light-textured soils. A bias in the precipitation sum is not such a crucial factor here; much more important is a prediction of the event. In Hartberg, crop yields with RA_{ASC} and TRMMRT input data correspond best with $INCA_{23km}$ input data (except RA_{ASC} soil 1). In Kremsmünster, both SM-based products present good yield results for soils 1 and 2; even if high monthly precipitation differences to $INCA_{23km}$ were calculated (Figure 3). Winter wheat and spring barley show similar yield predictions in both locations.

The poorest performances in all three locations and for both crops were found with CMORPH input data. The general underestimation of rainfall provided by CMORPH is in line with the finding of Stampoulis and Anagnostou [82], who assess the quality of this product over Europe.

Looking at SM estimated rainfall in more detail, $SM2R_{ASC}$ and RA_{ASC} perform well in this study, especially on light-textured soils in Kremsmünster and Hartberg compared to the two satellite precipitation data. Here, for example, the use of information regarding the spatial–temporal variability of top soil moisture could improve spatial crop yield simulations against the use of single point information for single weather stations for a given area. Therefore, the SM estimations ($SM2R_{ASC}$, RA_{ASC}) could be an alternative for potential agriculture applications in regions where other products are not available once calibrated to the specific climatic conditions. In addition, a remote sensing product does not necessarily have to be "better" than the model. It should be considered whether the data add value or new information. Hence, even when r^2 values are lower than for models, clever data assimilation approaches may take advantage of the data (see e.g., [28]).

5. Conclusions

In the current study, different types of spatial precipitation data as inputs were tested for a crop model application. Two daily satellite precipitation and two estimated rainfall data based on a satellite SM dataset were evaluated with INCA-input data at a spatial resolution of around 25 km in three locations in Austria. A bias in precipitation model input has lower impacts on simulated spring barley and winter wheat yield under humid (Kremsmünster and Hartberg) than under dry conditions (Groß-Enzersdorf). This can be very well observed in TMPA and in the two SM-based product simulations. Additionally, light-textured soils (especially soil class 1) show more sensitivity to different precipitation inputs than the other soils, regardless of the studied region.

This study represents one of the first attempts to integrate estimated rainfall datasets from SM for crop models. More comprehensive analyses will be approached henceforth in order to better understand and improve the capability of satellite-derived rainfall.

Author Contributions: The work has been performed in collaboration with all co-authors. S.T. and J.E. conceived the research. L.B. and L.C. provided $SM2R_{ASC}$ data as well as the two satellite precipitation data. S.H. and W.W. provided the daily ASCAT SM data. S.T. performed the statistical analysis and prepared the manuscript. A critical analysis of obtained results, reading, and commenting of the manuscript throughout all processes were done of all authors.

Funding: This research was funded by the European Unions Horizon 2020 research and innovation programme grant number 691998.

Acknowledgments: This paper is supported by the H2020-TWINN-2015 SERBIA FOR EXCELL project. This project has received funding from the European Unions Horizon 2020 research and innovation programme under grant agreement No. 691998. The work described in this paper was realized as a part of the project "COMBIRISK" of the Austrian Climate Research Programme (ACRP).

Conflicts of Interest: The authors declare no conflict of interest.

References

1. Penning de Vries, F.W.T.; Jansen, D.M.; ten Berge, H.F.M.; Bakema, A. *Simulation of Ecophysiological Processes of Growth in Several Annual Crops*; Centre for Agricultural Publishing and Documentation (Pudoc): Wageningen, The Netherlands, 1989.
2. Dadhwal, V.K. Crop growth and productivity monitoring and simulation using remote sensing and GIS. In *Satellite Remote Sensing and GIS Applications in Agricultural Meteorology, Proceedings of the Training Workshop, Dehra Dun, India, 7–11 July 2003*; Sivakumar, M.V.K., Roy, P.S., Harmsen, K., Saha, S.K., Eds.; World Meteorological Organization: Geneva, Switzerland, 2003; pp. 263–290.
3. De Wit, A.J.W.; Boogaard, H.L.; van Diepen, C.A. Spatial resolution of precipitation and radiation: The effect on regional crop yield forecasts. *Agric. For. Meteorol.* **2005**, *135*, 156–168. [CrossRef]
4. Delécolle, R.; Maas, S.J.; Guerif, M.; Baret, F. Remote sensing and crop production models: Present trends. *ISPRS J. Photogramm. Remote Sens.* **1992**, *47*, 145–161. [CrossRef]
5. Ewert, F.; van Ittersum, M.K.; Heckelei, T.; Therond, O.; Bezlepkina, I.; Andersen, E. Scale changes and model linking methods for integrated assessment of agri-environmental systems. *Agric. Ecosyst. Environ.* **2011**, *142*, 6–17. [CrossRef]
6. De Wit, A.J.W.; van Diepen, C.A. Crop growth modelling and crop yield forecasting using satellite-derived meteorological inputs. *Int. J. Appl. Earth Obs. Geoinf.* **2008**, *10*, 414–442. [CrossRef]
7. De Wit, A.; Baruth, B.; Boogaard, H.; van Diepen, K.; van Kraalingen, D.; Micale, F.; te Roller, J.; Supit, I.; van den Wijngaart, R. Using ERA-INTERIM for regional crop yield forecasting in Europe. *Clim. Res.* **2010**, *44*, 41–53. [CrossRef]
8. Ma, H.; Huang, J.; Zhu, D.; Liu, J.; Zhang, C.; Su, W.; Fan, J. Estimating regional winter wheat yield by assimilation of time series of HJ-1 CCD into WOFOST-ACRM model. *Math. Comput. Model.* **2013**, *58*, 753–764. [CrossRef]
9. Patel, N.R.; Mandal, U.K.; Pande, L.M. Agro-ecological zoning system. A Remote Sensing and GIS Perspective. *J. Agrometeorol.* **2000**, *2*, 1–13.
10. Ismail, M. Using Remote Sensing and GIS Application in Agro-ecological Zoning of Egypt. *Int. J. Environ. Sci.* **2012**, *1*, 85–94.
11. Taati, A.; Sarmadian, F.; Mousavi, A.; Rahmani, A. Agro-ecological zoning for cultivation of Alfalfa (*Medicago sativa* L.) using RS and GIS. *Sci. Agric.* **2015**, *9*, 93–100. [CrossRef]
12. Mustak, S.K.; Baghmar, N.K.; Singh, S.K. Land Suitability Modeling for gram crop using remote sensing and GIS: A case study of Seonath basin, India. *Bull. Environ. Sci. Res.* **2015**, *4*, 6–17.
13. Kamau, S.W.; Kuria, D.; Gachari, M.K. Crop-land Suitability Analysis Using GIS and Remote Sensing in Nyandarua County, Kenya. *J. Environ. Earth Sci.* **2015**, *5*, 121–131.
14. Mustafa, A.A.; Singh, M.; Sahoo, R.N.; Ahmed, N.; Khanna, M.; Sarangi, A.; Mishra, A.K. Land Suitability Analysis for Different Crops: A Multi Criteria Decision Making Approach using Remote Sensing and GIS. *Researcher* **2011**, *3*, 61–84.
15. Lobell, D.B. The use of satellite data for crop yield gap analysis. *Field Crop. Res.* **2013**, *143*, 56–64. [CrossRef]
16. Sibley, A.M.; Grassini, P.; Thomas, N.E.; Cassman, K.G.; Lobell, D.B. Testing Remote Sensing Approaches for Assessing Yield Variability among Maize Fields. *Agron. J.* **2014**, *106*, 24–32. [CrossRef]
17. Seelan, S.K.; Laguette, S.; Casady, G.M.; Seielstad, G.A. Remote sensing applications for precision agriculture: A learning community approach. *Remote Sens. Environ.* **2003**, *88*, 157–169. [CrossRef]
18. Mulla, D.J. Twenty five years of remote sensing in precision agriculture: Key advances and remaining knowledge gaps. *Biosyst. Eng.* **2013**, *114*, 358–371. [CrossRef]
19. Dorigo, W.A.; Zurita-Milla, R.; de Wit, A.J.; Brazile, J.; Singh, R.; Schaepman, M.E. A review on reflective remote sensing and data assimilation techniques for enhanced agroecosystem modeling. *Int. J. Appl. Earth Obs. Geoinf.* **2007**, *9*, 165–193. [CrossRef]

20. Morel, J.; Begue, A.; Todoroff, P.; Martine, J.; Lebourgeois, V.; Petit, M. Coupling a sugarcane crop model with the remotely sensed time series of fIPAR to optimise the yield estimation. *Eur. J. Agron.* **2014**, *61*, 60–68. [CrossRef]
21. Moulin, S.; Bondeau, A.; Delécolle, R. Combining agricultural crop models and satellite observations: From field to regional scales. *Int. J. Remote Sens.* **1998**, *19*, 1021–1036. [CrossRef]
22. Launay, M.; Guerif, M. Assimilating remote sensing data into a crop model to improve predictive performance for spatial applications. *Agric. Ecosyst. Environ.* **2005**, *111*, 321–339. [CrossRef]
23. De Wit, A.J.W.; Van Diepen, C.A. Crop model data assimilation with the Ensemble Kalman filter for improving regional crop yield forecasts. *Agric. For. Meteorol.* **2007**, *146*, 38–56. [CrossRef]
24. Fang, H.; Liang, S.; Hoogenboom, G.; Teasdale, J.; Cavigelli, M. Corn-yield estimation through assimilation of remotely sensed data into the CSM-CERES-Maize model. *Int. J. Remote Sens.* **2008**, *29*, 3011–3032. [CrossRef]
25. Dong, Y.; Zhao, C.; Yang, G.; Chen, L.; Wang, J.; Feng, H. Integrating a very fast simulated annealing optimization algorithm for crop leaf area index variational assimilation. *Math. Comput. Model.* **2013**, *58*, 877–885. [CrossRef]
26. Li, Y.; Zhou, Q.; Zhou, J.; Zhang, G.; Chen, C.; Wang, J. Assimilating remote sensing information into a coupled hydrology-crop growth model to estimate regional maize yield in arid regions. *Ecol. Model.* **2014**, *291*, 15–27. [CrossRef]
27. Jongschaap, R.E. Run-time calibration of simulation models by integrating remote sensing estimates of leaf area index and canopy nitrogen. *Eur. J. Agron.* **2006**, *24*, 316–324. [CrossRef]
28. Draper, C.S.; Reichle, R.H.; De Lannoy, G.J.M.; Liu, Q. Assimilation of passive and active microwave soil moisture retrievals. *Geophys. Res. Lett.* **2012**, *39*, L04401. [CrossRef]
29. Thorp, K.R.; Wang, G.; West, A.L.; Moran, M.S.; Bronson, K.F.; White, J.W.; Mon, J. Estimating crop biophysical properties from remote sensing data by inverting linked radiative transfer and ecophysiological models. *Remote Sens. Environ.* **2012**, *124*, 224–233. [CrossRef]
30. Li, Z.; Jin, X.; Zhao, C.; Wang, J.; Xu, X.; Yang, G.; Li, C.; Shen, J. Estimating wheat yield and quality by coupling the DSSAT-CERES model and proximal remote sensing. *Eur. J. Agron.* **2015**, *71*, 53–62. [CrossRef]
31. Wiegand, C.L.; Richardsons, A.J.; Kanemasu, E.T. Leaf area index estimates for wheat from LANDSAT and their implications for evapotranspiration and crop modeling. *Agron. J. Abstr.* **1979**, *71*, 336–342. [CrossRef]
32. Richardson, A.J.; Wiegand, C.L.; Arkin, G.F.; Nixon, P.R.; Gerbermann, A.H. Remotely sensed spectral indicators of sorghum development and their use in growth modelling. *Agric. Meteorol.* **1982**, *26*, 11–23. [CrossRef]
33. Reynolds, C.A.; Yitayew, M.; Slack, D.C.; Hutchinson, C.F.; Huete, A.; Peterson, M.S. Estimating crop yields and production by integrating the FAO Crop Specific Water Balance model with real-time satellite data and ground-based ancillary data. *Int. J. Remote Sens.* **2000**, *21*, 3487–3508. [CrossRef]
34. Ovando, G.; Sayago, S.; Bocco, M. Evaluating accuracy of DSSAT model for soybean yield estimation using satellite weather data. *ISPRS J. Photogramm. Remote Sens.* **2018**, *138*, 208–217. [CrossRef]
35. Dinku, T.; Ceccato, P.; Grover-Kopec, E.; Lemma, M.; Connor, S.J.; Ropelewsky, C.F. Validation of satellite rainfall products over East Africa's complex topography. *Int. J. Remote Sens.* **2007**, *28*, 1503–1526. [CrossRef]
36. Ciabatta, L.; Brocca, L.; Massari, C.; Moramarco, T.; Puca, S.; Rinollo, A.; Gabellani, S.; Wagner, W. Integration of satellite soil moisture and rainfall observations over the Italian territory. *J. Hydrometeorol.* **2015**, *16*, 1341–1355. [CrossRef]
37. Jones, J.W.; Hoogenboom, G.; Porter, C.H.; Boote, K.J.; Batchelor, W.D.; Hunt, L.A.; Wilkens, P.W.; Singh, U.; Gijsman, A.J.; Ritchie, J.T. The DSSAT cropping system model. *Eur. J. Agron.* **2003**, *18*, 235–265. [CrossRef]
38. Brocca, L.; Moramarco, T.; Melone, F.; Wagner, W. A new method for rainfall estimation through soil moisture observations. *Geophys. Res. Lett.* **2013**, *40*, 853–858. [CrossRef]
39. Brocca, L.; Ciabatta, L.; Massari, C.; Moramarco, T.; Hahn, S.; Hasenauer, S.; Kidd, R.; Dorigo, W.; Wagner, W.; Levizzani, V. Soil as a natural rain gauge: Estimating global rainfall from satellite soil moisture data. *J. Geophys. Res. Atmos.* **2014**, *119*, 5128–5141. [CrossRef]
40. Jones, J.W.; Keating, B.A.; Porter, C.H. Approaches to modular model development. *Agric. Syst.* **2001**, *70*, 241–443. [CrossRef]
41. Hunt, L.A.; White, J.W.; Hoogenboom, G. Agronomic data: Advances in documentation and protocols for exchange and use. *Agric. Syst.* **2001**, *70*, 477–492. [CrossRef]

42. Singh, A.K.; Tripathy, R.; Chopra, U.K. Evaluation of CERES-Wheat and CropSyst models for water-nitrogen interactions in wheat crop. *Agric. Water Manag.* **2008**, *95*, 776–786. [CrossRef]
43. Allen, G.A.; Pereira, L.S.; Raes, D.; Smith, M. *Crop Evapotranspiration: Guidelines for Computing Crop Water Requirements, Irrigation and Drainage Paper No. 56*; FAO: Rome, Italy, 1998.
44. Thaler, S.; Eitzinger, J.; Trnka, M.; Dubrovsky, M. Impacts of climate change and alternative adaptation options on winter wheat yield and water productivity in a dry climate in Central Europe. *J. Agric. Sci.* **2012**, *150*, 537–555. [CrossRef]
45. Eitzinger, J.; Trnka, M.; Semerádová, D.; Thaler, S.; Svobodová, E.; Hlavinka, P.; Siska, B.; Takác, J.; Malatinská, L.; Nováková, M.; et al. Regional climate change impacts on agricultural crop production in Central and Eastern Europe—Hotspots, regional differences and common trends. *J. Agric. Sci.* **2013**, *151*, 787–812. [CrossRef]
46. Haiden, T.; Kann, A.; Pistotnik, G. Nowcasting with INCA during SNOW-V_{10}. *Pure Appl. Geophys.* **2014**, *171*, 231–242. [CrossRef]
47. Huffman, G.J.; Adler, R.F.; Bolvin, D.T.; Gu, G.; Nelkin, E.J.; Bowman, K.P.; Hong, Y.; Stocker, E.F.; Wolff, D.B. The TRMM Multisatellite Precipitation Analysis (TMPA): Quasi-Global, Multiyear, Combined-Sensor Precipitation Estimates at Fine Scales. *J. Hydrometeorol.* **2007**, *8*, 38–55. [CrossRef]
48. Joyce, R.J.; Janowiak, J.E.; Arkin, P.A.; Xie, P. CMORPH: A method that produces global precipitation estimates from passive microwave and infrared data at high spatial and temporal resolution. *J. Hydrometeorol.* **2004**, *5*, 487–503. [CrossRef]
49. Karabatic, A.; Weber, R.; Haiden, T. Near real-time estimation of tropospheric water vapour content from ground based GNSS data and its potential contribution to weather now-casting in Austria. *Adv. Space Res.* **2011**, *4*, 1691–1703. [CrossRef]
50. Hussain, Y.; Satgé, F.; Hussain, M.B.; Martinez-Carvajal, H.; Bonnet, M.-P.; Cárdenas-Soto, M.; Llacer Roig, H.; Akhter, G. Performance of CMORPH, TMPA, and PERSIANN rainfall datasets over plain, mountainous, and glacial regions of Pakistan. *Theor. Appl. Clim.* **2018**, *131*, 1119–1132. [CrossRef]
51. Nayak, M.A.; Villarini, G. Remote sensing-based characterization of rainfall during atmospheric rivers over the central United States. *J. Hydrol.* **2018**, *556*, 1038–1049. [CrossRef]
52. Bartalis, Z.; Naeimi, V.; Hasenauer, S.; Wagner, W. *ASCAT Soil Moisture Product Handbook*; ASCAT Soil Moisture Rep. 15; Institute of Photogrammetry and Remote Sensing, Vienna University of Technology: Vienna, Austria, 2008.
53. Wagner, W.; Hahn, S.; Kidd, R.; Melzer, T.; Bartalis, Z.; Hasenauer, S.; Figa, J.; de Rosnay, P.; Jann, A.; Schneider, S.; et al. The ASCAT soil moisture product: A review of its specifications, validation results, and emerging applications. *Meteorol. Z.* **2013**, *22*, 5–33. [CrossRef]
54. Wagner, W.; Lemoine, G.; Rott, H. A method for estimating soil moisture from ERS scatterometer and soil data. *Remote Sens. Environ.* **1999**, *70*, 191–207. [CrossRef]
55. Brocca, L.; Liersch, S.; Melone, F.; Moramarco, T.; Volk, M. Application of a model-based rainfall-runoff database as efficient tool for flood risk management. *Hydrol. Earth Syst. Sci.* **2013**, *17*, 3159–3169. [CrossRef]
56. Ciabatta, L.; Brocca, L.; Massari, C.; Moramarco, T.; Gabellani, S.; Puca, S.; Wagner, W. Rainfall-runoff modelling by using SM2RAIN-derived and state-of-the-art satellite rainfall products over Italy. *Int. J. Appl. Earth Obs. Geoinf.* **2016**, *48*, 163–173. [CrossRef]
57. Kolassa, J.; Gentine, P.; Prigent, C.; Aires, F. Soil moisture retrieval from AMSR-E and ASCAT microwave observation synergy. Part 1: Satellite data analysis. *Remote Sens. Environ.* **2016**, *173*, 1–14. [CrossRef]
58. Angulo, C.; Rötter, R.; Trnka, M.; Pirttioja, N.; Gaiser, T.; Hlavinka, P.; Ewert, F. Characteristic 'fingerprints' of crop model responses to weather input data at different spatial resolutions. *Eur. J. Agron.* **2013**, *49*, 104–114. [CrossRef]
59. Faivre, R.; Leenhardt, D.; Voltz, M.; Benoît, M.; Papy, F.; Dedieu, G.; Wallach, D. Spatialising crop models. *Agronomie* **2004**, *24*, 205–217. [CrossRef]
60. Ciabatta, L.; Massari, C.; Brocca, L.; Gruber, A.; Reimer, C.; Hahn, S.; Paulik, C.; Dorigo, W.; Kidd, R.; Wagner, W. SM2RAIN-CCI: A new global long-term rainfall data set derived from ESA CCI soil moisture. *Earth Syst. Sci. Data* **2018**, *10*, 267–280. [CrossRef]
61. Hou, A.Y.; Kakar, R.K.; Neeck, S.; Azarbarzin, A.A.; Kummerow, C.D.; Kojima, M.; Oki, R.; Nakamura, K.; Iguchi, T. The Global Precipitation Measurement (GPM) mission. *Bull. Am. Meteorol. Soc.* **2014**, *95*, 701–722. [CrossRef]

62. Hsu, K.; Gao, X.; Sorooshian, S.; Gupta, H.V. Precipitation Estimation from Remotely Sensed Information Using Artificial Neural Networks. *J. Appl. Meteorol.* **1997**, *36*, 1176–1190. [CrossRef]
63. Funk, C.; Peterson, P.; Landsfeld, M.; Pedreros, D.; Verdin, J.; Shukla, S.; Husak, G.; Rowland, J.; Harrison, L.; Hoell, A.; et al. The climate hazards infrared precipitation with stations—A new environmental record for monitoring extremes. *Sci. Data* **2015**, 2. [CrossRef] [PubMed]
64. Lo Conti, F.; Hsu, K.L.; Noto, L.V.; Sorooshian, S. Evaluation and comparison of satellite precipitation estimates with reference to a local area in the Mediterranean Sea. *Atmos. Res.* **2014**, *138*, 189–204. [CrossRef]
65. Mei, Y.W.; Anagnostou, E.N.; Nikolopoulos, E.I.; Borga, M. Error analysis of satellite precipitation products in mountainous basins. *J. Hydrometeorol.* **2014**, *15*, 1778–1793. [CrossRef]
66. Trenberth, K.E.; Asrar, G.R. Challenges and opportunities in water cycle research: WCRP contributions. *Surv. Geophys.* **2014**, *35*, 515–532. [CrossRef]
67. Kucera, P.A.; Ebert, E.E.; Turk, F.J.; Levizzani, V.; Kirschbaum, D.; Tapiador, F.J.; Loew, A.; Borsche, M. Precipitation from space: Advancing earth system science. *Bull. Am. Meteorol. Soc.* **2013**, *94*, 365–375. [CrossRef]
68. Crow, W.T.; Huffman, G.F.; Bindlish, R.; Jackson, T.J. Improving satellite rainfall accumulation estimates using spaceborne soil moisture retrievals. *J. Hydrometeorol.* **2009**, *10*, 199–212. [CrossRef]
69. Pellarin, T.; Louvet, S.; Gruhier, C.; Quantin, G.; Legout, C. A simple and effective method for correcting soil moisture and precipitation estimates using AMSR-E measurements. *Remote Sens. Environ.* **2013**, *136*, 28–36. [CrossRef]
70. Wanders, N.; Pan, M.; Wood, E.F. Correction of real-time satellite precipitation with multi-sensor satellite observations of land surface variables. *Remote Sens. Environ.* **2015**, *160*, 206–221. [CrossRef]
71. Zhan, W.; Pan, M.; Wanders, N.; Wood, E.F. Correction of real-time satellite precipitation with satellite soil moisture observations. *Hydrol. Earth Syst. Sci.* **2015**, *19*, 4275–4291. [CrossRef]
72. Brocca, L.; Pellarin, T.; Crow, W.D.; Ciabatta, L.; Massari, C.; Ryu, D.; Su, C.H.; Rüdiger, C.; Kerr, Y. Rainfall estimation by inverting SMOS soil moisture estimates: A comparison of different methods over Australia. *J. Geophys. Res.-Atmos.* **2016**, *121*, 12062–12079. [CrossRef]
73. Ciabatta, L.; Marra, A.C.; Panegrossi, G.; Casella, D.; Sanò, P.; Dietrich, S.; Massari, C.; Brocca, L. Daily precipitation estimation through different microwave sensors: Verification study over Italy. *J. Hydrol.* **2017**, *545*, 436–450. [CrossRef]
74. Koster, R.D.; Brocca, L.; Crow, W.T.; Burgin, M.S.; De Lannoy, G.J.M. Precipitation Estimation Using LBand and C-Band Soil Moisture Retrievals. submitted to Water Resources Research. *Water Resour. Res.* **2016**, *52*, 7213–7225. [CrossRef] [PubMed]
75. Massari, C.; Crow, W.; Brocca, L. An assessment of the performance of global rainfall estimates without groundbased observations. *Hydrol. Earth Syst. Sci.* **2017**, *21*, 4347–4361. [CrossRef]
76. Isotta, F.A.; Frei, C.; Weilguni, V.; Perčec Tadić, M.; Lassègues, P.; Rudolf, B.; Pavan, V.; Cacciamani, C.; Antolini, G.; Ratto, S.M.; et al. The climate of daily precipitation in the Alps: Development and analysis of a high-resolution grid dataset from pan-Alpine rain-gauge data. *Int. J. Climatol.* **2014**, *34*, 1657–1675. [CrossRef]
77. Haylock, M.R.; Hofstra, N.; Klein Tank, A.M.G.; Klok, E.J.; Jones, P.D.; New, M. A European daily high-resolution gridded data set of surface temperature and precipitation for 1950–2006. *J. Geophys. Res.* **2008**, *113*, D20119. [CrossRef]
78. Eitzinger, J.; Thaler, S.; Schmid, E.; Strauss, F.; Ferrise, R.; Moriondo, M.; Bindi, M.; Palosuo, T.; Rötter, R.; Kersebaum, K.C.; et al. Sensitivities of crop models to extreme weather conditions during flowering period demonstrated for maize and winter wheat in Austria. *J. Agric. Sci.* **2013**, *151*, 813–835. [CrossRef]
79. Palosuo, T.; Kersebaum, K.C.; Angulo, C.; Hlavinka, P.; Moriondo, M.; Olesen, J.E.; Patil, R.H.; Ruget, F.; Rumbaur, C.; Takac, J.; et al. Simulation of winter wheat yield and its variability in different climates of Europe: A comparison of eight crop growth models. *Eur. J. Agron.* **2011**, *35*, 103–114. [CrossRef]
80. Rötter, R.P.; Palosuo, T.; Kersebaum, K.C.; Angulo, C.; Bindi, M.; Ewert, F.; Ferrise, R.; Hlavinka, P.; Moriondo, M.; Nendel, C.; et al. Simulation of spring barley yield in different climatic zones of Northern and Central Europe: A comparison of nine crop models. *Field Crop. Res.* **2012**, *133*, 23–36. [CrossRef]

81. Fronzek, S.; Pirttioja, N.; Carter, T.R.; Bindi, M.; Hoffmann, H.; Palosuo, T.; Ruiz-Ramos, M.; Tao, F.; Trnka, M.; Acutis, M.; et al. Classifying multi-model wheat yield impact response surfaces showing sensitivity to temperature and precipitation change. *Agric. Syst.* **2018**, *159*, 209–224. [CrossRef]
82. Stampoulis, D.; Anagnostou, E.N. Evaluation of global satellite rainfall products over continental Europe. *J. Hydrometeorol.* **2012**, *13*, 588–603. [CrossRef]